

Two-sample inference for high-dimensional Markov networks

Byol Kim^{*1}, Song Liu^{†2}, and Mladen Kolar^{‡3}

¹Department of Statistics, The University of Chicago, Chicago, IL 60637, USA.

²School of Mathematics, University of Bristol, Bristol, BS8 1UG, UK; Alan Turing Institute, London, NW1 2DB, UK.

³Booth School of Business, The University of Chicago, Chicago, IL 60637, USA.

Abstract

Markov networks are frequently used in sciences to represent conditional independence relationships underlying observed variables arising from a complex system. It is often of interest to understand how an underlying network differs between two conditions. In this paper, we develop methods for comparing a pair of high-dimensional Markov networks where we allow the number of observed variables to increase with the sample sizes. By taking the density ratio approach, we are able to learn the network difference directly and avoid estimating the individual graphs. Our methods are thus applicable even when the individual networks are dense as long as their difference is sparse. We prove finite-sample Gaussian approximation error bounds for the estimator we construct under significantly weaker assumptions than are typically required for model selection consistency. Furthermore, we propose bootstrap procedures for estimating quantiles of a max-type statistics based on our estimator, and show how they can be used to test the equality of two Markov networks or construct simultaneous confidence intervals. The performance of our methods is demonstrated through extensive simulations. The scientific usefulness is illustrated with an analysis of a new fMRI dataset.

Keywords: Differential networks; High-dimensional inference; Kullback-Leibler Importance Estimation Procedure; Markov networks; Post-regularization inference.

1 Introduction

Markov networks, also known as Markov random fields or undirected probabilistic graphical models, are successfully used in many application domains to represent interactions between measured components of a complex system and help scientists in uncovering structured information from large amounts of unstructured data (Lauritzen, 1996; MacKay, 2003; Koller and Friedman, 2009). In genetics the graph structure can be used, for example, to model regulatory activities in gene expressions (Hartemink et al., 2001; Dobra et al., 2004), while in neuroscience it can be used to model brain network in order to identify features associated with different mental diseases (Supekar et al., 2008). Other successful application areas include social and political sciences (Banerjee et al., 2008), analysis of financial data (Barber and Kolar, 2018), and many others. One of the fundamental problems in statistics is that of learning the graph structure of a probabilistic graphical model based on independent and identically distributed (i.i.d.) samples. See Drton and Maathuis (2017) for a recent overview.

The focus of this paper is on developing a method for statistical inference of parameters in a differential network. For a recent survey, see Shojaie (2021), and references therein. In many applications, interest centres not on a particular network, but rather on whether and how the network changes between different states. For example, genes may regulate each other differently when the external environment is altered. The way different regions of a brain interact together may be altered depending on the activity that a patient

*byolkim@uchicago.edu

†song.liu@bristol.ac.uk

‡mkolar@chicagobooth.edu

is performing. A single graphical model lacks the ability to capture such changes and cannot reflect the dynamic nature of such data, therefore limiting our ability to gain key insights into the underlying system under consideration.

We develop a collection of methods for performing statistical inference on the difference of parameters in high-dimensional Markov networks. Subtleties arise when the target of inference is the difference of parameters rather than the parameters themselves. In high-dimensional regimes, consistent estimation requires an assumption of inherent low-dimensionality such as sparsity (Yuan and Lin, 2007; Friedman et al., 2008; Yuan, 2010; Cai et al., 2011; Ravikumar et al., 2011). Therefore, a crude procedure that estimates the network parameters separately, and then takes the difference, can only work when *all* the individual networks are sparse. This is quite restrictive for applications where the individual networks may be dense, but the differences are expected to be sparse, say, due to the experimental set-up. Moreover, even when the assumption is satisfied, many such methods have tuning parameters that have an influence on the estimated structure, and it is unclear how they should be combined in practice to yield a consistent estimate of the difference.

This has led many researchers either to jointly estimate structurally similar networks (Chiquet et al., 2011; Danaher et al., 2014; Guo et al., 2011; Mohan et al., 2014; Ma and Michailidis, 2016; Majumdar and Michailidis, 2018) or to directly estimate the difference (Zhao et al., 2014; Xu and Gu, 2016; Liu et al., 2017; Fazayeli and Banerjee, 2016). The latter approaches tend to have better sample complexity as well as greater applicability. The methods we propose also belong to the latter category.

Our proposal tries to fill two gaps in the existing literature on differential network estimation. First, the majority of the literature on graphical models are developed assuming a particular observation model, and the growing literature on difference estimation is no exception. For example, Xia et al. (2015) assume that the data are Gaussian, whereas Cai et al. (2019) use an Ising model. By contrast, we work with *general* Markov random fields; we present a unified framework for statistical inference in differential networks, without the need for developing separate methodology for different distributional assumptions. Following the development of Sugiyama et al. (2008, 2012); Liu et al. (2014, 2017); Fazayeli and Banerjee (2016), we take the density ratio approach and estimate the difference directly. The last three assume a high-dimensional regime, and study consistency of point estimators defined as solutions to penalized procedures, but the question of statistical inference is unaddressed.

This brings us to the second gap. Most of the existing literature on network difference estimation focuses on producing consistent point estimates, leaving the question of quantifying uncertainty in those estimates largely untouched. The methods we develop in this paper can be used to construct confidence intervals and carry out hypothesis tests about the difference of networks parameters. The theoretical guarantees we provide hold under a fairly weak set of assumptions. In particular, they do not rely on perfect model selection at any stage, which would have necessitated strong assumptions, e.g., incoherence and strong signal strength. Certain features of our problem, e.g., nonlinearity, introduce technical challenges in establishing our theoretical results.

Our paper contributes to the growing literature on statistical inference on high-dimensional parameter estimates. Hypothesis testing and confidence intervals for high-dimensional M-estimators are studied in Zhang and Zhang (2013); Belloni et al. (2013, 2016); Javanmard and Montanari (2014); Meinshausen (2015); van de Geer et al. (2014). Related ideas have been developed in the context of Gaussian graphical models (Ren et al., 2015; Janková and van de Geer, 2015; Janková and van de Geer, 2017), elliptical copula models (Barber and Kolar, 2018; Lu et al., 2018), and Markov networks (Wang and Kolar, 2016; Yu et al., 2016). Existing inferential techniques for high-dimensional differential networks rely on Gaussian observation model and separate estimation (Xia et al., 2015; Belilovsky et al., 2016; Liu, 2017). By contrast, our methods also apply to non-Gaussian data and are based on direct difference estimation.

Our Gaussian bootstrap approximation results can be viewed as another contribution along the lines of Chen (2018) and Xue and Yao (2020), which build on the ideas of Chernozhukov et al. (2013, 2015a, 2017). In particular, the testing procedure developed in Xue and Yao (2020) relies on a Gaussian approximation result of the difference of two independent sums in high-dimensions. Our equal graph test is similar in flavor, but as our estimator cannot be represented as an independent sum, the proof of validity requires a careful control of the remainder. Furthermore, our empirical bootstrap heuristic is an interesting generalization of Dezeure et al. (2017) to a non-linear and two-sample problem, the theoretical exploration of which we leave up to future work.

The rest of this paper is organized as follows. Section 2 discusses some background. Our methods are presented in Section 3, and their theoretical guarantees are given in Section 4. We report the results of our extensive simulation study in Section 5, and analyze a real fMRI dataset in Section 6. We conclude with a discussion of alternatives and future directions in Section 7. The proofs of the main results are found in Appendix. A Julia package implementing the proposed methods may be obtained from <https://github.com/mlakolar/KLIEPInference.jl>, together with the code to reproduce the results.

2 Preliminaries

We list notations that are used frequently throughout this paper. Vectors are distinguished from scalars by bold font, e.g., \mathbf{v} . Bold uppercase letters are reserved for matrices, e.g., \mathbf{M} . For $d \in \mathbb{N}$, $[d] = \{1, \dots, d\}$. For $k \in [d]$, $\mathbf{e}_k \in \mathbb{R}^d$ is the k th standard basis vector. For $\mathbf{v} \in \mathbb{R}^d$ and $k \in [d]$, we write v_k for the k th component of \mathbf{v} . For $S \subseteq [d]$, $\mathbf{v}_S \in \mathbb{R}^d$ with $v_{S,k} = v_k$ for $k \in S$, $v_{S,k} = 0$ else. Let $\mathcal{I} \subseteq [d]$ be an index set. For a set of scalars $\{v_k\}_{k \in \mathcal{I}}$, $(v_k)_{k \in \mathcal{I}}$ denotes the $|\mathcal{I}|$ -vector with the components given by the set. Similarly, for a set of vectors $\{\mathbf{v}_k\}_{k \in \mathcal{I}}$ with all $\mathbf{v}_k \in \mathbb{R}^d$, $[\mathbf{v}_k]_{k \in \mathcal{I}}$ denotes the $d \times |\mathcal{I}|$ -matrix with the columns given by the set. Given $\mathbf{v}_1 \in \mathbb{R}^{d_1}$ and $\mathbf{v}_2 \in \mathbb{R}^{d_2}$, $\mathbf{v}_1 \cup \mathbf{v}_2 \in \mathbb{R}^{d_1+d_2}$ denotes their concatenation. For $\mathbf{v} \in \mathbb{R}^d$, the partition of \mathbf{v} induced by a partition $d_1 + d_2 = d$ is denoted $\mathbf{v} = [\mathbf{v}_1^1 \mathbf{v}_2^1]$. Similarly, for $\mathbf{M} \in \mathbb{R}^{d \times d}$, $\mathbf{M} = \begin{bmatrix} \mathbf{M}_{11} & \mathbf{M}_{12} \\ \mathbf{M}_{21} & \mathbf{M}_{22} \end{bmatrix}$.

The inner product is denoted as $\langle \mathbf{u}, \mathbf{v} \rangle = \mathbf{u}^\top \mathbf{v} = \sum_{k=1}^d u_k v_k$. We use $\|\cdot\|$ to denote a norm on \mathbb{R}^d , and $\|\cdot\|_*$ to denote its dual, $\|\mathbf{v}\|_* = \sup_{\|\mathbf{u}\| \leq 1} |\langle \mathbf{u}, \mathbf{v} \rangle|$. For $p \in [1, \infty]$, $\|\mathbf{v}\|_p = \left(\sum_{k=1}^d |v_k|^p\right)^{1/p}$ is the usual ℓ_p -norm of \mathbf{v} . This is extended first to $q \in (0, 1]$ as $\|\mathbf{v}\|_q = \sum_{k'} |v_{k'}|^q$, and then to $q = 0$ by adopting the convention $0^0 \equiv 0$ so that $\|\mathbf{v}\|_0 = |\text{supp}(\mathbf{v})| = |\{k : v_k \neq 0\}|$. For $q \in [0, 1)$, ℓ_q -“norms” can be thought of as generalized sparsity measures. For a matrix $\mathbf{M} \in \mathbb{R}^{d \times d}$, $\|\mathbf{M}\| = \|\text{vec}(\mathbf{M})\|$, e.g., $\|\mathbf{M}\|_\infty = \max_{1 \leq k, k' \leq d} |M_{kk'}|$. For $s > 0$, $\|\mathbf{M}\|_s$ is the maximum s -sparse eigenvalue of \mathbf{M} : $\|\mathbf{M}\|_s = \sup_{\|\mathbf{v}\|_0 \leq s, \|\mathbf{v}\| = 1} |\mathbf{v}^\top \mathbf{M} \mathbf{v}|$. Also, $\|\mathbf{M}\|_* = \sup_{\|\mathbf{v}\| \leq 1} \|\mathbf{M} \mathbf{v}\|_*$.

Let $(a_n)_{n \geq 1}$ and $(b_n)_{n \geq 1}$ be sequences. $a_n \lesssim b_n$ or $a_n = O(b_n)$ whenever $|a_n/b_n| \leq M$ for some $M > 0$ for all sufficiently large n . $a_n \asymp b_n$ when both $a_n \lesssim b_n$ and $b_n \lesssim a_n$. $a_n = o(b_n)$ means $|a_n/b_n| \rightarrow 0$ as $n \rightarrow \infty$. If such a relationship holds with probability approaching 1, this is distinguished by \mathbb{P} in the subscript, for example, $O_{\mathbb{P}}$, $o_{\mathbb{P}}$, $\lesssim_{\mathbb{P}}$, $\asymp_{\mathbb{P}}$.

REM is a catch-all symbol for the remainder of an approximation, whose precise definition varies according to the context and from line to line. Φ is the cdf of the standard Gaussian: $\Phi(z) = \int_{-\infty}^z \phi(t) dt$, where $\phi(z) = e^{-z^2/2}/\sqrt{2\pi}$. Φ^{-1} denotes its inverse function, i.e., the standard Gaussian quantile function.

2.1 Statement of the problem

A *Markov network* describes conditional dependencies among a collection of random variables (Lauritzen, 1996; Drton and Maathuis, 2017). Let $\mathbf{x} = (x_v)_{v=1}^m$ be a random vector taking values in $\mathbb{X} \subseteq \mathbb{R}^m$. Consider an *undirected graph* G on the node set $V = [m]$, i.e., a pair $G = (V, E)$, where E , called the edge set, contains unordered pairs of nodes. We say that nodes $u, v \in V$ are connected by an edge if $\{u, v\} \in E$. Formally, a Markov network associated with $G = ([m], E)$ is a collection of m -variate distributions such that $x_u \perp\!\!\!\perp x_v \mid (x_w)_{w \neq u, v}$ if and only if $\{u, v\} \notin E$. Thus, the edge set E describes which pairs of random variables are conditionally independent given all the other variables.

Let $\mathcal{C}(G)$ denote the set of all *cliques* of G , i.e., subsets of V for which every pair of nodes is connected by an edge. It is well-known that any such \mathbf{x} with a strictly positive density is an exponential family $f(\mathbf{x}; \gamma) = \exp(\gamma^\top \boldsymbol{\psi}(\mathbf{x}))/Z(\gamma)$ for some $\gamma = (\gamma_C)_{C \in \mathcal{C}(G)}$, $\boldsymbol{\psi} = (\psi_C)_{C \in \mathcal{C}(G)}$, and the normalizing constant $Z(\gamma) = \int \exp(\gamma^\top \boldsymbol{\psi}(\mathbf{x})) d\mathbf{x}$, where $\gamma_C \in \mathbb{R}$ and ψ_C is a function of the clique variables $(x_v)_{v \in C}$ only (Hammersley and Clifford, 1971). A parametric class \mathcal{F}_γ of Markov networks is obtained by assuming a fixed $\boldsymbol{\psi}$.

A special case of significance is the class of *pairwise* Markov networks (Wainwright and Jordan, 2008b; Yang et al., 2015) that have densities of the form

$$f(\mathbf{x}; \gamma) = \frac{1}{Z(\gamma)} \exp \left(\sum_{v=1}^m \gamma_v \psi_v(x_v) + \sum_{u=1}^m \sum_{v=u+1}^m \gamma_{uv} \psi_{uv}(x_u, x_v) \right), \quad (1)$$

where $\boldsymbol{\gamma} = (\gamma_v)_{v=1}^m \cup (\gamma_{uv})_{1 \leq u < v \leq m}$, $\boldsymbol{\psi} = (\psi_v)_{v=1}^m \cup (\psi_{uv})_{1 \leq u < v \leq m}$. For this class, each component function of $\boldsymbol{\psi}$ is at most a function of two variables, and hence $x_u \perp\!\!\!\perp x_v \mid (x_w)_{w \neq u, v}$ if and only if $\gamma_{uv} = 0$, $u \neq v$. Thus, for a pairwise Markov network, the edge set E dictates which of the pairwise parameters $(\gamma_{uv})_{1 \leq u < v \leq m}$ are nonzero. A number of well-studied models belong to the pairwise class.

Example 1 (Ising models). An Ising model is a family of discrete probability distribution on the vertices of the m -dimensional hypercube $\mathbb{X} = \{\pm 1\}^m$ given by the probability mass function of the form (1) with $\psi_v(x_v) = x_v$, $\psi_{uv}(x_u, x_v) = x_u x_v$, and $\gamma_v, \gamma_{uv} \in \mathbb{R}$. Thus, the Markov network associated with $G = ([m], E)$ are all Ising models with $\gamma_{uv} \neq 0$ if and only if $\{u, v\} \in E$.

Example 2 (Gaussian graphical models). The most-studied example of a probabilistic graphical model is the case of the undirected Gaussian graphical model. Suppose $\mathbf{x} \sim \mathcal{N}(\boldsymbol{\mu}, \boldsymbol{\Sigma})$. Then, \mathbf{x} has a density of the form (1) with $\psi_v(x_v) = x_v$, $\psi_{uv}(x_u, x_v) = x_u x_v$, $\gamma_v = (\boldsymbol{\Sigma}^{-1} \boldsymbol{\mu})_v$, and $\gamma_{uv} = -[\boldsymbol{\Sigma}^{-1}]_{uv}/2$. Thus, if \mathbf{x} is in a Gaussian graphical model with the graph $G = ([m], E)$, then the inverse covariance matrix satisfies $[\boldsymbol{\Sigma}^{-1}]_{uv} \neq 0$ if and only if $\{u, v\} \in E$.

Suppose $f_x = f(\cdot; \boldsymbol{\gamma}_x)$ and $f_y = f(\cdot; \boldsymbol{\gamma}_y)$ are two distributions from the same pairwise family (1) corresponding to parameters $\boldsymbol{\gamma}_x$ and $\boldsymbol{\gamma}_y$, respectively. Then, the *change* from $f_x = f(\cdot; \boldsymbol{\gamma}_y)$ to $f_y = f(\cdot; \boldsymbol{\gamma}_x)$ can be described by the *difference* $\boldsymbol{\theta}^* = \boldsymbol{\gamma}_x - \boldsymbol{\gamma}_y$. In particular, whenever $x_u \perp\!\!\!\perp x_v \mid (x_w)_{w \neq u, v}$ is true for only one of f_x or f_y , we have $\theta_{uv}^* = \gamma_{x,uv} - \gamma_{y,uv} \neq 0$. More generally, the support of $\boldsymbol{\theta}^*$ gives the pairs of random variables for which the conditional dependence relationship has changed.

The *differential network* is defined as the difference $\boldsymbol{\theta}^*$ of $\boldsymbol{\gamma}_x$ and $\boldsymbol{\gamma}_y$. We represent the differential network with a graph $G = (V, E)$ where an edge $\{u, v\} \in E$ is drawn between vertices u and v if and only if $\theta_{uv}^* \neq 0$. Our goal here is to learn the differential network given independent and identically distributed (i.i.d.) observations from each of $f_x = f(\cdot; \boldsymbol{\gamma}_x)$ and $f_y = f(\cdot; \boldsymbol{\gamma}_y)$. More precisely, using $\mathbf{x}^{(1)}, \dots, \mathbf{x}^{(n_x)} \stackrel{iid}{\sim} f_x$ and $\mathbf{y}^{(1)}, \dots, \mathbf{y}^{(n_y)} \stackrel{iid}{\sim} f_y$, we would like to construct confidence intervals or conduct hypothesis tests over possibly high-dimensional sub-vectors of $\boldsymbol{\theta}^*$ with provably valid simultaneous guarantee at arbitrary user-specified confidence level of $1 - \alpha$ for small $\alpha \in [0, 1]$. This requires an estimate of $\boldsymbol{\theta}^*$, which we construct in the next section based on the density ratio f_x/f_y without separately estimating the individual parameters $\boldsymbol{\gamma}_x$ and $\boldsymbol{\gamma}_y$.

2.2 Direct difference estimation via density ratio

We describe the Kullback-Leibler Importance Estimation Procedure (KLIEP) (Sugiyama et al., 2008) and how it can be used to directly estimate the differential network $\boldsymbol{\theta}^*$.

KLIEP is a framework for estimating the density ratio of two probability distributions based on i.i.d. observations from each. When the distributions are from the same parametric exponential family, the density ratio depends on the underlying pair of parameters only through their *difference* while maintaining the exponential form. Indeed, let $r_{\boldsymbol{\theta}^*} = f_x/f_y$. Then,

$$r_{\boldsymbol{\theta}^*}(\mathbf{x}) = \frac{f_x(\mathbf{x})}{f_y(\mathbf{x})} = \frac{Z(\boldsymbol{\gamma}_y) \exp(\boldsymbol{\gamma}_y^\top \boldsymbol{\psi}(\mathbf{x}))}{Z(\boldsymbol{\gamma}_x) \exp(\boldsymbol{\gamma}_x^\top \boldsymbol{\psi}(\mathbf{x}))} = \frac{\exp(\boldsymbol{\theta}^{*\top} \boldsymbol{\psi}(\mathbf{x}))}{Z_y(\boldsymbol{\theta}^*)},$$

where we have $Z_y(\boldsymbol{\theta}^*) = \mathbb{E}_y[\exp(\boldsymbol{\theta}^{*\top} \boldsymbol{\psi}(\mathbf{y}))]$, because

$$\begin{aligned} Z_y(\boldsymbol{\theta}^*) &= \frac{Z(\boldsymbol{\gamma}_x)}{Z(\boldsymbol{\gamma}_y)} = \frac{\int \exp(\boldsymbol{\gamma}_x^\top \boldsymbol{\psi}(\mathbf{x})) d\mathbf{x}}{Z(\boldsymbol{\gamma}_y)} \\ &= \int \exp(\boldsymbol{\theta}^{*\top} \boldsymbol{\psi}(\mathbf{x})) \frac{\exp(\boldsymbol{\gamma}_y^\top \boldsymbol{\psi}(\mathbf{x}))}{Z(\boldsymbol{\gamma}_y)} d\mathbf{x} = \mathbb{E}_y[\exp(\boldsymbol{\theta}^{*\top} \boldsymbol{\psi}(\mathbf{y}))]. \end{aligned}$$

This can be used to derive a procedure that directly learns $\boldsymbol{\theta}^*$ without having to learn either $\boldsymbol{\gamma}_x$ or $\boldsymbol{\gamma}_y$. Let $D_{\text{KL}}(f||g)$ be the *Kullback-Leibler (KL) divergence* for probability densities f and g . Recall that $D_{\text{KL}}(f||g) \geq 0$ with equality if and only if $f = g$ almost everywhere. Since $f_x = r_{\boldsymbol{\theta}^*} f_y$, $\boldsymbol{\theta}^* = \arg \min_{\boldsymbol{\theta}} D_{\text{KL}}(f_x || r_{\boldsymbol{\theta}} f_y)$. Moreover, it is proved in Appendix A.1 that

$$\begin{aligned} \boldsymbol{\theta}^* &= \arg \min_{\boldsymbol{\theta}} D_{\text{KL}}(f_x || r_{\boldsymbol{\theta}} f_y) \\ &= \arg \min_{\boldsymbol{\theta}} \{-\mathbb{E}_x[\boldsymbol{\theta}^\top \boldsymbol{\psi}(\mathbf{x})] + \log \mathbb{E}_y[\exp(\boldsymbol{\theta}^\top \boldsymbol{\psi}(\mathbf{y}))]\}, \end{aligned} \tag{2}$$

where \mathbb{E}_x denotes the expectation with respect to f_x and \mathbb{E}_y the expectation with respect to f_y . The *empirical KLIEP loss* ℓ_{KLIEP} is obtained by replacing each expectation with the corresponding sample average:

$$\begin{aligned} \ell_{\text{KLIEP}}(\boldsymbol{\theta}) &= \ell_{\text{KLIEP}}(\boldsymbol{\theta}; \mathbf{x}^{(1)}, \dots, \mathbf{x}^{(n_x)}, \mathbf{y}^{(1)}, \dots, \mathbf{y}^{(n_y)}) \\ &= -\frac{1}{n_x} \sum_{i=1}^{n_x} \boldsymbol{\theta}^\top \boldsymbol{\psi}(\mathbf{x}^{(i)}) + \log \left\{ \frac{1}{n_y} \sum_{j=1}^{n_y} \exp(\boldsymbol{\theta}^\top \boldsymbol{\psi}(\mathbf{y}^{(j)})) \right\}. \end{aligned} \quad (3)$$

Minimizing ℓ_{KLIEP} yields the KLIEP estimate $\hat{\boldsymbol{\theta}}_{\text{KLIEP}} = \arg \min_{\boldsymbol{\theta}} \ell_{\text{KLIEP}}(\boldsymbol{\theta})$ as a direct estimate of the differential network $\boldsymbol{\theta}^*$. ℓ_{KLIEP} is convex in $\boldsymbol{\theta}$, and when it is strictly convex — which requires $n_y > p$ — the KLIEP estimate $\hat{\boldsymbol{\theta}}_{\text{KLIEP}}$ is known to be approximately normal and unbiased (Sugiyama et al., 2012, Chapter 13).

In the high-dimensional setting with $n_y \leq p$, the minimizer of ℓ_{KLIEP} is no longer unique, and regularization becomes necessary for consistent estimation. In this setting, Liu et al. (2017) and Fazayeli and Banerjee (2016) proposed regularized versions of KLIEP using norm penalties. In particular, Liu et al. (2017) proposed the *sparse KLIEP*

$$\check{\boldsymbol{\theta}} = \check{\boldsymbol{\theta}}(\lambda) = \arg \min_{\boldsymbol{\theta}} \ell_{\text{KLIEP}}(\boldsymbol{\theta}; \mathbf{x}^{(1)}, \dots, \mathbf{x}^{(n_x)}, \mathbf{y}^{(1)}, \dots, \mathbf{y}^{(n_y)}) + \lambda \|\boldsymbol{\theta}\|_1, \quad (4)$$

where $\lambda > 0$ is a regularization parameter to be chosen by the user. They show that when $\boldsymbol{\theta}^*$ is sparse, the support of $\check{\boldsymbol{\theta}}$ consistently recovers the support of $\boldsymbol{\theta}^*$ for suitable choices of λ . However, such results typically require additional conditions, e.g., a lower bound on the minimal signal strength and incoherence of the Hessian, which may be restrictive for many real data applications. Furthermore, these are essentially results about the accuracy of the point estimates, whereas to construct confidence intervals or conduct hypothesis tests, one needs information about the distribution of the estimators. This is difficult for regularized estimators, as we shall see next.

2.3 De-biasing

Challenges arise when a regularized estimator $\check{\boldsymbol{\theta}}$, e.g., the sparse KLIEP estimator (4), is used for statistical inference. Regularization produces a non-negligible bias, and the distribution of the resulting estimator is typically intractable (see Ning and Liu, 2017, and references therein).

We propose to deal with this issue by de-biasing each component of $\check{\boldsymbol{\theta}}$. For convenience, adopt a linear indexing so that $\boldsymbol{\gamma} = (\gamma_k)_{k=1}^p$ and $\boldsymbol{\psi} = (\psi_k)_{k=1}^p$, where p is the total number of parameters. Suppose we wish to obtain a de-biased estimate of θ_k^* for some $k \in [p]$. Let $\boldsymbol{\theta}_{k^c}^* = \boldsymbol{\theta}_{[p] \setminus \{k\}}^* \in \mathbb{R}^{p-1}$ denote the vector of remaining $p-1$ parameters. This is the nuisance parameter for carrying out statistical inference for θ_k^* . Abusing the notation somewhat, we write the resulting partition as $\boldsymbol{\theta} = (\theta_k, \boldsymbol{\theta}_{k^c})$. Define $\boldsymbol{\omega}_k^*$ as the vector satisfying $\mathbb{E}[\nabla^2 \ell_{\text{KLIEP}}(\boldsymbol{\theta}^*)] \boldsymbol{\omega}_k^* = \mathbf{e}_k$, and let $\check{\boldsymbol{\omega}}_k$ be a consistent estimator of $\boldsymbol{\omega}_k^*$.

Our method offers two options for constructing an approximately normal and unbiased estimator $\hat{\theta}_k$ of θ_k^* that are asymptotically equivalent (Chernozhukov et al., 2015b). The first option is to use the *one-step* estimator (van der Vaart, 1998; Zhang and Zhang, 2013; van de Geer et al., 2014):

$$\hat{\theta}_k^{1+} = \check{\theta}_k - \check{\boldsymbol{\omega}}_k^\top \nabla \ell_{\text{KLIEP}}(\check{\boldsymbol{\theta}}). \quad (5)$$

This approximately solves a modified score equation $\check{\boldsymbol{\omega}}_k^\top \nabla \ell_{\text{KLIEP}}(\theta_k, \check{\boldsymbol{\theta}}_{k^c}) = 0$, where $\check{\boldsymbol{\theta}}_{k^c}$ is defined via $\check{\boldsymbol{\theta}} = (\theta_k, \check{\boldsymbol{\theta}}_{k^c})$, by taking one Newton iteration starting from θ_k . In Section 4.2, we prove that the one-step estimator $\hat{\theta}_k^{1+}$ is an approximately normal and unbiased estimator of θ_k^* .

When $\check{\boldsymbol{\theta}}$ and $\check{\boldsymbol{\omega}}_k$ are both sparse vectors, de-biasing may be carried out via the so-called *double selection* (Chernozhukov et al., 2015b). Let $\tilde{\boldsymbol{\theta}}$ be the estimate obtained by re-fitting to the union of the supports of $\check{\boldsymbol{\theta}}$ and $\check{\boldsymbol{\omega}}_k$, i.e.,

$$\tilde{\boldsymbol{\theta}} = \arg \min_{\boldsymbol{\theta}} \ell_{\text{KLIEP}}(\boldsymbol{\theta}) \quad \text{subject to} \quad \text{supp}(\boldsymbol{\theta}) \subseteq \{k\} \cup \text{supp}(\check{\boldsymbol{\theta}}) \cup \text{supp}(\check{\boldsymbol{\omega}}_k). \quad (6)$$

Then, the double-selection estimator $\hat{\theta}_k^{2+}$ is defined as the k th component of $\tilde{\boldsymbol{\theta}}$. Intuitively, by including the estimated supports of both $\boldsymbol{\theta}^*$ and $\boldsymbol{\omega}_k^*$, the double selection procedure achieves robustness to errors from

either model selection procedure. Provided that $\tilde{\theta}$ is as accurate as $\check{\theta}$ — which would be the case for sparse or approximately sparse θ^* and ω_k^* — $\tilde{\theta}_k^{2+}$ is asymptotically equivalent to $\hat{\theta}_k^{1+}$.

For a derivation of (5) in the context of KLIEP, see Appendix B.1. A general discussion of the relationship of one-step estimation and double selection may be found in Chernozhukov et al. (2015b).

3 Methodology

We propose a procedure for constructing an approximately normal and unbiased estimator of the differential network (Section 3.1). We then give two bootstrap sketching procedures for estimating the quantiles of a max-type statistic based on the estimator from Section 3.1, and show how they can be used for simultaneous inference (Section 3.2).

3.1 Sparse Kullback-Leibler Importance Estimation With de-biasing (SparKLIE+)

We present Procedure 1, which is a general recipe for de-biasing regularized KLIEP estimates for each θ_k^* in $k \in \mathcal{I}$, where $\mathcal{I} \subseteq [p]$ is the set of indices for the parameters of inferential interest. The procedure uses a general norm penalty for regularization.

Procedure 1. Kullback-Leibler Importance Estimation With de-biasing (KLIE+)

Input: Data $\mathbf{X}_{n_x} = \{\mathbf{x}^{(i)}\}_{i=1}^{n_x}$, $\mathbf{Y}_{n_y} = \{\mathbf{y}^{(j)}\}_{j=1}^{n_y}$, positive regularization parameters $\lambda_\theta, \lambda_k$, $k \in \mathcal{I}$

Output: De-biased estimates $\hat{\theta}_k$, $k \in \mathcal{I}$

Step 1. Find an initial estimate of θ^*

$$\check{\theta} = \arg \min_{\theta} \ell_{\text{KLIEP}}(\theta; \mathbf{X}_{n_x}, \mathbf{Y}_{n_y}) + \lambda_\theta \|\theta\|. \quad (7)$$

for $k \in \mathcal{I}$ **do**

Step 2. Find an initial estimate of ω_k^*

$$\check{\omega}_k = \arg \min_{\omega} \frac{1}{2} \omega^\top \nabla^2 \ell_{\text{KLIEP}}(\check{\theta}) \omega - \omega^\top \mathbf{e}_k + \lambda_k \|\omega\|. \quad (8)$$

Step 3. De-bias, either by (5) or by (6), to obtain $\hat{\theta}_k$.

end for

return $\hat{\theta}_k$, $k \in \mathcal{I}$

A general Gaussian approximation bound for Procedure 1 will be given below in Theorem 1 in Section 4.2. The result is valid as long as the initial estimators from (7) and (8) are sufficiently accurate. For example, this is the case for sparse or approximately sparse θ^* and ω_k^* when the ℓ_1 -penalty is used (Lemmas 2 and 3 in Appendix C.3). We call this procedure Sparse Kullback-Leibler Importance Estimation with de-biasing (SparKLIE+), with SparKLIE+1 referring to SparKLIE+ that uses one-step (5) for de-biasing and SparKLIE+2 referring to the double selection (6) option.

Remark 1 (Alternative procedures for initial estimation). It is possible to use other procedures for either of the initial estimation steps as long as the errors satisfy $\|\check{\theta} - \theta^*\| \cdot \|\check{\omega}_k - \omega_k^*\| = o_{\mathbb{P}}(n^{-1/2})$. We give examples in the case of the ℓ_1 -penalty. In Appendix G.1, we detail an autoscaling procedure for each step that allows the regularization parameter to be chosen in a data-independent way while yielding consistent estimation. We may also re-fit the model on the estimated support (Belloni and Chernozhukov, 2013). Finally, it is also possible to use a constrained procedure, similar to the method of Ning and Liu (2017), where instead of (8), one solves

$$\min \|\omega\|_1 \quad \text{subject to} \quad \|\nabla^2 \ell_{\text{KLIEP}}(\check{\theta}) \omega - \mathbf{e}_k\|_\infty \leq \lambda_k.$$

Remark 2 (Regularization parameters). Procedure 1 assumes that the user has already picked out the regularization parameters $\lambda_\theta, \lambda_k, k \in \mathcal{I}$. However, the optimal choice, as dictated by Lemmas 8 and 9 in Appendix E.1, depends on constants related to the regularity of the density ratio, which are typically unknown. In Appendix I.3, we empirically study the sensitivity of Procedure 1 to the choice of regularization parameters and find that the performance is robust across a wide range of regularization levels. Furthermore, in Appendix G.1, we further provide alternative procedures for Steps 1 and 2 that allows for problem-independent choices of penalty levels. This is the version of Procedure 1 we use in Sections 5 and 6.

3.1.1 Variance of the SparKLIE+ estimator

For statistical inference, we also need a consistent estimator of the variance of $\sqrt{n}\hat{\theta}_k$, $n = n_x + n_y$. Define the *empirical density ratio estimate*

$$\hat{r}_\theta(\mathbf{y}) = \exp(\boldsymbol{\theta}^\top \boldsymbol{\psi}(\mathbf{y})) / \hat{Z}_y(\boldsymbol{\theta}), \quad \text{where} \quad \hat{Z}_y(\boldsymbol{\theta}) = \frac{1}{n_y} \sum_{j=1}^{n_y} \exp(\boldsymbol{\theta}^\top \boldsymbol{\psi}(\mathbf{y}^{(j)})). \quad (9)$$

Let $\hat{\mathbf{S}}_\psi$ and $\hat{\mathbf{S}}_{\psi\hat{r}}(\check{\boldsymbol{\theta}})$ be the sample covariance matrices of $\{\boldsymbol{\psi}(\mathbf{x}^{(i)})\}_{i=1}^{n_x}$ and $\{\boldsymbol{\psi}(\mathbf{y}^{(j)})\hat{r}_\theta(\mathbf{y}^{(j)})\}_{j=1}^{n_y}$, i.e.,

$$\begin{aligned} \hat{\mathbf{S}}_\psi &= \frac{1}{n_x} \sum_{i=1}^{n_x} \boldsymbol{\psi}(\mathbf{x}^{(i)})\boldsymbol{\psi}(\mathbf{x}^{(i)})^\top - \overline{\boldsymbol{\psi}}\overline{\boldsymbol{\psi}}^\top, \\ \hat{\mathbf{S}}_{\psi\hat{r}}(\boldsymbol{\theta}) &= \frac{1}{n_y} \sum_{j=1}^{n_y} \hat{r}_\theta^2(\mathbf{y}^{(j)})\boldsymbol{\psi}(\mathbf{y}^{(j)})\boldsymbol{\psi}(\mathbf{y}^{(j)})^\top - \hat{\boldsymbol{\mu}}(\boldsymbol{\theta})\hat{\boldsymbol{\mu}}(\boldsymbol{\theta})^\top, \end{aligned}$$

where

$$\overline{\boldsymbol{\psi}} = \frac{1}{n_x} \sum_{i=1}^{n_x} \boldsymbol{\psi}(\mathbf{x}^{(i)}), \quad \hat{\boldsymbol{\mu}}(\boldsymbol{\theta}) = \frac{1}{n_y} \sum_{j=1}^{n_y} \boldsymbol{\psi}(\mathbf{y}^{(j)})\hat{r}_\theta(\mathbf{y}^{(j)}). \quad (10)$$

Let $\hat{\mathbf{S}}_{\text{pooled}}(\check{\boldsymbol{\theta}})$ be the pooled covariance

$$\hat{\mathbf{S}}_{\text{pooled}}(\check{\boldsymbol{\theta}}) = \frac{n}{n_x} \hat{\mathbf{S}}_\psi + \frac{n}{n_y} \hat{\mathbf{S}}_{\psi\hat{r}}(\check{\boldsymbol{\theta}}).$$

Finally, a consistent estimator of the variance of $\sqrt{n}\hat{\theta}_k$ is

$$\hat{\sigma}_k^2 = \check{\boldsymbol{\omega}}_k^\top \hat{\mathbf{S}}_{\text{pooled}}(\check{\boldsymbol{\theta}}) \check{\boldsymbol{\omega}}_k. \quad (11)$$

This estimates the variance of $\sqrt{n}\boldsymbol{\omega}_k^{*\top} \nabla \ell_{\text{KLIEP}}(\boldsymbol{\theta}^*)$, which we show is asymptotically equivalent to $\sqrt{n}(\hat{\theta}_k - \theta_k^*)$ in the proof of Theorem 1 in Appendix B.2. By Lemma 19 in Appendix F.2, $\hat{\sigma}_k^2$ is consistent if both $\check{\boldsymbol{\theta}}$ and $\check{\boldsymbol{\omega}}_k$ are.

Theorem 2 in Section 4.2 implies that if $z_q = \Phi^{-1}(q)$ is the q -quantile of a standard Gaussian, then $\mathbb{P}\{\sqrt{n}(\hat{\theta}_k - \theta_k^*)/\hat{\sigma}_k \leq z_q\} \approx \Phi^{-1}(z_q) = q$. Thus, $\hat{\theta}_k \pm z_{1-\alpha/2} \times \hat{\sigma}_k/\sqrt{n}$ is an asymptotically valid $100 \times (1-\alpha)\%$ confidence interval (CI) for θ_k^* . Similarly, the test that rejects for $\sqrt{n}|\hat{\theta}_k - \theta_{0k}|/\hat{\sigma}_k > z_{1-\alpha/2}$ is asymptotically level- α for the one-dimensional null hypothesis $\mathcal{H}_{0k} : \theta_k^* = \theta_{0k}$. In Section 5, we verify with simulations that the approximations are fairly accurate and robust even at small sample sizes.

3.2 High-dimensional inference via bootstrap sketched quantiles

In Section 3.1, we proposed SparKLIE+, a procedure for obtaining an asymptotically unbiased estimator of a component of the differential network. Iterating Step 3 of SparKLIE+ over all edges yields an unbiased estimator $\hat{\boldsymbol{\theta}}$ of the differential network $\boldsymbol{\theta}^*$. To make inferences about the structure of $\boldsymbol{\theta}^*$ using $\hat{\boldsymbol{\theta}}$, one may construct a simultaneous confidence region or conduct a simultaneous hypothesis test. This raises issues of multiple comparisons.

We deal with this problem by a bootstrap approximation of the quantiles of the following statistic

$$T = T_{n_x, n_y} = \max_{k=1, \dots, p} \sqrt{n} |\hat{\theta}_k - \theta_k^*|, \quad \text{where } n = n_x + n_y. \quad (12)$$

Let $c_{T,q}$ be the q -quantile of T . Then, it is easy to verify that $\hat{\boldsymbol{\theta}} \pm c_{T,1-\alpha}/\sqrt{n}$ is a $100 \times (1 - \alpha)\%$ confidence region for $\boldsymbol{\theta}^*$. Similarly, the test that rejects if $\max_k |\hat{\theta}_k| > c_{T,1-\alpha}/\sqrt{n}$ controls the family-wise error rate at level α for the null hypothesis $H_0 : \theta_k^* = 0$ for all $k \in [p]$. This approach has the advantage of adapting to the correlations among $\hat{\theta}_k$'s. Thus, given $c_{T,q}$ — or an accurate estimator thereof — we can learn the differential network structure while controlling the type I error rate.

However, in high-dimensions, it is itself a highly nontrivial problem to estimate $c_{T,q}$ with sufficient accuracy (see Chernozhukov et al., 2013, 2017; Deng and Zhang, 2020, and references therein). In this section, we present two bootstrap-based methods for estimating $c_{T,q}$.

Our first proposal employs the Gaussian multiplier bootstrap. Recall the definitions of \hat{r}_θ from (9), and of $\bar{\boldsymbol{\psi}}$ and $\hat{\boldsymbol{\mu}}(\boldsymbol{\theta})$ from (10).

Procedure 2. Gaussian multiplier bootstrap sketching for estimating quantiles of T

Input: Data $\mathbf{X}_{n_x} = \{\mathbf{x}^{(i)}\}_{i=1}^{n_x}$, $\mathbf{Y}_{n_y} = \{\mathbf{y}^{(j)}\}_{j=1}^{n_y}$; the outputs $\check{\boldsymbol{\theta}}$ and $\check{\boldsymbol{\omega}}_k$, $k \in \mathcal{I}$, of (7) and (8) from Procedure 1

Output: A Gaussian bootstrap estimate $\hat{c}_{T,q}$ of $c_{T,q}$

for $b = 1, \dots, n_b$ **do**

Draw Gaussian weights $\xi_x^{(b,1)}, \dots, \xi_x^{(b,n_x)}, \xi_y^{(b,1)}, \dots, \xi_y^{(b,n_y)} \stackrel{iid}{\sim} \mathcal{N}(0, 1)$.

Compute

$$\hat{T}^{(b)} = \max_k \sqrt{n} \left| \left\langle \check{\boldsymbol{\omega}}_k, \frac{1}{n_x} \sum_{i=1}^{n_x} (\boldsymbol{\psi}(\mathbf{x}^{(i)}) - \bar{\boldsymbol{\psi}}) \xi_x^{(b,i)} - \frac{1}{n_y} \sum_{j=1}^{n_y} (\boldsymbol{\psi}(\mathbf{y}^{(j)}) \hat{r}_{\check{\boldsymbol{\theta}}}(\mathbf{y}^{(j)}) - \hat{\boldsymbol{\mu}}(\check{\boldsymbol{\theta}})) \xi_y^{(b,j)} \right\rangle \right|. \quad (13)$$

end for

return $\hat{c}_{T,q}$, the q sample quantile of $\{\hat{T}^{(b)} : b = 1, \dots, n_b\}$.

Procedure 2 may be procedure for estimating the $(1 - \alpha)$ -quantile of the maximum of $|\mathcal{N}(\mathbf{0}, \hat{\boldsymbol{\Sigma}})|$, where $\hat{\boldsymbol{\Sigma}} = \check{\boldsymbol{\Omega}}^\top \hat{\mathbf{S}}_{\text{pooled}} \check{\boldsymbol{\Omega}}$, $\check{\boldsymbol{\Omega}} = [\check{\boldsymbol{\omega}}_k]_{k=1}^p$, and $\hat{\mathbf{S}}_{\text{pooled}}$ is defined in (11). Since we can show that $\hat{\boldsymbol{\theta}} - \boldsymbol{\theta}^* \approx \mathcal{N}(\mathbf{0}, \boldsymbol{\Sigma}^*)$ for some fixed $\boldsymbol{\Sigma}^*$ and, moreover, $\hat{\boldsymbol{\Sigma}} \approx \boldsymbol{\Sigma}^*$, we claim that $\hat{c}_{T,q}$ is a good estimate of the q -quantile of T . This intuition is formally stated in Theorem 3 in Section 4.3.

Although Procedure 2 is accurate for sufficiently large sample sizes, at smaller values of n_x and n_y , empirical bootstrap tends to yield more robust estimates of the quantiles. The procedure below, based on the empirical bootstrap, is what we recommend in practice.

Procedure 3. Empirical bootstrap sketching for estimating quantiles of T

Input: Data $\mathbf{X}_{n_x} = \{\mathbf{x}^{(i)}\}_{i=1}^{n_x}$, $\mathbf{Y}_{n_y} = \{\mathbf{y}^{(j)}\}_{j=1}^{n_y}$; the outputs $\check{\boldsymbol{\theta}}$ and $\check{\boldsymbol{\omega}}_k$, $k \in \mathcal{I}$, of (7) and (8) from Procedure 1

Output: An empirical bootstrap estimate $\hat{c}_{T,q}$ of $c_{T,q}$

for $b = 1, \dots, n_b$ **do**

Re-sample $\mathbf{X}_{n_x}^{(b)} = \{\mathbf{x}^{(b,1)}, \dots, \mathbf{x}^{(b,n_x)}\}$ and $\mathbf{Y}_{n_y}^{(b)} = \{\mathbf{y}^{(b,1)}, \dots, \mathbf{y}^{(b,n_y)}\}$ uniformly at random with replacement.

for $k \in \mathcal{I}$ **do**

For replicating SparkLIE+1 estimate (5), $\hat{\theta}_k^{(b)} = \check{\theta}_k - \check{\boldsymbol{\omega}}_k^\top \nabla \ell_{\text{KLIEP}}(\check{\boldsymbol{\theta}}; \mathbf{X}_{n_x}^{(b)}, \mathbf{Y}_{n_y}^{(b)})$.

For replicating SparKLIE+2 estimate (6), $\hat{\theta}_k^{(b)}$, the k th component of

$$\arg \min_{\theta} \ell_{\text{KLIEP}}(\theta; \mathbf{X}_{n_x}^{(b)}, \mathbf{Y}_{n_y}^{(b)}) \text{ subject to } \text{supp}(\theta) \subseteq \{k\} \cup \text{supp}(\check{\theta}) \cup \text{supp}(\check{\omega}_k).$$

end for
Compute

$$\hat{T}^{(b)} = \max_k \sqrt{n} |\hat{\theta}_k^{(b)} - \hat{\theta}_k|. \quad (14)$$

end for

return $\hat{c}_{T,q}$, the q sample quantile of $\{\hat{T}^{(b)} : b = 1, \dots, n_b\}$.

Note that only Step 3 of Procedure 1 is repeated in Procedure 3. This is akin to the use of $\check{\theta}$ and $\check{\omega}_k$, $k \in \mathcal{I}$, in Procedure 2.

We give a heuristic argument in support of Procedure 3, leaving the formal proof to future work. For the sake of argument, consider the infeasible estimator $\hat{\theta}_k^{1*} = \theta_k^* - \omega_k^{*\top} \nabla \ell_{\text{KLIEP}}(\theta^*)$ or $\hat{\theta}_k^{2*}$, the k th component of $\arg \min_{\theta} \nabla \ell_{\text{KLIEP}}(\theta)$ subject to $\text{supp}(\theta) \subseteq \{k\} \cup \text{supp}(\theta^*) \cup \text{supp}(\omega_k^*)$. In other words, $\hat{\theta}_k^{1*}$ or $\hat{\theta}_k^{2*}$ is the result of applying (5) or (6), but with the true parameters θ^* and ω_k^* replacing the initial estimates $\check{\theta}$ and $\check{\omega}_k$. It is easy to see that both $\hat{\theta}_k^{1*}$ and $\hat{\theta}_k^{2*}$ are approximately normal and unbiased estimators, and that making the same replacement in Procedure 3 would yield bootstrap replicates of $\hat{\theta}_k^{1*}$ and $\hat{\theta}_k^{2*}$. Because $\check{\theta}$ and $\check{\omega}_k$ are consistent estimators, we expect Procedure 3 to be approximately valid for bootstrapping the SparKLIE+ estimator $\hat{\theta}_k^{1+}$ or $\hat{\theta}_k^{2+}$. This intuition is verified in simulations in Section 5.2.

4 Theory

In this section, we establish statistical validity of the inference procedures discussed in Section 3.1 and Section 3.2 under two model assumptions introduced in Section 4.1.

4.1 Assumptions

We discuss two sufficient conditions that imply the accuracy of Gaussian approximation. The first is about the regularity of the density ratio $r_{\theta}(\mathbf{y})$.

Condition 1 (bounded density ratio model). There exist $\varrho > 0$ such that

$$M_r^{-1} \leq r_{\theta}(\mathbf{y}) \leq M_r \text{ a.s. for all } \theta \text{ with } \|\theta - \theta^*\| \leq \varrho$$

for some $M_r = M_r(\varrho) \geq 1$.

For convenience, we fix $\varrho = \|\theta^*\|$. Proposition 1 says that Condition 1 is equivalent to a boundedness condition on the sufficient statistics, a claim that was stated without proof for ℓ_2 -norm in Liu et al. (2017). We generalize the statement, and prove it in Appendix D.1.

Proposition 1 (bounded sufficient statistics). *Condition 1 is satisfied if and only if $\|\psi(\mathbf{x})\|_* \leq M_{\psi}$ a.s. for some $M_{\psi} < \infty$.*

In general, regularity conditions on the density ratio tend to induce even stronger regularity conditions on the sufficient statistics. The identity $\hat{Z}_y(\theta)/Z_y(\theta) \equiv n_y^{-1} \sum_{j=1}^{n_y} r_{\theta}(\mathbf{y}^{(j)})$ implies $\hat{Z}_y(\theta)/Z_y(\theta) \in [M_r^{-1}, M_r]$. Moreover, $\hat{r}_{\theta}(\mathbf{y}) \equiv (\hat{Z}_y(\theta)/Z_y(\theta))r_{\theta}(\mathbf{y})$, so that

$$M_r^{-2} \leq M_r^{-1} (1 - o_{\mathbb{P}}(1)) \leq \hat{r}_{\theta}(\mathbf{y}) \leq M_r (1 + o_{\mathbb{P}}(1)) \leq M_r^2.$$

The outer bounds are obvious. The inner bounds require a concentration result (Lemma 6 in Appendix D.1).

When Procedure 1 is implemented with the ℓ_1 -penalty, it is natural to impose Condition 1 with the ℓ_1 -norm, which by Proposition 1 is equivalent to imposing an ℓ_{∞} -bound on the sufficient statistics. Thus,

this choice of penalty works nicely with models that take values on a bounded domain, such as Ising models, Potts models, or truncated Gaussians with bounded support. Indeed, for the Ising model defined in Example 1, $\|\boldsymbol{\psi}(\mathbf{x})\|_\infty = 1$ but $\|\boldsymbol{\psi}(\mathbf{x})\|_2^2 = p$.

The second are regularity conditions on the population covariances of $\boldsymbol{\psi}(\mathbf{x})$ under f_x and f_y , as well as that of $(\boldsymbol{\psi}(\mathbf{y}) - \boldsymbol{\mu}_\psi)r_{\theta^*}(\mathbf{y})$ under f_y . Recall $\boldsymbol{\Sigma}_\psi = \text{Cov}_x[\boldsymbol{\psi}(\mathbf{x})]$, and let $\boldsymbol{\Sigma}_{\psi r} = \text{Cov}_y[(\boldsymbol{\psi}(\mathbf{y}) - \boldsymbol{\mu}_\psi)r_{\theta^*}(\mathbf{y})]$, where $\boldsymbol{\mu}_\psi = \mathbb{E}_x[\boldsymbol{\psi}(\mathbf{x})] = \mathbb{E}_y[\boldsymbol{\psi}(\mathbf{y})r_{\theta^*}(\mathbf{y})]$.

Condition 2 (bounded population eigenvalues). There exist $0 < \underline{\kappa} \leq \bar{\kappa} < \infty$ such that

$$\begin{aligned} \underline{\kappa} &\leq \min_{\|\mathbf{v}\|=1, \mathbf{v} \neq \mathbf{0}} \mathbf{v}^\top \boldsymbol{\Sigma}_\psi \mathbf{v} \leq \max_{\|\mathbf{v}\|=1, \mathbf{v} \neq \mathbf{0}} \mathbf{v}^\top \boldsymbol{\Sigma}_\psi \mathbf{v} \leq \bar{\kappa}, \\ \underline{\kappa} &\leq \min_{\|\mathbf{v}\|=1, \mathbf{v} \neq \mathbf{0}} \mathbf{v}^\top \boldsymbol{\Sigma}_{\psi r} \mathbf{v} \leq \max_{\|\mathbf{v}\|=1, \mathbf{v} \neq \mathbf{0}} \mathbf{v}^\top \boldsymbol{\Sigma}_{\psi r} \mathbf{v} \leq \bar{\kappa}. \end{aligned}$$

Condition 2 is a natural one, and ensures that the problem is well behaved (Liu et al., 2017). A lower bound on the minimum eigenvalues ensures that the model is non-degenerate. The upper bound ensures that ℓ_{KLIEP} (3) is smooth, and can be regarded as analogous to the assumption on the log-normalizing function in Yang et al. (2015). These bounds will naturally appear in bounding the convergence of $\nabla^2 \ell_{\text{KLIEP}}(\boldsymbol{\theta})$ to $\boldsymbol{\Sigma}_\psi$, as well as in bounding the variance of the estimator σ_k^2 .

Conditions imposed here are weaker than those in Liu et al. (2017), as we do not hope to correctly identify the support of the parameter $\boldsymbol{\theta}^*$. In particular, we do not need to assume the incoherence condition, nor do we need to require that the nonzero components of $\boldsymbol{\theta}^*$ be large enough.

Recall $\boldsymbol{\theta}^* = \gamma_x - \gamma_y$ and $\boldsymbol{\omega}_k^* = \boldsymbol{\Sigma}_\psi^{-1} \mathbf{e}_k$ where $\boldsymbol{\Sigma}_\psi = \text{Cov}_x[\boldsymbol{\psi}(\mathbf{x})]$ and $k \in [p]$. To facilitate the discussion of rates in the next two sections, we introduce additional notations. Let $n = n_x + n_y$. We view $n_x, n_y, p, s_\theta = s_{\theta, q_\theta} = \|\boldsymbol{\theta}^*\|_{q_\theta}, s_k = s_{k, q_k} = \|\boldsymbol{\omega}_k^*\|_{q_k}$ as sequences indexed by n and possibly diverging to ∞ . n_x and n_y are characterized by sequences $\eta_{x,n}$ and $\eta_{y,n}$ in $(0, 1)$ such that $\eta_{x,n} + \eta_{y,n} \equiv 1, n_x = n_{x,n} = \eta_{x,n}n$ and $n_y = n_{y,n} = \eta_{y,n}n$. In particular, this implies that $n \asymp n_x \asymp n_y$.

The bounds we give below are finite-sample in the sense that they are given as functions of n, p, s_θ, s_k . They can be used to study the asymptotic behavior as $n \rightarrow \infty$ by considering a sequence of models $(\boldsymbol{\theta}^*, \boldsymbol{\Sigma}_\psi) = (\boldsymbol{\theta}_n^*, \boldsymbol{\Sigma}_{\psi,n})$ such that the induced sequence of p, s_θ, s_k , etc. satisfy the side conditions of each theorem.

4.2 Finite-sample Gaussian approximation result for the SparkLIE+1

Theorem 1 gives a family of Gaussian approximation bounds for Procedure 1.

Let $k \in [p]$. Let $\hat{\boldsymbol{\theta}}$ and $\hat{\boldsymbol{\omega}}_k$ denote the outputs of Steps 1 and 2 of Procedure 1. For $\lambda_\theta, \lambda_k, \delta_\theta, \delta_k, \delta_\sigma \in [0, 1)$, define an event

$$\mathcal{E}_{\text{one}} = \mathcal{E}_{\text{one}}(\lambda_\theta, \lambda_k, \delta_\theta, \delta_k, \delta_\sigma) = \left\{ \begin{array}{ll} \text{(G.1)} & 2\|\nabla \ell_{\text{KLIEP}}(\boldsymbol{\theta}^*)\|_* \leq \lambda_\theta, \quad \text{(G.2)} & 2\|\nabla^2 \ell_{\text{KLIEP}}(\boldsymbol{\theta}^*)\boldsymbol{\omega}_k^* - \mathbf{e}_k\|_* \leq \lambda_k, \\ \text{(E.1)} & \|\hat{\boldsymbol{\theta}} - \boldsymbol{\theta}^*\| \leq \delta_\theta, \quad \text{(E.2)} & \|\hat{\boldsymbol{\omega}}_k - \boldsymbol{\omega}_k^*\| \leq \delta_k, \\ \text{(B.1)} & \left|1 - \frac{\hat{Z}_y(\boldsymbol{\theta}^*)}{Z_y(\boldsymbol{\theta}^*)}\right| \lesssim \lambda_\theta, \quad \text{(B.2)} & \left|\frac{1}{n_y} \sum_{j=1}^{n_y} \langle \boldsymbol{\omega}_k^*, \boldsymbol{\mu}_\psi - \boldsymbol{\psi}(\mathbf{y}^{(j)}) \rangle r_{\theta^*}(\mathbf{y}^{(j)})\right| \lesssim \lambda_k, \\ \text{(V.1)} & 4\|\hat{\boldsymbol{\Sigma}}_\psi - \boldsymbol{\Sigma}_\psi\|_* \leq \delta_\sigma, \quad \text{(V.2)} & 4\|\hat{\boldsymbol{\Sigma}}_{\psi r}(\boldsymbol{\theta}^*) - \boldsymbol{\Sigma}_{\psi r}\|_* \leq \delta_\sigma \end{array} \right\}.$$

Theorem 1. Assume Conditions 1 and 2. Let $\hat{\theta}_k$ be the estimator constructed by Procedure 1 with one-step approximation as

$$\hat{\theta}_k = \hat{\theta}_k - \hat{\boldsymbol{\omega}}_k^\top \nabla \ell_{\text{KLIEP}}(\hat{\boldsymbol{\theta}}).$$

Suppose $\mathbb{P}(\mathcal{E}_{\text{one}}) \geq 1 - \varepsilon_{\text{one},n}$ for some $\lambda_\theta, \lambda_k, \delta_\theta, \delta_k, \delta_\sigma \in [0, 1)$. Then,

$$\sup_{t \in \mathbb{R}} \left| \mathbb{P} \left\{ \sqrt{n} (\hat{\theta}_k - \theta_k^*) / \hat{\sigma}_k \leq t \right\} - \Phi(t) \right| \leq \Delta_1 + \Delta_2 + \Delta_3 + \varepsilon_{\text{one},n},$$

where

$$\begin{aligned} \Delta_1 &\lesssim \sqrt{\frac{\bar{\kappa}^2 / \underline{\kappa}}{\eta_{x,n} \eta_{y,n}}} \frac{\|\boldsymbol{\omega}_k^*\|}{\sqrt{n}}, \quad \Delta_2 \lesssim \sqrt{\frac{\eta_{x,n} \eta_{y,n}}{\underline{\kappa} / \bar{\kappa}^2}} ((\delta_\theta + \lambda_\theta)(\delta_k + \lambda_k) + \|\boldsymbol{\omega}_k^*\| \delta_\theta^2) \sqrt{n}, \\ \Delta_3 &\lesssim (\bar{\kappa}^2 / \underline{\kappa}) \|\boldsymbol{\omega}_k^*\|^2 (\delta_\sigma + \delta_\theta) + \delta_k^2. \end{aligned}$$

The proof is in Appendix B.2. We highlight some of the main technical difficulties. To prove Theorem 1, we need to find a linear approximation of $\sqrt{n}(\hat{\theta}_k - \theta_k^*)$ that is easy to analyze. This is not so obvious due to nonlinearity of ℓ_{KLIEP} . Our results require a delicate control of the bias that arises from using the empirical density ratio estimates, as we need to make sure that the error terms are vanishing even after \sqrt{n} scaling. This is in contrast to Liu et al. (2017) or Fazayeli and Banerjee (2016) where it sufficed to control the gradient in the dual norm.

Theorem 1 gives a result for a general norm penalty in Procedure 1. When specialized to SparKLIE+1, we have the following result.

Theorem 2. *Assume Condition 1 with the ℓ_1 -norm and Condition 2. Let $\hat{\theta}_k$ be the SparKLIE+1 estimator with tuning parameters*

$$\lambda_\theta \asymp \left(\frac{\log p}{n}\right)^{1/2} \quad \text{and} \quad \lambda_k \asymp s_{k,q_k}^{1/(2-q_k)} \left(\frac{\log p}{n}\right)^{1/2}.$$

Let s be a sequence of integers satisfying $s \geq s_{\theta,0}, s_{k,q_k} \lambda_k^{-q_k}$. Let $\varepsilon_{\text{RSC},n}$ be a sequence in $(0, 1)$ decreasing to 0. Then, subject to additional conditions on n_y and the growth regime detailed in Appendix C.1,

$$\begin{aligned} \sup_{t \in \mathbb{R}} \left| \mathbb{P} \left\{ \sqrt{n}(\hat{\theta}_k - \theta_k^*)/\hat{\sigma}_k \leq t \right\} - \Phi(t) \right| \\ \leq O \left(s_{\theta,0}^{2+\frac{1-2q_k}{2-q_k}} \left(\frac{\log p}{n}\right)^{1-q_k} \sqrt{n} \right) + \varepsilon_{\text{RSC},n} + c \exp(-c' \log p), \end{aligned}$$

where $c, c' > 0$ are constants that do not depend on $n, p, s_{\theta,0}$ or s_{k,q_k} .

The proof in Appendix C.1 relies on numerous technical lemmas to derive the rates of $\check{\theta}$ and $\check{\omega}_k$. In particular, we prove a restricted strong convexity (RSC) of the Hessian starting from a population-level assumption (Condition 2). The proof is quite involved as the Hessian is a weighted sample covariance where the weights are given by the empirical density ratio estimates, which makes application of existing results impossible. The details are in Appendix E.

Remark 3. Theorem 2 gives a nontrivial bound only for sufficiently (weakly) sparse θ^* and ω_k^* . The additional condition on n_y is a consequence of proving RSC from the population-level assumptions. In particular, it is linked to the probability that the Hessian fails to satisfy RSC. Analogous results for other sparsity regimes can be obtained from Theorem 1 as well (see earlier version of this paper on arXiv). Due to space limitations, we have singled out this regime as being arguably the most interesting.

Remark 4. We note that the inverse of the Hessian Σ_ψ^{-1} is determined by γ_x , since $\Sigma_\psi = \text{Cov}_x[\psi(\mathbf{x})]$, and, therefore, the sparsity of Σ_ψ^{-1} is related to that of γ_x . In the case of Gaussian graphical models, we can explicitly characterize Σ_ψ^{-1} and we observe that the rows of the inverse of the Hessian are sparse if the maximum degree of the underlying graph is small. The proof strategy critically relies on the properties of a Gaussian distribution and its log-partition function and is intractable for general Markov random fields. However, we further provide numerical evidence on the relationship between the support of Σ_ψ^{-1} and that of γ_x for Ising models. For our method to perform well, it suffices that the ℓ_q -“norm” is controlled for a small $q \in [0, 1)$, which we numerically verify. See Appendix D.3. Finally, we note that in some cases the rows of Σ_ψ^{-1} are neither sparse nor approximately sparse, but have bounded ℓ_1 norm. In this case, a possible direction for developing a valid inference procedure would be to modify the three step procedure in Ma et al. (2017) or Yu et al. (2020).

Remark 5. As pointed out by a reviewer, there is an inherent asymmetry in KLIEP, and Theorem 2 is one place where this can be observed. Specifically, the quality of Gaussian approximation depends on which set of observations is used as \mathbf{X} and which as \mathbf{Y} . First, r_θ may be more regular than $1/r_\theta$ as measured by the bounds. This affects the magnitude of λ_θ or λ_k . Second, the larger sample will satisfy the sample complexity condition with a smaller $\varepsilon_{\text{RSC},n}$, which is the probability that the Hessian fails to satisfy RSC. For the bounded sufficient statistics model we consider, we have found the latter to have a larger impact on the results. Therefore, we recommend choosing f_x and f_y so that $n_x \leq n_y$. In Section 7, we discuss alternative approaches to differential network estimation that are not asymmetric in nature. These, however, require imposing stronger conditions.

4.3 Finite-sample consistency for Gaussian multiplier bootstrap sketched quantiles

Theorem 3 is a finite-sample consistency result for the Gaussian multiplier bootstrap. Recall $T = \max_k \sqrt{n} |\hat{\theta}_k - \theta_k^*|$, and let $\hat{c}_{T,\alpha}$ denote the estimator of $(1 - \alpha)$ -quantile of T from Procedure 2. Define Σ_{pooled} analogously as in (11), and let $\Omega^* = \Sigma_{\psi}^{-1}$. Recall that the k th column of Ω^* is ω_k^* . For $\lambda_\theta, (\lambda_k)_{k=1}^p, \delta_\theta, (\delta_k)_{k=1}^p \in [0, 1)$, define an event

$$\mathcal{E}_{\text{all}} = \mathcal{E}_{\text{all}}(\lambda_\theta, (\lambda_k)_{k=1}^p, \delta_\theta, (\delta_k)_{k=1}^p) = \left. \begin{array}{ll} \text{(G.1)} & 2\|\nabla \ell_{\text{KLIEP}}(\theta^*)\|_* \leq \lambda_\theta, & \text{(G.2)} & 2\|\nabla^2 \ell_{\text{KLIEP}}(\theta^*)\omega_k^* - \mathbf{e}_k\|_* \leq \lambda_k \quad \forall k, \\ \text{(E.1)} & \|\hat{\theta} - \theta^*\| \leq \delta_\theta, & \text{(E.2)} & \|\check{\omega}_k - \omega_k^*\| \leq \delta_k \quad \forall k, \\ \text{(B.1)} & \left|1 - \frac{\bar{Z}_y(\theta^*)}{Z_y(\theta^*)}\right| \lesssim \lambda_\theta, & \text{(B.2)} & \left|\frac{1}{n_y} \sum_{j=1}^{n_y} \langle \omega_k^*, \mu_\psi - \psi(\mathbf{y}^{(j)}) \rangle r_{\theta^*}(\mathbf{y}^{(j)})\right| \lesssim \lambda_k \quad \forall k \end{array} \right\}.$$

Put $\nu_n = 1 \vee \max\{\|\omega_k^*\| : k = 1, \dots, p\}$, and set

$$B_n = \frac{(1 \vee \bar{\kappa})^3 (1 \vee M_\psi)^3 M_r^3 \nu_n^{21/2}}{\sqrt{\bar{\kappa}^3 \eta_{x,n} \eta_{y,n}}} \quad \text{and} \quad \delta_n = \left(\frac{B_n^2 \log^7(pn)}{n} \right)^{1/6}.$$

Theorem 3. *Assume Conditions 1 and 2. Let $\hat{\theta}$ be the estimator constructed by Procedure 1 with one-step approximation as*

$$\hat{\theta} = \check{\theta} - \check{\Omega}^\top \nabla \ell_{\text{KLIEP}}(\check{\theta}),$$

where $\check{\Omega} = [\check{\omega}_k]_{k=1}^p \in \mathbb{R}^{p \times p}$ is the matrix with the k th column given by $\check{\omega}_k$. Suppose

$$D_1 := \max_k \sqrt{\frac{\eta_{x,n} \eta_{y,n}}{\bar{\kappa}/\bar{\kappa}^2}} \left((\delta_\theta + \lambda_\theta)(\delta_k + \lambda_k) + \|\omega_k^*\| \delta_\theta^2 \right) \sqrt{n} \lesssim \left(\frac{B_n^2 \log^4(pn)}{n} \right)^{1/6},$$

$$D_2 := \max_k \frac{\bar{\kappa}/\bar{\kappa}^2}{\eta_{x,n}^2 \eta_{y,n}^2} \left(\delta_k^2 + \eta_{x,n} \|\omega_k^*\|^2 (\delta_\theta + \lambda_\theta)^2 \right) \lesssim \left(\frac{B_n^2 \log(pn)}{n} \right)^{1/3}.$$

If $\mathbb{P}(\mathcal{E}_{\text{all}}) \geq 1 - \varepsilon_{\text{all},n}$, then

$$\sup_{\alpha \in (0,1)} |\mathbb{P}\{T \leq \hat{c}_{T,\alpha}\} - (1 - \alpha)| = O(\delta_n + \varepsilon_{\text{all},n}) \quad (15)$$

with probability at least $1 - \varepsilon_{\text{all},n} - n^{-1}$.

The proof is in Appendix B.3. The bulk of hard work was done in establishing a linear approximation to $\sqrt{n}(\hat{\theta}_k - \theta_k^*)$ in the proof of Theorem 1. Theorem 3 follows by showing that the error in the linear approximation can be controlled, allowing for application of results in Belloni et al. (2018). Due to the nonlinearity of ℓ_{KLIEP} (3) and the fact that we are using a two sample estimator, the detailed calculations are rather complicated.

As an application of Theorem 3, we evaluate the bound in (15) in the case of SparKLIE+1 with $s_\theta = s_{\theta,0} = \|\theta^*\|_0$ and $s_k = s_{k,0} = \|\omega_k^*\|_0$.

Theorem 4. *Assume Condition 1 with ℓ_1 -norm and Condition 2. Suppose $T = \max_k \sqrt{n} |\hat{\theta}_k - \theta_k^*|$, where $\hat{\theta}$ is the SparKLIE+1 estimator with tuning parameters*

$$\lambda_\theta \asymp \left(\frac{\log p}{n} \right)^{1/2} \quad \text{and} \quad \lambda_k \asymp \left(\frac{s_{k,0} \log p}{n} \right)^{1/2}, \quad k = 1, \dots, p.$$

Let s be a sequence of integers satisfying $s \geq s_{\theta,0}, s_{k,0}$, $k = 1, \dots, p$. Let $\varepsilon_{\text{RSC},n}$ be a sequence in $(0, 1)$ decreasing to 0. Then, subject to an additional condition on n_y detailed in Appendix C.2,

$$\sup_{\alpha \in (0,1)} |\mathbb{P}\{T \leq \hat{c}_{T,\alpha}\} - (1 - \alpha)| = O(\delta_n + \varepsilon_{\text{RSC},n} + c \exp(-c' \log p))$$

with probability at least $1 - \varepsilon_{\text{RSC},n} - c \exp(-c' \log p) - n^{-1}$, where $c, c' > 0$ are constants that do not depend on $n, p, s_{\theta,0}$ or $s_{k,0}$.

Table 1: Empirical coverage of the 95% CI $\hat{\theta}_k \pm z_{0.975}\hat{\sigma}_k/\sqrt{n}$, where k is a fixed edge of interest and $z_{0.975}$ is the 0.975-quantile of $\mathcal{N}(0, 1)$, of SparKLIE+1 and +2 estimators compared with the oracle and a naïve re-fitted estimators. The results are averages over 1000 independent replications.

γ_x	γ_y	m	n_x	n_y	oracle	naïve	SparKLIE	
							+1	+2
chain	1	25	150	300	0.960	0.850	0.934	0.945
		50	300	600	0.946	0.822	0.943	0.948
	2	25	150	300	0.962	0.907	0.948	0.948
		50	300	600	0.962	0.839	0.953	0.955
ternary tree	1	25	150	300	0.972	0.925	0.932	0.958
		50	300	600	0.976	0.874	0.973	0.979
	2	25	150	300	0.972	0.946	0.957	0.977
		50	300	600	0.968	0.913	0.952	0.977

5 Simulation studies

Through extensive simulations, we illustrate the finite-sample performance of our methods: SparKLIE+ (Section 5.1) and empirical bootstrap sketching (Section 5.2).

5.1 Inference for a single edge via Gaussian approximation

In Experiments 1 and 2, we look at the performance of statistical inference procedures based on Gaussian approximation when an edge has been fixed as a target of inferential interest.

Experiment 1. We check the coverage of the 95% CI $\hat{\theta}_k \pm z_{0.975}\hat{\sigma}_k/\sqrt{n}$, where k is a fixed edge of interest and $z_{0.975}$ is the 0.975-quantile of $\mathcal{N}(0, 1)$. Here, SparKLIE+1 and +2 are compared with two other procedures: an oracle procedure with the knowledge of $\text{supp}(\theta^*)$ and a naïve re-estimation procedure that re-fits the model based on the estimated support $\text{supp}(\hat{\theta})$, where $\hat{\theta}$ is a sparse KLIEP estimate. See Appendix H.1 for precise definitions.

The results below were obtained using autoscaling procedures for both initial estimation steps. For each step, we used the canonical penalty level, which was $\lambda_{\theta_0} = 1.01\Phi^{-1}(1 - 0.05/p)$ for Step 1 and $\lambda_0 = \sqrt{2\log p/n_y}$ for Step 2. However, we remark that even with the vanilla sparse KLIEP procedure (4) in Step 1, we have found the performance of Procedure 1 to be robust to the choice of λ_θ . See Remarks 1 and 2, as well as Appendix I.3.

The data are pairs of samples of i.i.d. observations from a pair of Ising models γ_x and γ_y . Eight pairs of γ_x and γ_y are compared, arising from all possible combinations of the number of nodes ($m = 25$ or 50), the topology of γ_x (a chain or a ternary tree), and two choices of θ^* from which $\gamma_y = \gamma_x - \theta^*$ is obtained. Each differential network has five nonzero edges, one of which has been fixed as the target of inference. For illustration, see Figures 4 – 7 in Appendix H.2.

Table 1 gives the proportions of successful coverage out of 1000 independent replications at the nominal confidence level of 95%. In spite of the small sample sizes, the coverage of 95% CIs based on either of the two SparKLIE+ estimators are close to the nominal level, and on par with the performance of the oracle procedure across all the data generating processes considered. By contrast, we see that the naïve re-fitted estimator can undercover by as much as $\approx 13\%$.

In Appendix H.4, we further provide normal Q-Q plots (Figures 8 – 11) and empirical estimates of the biases (Table 3) for the four estimators. These reveal that the inferior performance of the naïve re-fitted estimator can be attributed to the larger bias.

In *Experiment 2* in Appendix I.1, we study the power SparKLIE+1 and +2 for testing the null hypothesis $\mathcal{H}_0 : \theta_k^* = 0$, where k is a fixed edge of interest.

Table 2: Sample sizes by group

	T1	T2	T3
HC	342	300	306
MS	342	300	311

5.2 Global inference with empirical bootstrap quantile estimates

In Experiments 3 and 4, we look at the performance of Procedure 3 for making inferences about the entire differential network θ^* .

Experiment 3. We check that Procedure 3 produces consistent estimates of the quantiles $c_{T,1-\alpha}$ of $T = \max_k \sqrt{n} |\hat{\theta}_k - \theta_k^*|$. Here, we focus on the setting $\gamma = \gamma_x = \gamma_y$, i.e., $\theta^* = \mathbf{0}$. We generate a pair of samples of the same size $n_x = n_y = 500$ from the same Ising model with the parameter γ . The parameter γ was generated as a disjoint union of $m/5$ chains of length 5 for $m \in \{25, 50, 100\}$. The nonzero edge weights were drawn i.i.d. from one of the three distributions: $\text{sgn} = 1$, $\text{Unif}(0.2, 0.4)$; $\text{sgn} = -1$, $\text{Unif}(-0.4, -0.2)$; or $\text{sgn} = 0$, $\text{Unif}(-0.4, -0.2) \cup (0.2, 0.4)$.

For each draw of samples from γ_x and γ_y , we use Procedure 3 with $n_b = 1000$ bootstrap replicates to estimate $\hat{c}_{T,1-\alpha}$, and record $\mathbb{1}\{T \leq \hat{c}_{T,1-\alpha}\}$ for each $1 - \alpha = 0.05, \dots, 0.95$. Then, the results are averaged across 1000 independent draws of the pair of samples. If Procedure 3 is consistent, $\mathbb{1}\{T \leq \hat{c}_{T,1-\alpha}\} \approx \mathbb{1}\{T \leq c_{T,1-\alpha}\}$, and hence the average over independent replicates would be close to $1 - \alpha$. This is indeed what we see in Figure 1.

In *Experiment 4* in Appendix I.2, we study the power of the level- α test obtained by inverting the simultaneous confidence region $\hat{\theta}_k \pm \hat{c}_{T,1-\alpha}/\sqrt{n}$ for testing the null hypothesis $\mathcal{H}_0 : \theta_k^* = 0$ for all k .

6 Real data example: Alertness and motor control, an fMRI study

We apply Procedure 1 and Procedure 3 to analyze a new fMRI dataset, made available courtesy of Dr. Jade Thai and Dr. Christelle Langley at the University of Bristol. The dataset comes from a pilot study involving a multiple sclerosis subject (MS) and a healthy control (HC) with the purpose of exploring the relationship between alertness and motor control. It consists of two time series, one for each participant of the study, of fMRI measurements at 0.906 second intervals from 116 regions of interest (ROI) in the brain. We further restrict to $m = 25$ ROIs pre-specified by the neuroscientists. The measurements were taken while the participants were performing one of three types of tasks: a sensorimotor task (T1), an intrinsic alertness task (T2), and an extrinsic alertness task (T3). For details concerning the study design and data post-processing, see Appendix J.

We model the fMRI measurements as independent observations from six Gaussian graphical models, where the groups are given by the disease status and the task type. For example, the measurements collected while the HC subject performed T1 are modeled as

$$f_{\text{HC},\text{T1}}(\mathbf{x}) = \det(\mathbf{G}_{\text{HC},\text{T1}}/(2\pi))^{1/2} \exp(-(\mathbf{x} - \mu_{\text{HC},\text{T1}})^\top \mathbf{G}_{\text{HC},\text{T1}}(\mathbf{x} - \mu_{\text{HC},\text{T1}})/2).$$

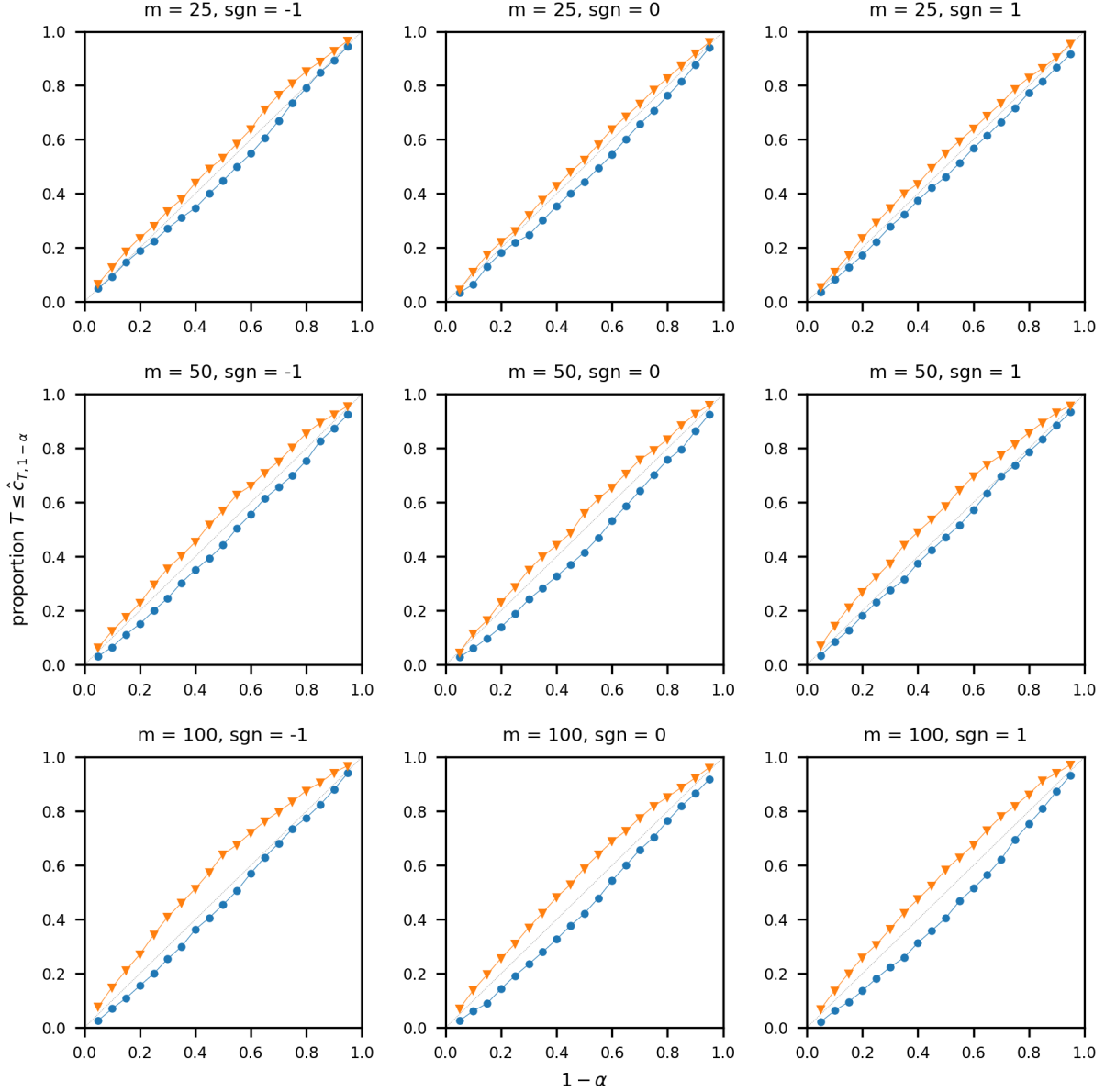
Since we are interested in the difference in the graph structure, we work with the data after centering by the group means. The sample sizes are given in Table 6.

For either the HC or the MS subject, we study the pairwise differences for the tasks. Specifically, we would like to obtain, with FWER control at 0.05, six differential networks:

$$\begin{aligned} \Delta_1^* &= \mathbf{G}_{\text{HC}, \text{T1}} - \mathbf{G}_{\text{HC}, \text{T2}}, & \Delta_2^* &= \mathbf{G}_{\text{HC}, \text{T1}} - \mathbf{G}_{\text{HC}, \text{T3}}, & \Delta_3^* &= \mathbf{G}_{\text{HC}, \text{T2}} - \mathbf{G}_{\text{HC}, \text{T3}}, \\ \Delta_4^* &= \mathbf{G}_{\text{MS}, \text{T1}} - \mathbf{G}_{\text{MS}, \text{T2}}, & \Delta_5^* &= \mathbf{G}_{\text{MS}, \text{T1}} - \mathbf{G}_{\text{MS}, \text{T3}}, & \Delta_6^* &= \mathbf{G}_{\text{MS}, \text{T2}} - \mathbf{G}_{\text{MS}, \text{T3}}. \end{aligned}$$

The six differential networks $\hat{\Delta}_g^*$, $g = 1, \dots, 6$, were estimated using Procedure 1 with the autoscaling formulations for Steps 1 and 2 with the universal penalty levels as explained in Remark 2 in Section 3.1. The test statistic $T_0 = \max_{g=1, \dots, 6} \max_{1 \leq u \leq v \leq 25} |\hat{\Delta}_{g,uv}|$ was used to test the null hypothesis $\mathcal{H}_0 : \Delta_g^* = \mathbf{0}$ for all $g = 1, \dots, 6$ at level 0.05 based on the rejection threshold $\hat{c}_{T_0,0.05}$ obtained from Procedure 3. The test found *no edges* to be statistically significant. However, the conclusion is based on a pilot study from two individuals, and more data are needed.

Figure 1: Consistency of the quantile estimates $\hat{c}_{T,1-\alpha}$ from Procedure 3 in nine different settings, corresponding to all possible combinations of the number of nodes $m = 25, 50,$ or 100 and the distribution of edge parameters $\text{sgn} = -1, 0,$ or 1 , where $\text{sgn} = 1, \text{Unif}(0.2, 0.4)$; $\text{sgn} = -1, \text{Unif}(-0.4, -0.2)$; or $\text{sgn} = 0, \text{Unif}(-0.4, -0.2) \cup (0.2, 0.4)$. The blue line with \bullet indicates SparKLIIE+1. The orange line with \blacktriangledown indicates SparKLIIE+2. The 45° line marks perfect calibration.



7 Discussion

We have developed novel methods for making statistically valid comparisons of general Markov networks based on i.i.d. observations from each. To our knowledge, this is the first work that allows one to conduct provably-valid inference using a direct estimate of the network difference for general Markov networks in high-dimensional settings. This means that our methods can deal with dense networks as long as their *difference* is sparse. Also, our framework can easily handle non-Gaussian data. Furthermore, our theory does not require the conditions that are typically necessary to guarantee consistent support recovery, increasing

applicability of our proposal. In addition, we develop the bootstrap sketching procedures to estimate the quantiles of extreme statistics accurately and in a computationally efficient manner even at large p .

As remarked by a reviewer, it is natural to ask whether it is possible to use other divergences to derive similar procedures. For closely-related varieties, such as the reverse and the symmetric KL, the answer is clearly yes. For arbitrary divergences, however, exact analogues may not exist. The derivation of KLIEP uses more than just the properties of a divergence. Indeed, the logarithm in KL plays an essential role in linearizing the ratio $f_x/(r_\theta f_y)$, yielding a population-level loss that involves expectations of only known functions of θ . In addition the loss is convex in θ , leading to a computationally attractive procedure. Using other divergences to measure discrepancy between f_x and $r_\theta f_y$ would, to the best of our knowledge, lead to an estimator that is not convex in θ . Establishing statistical properties of such an estimator is beyond the scope of this paper.

It can be checked that the special case of the reverse KL reduces to KLIEP with the role of f_x and f_y swapped. The effect of switching the samples was discussed in Remark 5 in Section 4.2. The symmetric KL leads to a procedure that minimizes the sum of the KLIEP and the reversed KLIEP loss functions. The theory developed in this paper extends in an obvious way to the symmetrized procedure. This means that the conditions that were previously imposed on only one of f_x and f_y now need to hold for both, reducing the applicability of our methods. Moreover, although the change is not expected to alter the order of error bounds, the constants are expected to be larger, and this is likely to result in a more brittle approximation at the same sample sizes, as corroborated by empirical evidence (Appendix I.3).

In addition to the approach followed in this paper, where the density ratio is estimated by minimizing the divergence between one density and the product of the density ratio and another density, alternative approaches have been considered in the literature. For example, Nguyen et al. (2010) estimate the density ratio by maximizing a lower bound on an f -divergence. Kanamori et al. (2009) estimate a density ratio by minimizing a squared loss between the true density ratio and the model of a density ratio. Developing inferential results for the parameters of differential networks obtained by such approaches is an interesting topic for future research.

Although we never place explicit assumptions on the form of dependence, some restraint is necessary in practice for good performance. This can already be seen from the results in Section 4: the bounds deteriorate rapidly as p increases to accommodate higher order dependencies. This is why we chose to focus exclusively on *pairwise* models in our simulations and real data analysis. It is of future interest to develop an efficient search procedure to include only the relevant higher-order terms.

Finally, although it is a huge advantage of our methods that they can be used to compare general Markov networks, it may be possible to obtain more sample efficient procedures for particular models by utilizing distribution-specific properties. For example, it is of interest to develop inferential procedures for the network difference of Gaussian or Gaussian copula models.

Acknowledgments

This work was completed in part with resources provided by the University of Chicago Research Computing Center. The fMRI dataset collection is funded by MS Research Treatment and Education whose Registered Charity Number is 1043280.

References

- O. Banerjee, L. El Ghaoui, and A. d’Aspremont. Model selection through sparse maximum likelihood estimation. *J. Mach. Learn. Res.*, 9(3):485–516, 2008.
- R. F. Barber and M. Kolar. Rocket: Robust confidence intervals via kendall’s tau for transelliptical graphical models. *Ann. Statist.*, 46(6B):3422–3450, 2018.
- E. Belilovsky, G. Varoquaux, and M. B. Blaschko. Testing for differences in gaussian graphical models: Applications to brain connectivity. In D. D. Lee, M. Sugiyama, U. V. Luxburg, I. Guyon, and R. Garnett, editors, *Advances in Neural Information Processing Systems 29*, pages 595–603. Curran Associates, Inc., 2016.

- A. Belloni, V. Chernozhukov, and L. Wang. Square-root lasso: pivotal recovery of sparse signals via conic programming. *Biometrika*, 98(4):791–806, 2011.
- A. Belloni and V. Chernozhukov. Least squares after model selection in high-dimensional sparse models. *Bernoulli*, 19(2):521–547, 2013.
- A. Belloni, V. Chernozhukov, and C. B. Hansen. Inference on treatment effects after selection amongst high-dimensional controls. *Rev. Econ. Stud.*, 81(2):608–650, 2013.
- A. Belloni, V. Chernozhukov, and L. Wang. Pivotal estimation via square-root Lasso in nonparametric regression. *The Annals of Statistics*, 42(2):757 – 788, 2014.
- A. Belloni, V. Chernozhukov, and Y. Wei. Post-selection inference for generalized linear models with many controls. *J. Bus. Econom. Statist.*, 34(4):606–619, 2016.
- A. Belloni, V. Chernozhukov, D. Chetverikov, C. Hansen, and K. Kato. High-dimensional econometrics and regularized GMM. *arxiv: 1806.01888*, 2018.
- A. Belloni, A. Kaul, and M. Rosenbaum. Pivotal estimation via self-normalization for high-dimensional linear models with error in variables, 2019.
- T. T. Cai, H. Li, J. Ma, and Y. Xia. Differential Markov random field analysis with an application to detecting differential microbial community networks. *Biometrika*, 106(2):401–416, 2019.
- T. T. Cai, W. Liu, and X. Luo. A constrained ℓ_1 minimization approach to sparse precision matrix estimation. *J. Am. Stat. Assoc.*, 106(494):594–607, 2011.
- L. H. Y. Chen, L. Goldstein, and Q.-M. Shao. *Normal approximation by Stein’s method*. Probability and its Applications (New York). Springer, Heidelberg, 2011.
- X. Chen. Gaussian and bootstrap approximations for high-dimensional U-statistics and their applications. *Ann. Statist.*, 46(2):642–678, 2018.
- V. Chernozhukov, D. Chetverikov, and K. Kato. Gaussian approximations and multiplier bootstrap for maxima of sums of high-dimensional random vectors. *Ann. Stat.*, 41(6):2786–2819, 2013.
- V. Chernozhukov, D. Chetverikov, and K. Kato. Comparison and anti-concentration bounds for maxima of Gaussian random vectors. *Probab. Theory Related Fields*, 162(1-2):47–70, 2015a.
- V. Chernozhukov, C. Hansen, and M. Spindler. Valid post-selection and post-regularization inference: An elementary, general approach. *Annual Review of Economics*, 7(1):649–688, 2015b.
- V. Chernozhukov, D. Chetverikov, and K. Kato. Central limit theorems and bootstrap in high dimensions. *Ann. Probab.*, 45(4):2309–2352, 2017.
- J. Chiquet, Y. Grandvalet, and C. Ambroise. Inferring multiple graphical structures. *Stat. Comput.*, 21(4): 537–553, 2011.
- P. Danaher, P. Wang, and D. M. Witten. The joint graphical lasso for inverse covariance estimation across multiple classes. *J. R. Stat. Soc. B*, 76(2):373–397, 2014.
- V. H. de la Peña, T. L. Lai, and Q.-M. Shao. *Self-Normalized Processes*. Springer Berlin Heidelberg, 2009.
- H. Deng and C.-H. Zhang. Beyond Gaussian approximation: Bootstrap for maxima of sums of independent random vectors. *The Annals of Statistics*, 48(6):3643 – 3671, 2020.
- R. Dezeure, P. Bühlmann, and C.-H. Zhang. High-dimensional simultaneous inference with the bootstrap. *TEST*, 26(4):685–719, 2017.
- A. Dobra, C. Hans, B. Jones, J. R. Nevins, G. Yao, and M. West. Sparse graphical models for exploring gene expression data. *J. Multivariate Anal.*, 90(1):196–212, 2004.

- M. Drton and M. H. Maathuis. Structure learning in graphical modeling. *Annual Review of Statistics and Its Application*, 4(1):365–393, 2017, [arXiv:https://doi.org/10.1146/annurev-statistics-060116-053803](https://doi.org/10.1146/annurev-statistics-060116-053803).
- F. Fazayeli and A. Banerjee. Generalized direct change estimation in Ising model structure. In M. F. Balcan and K. Q. Weinberger, editors, *Proceedings of The 33rd International Conference on Machine Learning*, volume 48 of *Proceedings of Machine Learning Research*, pages 2281–2290, New York, New York, USA, 2016. PMLR.
- J. H. Friedman, T. J. Hastie, and R. J. Tibshirani. Sparse inverse covariance estimation with the graphical lasso. *Biostatistics*, 9(3):432–441, 2008.
- S. Geman and D. Geman. Stochastic relaxation, gibbs distributions, and the bayesian restoration of images. *IEEE Transactions on Pattern Analysis and Machine Intelligence*, PAMI-6(6):721–741, 1984.
- J. Guo, E. Levina, G. Michailidis, and J. Zhu. Joint estimation of multiple graphical models. *Biometrika*, 98(1):1–15, 2011.
- J. M. Hammersley and P. Clifford. Markov fields on finite graphs and lattices. *Unpublished manuscript*, 46, 1971.
- A. J. Hartemink, D. K. Gifford, T. S. Jaakkola, and R. A. Young. Using graphical models and genomic expression data to statistically validate models of genetic regulatory networks. In R. B. Altman, A. K. Dunker, L. Hunter, and T. E. Klein, editors, *Proceedings of the 6th Pacific Symposium on Biocomputing, PSB 2001, Hawaii, USA, January 3-7, 2001*, pages 422–433, 2001.
- J. Janková and S. van de Geer. Confidence intervals for high-dimensional inverse covariance estimation. *Electron. J. Stat.*, 9(1):1205–1229, 2015.
- J. Janková and S. A. van de Geer. Honest confidence regions and optimality in high-dimensional precision matrix estimation. *TEST*, 26(1):143–162, 2017.
- A. Javanmard and A. Montanari. Confidence intervals and hypothesis testing for high-dimensional regression. *J. Mach. Learn. Res.*, 15(Oct):2869–2909, 2014.
- B.-Y. Jing, Q.-M. Shao, and Q. Wang. Self-normalized Cramér-type large deviations for independent random variables. *The Annals of Probability*, 31(4):2167 – 2215, 2003.
- T. Kanamori, S. Hido, and M. Sugiyama. A least-squares approach to direct importance estimation. *J. Mach. Learn. Res.*, 10:1391–1445, 2009.
- D. Koller and N. Friedman. *Probabilistic graphical models: principles and techniques*. MIT press, 2009.
- S. L. Lauritzen. *Graphical Models*, volume 17 of *Oxford Statistical Science Series*. The Clarendon Press Oxford University Press, New York, 1996. Oxford Science Publications.
- S. Liu, J. A. Quinn, M. U. Gutmann, T. Suzuki, and M. Sugiyama. Direct learning of sparse changes in Markov networks by density ratio estimation. *Neural Comput.*, 26(6):1169–1197, 2014.
- S. Liu, T. Suzuki, R. Relator, J. Sese, M. Sugiyama, and K. Fukumizu. Support consistency of direct sparse-change learning in Markov networks. *Ann. Statist.*, 45(3):959–990, 2017.
- W. Liu. Structural similarity and difference testing on multiple sparse Gaussian graphical models. *Ann. Statist.*, 45(6):2680–2707, 2017.
- P.-L. Loh and M. J. Wainwright. Structure estimation for discrete graphical models: generalized covariance matrices and their inverses. *Ann. Statist.*, 41(6):3022–3049, 2013.
- J. Lu, M. Kolar, and H. Liu. Post-regularization inference for time-varying nonparanormal graphical models. *Journal of Machine Learning Research*, 18(203):1–78, 2018.

- C. Ma, J. Lu, and H. Liu. Inter-subject analysis: Inferring sparse interactions with dense intra-graphs, 2017.
- J. Ma and G. Michailidis. Joint structural estimation of multiple graphical models. *Journal of Machine Learning Research*, 17(166):1–48, 2016.
- D. J. C. MacKay. *Information theory, inference and learning algorithms*. Cambridge University Press, New York, 2003.
- S. Majumdar and G. Michailidis. Joint estimation and inference for data integration problems based on multiple multi-layered gaussian graphical models. *arxiv: 1803.03348*, 2018.
- N. Meinshausen. Group bound: confidence intervals for groups of variables in sparse high dimensional regression without assumptions on the design. *J. R. Stat. Soc. Ser. B. Stat. Methodol.*, 77(5):923–945, 2015.
- K. Mohan, P. London, M. Fazel, D. M. Witten, and S.-I. Lee. Node-based learning of multiple gaussian graphical models. *J. Mach. Learn. Res.*, 15:445–488, 2014.
- S. N. Negahban, P. Ravikumar, M. J. Wainwright, and B. Yu. A unified framework for high-dimensional analysis of m -estimators with decomposable regularizers. *Stat. Sci.*, 27(4):538–557, 2012.
- X. Nguyen, M. J. Wainwright, and M. I. Jordan. Estimating divergence functionals and the likelihood ratio by convex risk minimization. *IEEE Trans. Inform. Theory*, 56(11):5847–5861, 2010.
- Y. Ning and H. Liu. A general theory of hypothesis tests and confidence regions for sparse high dimensional models. *Ann. Statist.*, 45(1):158–195, 2017.
- P. Ravikumar, M. J. Wainwright, G. Raskutti, and B. Yu. High-dimensional covariance estimation by minimizing ℓ_1 -penalized log-determinant divergence. *Electron. J. Stat.*, 5:935–980, 2011.
- Z. Ren, T. Sun, C.-H. Zhang, and H. H. Zhou. Asymptotic normality and optimalities in estimation of large Gaussian graphical models. *Ann. Stat.*, 43(3):991–1026, 2015.
- S. Roy, Y. Atchadé, and G. Michailidis. Change point estimation in high dimensional Markov random-field models. *J. R. Stat. Soc. Ser. B. Stat. Methodol.*, 79(4):1187–1206, 2017.
- A. Shojaie. Differential network analysis: a statistical perspective. *Wiley Interdiscip. Rev. Comput. Stat.*, 13(2):e1508, 16, 2021.
- M. Sugiyama, S. Nakaajima, H. Kashima, P. V. Buenau, and M. Kawanabe. Direct importance estimation with model selection and its application to covariate shift adaptation. In J. C. Platt, D. Koller, Y. Singer, and S. T. Roweis, editors, *Advances in Neural Information Processing Systems 20*, pages 1433–1440. Curran Associates, Inc., 2008.
- M. Sugiyama, T. Suzuki, and T. Kanamori. *Density ratio estimation in machine learning*. Cambridge University Press, Cambridge, 2012. With a foreword by Thomas G. Dietterich.
- T. Sun and C.-H. Zhang. Scaled sparse linear regression. *Biometrika*, 99(4):879–898, 2012.
- T. Sun and C.-H. Zhang. Sparse matrix inversion with scaled lasso. *J. Mach. Learn. Res.*, 14:3385–3418, 2013.
- K. Supekar, V. Menon, D. Rubin, M. Musen, and M. D. Greicius. Network analysis of intrinsic functional brain connectivity in alzheimer’s disease. *PLoS Computational Biology*, 4(6):e1000100, 2008.
- N. Tzourio-Mazoyer, B. Landeau, D. Papathanassiou, F. Crivello, O. Etard, N. Delcroix, B. Mazoyer, and M. Joliot. Automated anatomical labeling of activations in SPM using a macroscopic anatomical parcellation of the MNI MRI single-subject brain. *NeuroImage*, 15(1):273–289, 2002.
- S. A. van de Geer, P. Bühlmann, Y. Ritov, and R. Dezeure. On asymptotically optimal confidence regions and tests for high-dimensional models. *Ann. Stat.*, 42(3):1166–1202, 2014.

- A. W. van der Vaart. *Asymptotic statistics*, volume 3 of *Cambridge Series in Statistical and Probabilistic Mathematics*. Cambridge University Press, Cambridge, 1998.
- M. J. Wainwright and M. I. Jordan. Graphical models, exponential families, and variational inference. *Foundations and Trends® in Machine Learning*, 1(1-2):1–305, 2008a.
- M. J. Wainwright and M. I. Jordan. Graphical models, exponential families, and variational inference. *Found. and Trends Mach. Learn.*, 1(1-2):1–305, 2008b.
- J. Wang and M. Kolar. Inference for high-dimensional exponential family graphical models. In A. Gretton and C. C. Robert, editors, *Proc. of AISTATS*, volume 51, pages 751–760, 2016.
- Y. Xia, T. Cai, and T. T. Cai. Testing differential networks with applications to the detection of gene-gene interactions. *Biometrika*, 102(2):247–266, 2015.
- P. Xu and Q. Gu. Semiparametric differential graph models. In D. D. Lee, M. Sugiyama, U. V. Luxburg, I. Guyon, and R. Garnett, editors, *Advances in Neural Information Processing Systems 29*, pages 1064–1072. Curran Associates, Inc., 2016.
- K. Xue and F. Yao. Distribution and correlation-free two-sample test of high-dimensional means. *Ann. Statist.*, 48(3):1304–1328, 2020.
- E. Yang, P. Ravikumar, G. I. Allen, and Z. Liu. On graphical models via univariate exponential family distributions. *J. Mach. Learn. Res.*, 16:3813–3847, 2015.
- M. Yu, V. Gupta, and M. Kolar. Statistical inference for pairwise graphical models using score matching. In *Advances in Neural Information Processing Systems 29*. Curran Associates, Inc., 2016.
- M. Yu, V. Gupta, and M. Kolar. Simultaneous inference for pairwise graphical models with generalized score matching. *Journal of Machine Learning Research*, 21(91):1–51, 2020.
- M. Yuan. High dimensional inverse covariance matrix estimation via linear programming. *J. Mach. Learn. Res.*, 11:2261–2286, 2010.
- M. Yuan and Y. Lin. Model selection and estimation in the gaussian graphical model. *Biometrika*, 94(1): 19–35, 2007.
- C.-H. Zhang and S. S. Zhang. Confidence intervals for low dimensional parameters in high dimensional linear models. *J. R. Stat. Soc. B*, 76(1):217–242, 2013.
- S. D. Zhao, T. T. Cai, and H. Li. Direct estimation of differential networks. *Biometrika*, 101(2):253–268, 2014.

A The empirical KLIEP loss ℓ_{KLIEP}

A.1 Derivation of KLIEP

We derive the form for $\boldsymbol{\theta}^*$ in Section 2.2. We have

$$\boldsymbol{\theta}^* = \arg \min_{\boldsymbol{\theta}} D_{\text{KL}}(f_x \| f_y r_{\boldsymbol{\theta}}) \quad (16)$$

$$= \arg \min_{\boldsymbol{\theta}} \int \log \left(\frac{f_x(\mathbf{x})}{r_{\boldsymbol{\theta}}(\mathbf{x}) f_y(\mathbf{x})} \right) f_x(\mathbf{x}) d\mathbf{x} \quad (17)$$

$$= \arg \min_{\boldsymbol{\theta}} - \int \log r_{\boldsymbol{\theta}}(\mathbf{x}) f_x(\mathbf{x}) d\mathbf{x} \quad (18)$$

$$= \arg \min_{\boldsymbol{\theta}} - \int \boldsymbol{\theta}^{\top} \boldsymbol{\psi}(\mathbf{x}) f_x(\mathbf{x}) d\mathbf{x} + \log Z_y(\boldsymbol{\theta}) \quad (19)$$

$$= \arg \min_{\boldsymbol{\theta}} -\mathbb{E}_x [\boldsymbol{\theta}^{\top} \boldsymbol{\psi}(\mathbf{x})] + \log \mathbb{E}_y [\exp(\boldsymbol{\theta}^{\top} \boldsymbol{\psi}(\mathbf{y}))]. \quad (20)$$

(18) applies log to the ratio, and then notes that $\log r_{\boldsymbol{\theta}}$ is the only term with dependency on $\boldsymbol{\theta}$. (19) follows from the definition of $r_{\boldsymbol{\theta}}$. (20) is just the definition of expectation. In particular, $Z_y(\boldsymbol{\theta}) = \mathbb{E}_y[\exp(\boldsymbol{\theta}^{\top} \boldsymbol{\psi}(\mathbf{y}))] = \int \exp(\boldsymbol{\theta}^{\top} \boldsymbol{\psi}(\mathbf{x})) f_y(\boldsymbol{\theta}) d\mathbf{x}$.

A.2 Derivatives and approximate moment-matching

Recall

$$\widehat{Z}_y(\boldsymbol{\theta}) = \frac{1}{n_y} \sum_{j=1}^{n_y} \exp(\boldsymbol{\theta}^{\top} \boldsymbol{\psi}(\mathbf{y}^{(j)})), \quad \widehat{r}_{\boldsymbol{\theta}}(\mathbf{y}) = \frac{\exp(\boldsymbol{\theta}^{\top} \boldsymbol{\psi}(\mathbf{y}))}{\widehat{Z}_y(\boldsymbol{\theta})}, \quad \widehat{\boldsymbol{\mu}}(\boldsymbol{\theta}) = \frac{1}{n_y} \sum_{j=1}^{n_y} \boldsymbol{\psi}(\mathbf{y}^{(j)}) \widehat{r}_{\boldsymbol{\theta}}(\mathbf{y}^{(j)}).$$

The following identities hold:

$$\frac{\partial \log \widehat{Z}_y(\boldsymbol{\theta})}{\partial \theta_k} = \widehat{\mu}_k(\boldsymbol{\theta}), \quad (21)$$

$$\frac{\partial \widehat{r}_{\boldsymbol{\theta}}(\mathbf{y})}{\partial \theta_k} = (\psi_k(\mathbf{y}_k) - \widehat{\mu}_k(\boldsymbol{\theta})) \widehat{r}_{\boldsymbol{\theta}}(\mathbf{y}), \quad (22)$$

$$\frac{\partial \ell_{\text{KLIEP}}(\boldsymbol{\theta})}{\partial \theta_k} = -\frac{1}{n_x} \sum_{i=1}^{n_x} \psi_k(\mathbf{x}_k^{(i)}) + \widehat{\mu}_k(\boldsymbol{\theta}), \quad (23)$$

$$\frac{\partial^2 \ell_{\text{KLIEP}}(\boldsymbol{\theta})}{\partial \theta_{k'} \partial \theta_k} = \frac{1}{n_y} \sum_{j=1}^{n_y} \psi_{k'}(\mathbf{y}_{k'}^{(j)}) \psi_k(\mathbf{y}_k^{(j)}) \widehat{r}_{\boldsymbol{\theta}}(\mathbf{y}^{(j)}) - \widehat{\mu}_{k'}(\boldsymbol{\theta}) \widehat{\mu}_k(\boldsymbol{\theta}) \quad (24)$$

$$= \frac{1}{n_y^2} \sum_{1 \leq j < j' \leq n_y} \left(\psi_{k'}(\mathbf{y}_{k'}^{(j)}) - \psi_{k'}(\mathbf{y}_{k'}^{(j')}) \right) \left(\psi_k(\mathbf{y}_k^{(j)}) - \psi_k(\mathbf{y}_k^{(j')}) \right) \widehat{r}_{\boldsymbol{\theta}}(\mathbf{y}^{(j)}) \widehat{r}_{\boldsymbol{\theta}}(\mathbf{y}^{(j')}), \quad (25)$$

$$\frac{\partial^3 \ell_{\text{KLIEP}}(\boldsymbol{\theta})}{\partial \theta_{k''} \partial \theta_{k'} \partial \theta_k} = \frac{1}{n_y} \sum_{j=1}^{n_y} \psi_k(\mathbf{y}_k^{(j)}) \psi_{k'}(\mathbf{y}_{k'}^{(j)}) \psi_{k''}(\mathbf{y}_{k''}^{(j)}) \widehat{r}_{\boldsymbol{\theta}}(\mathbf{y}^{(j)}) \quad (26)$$

$$\begin{aligned} & - \widehat{\mu}_{k''}(\boldsymbol{\theta}) \times \frac{1}{n_y} \sum_{j=1}^{n_y} \psi_k(\mathbf{y}_k^{(j)}) \psi_{k'}(\mathbf{y}_{k'}^{(j)}) \widehat{r}_{\boldsymbol{\theta}}(\mathbf{y}^{(j)}) \\ & - \widehat{\mu}_{k'} \nabla_{k''k}^2 \ell_{\text{KLIEP}}(\boldsymbol{\theta}) - \widehat{\mu}_k(\boldsymbol{\theta}) \nabla_{k''k'}^2 \ell_{\text{KLIEP}}(\boldsymbol{\theta}). \end{aligned}$$

These identities are useful in obtaining various uniform bounds.

The suggestive notation is by design: $\widehat{Z}_y(\boldsymbol{\theta}) \approx Z_y(\boldsymbol{\theta})$ and $\widehat{r}_{\boldsymbol{\theta}}(\mathbf{y}) \approx r_{\boldsymbol{\theta}}(\mathbf{y})$, obviously. In fact, it is the message of Lemma 1 below that

$$\widehat{\boldsymbol{\mu}}(\boldsymbol{\theta}) \approx \mathbb{E}_{\boldsymbol{\theta} + \gamma_y}[\boldsymbol{\psi}(\mathbf{x})] \quad \text{and} \quad \mathbb{E}_{\boldsymbol{\theta} + \gamma_y}[\nabla^2 \ell_{\text{KLIEP}}(\boldsymbol{\theta})] \approx \text{Cov}_{\boldsymbol{\theta} + \gamma_y}[\boldsymbol{\psi}(\mathbf{x})].$$

$\nabla^3 \ell_{\text{KLIEP}}(\boldsymbol{\theta})$ also approximates the third central moment tensor of $\boldsymbol{\psi}(\mathbf{x})$ under $\boldsymbol{\gamma} = \boldsymbol{\theta} + \boldsymbol{\gamma}_y$, but we will not need this fact.

Lemma 1.

$$\mathbb{E}_y[\boldsymbol{\psi}(\mathbf{y})r_\theta(\mathbf{y})] = \mathbb{E}_{\theta+\gamma_y}[\boldsymbol{\psi}(\mathbf{x})].$$

and

$$\mathbb{E}_y[\mathbf{H}(\boldsymbol{\theta})] := \mathbb{E}_y \left[\frac{\widehat{Z}_y(\boldsymbol{\theta})^2}{Z_y(\boldsymbol{\theta})^2} \nabla^2 \ell_{\text{KLIEP}}(\boldsymbol{\theta}) \right] = \left(1 - \frac{1}{n_y} \right) \text{Cov}_{\theta+\gamma_y}[\boldsymbol{\psi}(\mathbf{x})]. \quad (27)$$

Proof. Let $f_\theta = f_{\theta+\gamma_y}$. To prove the first identity,

$$\mathbb{E}_y[\psi_k(\mathbf{y}_k)r_\theta(\mathbf{y})] = \int \psi_k(\mathbf{y}_k)r_\theta(\mathbf{y})f_y(\mathbf{y})d\mathbf{y} = \int \psi_k(\mathbf{y}_k)f_\theta(\mathbf{y})d\mathbf{y} = \mathbb{E}_{\theta+\gamma_y}\psi(\mathbf{y}_k) = \mu_k(\boldsymbol{\theta}).$$

To prove the second identity, let $\mathbf{y}, \mathbf{y}' \sim f_y$ be independent, so that

$$\begin{aligned} \mathbb{E}_y [(\psi_{k'}(\mathbf{y}_{k'}) - \psi_{k'}(\mathbf{y}'_{k'}))(\psi_k(\mathbf{y}_k) - \psi_k(\mathbf{y}'_k))r_\theta(\mathbf{y})r_\theta(\mathbf{y}')] \\ &= \iint (\psi_{k'}(\mathbf{y}_{k'}) - \psi_{k'}(\mathbf{y}'_{k'}))(\psi_k(\mathbf{y}_k) - \psi_k(\mathbf{y}'_k))r_\theta(\mathbf{y})r_\theta(\mathbf{y}')f_y(\mathbf{y})f_y(\mathbf{y}')d\mathbf{y}d\mathbf{y}' \\ &= 2 \iint \psi_{k'}(\mathbf{y}_{k'})\psi_k(\mathbf{y}_k)r_\theta(\mathbf{y})r_\theta(\mathbf{y}')f_y(\mathbf{y})f_y(\mathbf{y}')d\mathbf{y}d\mathbf{y}' \\ &\quad - 2 \iint \psi_{k'}(\mathbf{y}_{k'})\psi_k(\mathbf{y}'_k)r_\theta(\mathbf{y})r_\theta(\mathbf{y}')f_y(\mathbf{y})f_y(\mathbf{y}')d\mathbf{y}d\mathbf{y}'. \end{aligned}$$

The first integral is

$$\begin{aligned} \iint \psi_{k'}(\mathbf{y}_{k'})\psi_k(\mathbf{y}_k)r_\theta(\mathbf{y})r_\theta(\mathbf{y}')f_y(\mathbf{y})f_y(\mathbf{y}')d\mathbf{y}d\mathbf{y}' \\ &= \int \psi_{k'}(\mathbf{y}_{k'})\psi_k(\mathbf{y}_k)r_\theta(\mathbf{y})f_y(\mathbf{y})d\mathbf{y} \int r_\theta(\mathbf{y}')f_y(\mathbf{y}')d\mathbf{y}' \\ &= \int \psi_{k'}(\mathbf{y}_{k'})\psi_k(\mathbf{y}_k)\tilde{f}_{\theta+\gamma_y}(\mathbf{y})d\mathbf{y} \int \tilde{f}_{\theta+\gamma_y}(\mathbf{y}')d\mathbf{y}' \\ &= \mathbb{E}_{\theta+\gamma_y}[\psi_{k'}(\mathbf{y}_{k'})\psi_k(\mathbf{y}_k)]. \end{aligned}$$

As for the second integral,

$$\begin{aligned} \iint \psi_{k'}(\mathbf{y}_{k'})\psi_k(\mathbf{y}'_k)r_\theta(\mathbf{y})r_\theta(\mathbf{y}')f_y(\mathbf{y})f_y(\mathbf{y}')d\mathbf{y}d\mathbf{y}' \\ &= \int \psi_{k'}(\mathbf{y}_{k'})r_\theta(\mathbf{y})f_y(\mathbf{y})d\mathbf{y} \int \psi_k(\mathbf{y}'_k)r_\theta(\mathbf{y}')f_y(\mathbf{y}')d\mathbf{y}' \\ &= \int \psi_{k'}(\mathbf{y}_{k'})\tilde{f}_{\theta+\gamma_y}(\mathbf{y})d\mathbf{y} \int \psi_k(\mathbf{y}'_k)\tilde{f}_{\theta+\gamma_y}(\mathbf{y}')d\mathbf{y}' \\ &= \mathbb{E}_{\theta+\gamma_y}[\psi_{k'}(\mathbf{y}_{k'})]\mathbb{E}_{\theta+\gamma_y}[\psi_k(\mathbf{y}_k)] = \mu_{k'}(\boldsymbol{\theta})\mu_k(\boldsymbol{\theta}). \end{aligned}$$

Thus,

$$\begin{aligned} \mathbb{E}_y [(\psi_{k'}(\mathbf{y}_{k'}) - \psi_{k'}(\mathbf{y}'_{k'}))(\psi_k(\mathbf{y}_k) - \psi_k(\mathbf{y}'_k))r_\theta(\mathbf{y})r_\theta(\mathbf{y}')] \\ &= \mathbb{E}_{\theta+\gamma_y}[\psi_{k'}(\mathbf{y}_{k'})\psi_k(\mathbf{y}_k)] - \mu_{k'}(\boldsymbol{\theta})\mu_k(\boldsymbol{\theta}) = \text{Cov}_{\theta+\gamma_y}[\psi_{k'}(\mathbf{y}_{k'}), \psi_k(\mathbf{y}_k)], \end{aligned}$$

and therefore,

$$\begin{aligned}\mathbb{E}_y[\mathbf{H}(\boldsymbol{\theta})] &= \mathbb{E}_y \left[\frac{\widehat{Z}_y^2(\boldsymbol{\theta})}{Z_y^2(\boldsymbol{\theta})} \nabla^2 \ell_{\text{KLIEP}}(\boldsymbol{\theta}) \right] \\ &= \mathbb{E}_y \left[\frac{1}{n_y^2} \sum_{1 \leq j < j' \leq n_y} \left(\boldsymbol{\psi}(\mathbf{y}^{(j)}) - \boldsymbol{\psi}(\mathbf{y}^{(j')}) \right) \left(\boldsymbol{\psi}(\mathbf{y}^{(j)}) - \boldsymbol{\psi}(\mathbf{y}^{(j')}) \right) r_{\boldsymbol{\theta}}(\mathbf{y}^{(j)}) r_{\boldsymbol{\theta}}(\mathbf{y}^{(j')}) \right] \\ &= \left(1 - \frac{1}{n_y} \right) \boldsymbol{\Sigma}(\boldsymbol{\theta}).\end{aligned}$$

□

In KLIEP, the difference $\boldsymbol{\theta}^*$ of γ_x from γ_y is estimated by matching the moments of $\boldsymbol{\psi}(\mathbf{x})$ with $\boldsymbol{\psi}(\mathbf{y})$ by exponential tilting of the baseline pdf f_y .

KLIEP can be viewed as an approximate version of maximum-likelihood estimation. Fixing $f_y \in \mathcal{F}_\gamma$, define a new parametrization of the family by $\boldsymbol{\theta} = \gamma - \gamma_y$. Abusing the notation somewhat,

$$f_{\boldsymbol{\theta}}(\mathbf{x}) = r_{\boldsymbol{\theta}}(\mathbf{x}) f_y(\mathbf{x}) = Z_y(\boldsymbol{\theta})^{-1} \exp(\boldsymbol{\theta}^\top \boldsymbol{\psi}(\mathbf{x})) f_y(\mathbf{x}),$$

where $Z_y(\boldsymbol{\theta})$ normalizes $f_{\boldsymbol{\theta}}$ albeit with respect to the baseline f_y , that is to say,

$$Z_y(\boldsymbol{\theta}) = \int_{\mathbb{X}} \exp(\boldsymbol{\theta}^\top \boldsymbol{\psi}(\mathbf{x})) f_y(\mathbf{x}) d\mathbf{x} = Z(\boldsymbol{\theta} + \gamma_y) / Z(\gamma_y).$$

Clearly, each γ in the original parameter space corresponds to a unique $\boldsymbol{\theta}$ in the new parameter space.

Given $\mathbf{x}^{(1)}, \dots, \mathbf{x}^{(n_x)} \stackrel{iid}{\sim} f_x$, the negative log-likelihood of the data with respect to the difference parametrization $\boldsymbol{\theta}$ is

$$\ell_y(\boldsymbol{\theta}; \mathbf{X}_{n_x}) = -\frac{1}{n_x} \sum_{i=1}^{n_x} \boldsymbol{\theta}^\top \boldsymbol{\psi}(\mathbf{x}^{(i)}) + \log Z_y(\boldsymbol{\theta}).$$

Let $\boldsymbol{\mu}(\boldsymbol{\theta})$ and $\boldsymbol{\Sigma}(\boldsymbol{\theta})$ be, respectively, the mean and the covariance of $\boldsymbol{\psi}(\mathbf{x})$ under $f_{\boldsymbol{\theta}}$:

$$\boldsymbol{\mu}(\boldsymbol{\theta}) = \int_{\mathbb{X}} \boldsymbol{\psi}(\mathbf{x}) r_{\boldsymbol{\theta}}(\mathbf{x}) f_y(\mathbf{x}) d\mathbf{x}$$

and

$$\boldsymbol{\Sigma}(\boldsymbol{\theta}) = \int_{\mathbb{X}} \boldsymbol{\psi}(\mathbf{x}) \boldsymbol{\psi}(\mathbf{x})^\top r_{\boldsymbol{\theta}}(\mathbf{x}) f_y(\mathbf{x}) d\mathbf{x} - \left(\int_{\mathbb{X}} \boldsymbol{\psi}(\mathbf{x}) r_{\boldsymbol{\theta}}(\mathbf{x}) f_y(\mathbf{x}) d\mathbf{x} \right) \left(\int_{\mathbb{X}} \boldsymbol{\psi}(\mathbf{x}) r_{\boldsymbol{\theta}}(\mathbf{x}) f_y(\mathbf{x}) d\mathbf{x} \right)^\top.$$

It is straightforward to compute

$$\nabla \ell_y(\boldsymbol{\theta}; \mathbf{X}_{n_x}) = -\frac{1}{n} \sum_{i=1}^n \boldsymbol{\psi}(\mathbf{x}^{(i)}) + \boldsymbol{\mu}(\boldsymbol{\theta}) \quad \text{and} \quad \nabla^2 \ell_y(\boldsymbol{\theta}) = \boldsymbol{\Sigma}(\boldsymbol{\theta}).$$

Clearly, when $\mathbf{x}^{(1)}, \dots, \mathbf{x}^{(n_x)} \stackrel{iid}{\sim} f_{\boldsymbol{\theta}^*}$, $\boldsymbol{\theta}^* = \gamma_x - \gamma_y$ is the unique minimizer of $\mathbb{E}_x[\ell_y(\boldsymbol{\theta}; \mathbf{X}_{n_x})]$. In this setting, $\nabla^2 \ell_y$ is a deterministic function of the parameter and thus does not depend on the data. However, it is in general hard to minimize ℓ_y directly, so we look to minimize ℓ_{KLIEP} instead.

Using $\widehat{Z}_y(\boldsymbol{\theta})$ in place of $Z_y(\boldsymbol{\theta})$ recovers ℓ_{KLIEP} . As

$$\sup_{\boldsymbol{\theta}} |\ell_{\text{KLIEP}}(\boldsymbol{\theta}) - \ell_y(\boldsymbol{\theta})| = \left| \log \left\{ \frac{1}{n_y} \sum_{j=1}^{n_y} r_{\boldsymbol{\theta}}(\mathbf{y}^{(j)}) \right\} \right|,$$

ℓ_{KLIEP} converges to ℓ_y pointwise a.s. as $n_y \rightarrow \infty$. Consequently, the minimizer of ℓ_{KLIEP} and the minimizer of ℓ_y are asymptotically equivalent.

B Proofs of the general results

In the below, positive constants that depend only on the fixed problem parameters are denoted as $c_0, c_1, \dots, c'_0, c'_1, \dots, K_0, K_1, \dots$, and their precise definitions may change from line to line. They are never allowed to depend on the sample sizes n_x and n_y , the number of nodes m or the number of parameters p (usually $p = \binom{m}{2}$), or the sparsity level of the true parameters $s_\theta = s_{\theta, q_\theta} = \|\boldsymbol{\theta}^*\|_{q_\theta}$ or $s_k = s_{k, q_k} = \|\boldsymbol{\omega}_k^*\|_{q_k}$ for $k \in [p]$ and for fixed $q_\theta, q_k \in [0, 1]$.

B.1 Explaining de-biasing

Suppose we wish to construct an unbiased estimator of θ_k^* for some $k \in [p]$. Let $\boldsymbol{\theta}_{k^c}^* = \boldsymbol{\theta}_{[p] \setminus \{k\}}^* \in \mathbb{R}^{p-1}$ denote the vector of remaining $p - 1$ parameters; this is the nuisance parameter for carrying out statistical inference for θ_k^* . Abusing the notation somewhat, we write the resulting partition as $\boldsymbol{\theta} = (\theta_k, \boldsymbol{\theta}_{k^c})$. Let $n = n_x + n_y$.

We consider estimators that arise as zeros of modified score functions of the form $g(\theta_k; \check{\boldsymbol{\theta}}_{k^c}, \boldsymbol{\omega}_k) = \boldsymbol{\omega}_k^\top \nabla \ell_{\text{KLIEP}}(\theta_k; \boldsymbol{\theta}_{k^c})$, where $\check{\boldsymbol{\theta}}_{k^c}$ is a consistent, but not necessarily \sqrt{n} -consistent estimator of $\boldsymbol{\theta}_{k^c}^*$ and $\boldsymbol{\omega}_k \in \mathbb{R}^p$ is a fixed vector. g has the first-order Taylor expansion

$$\boldsymbol{\omega}_k^\top \nabla \ell_{\text{KLIEP}}(\theta_k; \check{\boldsymbol{\theta}}_{k^c}) = \boldsymbol{\omega}_k^\top \nabla \ell_{\text{KLIEP}}(\boldsymbol{\theta}^*) + \boldsymbol{\omega}_k^\top \nabla^2 \ell_{\text{KLIEP}}(\boldsymbol{\theta}^*) \begin{bmatrix} \theta_k - \theta_k^* \\ \check{\boldsymbol{\theta}}_{k^c} - \boldsymbol{\theta}_{k^c}^* \end{bmatrix} + \text{REM}. \quad (28)$$

In an oracle setting where the true nuisance parameter $\boldsymbol{\theta}_{k^c}^*$ is known, the choice $\boldsymbol{\omega}_k = \mathbf{e}_k$, which corresponds to the modified score function $g(\theta_k; \boldsymbol{\theta}_{k^c}^*, \mathbf{e}_k) = \nabla_k \ell_{\text{KLIEP}}(\theta_k; \boldsymbol{\theta}_{k^c}^*)$, leads to an approximately normal and unbiased estimation of θ_k^* . When $\boldsymbol{\theta}_{k^c}^*$ is unknown and has to be estimated from the data as well, $\boldsymbol{\theta}_{k^c}^*$ is replaced by an estimate $\check{\boldsymbol{\theta}}_{k^c}$ in the naive plug-in approach. This is acceptable when $\check{\boldsymbol{\theta}}_{k^c}$ is \sqrt{n} -consistent; for example, this would be the case in low dimensions with $n \gg p$. Unfortunately, this naive plug-in approach ceases to work when $\check{\boldsymbol{\theta}}_{k^c} \rightarrow \boldsymbol{\theta}_{k^c}^*$ at a rate slower than $n^{-1/2}$, which is typically the case for regularized estimators used in high dimensions. This is because estimation based on the modified score with $\boldsymbol{\omega}_k = \mathbf{e}_k$ is in general *not* insensitive to the error in $\check{\boldsymbol{\theta}}_{k^c}$. To see why, plug in $\boldsymbol{\omega}_k = \mathbf{e}_k$ in (28):

$$\begin{aligned} \nabla_k \ell_{\text{KLIEP}}(\theta_k; \check{\boldsymbol{\theta}}_{k^c}) &= \nabla_k \ell_{\text{KLIEP}}(\boldsymbol{\theta}^*) + \nabla_{kk}^2 \ell_{\text{KLIEP}}(\boldsymbol{\theta}^*) (\theta_k - \theta_k^*) \\ &\quad + \nabla_{kk^c}^2 \ell_{\text{KLIEP}}(\boldsymbol{\theta}^*) (\check{\boldsymbol{\theta}}_{k^c} - \boldsymbol{\theta}_{k^c}^*) + \text{REM}. \end{aligned} \quad (29)$$

As $n \rightarrow \infty$, $\nabla_{kk}^2 \ell_{\text{KLIEP}}(\boldsymbol{\theta}^*) \rightarrow \boldsymbol{\Sigma}_{\psi, kk}$ and $\nabla_{kk^c}^2 \ell_{\text{KLIEP}}(\boldsymbol{\theta}^*) \rightarrow \boldsymbol{\Sigma}_{\psi, kk^c}$, where $\boldsymbol{\Sigma}_\psi = \text{Cov}_x[\boldsymbol{\psi}(\mathbf{x})]$, by the Law of Large Numbers and Lemma 1. Thus, the estimator $\check{\theta}_k$, defined as a root of $g(\theta_k; \check{\boldsymbol{\theta}}_{k^c}, \mathbf{e}_k)$, has the asymptotic linear approximation

$$\sqrt{n} (\check{\theta}_k - \theta_k^*) = -\sqrt{n} \boldsymbol{\Sigma}_{\psi, kk}^{-1} \nabla_k \ell_{\text{KLIEP}}(\boldsymbol{\theta}^*) - \sqrt{n} \boldsymbol{\Sigma}_{\psi, kk}^{-1} \boldsymbol{\Sigma}_{\psi, kk^c} (\check{\boldsymbol{\theta}}_{k^c} - \boldsymbol{\theta}_{k^c}^*) + \text{REM}. \quad (30)$$

Looking at the right-hand side, although the first term $\sqrt{n} \boldsymbol{\Sigma}_{\psi, kk}^{-1} \nabla_k \ell_{\text{KLIEP}}(\boldsymbol{\theta}^*)$ is approximately mean-zero and normal, the same cannot be guaranteed for the second term $\sqrt{n} \boldsymbol{\Sigma}_{\psi, kk}^{-1} \boldsymbol{\Sigma}_{\psi, kk^c} (\check{\boldsymbol{\theta}}_{k^c} - \boldsymbol{\theta}_{k^c}^*)$ in many high-dimensional settings. Indeed, when $\check{\boldsymbol{\theta}}_{k^c}$ is given by the sparse KLIEP (4), we can only guarantee $\|\check{\boldsymbol{\theta}}_{k^c} - \boldsymbol{\theta}_{k^c}^*\|_1 \leq \sqrt{\|\boldsymbol{\theta}^*\|_0 \log p/n}$; this is insufficient if we are looking to use normal approximation as a basis of inference.

Comparing (28) and (29), it is clear that the reason that $\boldsymbol{\omega}_k = \mathbf{e}_k$ is a poor choice is because the nuisance components of $\boldsymbol{\Sigma}_\psi \mathbf{e}_k$ are in general nonzero, and hence, the product $\sqrt{n} \boldsymbol{\Sigma}_{\psi, kk^c} (\check{\boldsymbol{\theta}}_{k^c} - \boldsymbol{\theta}_{k^c}^*)$ is non-negligible whenever $\sqrt{n} (\check{\boldsymbol{\theta}}_{k^c} - \boldsymbol{\theta}_{k^c}^*)$ is non-negligible. Therefore, if $\boldsymbol{\omega}_k$ is chosen to satisfy $\boldsymbol{\Sigma}_\psi \boldsymbol{\omega}_k \approx \mathbf{e}_k$ instead — i.e., $\boldsymbol{\omega}_k$ approximates the k th column of the *inverse* of $\boldsymbol{\Sigma}_\psi$ — it would have the effect of counterbalancing the error in $\check{\boldsymbol{\theta}}_{k^c}$.

Of course, since $\boldsymbol{\Sigma}_\psi$ is itself an unknown parameter, $\boldsymbol{\omega}_k$ would have to be estimated from the data as well. However, the good news is that even in high-dimensions, it is often possible to find $\boldsymbol{\omega}_k$ satisfying

$$\{\nabla^2 \ell_{\text{KLIEP}}(\boldsymbol{\theta}^*) \boldsymbol{\omega}_k - \mathbf{e}_k\}^\top \begin{bmatrix} \hat{\theta}_k - \theta_k^* \\ \check{\boldsymbol{\theta}}_{k^c} - \boldsymbol{\theta}_{k^c}^* \end{bmatrix} = o_{\mathbb{P}}(n^{-1/2}), \quad (31)$$

provided that structural assumptions are reasonable for $\boldsymbol{\Sigma}_\psi^{-1}$.

With this ω_k , g has the first-order Taylor expansion

$$\begin{aligned} & \omega_k^\top \nabla \ell_{\text{KLIEP}}(\theta_k; \check{\theta}_{k^c}) \\ &= \omega_k^\top \nabla \ell_{\text{KLIEP}}(\theta^*) + (\theta_k - \theta_k^*) + \{\nabla^2 \ell_{\text{KLIEP}}(\theta^*) \omega_k - \mathbf{e}_k\}^\top \begin{bmatrix} \theta_k - \theta_k^* \\ \check{\theta}_{k^c} - \theta_{k^c}^* \end{bmatrix} + \text{REM}. \end{aligned} \quad (32)$$

The resulting estimator $\hat{\theta}_k$ then has the asymptotic linear approximation

$$\sqrt{n}(\hat{\theta}_k - \theta_k^*) = -\sqrt{n} \omega_k^\top \nabla \ell_{\text{KLIEP}}(\theta^*) - \sqrt{n} \{\nabla^2 \ell_{\text{KLIEP}}(\theta^*) \omega_k - \mathbf{e}_k\}^\top \begin{bmatrix} \hat{\theta}_k - \theta_k^* \\ \check{\theta}_{k^c} - \theta_{k^c}^* \end{bmatrix} + \text{REM}. \quad (33)$$

In contrast to (30), the bias terms in (33) are still vanishing after \sqrt{n} -scaling.

B.2 Proof of Theorem 1

Let $k \in [p]$. Let $\check{\theta}$ and $\check{\omega}_k$ denote the outputs of Steps 1 and 2 of Procedure 1. For $\lambda_\theta, \lambda_k, \delta_\theta, \delta_k, \delta_\sigma \in [0, 1)$, define an event

$$\mathcal{E}_{\text{one}} = \mathcal{E}_{\text{one}}(\lambda_\theta, \lambda_k, \delta_\theta, \delta_k, \delta_\sigma) = \left\{ \begin{array}{ll} \text{(G.1)} & 2\|\nabla \ell_{\text{KLIEP}}(\theta^*)\|_* \leq \lambda_\theta, \quad \text{(G.2)} & 2\|\nabla^2 \ell_{\text{KLIEP}}(\theta^*) \omega_k^* - \mathbf{e}_k\|_* \leq \lambda_k, \\ \text{(E.1)} & \|\check{\theta} - \theta^*\| \leq \delta_\theta, \quad \text{(E.2)} & \|\check{\omega}_k - \omega_k^*\| \leq \delta_k, \\ \text{(B.1)} & \left|1 - \frac{\widehat{Z}_y(\theta^*)}{Z_y(\theta^*)}\right| \lesssim \lambda_\theta, \quad \text{(B.2)} & \left|\frac{1}{n_y} \sum_{j=1}^{n_y} \langle \omega_k^*, \mu_\psi - \psi(\mathbf{y}^{(j)}) \rangle r_{\theta^*}(\mathbf{y}^{(j)})\right| \lesssim \lambda_k, \\ \text{(V.1)} & 4\|\widehat{\mathbf{S}}_\psi - \Sigma_\psi\|_* \leq \delta_\sigma, \quad \text{(V.2)} & 4\|\widehat{\mathbf{S}}_{\psi\widehat{r}}(\theta^*) - \Sigma_{\psi r}\|_* \leq \delta_\sigma \end{array} \right\}.$$

Theorem 5 (Re-statement of Theorem 1). *Assume Conditions 1 and 2. Let $\hat{\theta}_k$ be the estimator constructed by Procedure 1 with one-step approximation as*

$$\hat{\theta}_k = \check{\theta}_k - \check{\omega}_k^\top \nabla \ell_{\text{KLIEP}}(\check{\theta}).$$

Suppose $\mathbb{P}(\mathcal{E}_{\text{one}}) \geq 1 - \varepsilon_{\text{one},n}$ for some $\lambda_\theta, \lambda_k, \delta_\theta, \delta_k, \delta_\sigma \in [0, 1)$. Then,

$$\sup_{t \in \mathbb{R}} \left| \mathbb{P} \left\{ \sqrt{n}(\hat{\theta}_k - \theta_k^*) / \widehat{\sigma}_k \leq t \right\} - \Phi(t) \right| \leq \Delta_1 + \Delta_2 + \Delta_3 + \varepsilon_{\text{one},n},$$

where

$$\begin{aligned} \Delta_1 &\lesssim \sqrt{\frac{\bar{\kappa}^2 / \underline{\kappa}}{\eta_{x,n} \eta_{y,n}}} \frac{\|\omega_k^*\|}{\sqrt{n}}, \quad \Delta_2 \lesssim \sqrt{\frac{\eta_{x,n} \eta_{y,n}}{\underline{\kappa} / \bar{\kappa}^2}} ((\delta_\theta + \lambda_\theta)(\delta_k + \lambda_k) + \|\omega_k^*\| \delta_\theta^2) \sqrt{n}, \\ \Delta_3 &\lesssim (\bar{\kappa}^2 / \underline{\kappa}) \|\omega_k^*\|^2 (\delta_\sigma + \delta_\theta) + \delta_k^2. \end{aligned}$$

Proof. The proof combines two lemmas: a Berry-Esseen-type result for the leading linear term in the decomposition of $\sqrt{n}(\hat{\theta}_k - \theta_k^*)$ (Lemma 17) and a technical lemma for incorporating error bounds (Lemma 18).

Recall $\mu_\psi = \mathbb{E}_x[\psi(\mathbf{x})] = \mathbb{E}_y[\psi(\mathbf{y})r_{\theta^*}(\mathbf{y})]$. To use the lemmas, we break up $\hat{\theta}_k - \theta_k^*$ as

$$\hat{\theta}_k - \theta_k^* = A + B,$$

where

$$A = \frac{1}{n_x} \sum_{i=1}^{n_x} \langle \omega_k^*, \psi(\mathbf{x}^{(i)}) - \mu_\psi \rangle + \frac{1}{n_y} \sum_{j=1}^{n_y} \langle \omega_k^*, \mu_\psi - \psi(\mathbf{y}^{(j)}) \rangle r_{\theta^*}(\mathbf{y}^{(j)}),$$

and $B = (\hat{\theta}_k - \theta_k^*) - A$. Also, we let $C = (\widehat{\sigma}_k / \sigma_k) - 1$, so that

$$\sqrt{n}(\hat{\theta}_k - \theta_k^*) / \widehat{\sigma}_k = \sqrt{n} \{(A + B) / \sigma_k\} / (1 + C).$$

Since A is a sum of two i.i.d. sums, $\sqrt{n} A/\sigma_k$ is well-approximated by a Gaussian law. Indeed, Lemma 17 says

$$\sup_{t \in \mathbb{R}} |\mathbb{P} \{ \sqrt{n} A/\sigma_k \leq t \} - \Phi(t)| \lesssim \sqrt{\frac{\bar{\kappa}^2/\underline{\kappa}}{\eta_{x,n}\eta_{y,n}}} \frac{\|\boldsymbol{\omega}_k^*\|}{\sqrt{n}} := \Delta_1. \quad (34)$$

The remainder of the proof is about obtaining the bounds δ_B , δ_C , and ε_{BC} that can be used with Lemma 18.

First, we need an exact expression for B . By definition,

$$\begin{aligned} \widehat{\boldsymbol{\theta}}_k &= \check{\boldsymbol{\theta}}_k - \check{\boldsymbol{\omega}}_k^\top \nabla \ell_{\text{KLIEP}}(\check{\boldsymbol{\theta}}) \\ &= \check{\boldsymbol{\theta}}_k - \boldsymbol{\omega}_k^{*\top} \nabla \ell_{\text{KLIEP}}(\check{\boldsymbol{\theta}}) - (\check{\boldsymbol{\omega}}_k - \boldsymbol{\omega}_k^*)^\top \nabla \ell_{\text{KLIEP}}(\check{\boldsymbol{\theta}}). \end{aligned} \quad (35)$$

Expand $\check{\boldsymbol{\theta}}_k - \boldsymbol{\omega}_k^{*\top} \nabla \ell_{\text{KLIEP}}(\check{\boldsymbol{\theta}})$ about $\boldsymbol{\theta}^*$:

$$\check{\boldsymbol{\theta}}_k - \boldsymbol{\omega}_k^{*\top} \nabla \ell_{\text{KLIEP}}(\check{\boldsymbol{\theta}}) = \boldsymbol{\theta}_k^* - \boldsymbol{\omega}_k^{*\top} \nabla \ell_{\text{KLIEP}}(\boldsymbol{\theta}^*) - \{ \nabla^2 \ell_{\text{KLIEP}}(\boldsymbol{\theta}^*) \boldsymbol{\omega}_k^* - \mathbf{e}_k \}^\top (\check{\boldsymbol{\theta}} - \boldsymbol{\theta}^*) - \boldsymbol{\omega}_k^{*\top} \mathbf{r}, \quad (36)$$

where by Taylor's theorem, \mathbf{r} is given by

$$r_k = \frac{1}{2} \sum_{k''=1}^p \sum_{k'=1}^p \left\{ \int_0^1 (1-t) \partial_{k''k'}^3 \ell_{\text{KLIEP}}(\boldsymbol{\theta}^* + t(\check{\boldsymbol{\theta}} - \boldsymbol{\theta}^*)) dt \right\} (\check{\boldsymbol{\theta}}_{k''} - \boldsymbol{\theta}_{k''}^*) (\check{\boldsymbol{\theta}}_{k'} - \boldsymbol{\theta}_{k'}^*).$$

Combining (35) and (36), and rearranging,

$$\begin{aligned} \widehat{\boldsymbol{\theta}}_k - \boldsymbol{\theta}_k^* &= -\boldsymbol{\omega}_k^{*\top} \nabla \ell_{\text{KLIEP}}(\boldsymbol{\theta}^*) \\ &\quad - (\check{\boldsymbol{\omega}}_k - \boldsymbol{\omega}_k^*)^\top \nabla \ell_{\text{KLIEP}}(\check{\boldsymbol{\theta}}) - \{ \nabla^2 \ell_{\text{KLIEP}}(\boldsymbol{\theta}^*) \boldsymbol{\omega}_k^* - \mathbf{e}_k \}^\top (\check{\boldsymbol{\theta}} - \boldsymbol{\theta}^*) - \boldsymbol{\omega}_k^{*\top} \mathbf{r}. \end{aligned}$$

The leading term is

$$\begin{aligned} \boldsymbol{\omega}_k^{*\top} \nabla \ell_{\text{KLIEP}}(\boldsymbol{\theta}^*) &= \left\langle \boldsymbol{\omega}_k^*, \frac{1}{n_x} \sum_{i=1}^{n_x} \boldsymbol{\psi}(\mathbf{x}^{(i)}) - \frac{1}{n_y} \sum_{j=1}^{n_y} \boldsymbol{\psi}(\mathbf{y}^{(j)}) \widehat{r}_{\boldsymbol{\theta}^*}(\mathbf{y}^{(j)}) \right\rangle \\ &= \left\langle \boldsymbol{\omega}_k^*, \frac{1}{n_x} \sum_{i=1}^{n_x} (\boldsymbol{\psi}(\mathbf{x}^{(i)}) - \boldsymbol{\mu}_\psi) + \frac{1}{n_y} \sum_{j=1}^{n_y} (\boldsymbol{\mu}_\psi - \boldsymbol{\psi}(\mathbf{y}^{(j)})) \widehat{r}_{\boldsymbol{\theta}^*}(\mathbf{y}^{(j)}) \right\rangle \\ &= \left\langle \boldsymbol{\omega}_k^*, \frac{1}{n_x} \sum_{i=1}^{n_x} (\boldsymbol{\psi}(\mathbf{x}^{(i)}) - \boldsymbol{\mu}_\psi) + \frac{Z_y(\boldsymbol{\theta}^*)}{\widehat{Z}_y(\boldsymbol{\theta}^*)} \cdot \frac{1}{n_y} \sum_{j=1}^{n_y} (\boldsymbol{\mu}_\psi - \boldsymbol{\psi}(\mathbf{y}^{(j)})) r_{\boldsymbol{\theta}^*}(\mathbf{y}^{(j)}) \right\rangle \\ &= \left\langle \boldsymbol{\omega}_k^*, \frac{1}{n_x} \sum_{i=1}^{n_x} (\boldsymbol{\psi}(\mathbf{x}^{(i)}) - \boldsymbol{\mu}_\psi) + \frac{1}{n_y} \sum_{j=1}^{n_y} (\boldsymbol{\mu}_\psi - \boldsymbol{\psi}(\mathbf{y}^{(j)})) r_{\boldsymbol{\theta}^*}(\mathbf{y}^{(j)}) \right\rangle \\ &\quad + \left(\frac{Z_y(\boldsymbol{\theta}^*)}{\widehat{Z}_y(\boldsymbol{\theta}^*)} - 1 \right) \frac{1}{n_y} \sum_{j=1}^{n_y} \langle \boldsymbol{\omega}_k^*, \boldsymbol{\mu}_\psi - \boldsymbol{\psi}(\mathbf{y}^{(j)}) \rangle r_{\boldsymbol{\theta}^*}(\mathbf{y}^{(j)}), \end{aligned}$$

where in the second step, we have used $n_y^{-1} \sum_{j=1}^{n_y} \widehat{r}_{\boldsymbol{\theta}^*}(\mathbf{y}^{(j)}) \equiv 1$ for any $\boldsymbol{\theta}$. Recognizing A as the first term of the last line, we have

$$\begin{aligned} B &= \underbrace{\left(\frac{Z_y(\boldsymbol{\theta}^*)}{\widehat{Z}_y(\boldsymbol{\theta}^*)} - 1 \right) \frac{1}{n_y} \sum_{j=1}^{n_y} \langle \boldsymbol{\omega}_k^*, \boldsymbol{\mu}_\psi - \boldsymbol{\psi}(\mathbf{y}^{(j)}) \rangle r_{\boldsymbol{\theta}^*}(\mathbf{y}^{(j)})}_{B_0} \\ &\quad - \underbrace{(\check{\boldsymbol{\omega}}_k - \boldsymbol{\omega}_k^*)^\top \nabla \ell_{\text{KLIEP}}(\check{\boldsymbol{\theta}})}_{B_1} - \underbrace{\{ \nabla^2 \ell_{\text{KLIEP}}(\boldsymbol{\theta}^*) \boldsymbol{\omega}_k^* - \mathbf{e}_k \}^\top (\check{\boldsymbol{\theta}} - \boldsymbol{\theta}^*)}_{B_2} - \underbrace{\boldsymbol{\omega}_k^{*\top} \mathbf{r}}_{B_3}. \end{aligned}$$

We proceed to bound $|B|$ on \mathcal{E}_{one} using the defining conditions. (B.1) and (B.2) imply a bound on B_0 :

$$\begin{aligned}
|B_0| &= \left| \left(\frac{Z_y(\boldsymbol{\theta}^*)}{\widehat{Z}_y(\boldsymbol{\theta}^*)} - 1 \right) \frac{1}{n_y} \sum_{j=1}^{n_y} \langle \boldsymbol{\omega}_k^*, \boldsymbol{\mu}_\psi - \boldsymbol{\psi}(\mathbf{y}^{(j)}) \rangle r_{\theta^*}(\mathbf{y}^{(j)}) \right| \\
&= \left| \frac{Z_y(\boldsymbol{\theta}^*)}{\widehat{Z}_y(\boldsymbol{\theta}^*)} \right| \left| 1 - \frac{\widehat{Z}_y(\boldsymbol{\theta}^*)}{Z_y(\boldsymbol{\theta}^*)} \right| \left| \frac{1}{n_y} \sum_{j=1}^{n_y} \langle \boldsymbol{\omega}_k^*, \boldsymbol{\mu}_\psi - \boldsymbol{\psi}(\mathbf{y}^{(j)}) \rangle r_{\theta^*}(\mathbf{y}^{(j)}) \right| \leq K_1 \lambda_\theta \lambda_k, \quad (37)
\end{aligned}$$

because $Z_y(\boldsymbol{\theta}^*)/\widehat{Z}_y(\boldsymbol{\theta}^*) \in [M_r^{-1}, M_r]$ under Condition 1. B_1 is further decomposed as

$$B_1 = \underbrace{(\check{\boldsymbol{\omega}}_k - \boldsymbol{\omega}_k^*)^\top \nabla \ell_{\text{KLIEP}}(\boldsymbol{\theta}^*)}_{B_{11}} + \underbrace{(\check{\boldsymbol{\omega}}_k - \boldsymbol{\omega}_k^*)^\top (\nabla \ell_{\text{KLIEP}}(\check{\boldsymbol{\theta}}) - \nabla \ell_{\text{KLIEP}}(\boldsymbol{\theta}^*))}_{B_{12}}.$$

Using (G.1) and (E.2) for (38), and (G.2) and (E.1) for (39),

$$|B_{11}| \leq \|\check{\boldsymbol{\omega}}_k - \boldsymbol{\omega}_k^*\| \|\nabla \ell_{\text{KLIEP}}(\boldsymbol{\theta}^*)\|_* \leq \lambda_\theta \delta_k, \quad (38)$$

$$|B_{12}| \leq \|\nabla^2 \ell_{\text{KLIEP}}(\boldsymbol{\theta}^*) \boldsymbol{\omega}_k^* - \mathbf{e}_k\|_* \|\check{\boldsymbol{\theta}} - \boldsymbol{\theta}^*\| \leq \lambda_k \delta_\theta. \quad (39)$$

For B_{12} , we use the mean value theorem to express each component of $\nabla \ell_{\text{KLIEP}}(\check{\boldsymbol{\theta}}) - \nabla \ell_{\text{KLIEP}}(\boldsymbol{\theta}^*)$ as

$$\partial_k \ell_{\text{KLIEP}}(\check{\boldsymbol{\theta}}) - \partial_k \ell_{\text{KLIEP}}(\boldsymbol{\theta}^*) = \sum_{k'=1}^p \partial_{k'}^2 \ell_{\text{KLIEP}}(\bar{\boldsymbol{\theta}}_k) (\check{\theta}_{k'} - \theta_{k'}^*),$$

where $\bar{\boldsymbol{\theta}}_k$ is on the line segment connecting $\check{\boldsymbol{\theta}}$ and $\boldsymbol{\theta}^*$. Using (24), this can be written as

$$\begin{aligned}
&\partial_k \ell_{\text{KLIEP}}(\check{\boldsymbol{\theta}}) - \partial_k \ell_{\text{KLIEP}}(\boldsymbol{\theta}^*) \\
&= \sum_{k'=1}^p \left\{ \frac{1}{n_y} \sum_{j=1}^{n_y} \widehat{r}_{\bar{\boldsymbol{\theta}}_k}(\mathbf{y}^{(j)}) \psi_k(\mathbf{y}_k^{(j)}) \psi_{k'}(\mathbf{y}_{k'}^{(j)}) - \widehat{\mu}_k(\bar{\boldsymbol{\theta}}_k) \widehat{\mu}_{k'}(\bar{\boldsymbol{\theta}}_k) \right\} (\check{\theta}_{k'} - \theta_{k'}^*) \\
&= \frac{1}{n_y} \sum_{j=1}^{n_y} \widehat{r}_{\bar{\boldsymbol{\theta}}_k}(\mathbf{y}^{(j)}) \psi_k(\mathbf{y}_k^{(j)}) \left\{ \sum_{k'=1}^p \psi_{k'}(\mathbf{y}_{k'}^{(j)}) (\check{\theta}_{k'} - \theta_{k'}^*) \right\} - \widehat{\mu}_k(\bar{\boldsymbol{\theta}}_k) \left\{ \sum_{k'=1}^p \widehat{\mu}_{k'}(\bar{\boldsymbol{\theta}}_k) (\check{\theta}_{k'} - \theta_{k'}^*) \right\}.
\end{aligned}$$

Under Condition 1,

$$\sum_{k'=1}^p \psi_{k'}(\mathbf{y}_{k'}^{(j)}) (\check{\theta}_{k'} - \theta_{k'}^*) \leq M_\psi \|\check{\boldsymbol{\theta}} - \boldsymbol{\theta}^*\| \quad \text{and} \quad \sum_{k'=1}^p \widehat{\mu}_{k'}(\bar{\boldsymbol{\theta}}_k) (\check{\theta}_{k'} - \theta_{k'}^*) \leq M_\psi M_r^2 \|\check{\boldsymbol{\theta}} - \boldsymbol{\theta}^*\|,$$

so that

$$\|\nabla \ell_{\text{KLIEP}}(\check{\boldsymbol{\theta}}) - \nabla \ell_{\text{KLIEP}}(\boldsymbol{\theta}^*)\|_* \leq K_2 \|\check{\boldsymbol{\theta}} - \boldsymbol{\theta}^*\|.$$

With (E.1) and (E.2),

$$|B_{12}| \leq \|\check{\boldsymbol{\omega}}_k - \boldsymbol{\omega}_k^*\| \|\nabla \ell_{\text{KLIEP}}(\check{\boldsymbol{\theta}}) - \nabla \ell_{\text{KLIEP}}(\boldsymbol{\theta}^*)\|_* \leq K_2 \delta_\theta \delta_k. \quad (40)$$

We turn to B_3 . Under Condition 1, (26) implies a uniform bound on the third-order tensor, so

$$|B_3| \leq \|\boldsymbol{\omega}_k^*\| \|\mathbf{r}\|_* \leq K_3 \|\boldsymbol{\omega}_k^*\| \delta_\theta^2. \quad (41)$$

Combining (37) to (41),

$$\sqrt{n} |B| / \sigma_k \lesssim \sqrt{\frac{\eta_x \cdot n \eta_y \cdot n}{\underline{\kappa} / \bar{\kappa}^2}} ((\delta_\theta + \lambda_\theta)(\delta_k + \lambda_k) + \|\boldsymbol{\omega}_k^*\| \delta_\theta^2) \sqrt{n} := \Delta_2. \quad (42)$$

Next, we bound $|C|$ on \mathcal{E}_{one} . Using (E.1), (E.2), (V.1), (V.2),

$$\left| \frac{\widehat{\sigma}_k}{\sigma_k} - 1 \right| \leq \left| \frac{\widehat{\sigma}_k^2 - \sigma_k^2}{\sigma_k^2} \right| \lesssim (\bar{\kappa}^2 / \underline{\kappa}) \|\boldsymbol{\omega}_k^*\|^2 (\delta_\sigma + \delta_\theta) + \delta_k^2 := \Delta_3 \quad (43)$$

by Lemma 19.

Taking $A = \sqrt{n} A / \sigma_k$, $B = \sqrt{n} B / \sigma_k$, $C = (\widehat{\sigma}_k / \sigma_k) - 1$, $\varepsilon_A = \Delta_1$, $\delta_B = \Delta_2$, $\delta_C = \Delta_3$, $\varepsilon_{BC} = \varepsilon_{\text{one}}$ in Lemma 18 concludes the proof. \square

Remark 6. In the last step, one could just as well apply Lemma 18 with $A = \sqrt{n} A/\sigma_k$, $B = \sqrt{n} B/\sigma_k$, $C = 0$, $\varepsilon_A = \Delta_1$, $\delta_B = \Delta_2$, $\delta_C = 0$, $\varepsilon_{BC} = \varepsilon_{\text{one}}$ to end up with

$$\sup_{t \in \mathbb{R}} \left| \mathbb{P} \left\{ \sqrt{n} (\hat{\theta}_k - \theta_k^*)/\sigma_k \leq t \right\} - \Phi(t) \right| \leq \Delta_1 + \Delta_2 + \varepsilon_{\text{one}},$$

but this result is not as useful.

B.3 Proof of Theorem 3

For $k = 1, \dots, p$, let

$$\widehat{L}_{n_x, n_y, k}^B = -\frac{1}{\sqrt{n}} \check{\omega}_k^\top \left\{ \eta_{x,n}^{-1} \sum_{i=1}^{n_x} (\psi(\mathbf{x}^{(i)}) - \bar{\psi}) \xi_x^{(i)} - \eta_{y,n}^{-1} \sum_{j=1}^{n_y} (\psi(\mathbf{y}^{(j)}) \widehat{r}_{\check{\theta}}(\mathbf{y}^{(j)}) - \widehat{\mu}(\check{\theta})) \xi_y^{(j)} \right\}, \quad (44)$$

where $\check{\theta}$ is a consistent estimator of θ , and

$$\xi_x^{(1)}, \dots, \xi_x^{(n_x)}, \xi_y^{(1)}, \dots, \xi_y^{(n_y)} \stackrel{iid}{\sim} \mathcal{N}(0, 1).$$

Note that

$$\bar{\psi} = \frac{1}{n_x} \sum_{i=1}^{n_x} \psi(\mathbf{x}^{(i)}) \quad \text{and} \quad \widehat{\mu}(\check{\theta}) = \frac{1}{n_y} \sum_{j=1}^{n_y} \psi(\mathbf{y}^{(j)}) \widehat{r}_{\check{\theta}}(\mathbf{y}^{(j)})$$

are the two components of $\nabla \ell_{\text{KLIEP}}(\check{\theta})$. The centering is necessary for variance-matching, because $\nabla \ell_{\text{KLIEP}}(\check{\theta}) \neq \mathbf{0}$ for high-dimensional estimators. In terms of (44), the statistic to be bootstrapped is written as

$$\widehat{T}_{n_x, n_y} = \max_k |\widehat{L}_{n_x, n_y, k}^B|.$$

The multiplier bootstrap scheme presupposes that the conditional distribution of $\widehat{L}_{n_x, n_y, k}^B$ is a good proxy for the distribution of $\sqrt{n} (\hat{\theta}_k - \theta_k^*)$. It is not difficult to imagine that the conditional distribution of $\widehat{L}_{n_x, n_y, k}^B$ is a good proxy for the distribution of $L_{n_x, n_y, k}$, where

$$L_{n_x, n_y, k} = -\frac{1}{\sqrt{n}} \omega_k^{*\top} \left\{ \eta_{x,n}^{-1} \sum_{i=1}^{n_x} (\psi(\mathbf{x}^{(i)}) - \mu_\psi) - \eta_{y,n}^{-1} \sum_{j=1}^{n_y} (\psi(\mathbf{y}^{(j)}) r_{\theta^*}(\mathbf{y}^{(j)}) - \mu_\psi) \right\}.$$

Because $L_{n_x, n_y, k}$ is the leading term in the first-order Taylor approximation of $\sqrt{n} (\hat{\theta}_k - \theta_k^*)$, the distribution of the former is also close to the distribution of the latter, and hence, the conditional distribution of $\widehat{L}_{n_x, n_y, k}^B$ can be used to estimate the quantiles of $\sqrt{n} (\hat{\theta}_k - \theta_k^*)$.

Let Σ_{pooled} be defined as in (11), and let $\Omega^* = \Sigma_\psi^{-1}$. Recall that the k th column of Ω^* is ω_k^* . For $\lambda_\theta, (\lambda_k)_{k=1}^p, \delta_\theta, (\delta_k)_{k=1}^p \in [0, 1]$, define an event

$$\mathcal{E}_{\text{all}} = \mathcal{E}_{\text{all}}(\lambda_\theta, (\lambda_k)_{k=1}^p, \delta_\theta, (\delta_k)_{k=1}^p) = \left\{ \begin{array}{ll} \text{(G.1)} & 2 \|\nabla \ell_{\text{KLIEP}}(\theta^*)\|_* \leq \lambda_\theta, & \text{(G.2)} & 2 \|\nabla^2 \ell_{\text{KLIEP}}(\theta^*) \omega_k^* - \mathbf{e}_k\|_* \leq \lambda_k \quad \forall k, \\ \text{(E.1)} & \|\check{\theta} - \theta^*\| \leq \delta_\theta, & \text{(E.2)} & \|\check{\omega}_k - \omega_k^*\| \leq \delta_k \quad \forall k, \\ \text{(B.1)} & \left| 1 - \frac{\widehat{Z}_y(\theta^*)}{Z_y(\theta^*)} \right| \lesssim \lambda_\theta, & \text{(B.2)} & \left| \frac{1}{n_y} \sum_{j=1}^{n_y} \langle \omega_k^*, \mu_\psi - \psi(\mathbf{y}^{(j)}) r_{\theta^*}(\mathbf{y}^{(j)}) \rangle \right| \lesssim \lambda_k \quad \forall k \end{array} \right\}.$$

Put $\nu_n = 1 \vee \max\{\|\omega_k^*\| : k = 1, \dots, p\}$, and set

$$B_n = \frac{(1 \vee \bar{\kappa})^3 (1 \vee M_\psi)^3 M_r^3 \nu_n^{21/2}}{\sqrt{\underline{\kappa}^3 \eta_{x,n} \eta_{y,n}}} \quad \text{and} \quad \delta_n = \left(\frac{B_n^2 \log^7(pn)}{n} \right)^{1/6}.$$

Theorem 6 (Re-statement of Theorem 3). *Assume Conditions 1 and 2. Let $\widehat{\boldsymbol{\theta}}$ be the estimator constructed by Procedure 1 with one-step approximation as*

$$\widehat{\boldsymbol{\theta}} = \check{\boldsymbol{\theta}} - \check{\boldsymbol{\Omega}}^\top \nabla \ell_{KLIEP}(\check{\boldsymbol{\theta}}),$$

where $\check{\boldsymbol{\Omega}} = [\check{\boldsymbol{\omega}}_k]_{k=1}^p \in \mathbb{R}^{p \times p}$ is the matrix with the k th column given by $\check{\boldsymbol{\omega}}_k$. Suppose

$$D_1 := \max_k \sqrt{\frac{\eta_{x,n} \eta_{y,n}}{\underline{\kappa}/\bar{\kappa}^2}} \left((\delta_\theta + \lambda_\theta)(\delta_k + \lambda_k) + \|\boldsymbol{\omega}_k^*\| \delta_\theta^2 \right) \sqrt{n} \lesssim \left(\frac{B_n^2 \log^4(pn)}{n} \right)^{1/6},$$

$$D_2 := \max_k \frac{\kappa/\bar{\kappa}^2}{\eta_{x,n}^2 \eta_{y,n}^2} \left(\delta_k^2 + \eta_{x,n} \|\boldsymbol{\omega}_k\|^2 (\delta_\theta + \lambda_\theta)^2 \right) \lesssim \left(\frac{B_n^2 \log(pn)}{n} \right)^{1/3}.$$

If $\mathbb{P}(\mathcal{E}_{all}) \geq 1 - \varepsilon_{all,n}$, then

$$\sup_{\alpha \in (0,1)} \left| \mathbb{P} \{ T_{n_x, n_y} \leq \widehat{c}_{T,\alpha} \} - (1 - \alpha) \right| = O(\delta_n + \varepsilon_{all,n})$$

with probability at least $1 - \varepsilon_{all,n} - n^{-1}$.

Proof. We prove the result for the case where $\boldsymbol{\mu}_\psi = \mathbb{E}_x[\boldsymbol{\psi}(\mathbf{x})] = \mathbb{E}_y[\boldsymbol{\psi}(\mathbf{y})r_{\theta^*}(\mathbf{y})] = \mathbf{0}$. The general result follows by the consistency of empirical averages.

The proof is by Theorems 2.1 and 2.2 of Belloni et al. (2018). The two theorems are Gaussian approximation results for approximate means over the class \mathcal{A} of hyper-rectangles in \mathbb{R}^p , in other words, \mathcal{A} contains sets of the form

$$A = \{ \mathbf{v} \in \mathbb{R}^p : l_k \leq v_k \leq u_k \text{ for all } k = 1, \dots, p \},$$

where $-\infty \leq l_k \leq u_k \leq +\infty$ for all k . In the proof of Theorem 1, we saw that $\sqrt{n}(\widehat{\boldsymbol{\theta}} - \boldsymbol{\theta}^*)$ may be decomposed as

$$\sqrt{n}(\widehat{\boldsymbol{\theta}} - \boldsymbol{\theta}^*) = L_n + R_n,$$

where the leading linear term has the form

$$L_n = -\frac{1}{\sqrt{n}} \boldsymbol{\Omega}^{*\top} \left\{ \eta_{x,n}^{-1} \sum_{i=1}^{n_x} \boldsymbol{\psi}(\mathbf{x}^{(i)}) - \eta_{y,n}^{-1} \sum_{j=1}^{n_y} \boldsymbol{\psi}(\mathbf{y}^{(j)}) r_{\theta^*}(\mathbf{y}^{(j)}) \right\}$$

and the remainder is given by

$$R_n = \sqrt{n} \left\{ \boldsymbol{\Omega}^{*\top} \left(\frac{Z_y(\boldsymbol{\theta}^*)}{\widehat{Z}_y(\boldsymbol{\theta}^*)} - 1 \right) \frac{1}{n_y} \sum_{j=1}^{n_y} \boldsymbol{\psi}(\mathbf{y}^{(j)}) r_{\theta^*}(\mathbf{y}^{(j)}) \right. \\ \left. - \{ \check{\boldsymbol{\Omega}} - \boldsymbol{\Omega}^* \}^\top \nabla \ell_{KLIEP}(\check{\boldsymbol{\theta}}) - \{ \nabla^2 \ell_{KLIEP}(\boldsymbol{\theta}^*) \boldsymbol{\Omega}^* - \mathbf{I} \}^\top (\check{\boldsymbol{\theta}} - \boldsymbol{\theta}^*) + \boldsymbol{\Omega}^{*\top} \mathbf{r} \right\}.$$

This demonstrates that our problem also falls under the approximate means framework.

Let $\mathbf{P} = \mathbb{P}[\cdot \mid \mathbf{X}_{n_x}, \mathbf{Y}_{n_y}]$ denote the conditional probability given the data. If applicable, Theorem 2.1 would give us

$$\sup_{A \in \mathcal{A}} \left| \mathbb{P} \left\{ \sqrt{n}(\widehat{\boldsymbol{\theta}} - \boldsymbol{\theta}^*) \in A \right\} - \mathbb{P} \left\{ \mathcal{N}(\mathbf{0}, \boldsymbol{\Omega}^{*\top} \boldsymbol{\Sigma}_{\text{pooled}} \boldsymbol{\Omega}^*) \in A \right\} \right| = O(\delta_n + \varepsilon_{all,n}),$$

and Theorem 2.2 would give us

$$\sup_{A \in \mathcal{A}} \left| \mathbf{P} \left\{ \widehat{L}_n^B \in A \right\} - \mathbb{P} \left\{ \mathcal{N}(\mathbf{0}, \boldsymbol{\Omega}^{*\top} \boldsymbol{\Sigma}_{\text{pooled}} \boldsymbol{\Omega}^*) \in A \right\} \right| = O(\delta_n)$$

with probability at least $1 - \varepsilon_{all,n} - n^{-1}$. Combining the two statements,

$$\sup_{A \in \mathcal{A}} \left| \mathbb{P} \left\{ \sqrt{n}(\widehat{\boldsymbol{\theta}} - \boldsymbol{\theta}^*) \in A \right\} - \mathbf{P} \left\{ \widehat{L}_n^B \in A \right\} \right| = O(\delta_n + \varepsilon_{all,n}) \quad (45)$$

with probability at least $1 - \varepsilon_{\text{all},n} - n^{-1}$. Once (45) is established for \mathcal{A} , then *a fortiori* (45) is established for the sub-collection

$$A = \left\{ \mathbf{v} \in \mathbb{R}^p : \max_k |v_k| \leq t \text{ for all } k = 1, \dots, p \right\},$$

so that in particular

$$\sup_{A \in \mathcal{A}} \left| \mathbb{P} \{ T_{n_x, n_y} \leq \widehat{c}_{T, \alpha} \} - (1 - \alpha) \right| = O(\delta_n + \varepsilon_{\text{all},n}), \quad (46)$$

which is the statement of the theorem.

Thus, in a nutshell, our work here boils down to checking that our problem satisfies the conditions of Theorems 2.1 and 2.2 of Belloni et al. (2018) — Conditions M, E, and A — which we restate in context below.

Before we proceed, let

$$\widehat{L}_n = -\frac{1}{\sqrt{n}} \check{\Omega}^\top \left\{ \eta_{x,n}^{-1} \sum_{i=1}^{n_x} \boldsymbol{\psi}(\mathbf{x}^{(i)}) - \eta_{y,n}^{-1} \sum_{j=1}^{n_y} \boldsymbol{\psi}(\mathbf{y}^{(j)}) \widehat{r}_{\widehat{\theta}}(\mathbf{y}^{(j)}) \right\}.$$

This is a feasible approximation to L_n , and this is what we actually bootstrap as \widehat{L}_n^B .

Condition M. Translated to our problem, Condition M of Belloni et al. (2018) is

$$\text{Var}[L_{n,k}] = \boldsymbol{\omega}_k^{*\top} \{ \eta_{x,n}^{-1} \boldsymbol{\Sigma}_\psi + \eta_{y,n}^{-1} \boldsymbol{\Sigma}_{\psi r} \} \boldsymbol{\omega}_k^* \geq c \text{ for some } c > 0, \quad (47)$$

$$\eta_{x,n}^{-2} \mathbb{E}_x [|\boldsymbol{\omega}_k^{*\top} \boldsymbol{\psi}(\mathbf{x})|^3] + \eta_{y,n}^{-2} \mathbb{E}_y [|\boldsymbol{\omega}_k^{*\top} \boldsymbol{\psi}(\mathbf{y}) r_{\theta^*}(\mathbf{y})|^3] \leq c^{3/2} B_n, \quad (48)$$

$$\eta_{x,n}^{-3} \mathbb{E}_x [|\boldsymbol{\omega}_k^{*\top} \boldsymbol{\psi}(\mathbf{x})|^4] + \eta_{y,n}^{-3} \mathbb{E}_y [|\boldsymbol{\omega}_k^{*\top} \boldsymbol{\psi}(\mathbf{y}) r_{\theta^*}(\mathbf{y})|^4] \leq c^2 B_n^2 \quad (49)$$

for each $k \in [p]$.

Under Condition 2, (86) says

$$\text{Var}[L_{n,k}] = \boldsymbol{\omega}_k^{*\top} \{ \eta_{x,n}^{-1} \boldsymbol{\Sigma}_\psi + \eta_{y,n}^{-1} \boldsymbol{\Sigma}_{\psi r} \} \boldsymbol{\omega}_k^* \geq \underline{\kappa} / (\bar{\kappa}^2 \eta_{x,n} \eta_{y,n}) \quad \forall k.$$

Thus, (47) is satisfied with $c = \underline{\kappa} / (\bar{\kappa}^2 \eta_{x,n} \eta_{y,n})$.

By (85), for all k ,

$$|\boldsymbol{\omega}_k^{*\top} \boldsymbol{\psi}(\mathbf{x})| \leq M_\psi \|\boldsymbol{\omega}_k^*\| \quad (50)$$

and

$$|\boldsymbol{\omega}_k^{*\top} \boldsymbol{\psi}(\mathbf{y}) r_{\theta^*}(\mathbf{y})| \leq M_r M_\psi \|\boldsymbol{\omega}_k^*\|. \quad (51)$$

So,

$$c^{-3/2} (\eta_{x,n}^{-2} \mathbb{E}_x [|\boldsymbol{\omega}_k^{*\top} \boldsymbol{\psi}(\mathbf{x})|^3] + \eta_{y,n}^{-2} \mathbb{E}_y [|\boldsymbol{\omega}_k^{*\top} \boldsymbol{\psi}(\mathbf{y}) r_{\theta^*}(\mathbf{y})|^3]) \leq \frac{\bar{\kappa}^3 M_r^3 M_\psi^3 \nu_n^3}{\sqrt{\underline{\kappa}^3 \eta_{x,n} \eta_{y,n}}} \leq B_n$$

and

$$c^{-2} (\eta_{x,n}^{-3} \mathbb{E}_x [|\boldsymbol{\omega}_k^{*\top} \boldsymbol{\psi}(\mathbf{x})|^4] + \eta_{y,n}^{-3} \mathbb{E}_y [|\boldsymbol{\omega}_k^{*\top} \boldsymbol{\psi}(\mathbf{y}) r_{\theta^*}(\mathbf{y})|^4]) \leq \frac{\bar{\kappa}^4 M_r^4 M_\psi^4 \nu_n^4}{\underline{\kappa}^2 \eta_{x,n} \eta_{y,n}} \leq B_n^2.$$

Thus, both (48) and (49) are satisfied with B_n as defined in Section 4.3.

Condition E. Translated to our problem, Condition E of Belloni et al. (2018) is

$$\mathbb{E}_x \left[\exp \left\{ |\boldsymbol{\omega}_k^{*\top} \boldsymbol{\psi}(\mathbf{x})| / \left(\eta_{x,n} c^{1/2} B_n \right) \right\} \right] \leq 2$$

and

$$\mathbb{E}_y \left[\exp \left\{ |\boldsymbol{\omega}_k^{*\top} \boldsymbol{\psi}(\mathbf{y}) r_{\theta^*}(\mathbf{y})| / \left(\eta_{y,n} c^{1/2} B_n \right) \right\} \right] \leq 2$$

with

$$\left(\frac{B_n^2 \log^7(pn)}{n} \right)^{1/6} \leq \delta_n.$$

But these are all immediate by (50), (51), and how we defined B_n and δ_n in Section 4.3.

Condition A. Translated to our problem, Condition A of Belloni et al. (2018) is

$$\mathbb{P} \left\{ \max_k |R_{n,k}| > c^{1/2} \delta_n / \sqrt{\log(pn)} \right\} \leq \varepsilon_{\text{all},n} \quad (52)$$

and

$$\mathbb{P} \left\{ \max_k v_k^2 > c \delta_n^2 / \log^2(pn) \right\} \leq \varepsilon_{\text{all},n} \quad (53)$$

where

$$\begin{aligned} v_k^2 = v_{x,k}^2 + v_{y,k}^2 &= \frac{\eta_{x,n}^{-1}}{n_x} \sum_{i=1}^{n_x} \langle \tilde{\omega}_k - \omega_k^*, \psi(\mathbf{x}^{(i)}) \rangle^2 \\ &\quad + \frac{\eta_{y,n}^{-1}}{n_y} \sum_{j=1}^{n_y} \left(\langle \tilde{\omega}_k, \psi(\mathbf{y}^{(j)}) \widehat{r}_{\tilde{\theta}}(\mathbf{y}^{(j)}) \rangle - \langle \omega_k^*, \psi(\mathbf{y}^{(j)}) r_{\theta^*}(\mathbf{y}^{(j)}) \rangle \right)^2. \end{aligned}$$

We saw in the proof of Theorem 1 that on \mathcal{E}_{all} ,

$$c^{-1/2} |R_{n,k}| \lesssim \sqrt{\frac{\eta_{x,n} \eta_{y,n}}{\underline{\kappa} / \bar{\kappa}^2}} ((\delta_\theta + \lambda_\theta)(\delta_k + \lambda_k) + \|\omega_k^*\| \delta_\theta^2) \sqrt{n} \quad \forall k.$$

Under the conditions of the theorem,

$$c^{-1/2} |R_{n,k}| \lesssim \left(\frac{B_n^2 \log^4(pn)}{n} \right)^{1/6} = \left(\frac{B_n^2 \log^7(pn)}{n} \right)^{1/6} / \sqrt{\log(pn)} \lesssim \delta_n / \sqrt{\log(pn)} \quad \forall k.$$

v_k^2 is controlled by obtaining separate bounds for $v_{x,k}^2$ and $v_{y,k}^2$. For the former,

$$v_{x,k}^2 = \frac{1}{\eta_{x,n} n_x} \sum_{i=1}^{n_x} \langle \tilde{\omega}_k - \omega_k^*, \psi(\mathbf{x}^{(i)}) \rangle^2 \leq \eta_{x,n}^{-1} M_\psi^2 \|\tilde{\omega}_k - \omega_k^*\|^2 \lesssim \eta_{x,n}^{-1} \delta_k^2$$

In the case of the latter, we first decompose each summand using

$$\begin{aligned} \langle \tilde{\omega}_k, \psi(\mathbf{y}^{(j)}) \widehat{r}_{\tilde{\theta}}(\mathbf{y}^{(j)}) \rangle - \langle \omega_k^*, \psi(\mathbf{y}^{(j)}) r_{\theta^*}(\mathbf{y}^{(j)}) \rangle \\ = \langle \tilde{\omega}_k - \omega_k^*, \psi(\mathbf{y}^{(j)}) \widehat{r}_{\tilde{\theta}}(\mathbf{y}^{(j)}) \rangle + \langle \omega_k^*, \psi(\mathbf{y}^{(j)}) \rangle \left(\widehat{r}_{\tilde{\theta}}(\mathbf{y}^{(j)}) - r_{\theta^*}(\mathbf{y}^{(j)}) \right). \end{aligned}$$

Then,

$$|\langle \tilde{\omega}_k - \omega_k^*, \psi(\mathbf{y}^{(j)}) \widehat{r}_{\tilde{\theta}}(\mathbf{y}^{(j)}) \rangle| \leq M_\psi M_r^2 \|\tilde{\omega}_k - \omega_k^*\|,$$

and

$$\begin{aligned} \left| \langle \omega_k^*, \psi(\mathbf{y}^{(j)}) \rangle \left(\widehat{r}_{\tilde{\theta}}(\mathbf{y}^{(j)}) - r_{\theta^*}(\mathbf{y}^{(j)}) \right) \right| \\ = \left| \langle \omega_k^*, \psi(\mathbf{y}^{(j)}) \rangle \left\{ \left(\widehat{r}_{\tilde{\theta}}(\mathbf{y}^{(j)}) - \widehat{r}_{\theta^*}(\mathbf{y}^{(j)}) \right) + \left(\widehat{r}_{\theta^*}(\mathbf{y}^{(j)}) - r_{\theta^*}(\mathbf{y}^{(j)}) \right) \right\} \right| \\ \leq M_\psi \|\omega_k^*\| \left(L_1 \|\tilde{\theta} - \theta^*\| + M_r^2 \left| 1 - \frac{\widehat{Z}_y(\theta^*)}{Z_y(\theta^*)} \right| \right), \end{aligned}$$

where we have used Lemma 5, as well as (77) and (85). Hence,

$$\begin{aligned} v_{y,k}^2 &= \frac{n}{n_y^2} \sum_{j=1}^{n_y} \left(\langle \tilde{\omega}_k, \psi(\mathbf{y}^{(j)}) \widehat{r}_{\tilde{\theta}}(\mathbf{y}^{(j)}) \rangle - \langle \omega_k^*, \psi(\mathbf{y}^{(j)}) r_{\theta^*}(\mathbf{y}^{(j)}) \rangle \right)^2 \\ &\leq \eta_{y,n}^{-1} \left\{ M_\psi M_r^2 \|\tilde{\omega}_k - \omega_k^*\| + M_\psi \|\omega_k^*\| \left(L_1 \|\tilde{\theta} - \theta^*\| + M_r^2 \left| 1 - \frac{\widehat{Z}_y(\theta^*)}{Z_y(\theta^*)} \right| \right) \right\}^2. \end{aligned}$$

$$\lesssim \eta_{y,n}^{-1} \{ \delta_k + \|\boldsymbol{\omega}_k^*\| (\delta_\theta + \lambda_\theta) \}^2.$$

Thus,

$$v_k^2 \lesssim (\eta_{x,n} \eta_{y,n})^{-1} \delta_k^2 + \eta_{y,n}^{-1} \|\boldsymbol{\omega}_k\|^2 (\delta_\theta + \lambda_\theta)^2.$$

Under the conditions of the theorem,

$$c v_k^2 \lesssim \left(\frac{B_n^2 \log(pn)}{n} \right)^{1/3} = \left(\frac{B_n^2 \log^7(pn)}{n} \right)^{1/3} \Big/ \log^2(pn) \lesssim \delta_n^2 / \log(pn) \quad \forall k.$$

Clearly,

$$\mathbb{P} \left\{ \max_k |R_{n,k}| > c^{1/2} \delta_n / \sqrt{\log(pn)} \right\} \leq \mathbb{P}(\mathcal{E}^c) \leq \varepsilon_{\text{all},n} \quad (54)$$

and

$$\mathbb{P} \left\{ \max_k v_k^2 > c \delta_n^2 / \log^2(pn) \right\} \leq \mathbb{P}(\mathcal{E}^c) \leq \varepsilon_{\text{all},n}. \quad (55)$$

Conclusion. Subject to some growth constraints, all three of Conditions M, E, and A are satisfied by our problem. The result follows by the discussion at the start of the proof. \square

C Proofs for the ℓ_1 -penalty case

C.1 Proof of Theorem 2

Theorem 7 (Re-statement of Theorem 2). *Assume Condition 1 with ℓ_1 -norm and Condition 2. Assume additionally that*

$$\frac{s_{\theta,0}}{s_{k,q_k}} \left(\frac{n}{\log p} \right)^{\frac{q_k}{4}} \lesssim 1 \quad \text{and} \quad \frac{1}{s_{k,q_k}} \left(\frac{\log p}{n} \right)^{\frac{q_k}{4} \frac{2-q_k}{1-q_k}} \lesssim 1. \quad (56)$$

Let $\widehat{\theta}_k$ be the SparkKLIE+1 estimator with tuning parameters

$$\lambda_\theta \asymp \left(\frac{\log p}{n} \right)^{1/2} \quad \text{and} \quad \lambda_k \asymp s_{k,q_k}^{1/(2-q_k)} \left(\frac{\log p}{n} \right)^{1/2}. \quad (57)$$

Let s be a sequence of integers satisfying

$$s \geq s_{\theta,0} \vee s_{k,q_k} \lambda_k^{-q_k}.$$

Let $\varepsilon_{RSC,n}$ be a sequence in $(0, 1)$ decreasing to 0. Then, provided that

$$n_y \geq C' (\bar{\kappa} / \underline{\kappa}^2) M_\psi^2 M_r^2 s \log^2(s) \log(p \vee n_y) \log(n_y) / \varepsilon_{RSC,n}^2, \quad (58)$$

where $C' > 0$ is the known, absolute constant determined in Lemma 15, we have

$$\begin{aligned} \sup_{t \in \mathbb{R}} \left| \mathbb{P} \left\{ \sqrt{n} (\widehat{\theta}_k - \theta_k^*) / \widehat{\sigma}_k \leq t \right\} - \Phi(t) \right| \\ \leq O \left(s_{\theta,0} s_{k,q_k}^{2 + \frac{1-2q_k}{2-q_k}} \left(\frac{\log p}{n} \right)^{1-q_k} \sqrt{n} \right) + \varepsilon_{RSC,n} + c \exp(-c' \log p). \end{aligned}$$

Proof. For the sake of clarity, we ignore the factors of $\bar{\kappa}$, $\underline{\kappa}$, $\eta_{x,n}$, and $\eta_{y,n}$ in calculations. Detailed bounds are, albeit tedious, not difficult to derive.

By Theorem 1, it suffices to find an event $\mathcal{E} \subseteq \mathcal{E}_{\text{one}}$ with $\mathbb{P}(\mathcal{E}^c) \searrow 0$. Let

$$\mathbf{H}(\boldsymbol{\theta}) := \frac{\widehat{Z}_y^2(\boldsymbol{\theta})}{Z_y^2(\boldsymbol{\theta})} \nabla^2 \ell_{\text{KLIEP}}(\boldsymbol{\theta})$$

$$= \frac{1}{n_y^2} \sum_{1 \leq j < j' \leq n_y} \left(\boldsymbol{\psi}(\mathbf{y}^{(j)}) - \boldsymbol{\psi}(\mathbf{y}^{(j')}) \right) \left(\boldsymbol{\psi}(\mathbf{y}^{(j)}) - \boldsymbol{\psi}(\mathbf{y}^{(j')}) \right)^\top r_\theta(\mathbf{y}^{(j)}) r_\theta(\mathbf{y}^{(j')}).$$

Consider the event

$$\mathcal{E}_{\text{one}}^L = \left\{ \begin{array}{l} \text{(G.1)} \quad 2\|\nabla \ell_{\text{KLIEP}}(\boldsymbol{\theta}^*)\|_\infty \leq \lambda_\theta, \quad \text{(G.2)} \quad 2\|\nabla^2 \ell_{\text{KLIEP}}(\boldsymbol{\theta}^*) \boldsymbol{\omega}_k^* - \mathbf{e}_k\|_\infty \leq \lambda_k, \\ \text{(B.1)} \quad \left| 1 - \frac{\widehat{Z}_y(\boldsymbol{\theta}^*)}{Z_y(\boldsymbol{\theta}^*)} \right| \lesssim \lambda_\theta, \\ \text{(B.2)} \quad \left| \frac{1}{n_y} \sum_{j=1}^{n_y} \langle \boldsymbol{\omega}_k^*, \boldsymbol{\mu}_\psi - \boldsymbol{\psi}(\mathbf{y}^{(j)}) \rangle r_{\theta^*}(\mathbf{y}^{(j)}) \right| \lesssim \lambda_k, \\ \text{(V.1)} \quad \|\widehat{\mathbf{S}}_\psi - \boldsymbol{\Sigma}_\psi\|_\infty \lesssim s_{\theta,0} \lambda_\theta \quad \text{(V.2)} \quad \|\widehat{\mathbf{S}}_{\psi r}(\boldsymbol{\theta}^*) - \boldsymbol{\Sigma}_{\psi r}\|_\infty \lesssim s_{\theta,0} \lambda_\theta, \\ \text{(SE)} \quad \|\mathbf{H}(\boldsymbol{\theta}^*) - \mathbb{E}_y \mathbf{H}(\boldsymbol{\theta}^*)\|_s \leq \underline{\kappa}/128 \end{array} \right\}.$$

Note that (SE) replaces (E.1) and (E.2) in the definition of \mathcal{E}_{one} . We shall show

- (G.1) and (SE) imply (E.1), and
- (G.2) and (SE) in conjunction with (E.1) imply (E.2),

so that $\mathcal{E}_{\text{one}}^L \subseteq \mathcal{E}_{\text{one}}$.

Define

$$\mathcal{K}(S, \beta, \rho) = \{\mathbf{v} \in \mathbb{R}^p : \|\mathbf{v}_{S^c}\|_1 \leq \beta \|\mathbf{v}_S\|_1 + (1 + \beta)\rho, \|\mathbf{v}\| \leq 1\}$$

for any $S \subseteq [p]$, $S \neq \emptyset$, $\beta \geq 0$, $\rho \geq 0$. We shall use this with

$$S_\theta = \{k' : |\theta_{k'}^*| > \lambda_\theta\}, \quad s_\theta = |S_\theta|, \quad \rho_\theta = \|\boldsymbol{\theta}_{S_\theta^c}^*\|_1$$

and

$$S_k = \{k' : |\omega_{k,k'}^*| > \lambda_k\}, \quad s_k = |S_k|, \quad \rho_k = \|\boldsymbol{\omega}_{k,S_k^c}^*\|_1.$$

By the first part of Lemma 14, (B.1) and (SE) imply

$$\mathbf{v}^\top \nabla^2 \ell_{\text{KLIEP}}(\boldsymbol{\theta}^*) \mathbf{v} \geq c_1 \underline{\kappa} \|\mathbf{v}\|^2 - c_2 \rho_\theta^2 / s_\theta \quad \text{for all } \mathbf{v} \in \mathcal{K}(S_\theta, 3, \rho_\theta).$$

Combining this with (G.1), Lemma 2 gives us

$$\|\check{\boldsymbol{\theta}} - \boldsymbol{\theta}^*\|_1 \lesssim s_{\theta,0} \lambda_\theta \asymp s_{\theta,0} \left(\frac{\log p}{n} \right)^{1/2}, \quad (59)$$

where we have used the condition on λ_θ (57). Under the conditions of the corollary, the second part of Lemma 14 imply

$$\mathbf{v}^\top \nabla^2 \ell_{\text{KLIEP}}(\boldsymbol{\theta}^*) \mathbf{v} \geq c_3 \underline{\kappa} \|\mathbf{v}\|^2 \quad \text{for all } \mathbf{v} \in \mathcal{K}(S_k, 6, 0).$$

Combining this with (G.2), Lemma 3 gives us

$$\begin{aligned} \|\check{\boldsymbol{\omega}}_k - \boldsymbol{\omega}_k^*\|_1 &\lesssim \|\check{\boldsymbol{\theta}} - \boldsymbol{\theta}^*\|_1^2 s_{k,q_k} \lambda_k^{-1-q_k} + s_{k,q_k}^2 \lambda_k^{1-2q_k} + s_{k,q_k} \lambda_k^{1-q_k} \\ &\lesssim s_{\theta,0}^2 \lambda_\theta^2 s_{k,q_k} \lambda_k^{-1-q_k} + s_{k,q_k}^2 \lambda_k^{1-2q_k} + s_{k,q_k} \lambda_k^{1-q_k} \\ &\lesssim s_{\theta,0}^2 s_{k,q_k}^{1-\frac{1+q_k}{2-q_k}} \left(\frac{\log p}{n} \right)^{(1-q_k)/2} \\ &\quad + s_{k,q_k}^{2+\frac{1-2q_k}{2-q_k}} \left(\frac{\log p}{n} \right)^{(1-2q_k)/2} + s_{k,q_k}^{1+\frac{1-q_k}{2-q_k}} \left(\frac{\log p}{n} \right)^{(1-q_k)/2} \\ &\lesssim s_{k,q_k}^{2+\frac{1-2q_k}{2-q_k}} \left(\frac{\log p}{n} \right)^{(1-2q_k)/2}. \end{aligned}$$

where we have used the assumptions (56) and (57), as well as (59). Thus,

$$\Delta_2 \lesssim s_{\theta,0} s_{k,q_k}^{2+\frac{1-2q_k}{2-q_k}} \left(\frac{\log p}{n} \right)^{1-q_k} \sqrt{n}. \quad (60)$$

The terms corresponding to Δ_1 and Δ_3 are of smaller order, so we ignore them.

Next, we bound $\mathbb{P}(\mathcal{E}_{\text{one}}^{\text{L}^c})$. Let

$$\begin{aligned}\mathcal{E}_1 &= \{2\|\nabla\ell_{\text{KLIEP}}(\boldsymbol{\theta}^*)\|_\infty \leq \lambda_\theta\}, \\ \mathcal{E}_2 &= \{2\|\nabla^2\ell_{\text{KLIEP}}(\boldsymbol{\theta}^*)\boldsymbol{\omega}_k^* - \mathbf{e}_k\|_\infty \leq \lambda_k\}, \\ \mathcal{E}_3 &= \left\{ \left| 1 - \frac{\widehat{Z}_y(\boldsymbol{\theta}^*)}{Z_y(\boldsymbol{\theta}^*)} \right| \lesssim \lambda_\theta \right\}, \\ \mathcal{E}_4 &= \left\{ \left| \frac{1}{n_y} \sum_{j=1}^{n_y} \langle \boldsymbol{\omega}_k^*, \boldsymbol{\mu}_\psi - \boldsymbol{\psi}(\mathbf{y}^{(j)}) \rangle r_{\theta^*}(\mathbf{y}^{(j)}) \right| \lesssim \lambda_k \right\}, \\ \mathcal{E}_5 &= \left\{ \|\widehat{\mathbf{S}}_\psi - \boldsymbol{\Sigma}_\psi\|_\infty \lesssim s_{\theta,0}\lambda_\theta \right\}, \\ \mathcal{E}_6 &= \left\{ \|\widehat{\mathbf{S}}_{\psi\widehat{r}}(\boldsymbol{\theta}^*) - \boldsymbol{\Sigma}_{\psi r}\|_\infty \lesssim s_{\theta,0}\lambda_\theta \right\}, \\ \mathcal{E}_7 &= \left\{ \|\mathbf{H}(\boldsymbol{\theta}^*) - \mathbb{E}_y \mathbf{H}(\boldsymbol{\theta}^*)\|_2 \leq \underline{\kappa}/128 \right\}.\end{aligned}$$

Clearly,

$$\mathbb{P}(\mathcal{E}_{\text{one}}^{\text{L}^c}) \leq \sum_{\ell=1}^7 \mathbb{P}(\mathcal{E}_\ell^c).$$

Under the conditions of the corollary, Lemma 8 and Lemma 9 indicate that

$$\begin{aligned}\mathbb{P}(\mathcal{E}_1^c) &= \mathbb{P}\{2\|\nabla\ell_{\text{KLIEP}}(\boldsymbol{\theta}^*)\|_\infty > \lambda_\theta\} \leq c_4 \exp(-c'_4 \log p), \\ \mathbb{P}(\mathcal{E}_2^c) &= \mathbb{P}\left\{2\|\widehat{\mathbf{H}}(\boldsymbol{\theta}^*)\boldsymbol{\omega}_k^* - \mathbf{e}_k\|_\infty > \lambda_k\right\} \leq c_5 \exp(-c'_5 \log p).\end{aligned}$$

Lemma 6 says

$$\mathbb{P}(\mathcal{E}_3^c) = \mathbb{P}\left\{ \left| \frac{\widehat{Z}_y(\boldsymbol{\theta}^*)}{Z_y(\boldsymbol{\theta}^*)} - 1 \right| \gtrsim \lambda_\theta \right\} \leq c_6 \exp(-c'_6 \log p).$$

Because $\{\langle \boldsymbol{\omega}_k^*, \boldsymbol{\mu}_\psi - \boldsymbol{\psi}(\mathbf{y}^{(j)}) \rangle r_{\theta^*}(\mathbf{y}^{(j)})\}_{j=1}^{n_y}$ are bounded mean-zero i.i.d. random variables, we also have the following Hoeffding bound

$$\mathbb{P}(\mathcal{E}_4^c) = \mathbb{P}\left\{ \left| \frac{1}{n_y} \sum_{j=1}^{n_y} \langle \boldsymbol{\omega}_k^*, \boldsymbol{\mu}_\psi - \boldsymbol{\psi}(\mathbf{y}^{(j)}) \rangle r_{\theta^*}(\mathbf{y}^{(j)}) \right| \gtrsim \lambda_k \right\} \leq c_7 \exp(-c'_7 \log p).$$

Lemma 21 and Lemma 22 indicate that

$$\begin{aligned}\mathbb{P}(\mathcal{E}_5^c) &= \mathbb{P}\{\|\mathbf{S}_\psi - \boldsymbol{\Sigma}_\psi\|_\infty \gtrsim s_{\theta,0}\lambda_\theta\} \leq c_8 \exp(-c'_8 \log p), \\ \mathbb{P}(\mathcal{E}_6^c) &= \mathbb{P}\left\{ \|\widehat{\mathbf{S}}_{\psi\widehat{r}}(\boldsymbol{\theta}^*) - \boldsymbol{\Sigma}_{\psi r}\|_\infty \gtrsim s_{\theta,0}\lambda_\theta \right\} \leq c_9 \exp(-c'_9 \log p).\end{aligned}$$

Furthermore, Lemma 15 gives

$$\mathbb{P}(\mathcal{E}_7^c) \leq \varepsilon_{\text{RSC},n}.$$

Therefore,

$$\mathbb{P}(\mathcal{E}_{\text{one}}^{\text{L}^c}) \leq \varepsilon_{\text{RSC},n} + c \exp(-c' \log p) \tag{61}$$

for some constants $c, c' > 0$.

We complete the proof by combining the bound from (60) and the bound from (61) with (5):

$$\begin{aligned}\sup_{t \in \mathbb{R}} \left| \mathbb{P}\left\{ \sqrt{n}(\widehat{\theta}_k - \theta_k^*)/\widehat{\sigma}_k \leq t \right\} - \Phi(t) \right| \\ \leq O\left(s_{\theta,0} s_{k,q_k}^{2+\frac{1-2q_k}{2-q_k}} \left(\frac{\log p}{n} \right)^{1-q_k} \sqrt{n} \right) + \varepsilon_{\text{RSC},n} + c \exp(-c' \log p).\end{aligned}$$

□

C.2 Proof of Theorem 4

Theorem 8 (Re-statement of Theorem 4). *Assume Condition 1 with ℓ_1 -norm and Condition 2. Suppose $T_{n_x, n_y} = \max_k \sqrt{n} |\hat{\theta}_k - \theta_k^*|$, where $\hat{\boldsymbol{\theta}}$ is the SparKLIE+1 estimator with tuning parameters*

$$\lambda_\theta \asymp \left(\frac{\log p}{n} \right)^{1/2} \quad \text{and} \quad \lambda_k \asymp \left(\frac{s_{k,0} \log p}{n} \right)^{1/2}, \quad k = 1, \dots, p.$$

Let s be a sequence of integers satisfying $s \geq s_{\theta,0}, s_{k,0}$, $k = 1, \dots, p$. Let $\varepsilon_{RSC,n}$ be a sequence in $(0, 1)$ decreasing to 0. Then, provided that

$$n_y \geq C' (\bar{\kappa}/\underline{\kappa}^2) M_\psi^2 M_r^2 s \log^2(s) \log(p \vee n_y) \log(n_y) / \varepsilon_{RSC,n}^2,$$

where $C' > 0$ is the known, absolute constant determined in Lemma 15, we have

$$\sup_{\alpha \in (0,1)} |\mathbb{P}\{T_{n_x, n_y} \leq \hat{c}_{T, \alpha}\} - (1 - \alpha)| = O(\delta_n + \varepsilon_{RSC,n} + c \exp(-c' \log p))$$

with probability at least $1 - \varepsilon_{RSC,n} - c \exp(-c' \log p) - n^{-1}$.

Proof. For the sake of clarity, we ignore the factors of $\bar{\kappa}$, $\underline{\kappa}$, $\eta_{x,n}$, and $\eta_{y,n}$ in calculations. Detailed bounds are, albeit tedious, not difficult to derive.

As in the proof of Theorem 2, the key to the proof is in finding an event $\mathcal{E} \subseteq \mathcal{E}_{\text{all}}$ with $\mathbb{P}(\mathcal{E}^c) \searrow 0$. Let $\mathbf{H}(\boldsymbol{\theta}) = (\hat{Z}_y^2(\boldsymbol{\theta})/Z_y^2(\boldsymbol{\theta})) \nabla^2 \ell_{\text{KLIEP}}(\boldsymbol{\theta})$. Consider

$$\mathcal{E}_{\text{all}}^L = \left\{ \begin{array}{l} \text{(G.1)} \quad 2\|\nabla \ell_{\text{KLIEP}}(\boldsymbol{\theta}^*)\|_\infty \leq \lambda_\theta, \quad \text{(G.2)} \quad 2\|\nabla^2 \ell_{\text{KLIEP}}(\boldsymbol{\theta}^*) \boldsymbol{\omega}_k^* - \mathbf{e}_k\|_\infty \leq \lambda_k \quad \forall k, \\ \text{(B.1)} \quad \left| 1 - \frac{\hat{Z}_y(\boldsymbol{\theta}^*)}{Z_y(\boldsymbol{\theta}^*)} \right| \lesssim \lambda_\theta, \\ \text{(B.2)} \quad \left| \frac{1}{n_y} \sum_{j=1}^{n_y} \langle \boldsymbol{\omega}_k^*, \boldsymbol{\mu}_\psi - \boldsymbol{\psi}(\mathbf{y}^{(j)}) \rangle r_{\boldsymbol{\theta}^*}(\mathbf{y}^{(j)}) \right| \lesssim \lambda_k \quad \forall k, \\ \text{(SE)} \quad \|\mathbf{H}(\boldsymbol{\theta}^*) - \mathbb{E}_y \mathbf{H}(\boldsymbol{\theta}^*)\|_s \leq \underline{\kappa}/128 \end{array} \right\}.$$

Following the argument of the proof of Theorem 2, on $\mathcal{E}_{\text{all}}^L$,

$$\delta_\theta \lesssim \left(\frac{s^2 \log p}{n} \right)^{1/2} \quad \text{and} \quad \delta_k \lesssim \left(\frac{s^5 \log p}{n} \right)^{1/2} \quad \forall k,$$

and hence,

$$D_1 \lesssim \frac{s^{7/2} \log p}{\sqrt{n}} \lesssim \left(\frac{B_n^2 \log^4(pn)}{n} \right)^{1/6} \quad \text{and} \quad D_2 \lesssim \frac{s^5 \log p}{n} \lesssim \left(\frac{B_n^2 \log(pn)}{n} \right)^{1/3}.$$

We finish the proof by finding a bound for $\varepsilon_{\text{all},n}$. Let

$$\begin{aligned} \mathcal{E}_1 &= \{2\|\nabla \ell_{\text{KLIEP}}(\boldsymbol{\theta}^*)\|_\infty \leq \lambda_\theta\}, \\ \mathcal{E}_{2k} &= \{2\|\nabla^2 \ell_{\text{KLIEP}}(\boldsymbol{\theta}^*) \boldsymbol{\omega}_k^* - \mathbf{e}_k\|_\infty \leq \lambda_k\}, \\ \mathcal{E}_3 &= \left\{ \left| 1 - \frac{\hat{Z}_y(\boldsymbol{\theta}^*)}{Z_y(\boldsymbol{\theta}^*)} \right| \lesssim \lambda_\theta \right\}, \\ \mathcal{E}_{4k} &= \left\{ \left| \frac{1}{n_y} \sum_{j=1}^{n_y} \langle \boldsymbol{\omega}_k^*, \boldsymbol{\mu}_\psi - \boldsymbol{\psi}(\mathbf{y}^{(j)}) \rangle r_{\boldsymbol{\theta}^*}(\mathbf{y}^{(j)}) \right| \lesssim \lambda_k \right\}, \\ \mathcal{E}_5 &= \{ \|\mathbf{H}(\boldsymbol{\theta}^*) - \mathbb{E}_y \mathbf{H}(\boldsymbol{\theta}^*)\|_s \leq \underline{\kappa}/128 \}, \end{aligned}$$

so that

$$\varepsilon_{\text{all},n} \leq \mathbb{P}(\mathcal{E}_{\text{all}}^L)^c \leq \mathbb{P}(\mathcal{E}_1^c) + \sum_{k=1}^p \mathbb{P}(\mathcal{E}_{2k}^c) + \mathbb{P}(\mathcal{E}_3^c) + \sum_{k=1}^p \mathbb{P}(\mathcal{E}_{4k}^c) + \mathbb{P}(\mathcal{E}_5^c).$$

By a sequence of arguments similar to that in the proof of Theorem 2,

$$\varepsilon_{\text{all},n} \leq \varepsilon_{\text{RSC},n} + c \exp(-c' \log p).$$

□

C.3 Consistency of ℓ_1 -penalized estimators

In the following,

$$\mathcal{K}(S, \beta, \rho) = \{\mathbf{v} \in \mathbb{R}^p : \|\mathbf{v}_{S^c}\|_1 \leq \beta \|\mathbf{v}_S\|_1 + (1 + \beta)\rho, \|\mathbf{v}\| \leq 1\},$$

where $S \subseteq [p]$ is nonempty, $\beta \geq 0$, and $\rho \geq 0$.

Lemma 2. Consider the optimization problem (7) using ℓ_1 -penalty and a regularization parameter λ_θ satisfying

$$\lambda_\theta \geq 2\|\nabla \ell_{\text{KLIEP}}(\boldsymbol{\theta}^*)\|_\infty.$$

Suppose, in addition, it holds that

$$\mathbf{v}^\top \nabla^2 \ell_{\text{KLIEP}}(\boldsymbol{\theta}^*) \mathbf{v} \geq c\underline{\kappa} \|\mathbf{v}\|_2^2 - c' \frac{\rho_\theta^2}{s_{\theta,0}} \quad \text{for } \mathbf{v} \in \mathcal{K}(S_\theta, 3, \rho_\theta),$$

for some $c, c' > 0$, where

$$S_\theta = \{k' : |\theta_{k'}^*| > \lambda_\theta\}, \quad s_\theta = |S_\theta|, \quad \rho_\theta = \|\boldsymbol{\theta}_{S_\theta^c}^*\|_1.$$

Then any solution $\check{\boldsymbol{\theta}}$ satisfies

$$\|\check{\boldsymbol{\theta}} - \boldsymbol{\theta}^*\|_1 \lesssim (1 + \underline{\kappa}^{-1}) \|\boldsymbol{\theta}^*\|_{q_\theta} \lambda_\theta^{1-q_\theta}.$$

Proof. By a direct application of Theorem 1 of Negahban et al. (2012),

$$\|\check{\boldsymbol{\theta}} - \boldsymbol{\theta}^*\|_2^2 \leq \frac{9s_\theta \lambda_\theta^2}{c^2 \underline{\kappa}^2} + \frac{4\lambda_\theta \rho_\theta}{c \underline{\kappa}} + \frac{2c' \lambda_\theta \rho_\theta^2}{c \underline{\kappa} s_\theta}. \quad (62)$$

By (81) and (82),

$$s_\theta \leq \|\boldsymbol{\theta}^*\|_{q_\theta} \lambda_\theta^{-q_\theta} \quad \text{and} \quad \rho_\theta \leq \|\boldsymbol{\theta}^*\|_{q_\theta} \lambda_\theta^{1-q_\theta},$$

so that

$$\begin{aligned} \|\check{\boldsymbol{\theta}} - \boldsymbol{\theta}^*\|_2^2 &\leq \frac{9\|\boldsymbol{\theta}^*\|_{q_\theta} \lambda_\theta^{2-q_\theta}}{c^2 \underline{\kappa}^2} + \frac{4\|\boldsymbol{\theta}^*\|_{q_\theta} \lambda_\theta^{2-q_\theta}}{c \underline{\kappa}} + \frac{2c' \|\boldsymbol{\theta}^*\|_{q_\theta}^2 \lambda_\theta^{3-2q_\theta}}{c \underline{\kappa} s_\theta} \\ &= \underline{\kappa}^{-2} \|\boldsymbol{\theta}^*\|_{q_\theta} \lambda_\theta^{2-q_\theta} \left(\frac{9}{c^2} + \frac{4}{c} \underline{\kappa} + \frac{2c'}{c} \underline{\kappa} \|\boldsymbol{\theta}^*\|_{q_\theta} \lambda_\theta^{1-q_\theta} \right) \leq K_1 \underline{\kappa}^{-2} \|\boldsymbol{\theta}^*\|_{q_\theta} \lambda_\theta^{2-q_\theta} \end{aligned}$$

for an appropriate choice of $K_1 > 0$. Therefore,

$$\|\check{\boldsymbol{\theta}} - \boldsymbol{\theta}^*\|_1 \leq 4\sqrt{s_\theta} \|\check{\boldsymbol{\theta}} - \boldsymbol{\theta}^*\|_2 + 4\rho_\theta \leq K_2 \underline{\kappa}^{-1} \|\boldsymbol{\theta}^*\|_{q_\theta} \lambda_\theta^{1-q_\theta} + 4\|\boldsymbol{\theta}^*\|_{q_\theta} \lambda_\theta^{1-q_\theta} \leq K_3 (1 + \underline{\kappa}^{-1}) \|\boldsymbol{\theta}^*\|_{q_\theta} \lambda_\theta^{1-q_\theta}. \quad (63)$$

□

Lemma 3. Assume Condition 1. Consider the optimization problem (8) using ℓ_1 -penalty and a regularization parameter λ_k satisfying

$$\lambda_k \geq 2\|\nabla^2 \ell_{\text{KLIEP}}(\boldsymbol{\theta}^*) \boldsymbol{\omega}_k^* - \mathbf{e}_k\|_\infty.$$

Suppose, in addition, it holds that

$$\mathbf{v}^\top \nabla^2 \ell_{\text{KLIEP}}(\check{\boldsymbol{\theta}}) \mathbf{v} \geq c\underline{\kappa} \|\mathbf{v}\|_2^2 \quad \text{for } \mathbf{v} \in \mathcal{K}(S_k, 6, 0),$$

for some $c > 0$, where $S_k = \{k' : |\omega_{k'}^*| > \lambda_k\}$. Then any solution $\check{\boldsymbol{\omega}}_k$ satisfies

$$\|\check{\boldsymbol{\omega}}_k - \boldsymbol{\omega}_k^*\|_1 \lesssim \underline{\kappa}^{-2} \|\check{\boldsymbol{\theta}} - \boldsymbol{\theta}^*\|_1^2 s_{k,q_k} \lambda_k^{-1-q_k} + s_{k,q_k}^2 \lambda_k^{1-2q_k} + \underline{\kappa}^{-1} s_{k,q_k} \lambda_k^{1-q_k}.$$

Proof. Put $\widehat{\mathbf{H}}(\boldsymbol{\theta}) = \nabla^2 \ell_{\text{KLIEP}}(\boldsymbol{\theta})$. The objective function is

$$\frac{1}{2} \boldsymbol{\omega}^\top \widehat{\mathbf{H}}(\check{\boldsymbol{\theta}}) \boldsymbol{\omega} - \boldsymbol{\omega}^\top \mathbf{e}_k + \lambda_k \|\boldsymbol{\omega}\|_1.$$

For S_k in the statement of the theorem, set

$$s_k = |S_k| \quad \text{and} \quad \rho_k = \|\boldsymbol{\omega}_{S_k^c}^*\|_1.$$

Since $\check{\boldsymbol{\omega}}_k$ is the solution to (8) using ℓ_1 -penalty,

$$\frac{1}{2} \check{\boldsymbol{\omega}}_k^\top \widehat{\mathbf{H}}(\check{\boldsymbol{\theta}}) \check{\boldsymbol{\omega}}_k - \check{\boldsymbol{\omega}}_k^\top \mathbf{e}_k + \lambda_k \|\check{\boldsymbol{\omega}}_k\|_1 \leq \frac{1}{2} \boldsymbol{\omega}_{k,S_k}^{*\top} \widehat{\mathbf{H}}(\check{\boldsymbol{\theta}}) \boldsymbol{\omega}_{k,S_k}^* - \boldsymbol{\omega}_{k,S_k}^{*\top} \mathbf{e}_k + \lambda_k \|\boldsymbol{\omega}_{k,S_k}^*\|_1.$$

Setting $\mathbf{d} = \check{\boldsymbol{\omega}}_k - \boldsymbol{\omega}_{k,S_k}^*$, the above can be rearranged as

$$\begin{aligned} \frac{1}{2} \mathbf{d}^\top \widehat{\mathbf{H}}(\check{\boldsymbol{\theta}}) \mathbf{d} &\leq \lambda_k (\|\boldsymbol{\omega}_{k,S_k}^*\|_1 - \|\check{\boldsymbol{\omega}}_k\|_1) - \mathbf{d}^\top \{\widehat{\mathbf{H}}(\boldsymbol{\theta}^*) \boldsymbol{\omega}_k^* - \mathbf{e}_k\} \\ &\quad - \mathbf{d}^\top \{\widehat{\mathbf{H}}(\check{\boldsymbol{\theta}}) - \widehat{\mathbf{H}}(\boldsymbol{\theta}^*)\} \boldsymbol{\omega}_{k,S_k}^* + \mathbf{d}^\top \widehat{\mathbf{H}}(\boldsymbol{\theta}^*) \boldsymbol{\omega}_{k,S_k^c}^*. \end{aligned} \quad (64)$$

By Cauchy-Schwarz, the condition of the lemma implies

$$|\mathbf{d}^\top \{\widehat{\mathbf{H}}(\boldsymbol{\theta}^*) \boldsymbol{\omega}_k^* - \mathbf{e}_k\}| \leq \|\mathbf{d}\|_1 \|\widehat{\mathbf{H}}(\boldsymbol{\theta}^*) \boldsymbol{\omega}_k^* - \mathbf{e}_k\|_\infty \leq \frac{\lambda_k}{2} \|\mathbf{d}\|_1. \quad (65)$$

(73) of Lemma 4 yields

$$|\mathbf{d}^\top \{\widehat{\mathbf{H}}(\check{\boldsymbol{\theta}}) - \widehat{\mathbf{H}}(\boldsymbol{\theta}^*)\} \boldsymbol{\omega}_{k,S_k}^*| \leq \frac{1}{8} \mathbf{d}^\top \widehat{\mathbf{H}}(\check{\boldsymbol{\theta}}) \mathbf{d} + K_1 \|\check{\boldsymbol{\theta}} - \boldsymbol{\theta}^*\|_1^2 \|\boldsymbol{\omega}_{k,S_k}^*\|_1^2. \quad (66)$$

(72) of Lemma 4 yields

$$|\mathbf{d}^\top \widehat{\mathbf{H}}(\boldsymbol{\theta}^*) \boldsymbol{\omega}_{k,S_k^c}^*| \leq \frac{1}{8} \mathbf{d}^\top \widehat{\mathbf{H}}(\check{\boldsymbol{\theta}}) \mathbf{d} + K_2 \rho_k^2. \quad (67)$$

Combining (65) to (67) with (64), and noting $\|\boldsymbol{\omega}_{k,S_k}^*\|_1 - \|\check{\boldsymbol{\omega}}_k\|_1 \leq \|\mathbf{d}_{S_k}\|_1 - \|\mathbf{d}_{S_k^c}\|_1$,

$$\frac{1}{4} \mathbf{d}^\top \widehat{\mathbf{H}}(\boldsymbol{\theta}^*) \mathbf{d} + \frac{\lambda_k}{2} \|\mathbf{d}_{S_k^c}\|_1 \leq \frac{3\lambda_k}{2} \|\mathbf{d}_{S_k}\|_1 + K_1 \|\check{\boldsymbol{\theta}} - \boldsymbol{\theta}^*\|_1^2 \|\boldsymbol{\omega}_{k,S_k}^*\|_1^2 + K_2 \rho_k^2. \quad (68)$$

We consider two cases. First, suppose that

$$\frac{3\lambda_k}{2} \|\mathbf{d}_{S_k}\|_1 \leq K_1 \|\check{\boldsymbol{\theta}} - \boldsymbol{\theta}^*\|_1^2 \|\boldsymbol{\omega}_{k,S_k}^*\|_1^2 + K_2 \rho_k^2.$$

Then,

$$\frac{\lambda_k}{2} \|\mathbf{d}_{S_k^c}\|_1 \leq 2 (K_1 \|\check{\boldsymbol{\theta}} - \boldsymbol{\theta}^*\|_1^2 \|\boldsymbol{\omega}_{k,S_k}^*\|_1^2 + K_2 \rho_k^2).$$

easily, and hence

$$\|\mathbf{d}\|_1 \leq K_3 \|\check{\boldsymbol{\theta}} - \boldsymbol{\theta}^*\|_1^2 \|\boldsymbol{\omega}_{k,S_k}^*\|_1^2 \lambda_k^{-1} + K_4 \rho_k^2 \lambda_k^{-1}. \quad (69)$$

in the this case.

Next, suppose that

$$\frac{3\lambda_k}{2} \|\mathbf{d}_{S_k}\|_1 \geq K_1 \|\check{\boldsymbol{\theta}} - \boldsymbol{\theta}^*\|_1^2 \|\boldsymbol{\omega}_{k,S_k}^*\|_1^2 + K_2 \rho_k^2.$$

Then, (68) yields $\mathbf{d} \in \mathcal{K}(S_k, 6, 0)$, and hence

$$\|\mathbf{d}\|_1 \leq 7 \|\mathbf{d}_{S_k}\|_1 \leq 7 \sqrt{s_k} \|\mathbf{d}\|.$$

We are able to apply the restricted strong convexity assumption to (68), which yields

$$\|\mathbf{d}\|_1 \leq K_{5\underline{K}}^{-1} s_k \lambda_k. \quad (70)$$

Finally, combining the two error bounds (70) and (69),

$$\begin{aligned}\|\check{\boldsymbol{\omega}}_k - \boldsymbol{\omega}_k^*\|_1 &\leq \|\mathbf{d}\|_1 + \rho_k \\ &\leq K_3 \|\check{\boldsymbol{\theta}} - \boldsymbol{\theta}^*\|_1^2 \|\boldsymbol{\omega}_{k,S_k}^*\|_1^2 \lambda_k^{-1} + K_4 \rho_k^2 \lambda_k^{-1} + K_5 \underline{\kappa}^{-1} s_k \lambda_k + \rho_k.\end{aligned}$$

By (81) and (82),

$$s_k \leq s_{k,q_k} \lambda_k^{-q_k} \quad \text{and} \quad \rho_k \leq s_{k,q_k} \lambda_k^{1-q_k}. \quad (71)$$

Thus,

$$\|\check{\boldsymbol{\omega}}_k - \boldsymbol{\omega}_k^*\|_1 \leq K_6 \underline{\kappa}^{-2} \|\check{\boldsymbol{\theta}} - \boldsymbol{\theta}^*\|_1^2 s_{k,q_k} \lambda_k^{1-q_k} + K_7 s_{k,q_k}^2 \lambda_k^{1-2q_k} + K_8 \underline{\kappa}^{-1} s_{k,q_k} \lambda_k^{1-q_k}.$$

□

Lemma 4. Let $\boldsymbol{\theta} \in \bar{\mathcal{B}}_\rho(\boldsymbol{\theta}^*)$, $c > 0$. Under Condition 1,

$$|\mathbf{d}^\top \widehat{\mathbf{H}}(\boldsymbol{\theta}^*) \mathbf{v}| \leq \frac{1}{2c} \mathbf{d}^\top \widehat{\mathbf{H}}(\boldsymbol{\theta}) \mathbf{d} + c M_\psi^2 M_r^{16} \|\mathbf{v}\|_1^2 \quad (72)$$

and

$$|\mathbf{d}^\top \{\widehat{\mathbf{H}}(\check{\boldsymbol{\theta}}) - \widehat{\mathbf{H}}(\boldsymbol{\theta}^*)\} \mathbf{v}| \leq \frac{1}{2c} \mathbf{d}^\top \widehat{\mathbf{H}}(\boldsymbol{\theta}) \mathbf{d} + 4c L_1^2 M_\psi^2 M_r^{12} \|\check{\boldsymbol{\theta}} - \boldsymbol{\theta}^*\|_1^2 \|\mathbf{v}\|_1^2. \quad (73)$$

Proof. Because the geometric mean of nonnegative numbers is dominated by the arithmetic mean,

$$\begin{aligned}|\mathbf{d}^\top \widehat{\mathbf{H}}(\boldsymbol{\theta}^*) \mathbf{v}| &\leq \left(\mathbf{d}^\top \widehat{\mathbf{H}}(\boldsymbol{\theta}) \mathbf{d} \right)^{1/2} \left(\max_{j,j'} \left(\frac{\widehat{r}_{\boldsymbol{\theta}^*}(\mathbf{y}^{(j)}) \widehat{r}_{\boldsymbol{\theta}^*}(\mathbf{y}^{(j')})}{\widehat{r}_{\boldsymbol{\theta}}(\mathbf{y}^{(j)}) \widehat{r}_{\boldsymbol{\theta}}(\mathbf{y}^{(j')})} \right)^2 \mathbf{v}^\top \widehat{\mathbf{H}}(\boldsymbol{\theta}) \mathbf{v} \right)^{1/2} \\ &= \left(c^{-2} \mathbf{d}^\top \widehat{\mathbf{H}}(\boldsymbol{\theta}) \mathbf{d} \right)^{1/2} \left(c^2 \max_{j,j'} \left(\frac{\widehat{r}_{\boldsymbol{\theta}^*}(\mathbf{y}^{(j)}) \widehat{r}_{\boldsymbol{\theta}^*}(\mathbf{y}^{(j')})}{\widehat{r}_{\boldsymbol{\theta}}(\mathbf{y}^{(j)}) \widehat{r}_{\boldsymbol{\theta}}(\mathbf{y}^{(j')})} \right)^2 \frac{Z_y^2(\boldsymbol{\theta})}{\widehat{Z}_y^2(\boldsymbol{\theta})} \mathbf{v}^\top \mathbf{H}(\boldsymbol{\theta}) \mathbf{v} \right)^{1/2} \\ &\leq \frac{1}{2c} \mathbf{d}^\top \widehat{\mathbf{H}}(\boldsymbol{\theta}) \mathbf{d} + \frac{c}{2} \max_{j,j'} \left(\frac{\widehat{r}_{\boldsymbol{\theta}^*}(\mathbf{y}^{(j)}) \widehat{r}_{\boldsymbol{\theta}^*}(\mathbf{y}^{(j')})}{r_{\boldsymbol{\theta}}(\mathbf{y}^{(j)}) r_{\boldsymbol{\theta}}(\mathbf{y}^{(j')})} \right)^2 \frac{\widehat{Z}_y^2(\boldsymbol{\theta})}{Z_y^2(\boldsymbol{\theta})} \|\mathbf{H}(\boldsymbol{\theta})\|_\infty \|\mathbf{v}\|_1^2\end{aligned}$$

and

$$\begin{aligned}|\mathbf{d}^\top \{\widehat{\mathbf{H}}(\check{\boldsymbol{\theta}}) - \widehat{\mathbf{H}}(\boldsymbol{\theta}^*)\} \mathbf{v}| &\leq \left(\mathbf{d}^\top \widehat{\mathbf{H}}(\boldsymbol{\theta}) \mathbf{d} \right)^{1/2} \left(\max_{j,j'} \left(\frac{\widehat{r}_{\check{\boldsymbol{\theta}}}(\mathbf{y}^{(j)}) \widehat{r}_{\check{\boldsymbol{\theta}}}(\mathbf{y}^{(j')}) - \widehat{r}_{\boldsymbol{\theta}^*}(\mathbf{y}^{(j)}) \widehat{r}_{\boldsymbol{\theta}^*}(\mathbf{y}^{(j')})}{\widehat{r}_{\boldsymbol{\theta}}(\mathbf{y}^{(j)}) \widehat{r}_{\boldsymbol{\theta}}(\mathbf{y}^{(j')})} \right)^2 \frac{Z_y^2(\boldsymbol{\theta})}{\widehat{Z}_y^2(\boldsymbol{\theta})} \mathbf{v}^\top \mathbf{H}(\boldsymbol{\theta}) \mathbf{v} \right)^{1/2} \\ &\leq \frac{1}{2c} \mathbf{d}^\top \widehat{\mathbf{H}}(\check{\boldsymbol{\theta}}) \mathbf{d} + \frac{c}{2} \max_{j,j'} \left(\frac{\widehat{r}_{\check{\boldsymbol{\theta}}}(\mathbf{y}^{(j)}) \widehat{r}_{\check{\boldsymbol{\theta}}}(\mathbf{y}^{(j')}) - \widehat{r}_{\boldsymbol{\theta}^*}(\mathbf{y}^{(j)}) \widehat{r}_{\boldsymbol{\theta}^*}(\mathbf{y}^{(j')})}{r_{\boldsymbol{\theta}}(\mathbf{y}^{(j)}) r_{\boldsymbol{\theta}}(\mathbf{y}^{(j')})} \right)^2 \frac{\widehat{Z}_y^2(\boldsymbol{\theta})}{Z_y^2(\boldsymbol{\theta})} \|\mathbf{H}(\boldsymbol{\theta})\|_\infty \|\mathbf{v}\|_1^2.\end{aligned}$$

Under Condition 1, $\|\mathbf{H}(\boldsymbol{\theta})\|_\infty \leq 2M_\psi^2 M_r^2$ for all $\boldsymbol{\theta} \in \bar{\mathcal{B}}_\rho(\boldsymbol{\theta}^*)$. Furthermore,

$$M_r^{-6} \leq \frac{\widehat{r}_{\boldsymbol{\theta}^*}(\mathbf{y}^{(j)}) \widehat{r}_{\boldsymbol{\theta}^*}(\mathbf{y}^{(j')})}{r_{\boldsymbol{\theta}}(\mathbf{y}^{(j)}) r_{\boldsymbol{\theta}}(\mathbf{y}^{(j')})} \leq M_r^6,$$

and

$$\begin{aligned}\left| \frac{\widehat{r}_{\check{\boldsymbol{\theta}}}(\mathbf{y}^{(j)}) \widehat{r}_{\check{\boldsymbol{\theta}}}(\mathbf{y}^{(j')}) - \widehat{r}_{\boldsymbol{\theta}^*}(\mathbf{y}^{(j)}) \widehat{r}_{\boldsymbol{\theta}^*}(\mathbf{y}^{(j')})}{r_{\boldsymbol{\theta}}(\mathbf{y}^{(j)}) r_{\boldsymbol{\theta}}(\mathbf{y}^{(j')})} \right| &= \frac{\widehat{r}_{\check{\boldsymbol{\theta}}}(\mathbf{y}^{(j)}) \left| \widehat{r}_{\check{\boldsymbol{\theta}}}(\mathbf{y}^{(j')}) - \widehat{r}_{\boldsymbol{\theta}^*}(\mathbf{y}^{(j')}) \right| + \left| \widehat{r}_{\check{\boldsymbol{\theta}}}(\mathbf{y}^{(j)}) - \widehat{r}_{\boldsymbol{\theta}^*}(\mathbf{y}^{(j)}) \right| \widehat{r}_{\boldsymbol{\theta}^*}(\mathbf{y}^{(j')})}{r_{\boldsymbol{\theta}}(\mathbf{y}^{(j)}) r_{\boldsymbol{\theta}}(\mathbf{y}^{(j')})} \\ &\leq 2L_1 M_r^4 \|\check{\boldsymbol{\theta}} - \boldsymbol{\theta}^*\|_1.\end{aligned}$$

The inequalities follow. □

D Model assumptions

In this section, we go over some of the implications of the assumptions in Section 4.1. Appendix D.1 discusses the properties of the bounded density ratio model of Condition 1. In Appendix D.2, we derive bounds on the ℓ_2 - and ℓ_1 -norms of $\boldsymbol{\omega}_k^* = \boldsymbol{\Sigma}_\psi^{-1} \mathbf{e}_k$, as well as lower- and upper-bounds on the variance of the linearization $\sigma_{n,k}^2$, as direct consequences of Condition 2. In Appendix D.3 we characterize the sparsity of the rows of $\boldsymbol{\Sigma}_\psi^{-1}$.

D.1 Properties of the bounded density ratio model

Proposition 2 (Re-statement of Proposition 1). *Condition 1 is satisfied if and only if $\|\boldsymbol{\psi}(\mathbf{x})\|_* \leq M_\psi$ a.s. for some $M_\psi < \infty$.*

Proof. We shall first treat the case $\boldsymbol{\theta}^* = \mathbf{0}$, and then show how the general case follows from the special one. Assume $\|\boldsymbol{\psi}(\mathbf{x})\|_* \leq M_\psi$ for some $M_\psi < \infty$. For each \mathbf{x} , by the definition of the dual norm,

$$|\langle \boldsymbol{\psi}(\mathbf{x}), \boldsymbol{\theta} \rangle| = |\langle \boldsymbol{\psi}(\mathbf{x}), \boldsymbol{\theta} / \|\boldsymbol{\theta}\| \rangle| \|\boldsymbol{\theta}\| \leq \|\boldsymbol{\psi}(\mathbf{x})\|_* \|\boldsymbol{\theta}\| \leq \varrho M_\psi.$$

It is easy to see that for each $\boldsymbol{\theta} \in \bar{\mathcal{B}}_\varrho(\boldsymbol{\theta}^*)$,

$$e^{-\varrho M_\psi} \leq e^{\langle \boldsymbol{\psi}(\mathbf{x}), \boldsymbol{\theta} \rangle} \leq e^{\varrho M_\psi} \quad \text{and} \quad e^{-\varrho M_\psi} \leq Z_y(\boldsymbol{\theta}) \leq e^{\varrho M_\psi},$$

and hence,

$$e^{-2\varrho M_\psi} \leq r_\theta(\mathbf{x}) \leq e^{2\varrho M_\psi}.$$

In particular, one may choose $M_r = M_r(\varrho) = e^{2\varrho M_\psi}$.

This proves one direction of the claim. For the other direction, first note that Condition 1 implies

$$\langle \boldsymbol{\psi}(\mathbf{x}), \boldsymbol{\theta} \rangle \leq \log M_r(\varrho) + \log Z_y(\boldsymbol{\theta}) \quad \text{for all } \boldsymbol{\theta} \in \bar{\mathcal{B}}_\varrho(\boldsymbol{\theta}^*).$$

For each \mathbf{x} , $\varrho \|\boldsymbol{\psi}(\mathbf{x})\|_* = \langle \boldsymbol{\psi}(\mathbf{x}), \boldsymbol{\theta}_x \rangle$ for some $\boldsymbol{\theta}_x \in \bar{\mathcal{B}}_\varrho(\boldsymbol{\theta}^*)$ by compactness, so

$$\|\boldsymbol{\psi}(\mathbf{x})\|_* \leq \varrho^{-1} (\log M_r(\varrho) + \log Z_y(\boldsymbol{\theta}_x)).$$

Using compactness again,

$$\|\boldsymbol{\psi}(\mathbf{x})\|_* \leq \varrho^{-1} \left(\log M_r(\varrho) + \max_{\|\boldsymbol{\theta}\| \leq \varrho} \log Z_y(\boldsymbol{\theta}) \right),$$

and the bound is finite by assumption. Now, the right-hand side is a function of ϱ only, whereas the left-hand side is independent of ϱ . Thus,

$$\|\boldsymbol{\psi}(\mathbf{x})\|_* \leq \inf_{\varrho > 0} \varrho^{-1} \left(\log M_r(\varrho) + \max_{\|\boldsymbol{\theta}\| \leq \varrho} \log Z_y(\boldsymbol{\theta}) \right).$$

This completes the proof for the case $\boldsymbol{\theta}^* = \mathbf{0}$. For general $\boldsymbol{\theta}^*$,

$$|\langle \boldsymbol{\psi}(\mathbf{x}), \boldsymbol{\theta} \rangle| \leq |\langle \boldsymbol{\psi}(\mathbf{x}), \boldsymbol{\theta} - \boldsymbol{\theta}^* \rangle| + |\langle \boldsymbol{\psi}(\mathbf{x}), \boldsymbol{\theta}^* \rangle| \leq \|\boldsymbol{\psi}\|_* (\varrho + \|\boldsymbol{\theta}^*\|),$$

and

$$\langle \boldsymbol{\psi}(\mathbf{x}), \boldsymbol{\theta} - \boldsymbol{\theta}^* \rangle \leq \log (M_r^2 Z_y(\boldsymbol{\theta}) / Z_y(\boldsymbol{\theta}^*)),$$

and the proof goes through as before. \square

Under the bounded density ratio model, $\widehat{Z}_y(\boldsymbol{\theta})$, $\widehat{r}_\theta(\mathbf{y})$, and $\boldsymbol{\mu}(\boldsymbol{\theta})$ are all locally Lipschitz continuous in $\boldsymbol{\theta}$.

Lemma 5. *There exist $L_0, L_1, L_2 > 0$ such that for all $\boldsymbol{\theta} \in \bar{\mathcal{B}}_\varrho(\boldsymbol{\theta}^*)$,*

$$|\widehat{Z}_y(\boldsymbol{\theta}) - \widehat{Z}_y(\boldsymbol{\theta}^*)| \leq L_0 \|\boldsymbol{\theta} - \boldsymbol{\theta}^*\|, \tag{74}$$

$$|\widehat{r}_\theta(\mathbf{y}) - \widehat{r}_{\boldsymbol{\theta}^*}(\mathbf{y})| \leq L_1 \|\boldsymbol{\theta} - \boldsymbol{\theta}^*\|, \tag{75}$$

$$\|\widehat{\boldsymbol{\mu}}(\boldsymbol{\theta}) - \widehat{\boldsymbol{\mu}}(\boldsymbol{\theta}^*)\|_* \leq L_2 \|\boldsymbol{\theta} - \boldsymbol{\theta}^*\|. \tag{76}$$

Proof. $\widehat{Z}_y(\boldsymbol{\theta})$, $\widehat{r}_\theta(\mathbf{y})$, and $\widehat{\boldsymbol{\mu}}(\boldsymbol{\theta})$ are all differentiable functions of $\boldsymbol{\theta}$, and hence the mean value theorem and the boundedness assumption can be used to derive the required bounds. \square

It is not difficult to imagine that under the bounded density ratio model, all the relevant sample quantities concentrate sufficiently fast. The following lemma proves this intuition. It is always true that for any $\boldsymbol{\theta}$,

$$\frac{r_\theta(\mathbf{y})}{\widehat{r}_\theta(\mathbf{y})} = \frac{\widehat{Z}_y(\boldsymbol{\theta})}{Z_y(\boldsymbol{\theta})} = \frac{1}{n_y} \sum_{j=1}^{n_y} \frac{\exp(\boldsymbol{\theta}^\top \boldsymbol{\psi}(\mathbf{y}^{(j)}))}{Z_y(\boldsymbol{\theta})} = \frac{1}{n_y} \sum_{j=1}^{n_y} r_\theta(\mathbf{y}^{(j)}), \quad (77)$$

and

$$\mathbb{E}_y[r_\theta(\mathbf{y})] = \int r_\theta(\mathbf{y}) f_y(\mathbf{y}) d\mathbf{y} = \int f(\mathbf{y}; \boldsymbol{\theta} + \boldsymbol{\gamma}_y) d\mathbf{y} = 1. \quad (78)$$

If, in addition, $r_\theta(\mathbf{y})$ is bounded, then (77) and (78) can be used to derive the following results.

Lemma 6. *Suppose $\boldsymbol{\theta} \in \bar{\mathcal{B}}_\varrho(\boldsymbol{\theta}^*)$. For any $t > 0$,*

$$\mathbb{P} \left\{ \frac{\widehat{Z}_y(\boldsymbol{\theta})}{Z_y(\boldsymbol{\theta})} - 1 > t \right\} \leq \exp \left(-\frac{2t^2 n_y}{(M_r - M_r^{-1})^2} \right)$$

and

$$\mathbb{P} \left\{ \frac{\widehat{Z}_y(\boldsymbol{\theta})}{Z_y(\boldsymbol{\theta})} - 1 < -t \right\} \leq \exp \left(-\frac{2t^2 n_y}{(M_r - M_r^{-1})^2} \right).$$

Proof. Apply Hoeffding's inequality to the random variable $r_\theta(\mathbf{y}) \in [M_r^{-1}, M_r]$, $\mathbb{E}_y[r_\theta(\mathbf{y})] = 1$. \square

Having highlighted a few of the features of the bounded density ratio model, we proceed to explain why (7) or (8) are expected to yield consistent estimators of $\boldsymbol{\theta}^*$ or $\boldsymbol{\omega}_k^*$ under Condition 1.

The optimization problem described by (7) or (8) has a convex objective with ℓ_1 -penalty. It is well-understood that given a regularization level $\lambda > 0$, a minimizer of the corresponding regularized objective is consistent for the population optimum, provided that the gradient at the population optimum is bounded by $\lambda/2$ in ℓ_∞ -norm (the dual norm of the ℓ_1 -norm), and the Hessian behaves like a positive definite matrix when restricted to the right set. The boundedness of the density ratio and sufficient statistics help guarantee both.

The gradient of ℓ_{KLIEP} at $\boldsymbol{\theta}^*$ is

$$\nabla \ell_{\text{KLIEP}}(\boldsymbol{\theta}^*) = -\frac{1}{n_x} \sum_{i=1}^{n_x} \boldsymbol{\psi}(\mathbf{x}^{(i)}) + \frac{1}{n_y} \sum_{j=1}^{n_y} \boldsymbol{\psi}(\mathbf{y}^{(j)}) \widehat{r}_{\boldsymbol{\theta}^*}(\mathbf{y}^{(j)}). \quad (79)$$

Since $\boldsymbol{\mu}_\psi = \mathbb{E}_x[\boldsymbol{\psi}(\mathbf{x})] = \mathbb{E}_y[\boldsymbol{\psi}(\mathbf{y}) r_{\boldsymbol{\theta}^*}(\mathbf{y})]$, $\widehat{r}_{\boldsymbol{\theta}^*}(\mathbf{y}) = (Z_y(\boldsymbol{\theta}^*)/\widehat{Z}_y(\boldsymbol{\theta}^*)) r_{\boldsymbol{\theta}^*}(\mathbf{y})$, and $\widehat{Z}_y(\boldsymbol{\theta}^*)/Z_y(\boldsymbol{\theta}^*) \xrightarrow{P} 1$, each average in the gradient is a consistent estimator of $\boldsymbol{\mu}_\psi$, so that the gradient as a whole is converging to a zero vector. Because both $\boldsymbol{\psi}(\mathbf{x}^{(i)})$'s and $\boldsymbol{\psi}(\mathbf{y}^{(j)}) \widehat{r}_{\boldsymbol{\theta}^*}(\mathbf{y}^{(j)})$'s are bounded, a Hoeffding-type bound can be used to control the gradient.

The gradient of the quadratic part of (8), as well as the curvature of both (7) and (8), involves the Hessian of ℓ_{KLIEP} :

$$\nabla^2 \ell_{\text{KLIEP}}(\boldsymbol{\theta}) = \frac{1}{n_y^2} \sum_{1 \leq j < j' \leq n_y} \left(\boldsymbol{\psi}(\mathbf{y}^{(j)}) - \boldsymbol{\psi}(\mathbf{y}^{(j')}) \right) \left(\boldsymbol{\psi}(\mathbf{y}^{(j)}) - \boldsymbol{\psi}(\mathbf{y}^{(j')}) \right)^\top \widehat{r}_\theta(\mathbf{y}^{(j)}) \widehat{r}_\theta(\mathbf{y}^{(j')}).$$

Note that the above only uses the samples from f_y . The form of the Hessian makes it clear that if too many of $\widehat{r}_\theta(\mathbf{y}^{(j)})$'s are small, this results in a loss of curvature. Moreover, when many $\widehat{r}_\theta(\mathbf{y}^{(j)})$'s are small, the identity $n_y^{-1} \sum_{j=1}^{n_y} \widehat{r}_\theta(\mathbf{y}^{(j)}) \equiv 1$ makes it likely that many $\widehat{r}_\theta(\mathbf{y}^{(j)})$'s are also large to balance the sum. This is likely to lead to the Hessian becoming ill-conditioned. As before, the boundedness of the density ratio provides a protection against this kind of degeneracy.

D.2 Consequences of the bounds on the population eigenvalues

D.2.1 Bounds on ω_k^*

It is an easy consequence of the definitions of ω_k^* , $\underline{\kappa}$, and $\bar{\kappa}$ that

$$\bar{\kappa}^{-1} \leq \|\omega_k^*\|_2 \leq \underline{\kappa}^{-1} \quad \text{for all } k = 1, \dots, p. \quad (80)$$

Before we turn to bounding the ℓ_1 -norm of ω_k^* in terms of its ℓ_{q_k} -“norm”, we look at some useful inequalities related to ℓ_q -“norms”. Fix $\lambda > 0$, and let $S_\lambda = \{k : |v_k| > \lambda\}$ and $s_\lambda = |S_\lambda|$. Then,

$$\|\mathbf{v}\|_q \geq \sum_{k \in S_\lambda} |v_k|^q \geq s_\lambda \lambda^q,$$

so that

$$s_\lambda \leq \lambda^{-q} \|\mathbf{v}\|_q. \quad (81)$$

Moreover,

$$\|\mathbf{v}_{S_\lambda^c}\|_1 = \sum_{k \notin S_\lambda} |v_k| = \sum_{k \notin S_\lambda} |v_k|^{1-q} |v_k|^q \leq \lambda^{1-q} \|\mathbf{v}\|_q. \quad (82)$$

Thus,

$$\|\mathbf{v}\|_1 = \|\mathbf{v}_{S_\lambda}\|_1 + \|\mathbf{v}_{S_\lambda^c}\|_1 \leq \sqrt{s_\lambda} \|\mathbf{v}\|_2 + \|\mathbf{v}_{S_\lambda^c}\|_1 \leq \lambda^{-q/2} \|\mathbf{v}\|_q^{1/2} \|\mathbf{v}\|_2 + \lambda^{1-q} \|\mathbf{v}\|_q. \quad (83)$$

To simplify the form of the upper bound, we balance the two terms by seeking $r \in \mathbb{R}$ such that

$$\lambda \asymp \|\mathbf{v}\|_q^r \quad \text{and} \quad \lambda^{-q/2} \|\mathbf{v}\|_q^{1/2} \asymp \lambda^{1-q} \|\mathbf{v}\|_q.$$

This is solved by $r = -1/(2 - q)$. Substituting this into (83),

$$\|\mathbf{v}\|_1 \leq (1 + \|\mathbf{v}\|_2) \|\mathbf{v}\|_q^{1/(2-q)}. \quad (84)$$

Applying (84) to ω_k^* ,

$$\|\omega_k^*\|_1 \leq (1 + \|\omega_k^*\|_2) s_{k,q_k}^{1/(2-q_k)} \leq (1 + \underline{\kappa}^{-1}) s_{k,q_k}^{1/(2-q_k)} \quad \text{for } k = 1, \dots, p. \quad (85)$$

D.2.2 Bounds on σ_k^2

Define

$$\begin{aligned} \sigma_{n,k}^2 &= \text{Var} \left[\sqrt{n} \left\langle \omega_k^*, \frac{1}{n_x} \sum_{i=1}^{n_x} \psi(\mathbf{x}^{(i)}) - \frac{1}{n_y} \sum_{j=1}^{n_y} \psi(\mathbf{y}^{(j)}) r_{\theta^*}(\mathbf{y}^{(j)}) \right\rangle \right] \\ &= \omega_k^{*\top} \{ \eta_{x,n}^{-1} \Sigma_\psi + \eta_{y,n}^{-1} \Sigma_{\psi r} \} \omega_k^*, \end{aligned}$$

where $\Sigma_\psi = \text{Cov}_x[\psi(\mathbf{x})]$ and $\Sigma_{\psi r} = \text{Cov}_y[(\psi(\mathbf{y}) - \boldsymbol{\mu}_\psi) r_{\theta^*}(\mathbf{y})]$. Since Σ_ψ and $\Sigma_{\psi r}$ are symmetric and positive definite by Condition 2, we have

$$\lambda_{\max}(\eta_{x,n}^{-1} \Sigma_\psi + \eta_{y,n}^{-1} \Sigma_{\psi r}) \leq \eta_{x,n}^{-1} \lambda_{\max}(\Sigma_\psi) + \eta_{y,n}^{-1} \lambda_{\max}(\Sigma_{\psi r}) \leq \bar{\kappa}/(\eta_{x,n} \eta_{y,n}),$$

and, similarly,

$$\lambda_{\min}(\eta_{x,n}^{-1} \Sigma_\psi + \eta_{y,n}^{-1} \Sigma_{\psi r}) \geq \underline{\kappa}/(\eta_{x,n} \eta_{y,n}).$$

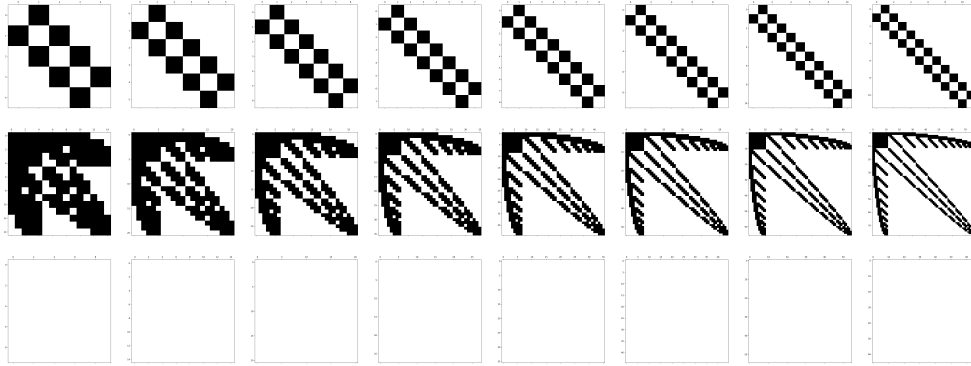
Thus,

$$\frac{\underline{\kappa}}{\bar{\kappa}^2 \eta_{x,n} \eta_{y,n}} \leq \frac{\underline{\kappa} \|\omega_k^*\|_2^2}{\eta_{x,n} \eta_{y,n}} \leq \sigma_k^2 \leq \frac{\bar{\kappa} \|\omega_k^*\|_2^2}{\eta_{x,n} \eta_{y,n}} \leq \frac{\bar{\kappa}}{\underline{\kappa}^2 \eta_{x,n} \eta_{y,n}}, \quad (86)$$

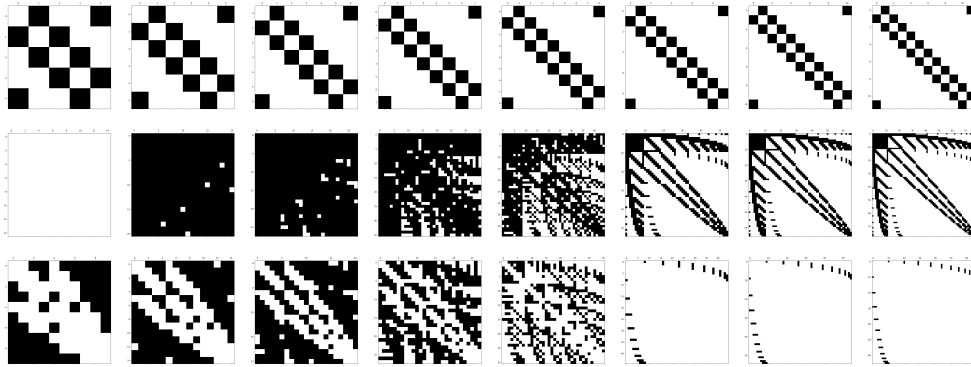
where the outer-most pair of inequalities use (80).

Figure 2: **The row sparsity of Σ_ψ^{-1} for some Ising models.** We examine the sparsity patterns of Γ_x (first row), Σ_ψ^{-1} (second row), and the symmetric difference of supports of $\Sigma_{\psi, \text{Gaussian}}^{-1}$ and the edge interaction diagonal block of Σ_ψ^{-1} (third row) for some Ising models for $m = 5, 6, \dots, 12$. Σ_ψ^{-1} is observed to have sparse rows when the maximum degree of Γ_x is small. In addition, the edge interaction diagonal block of Σ_ψ^{-1} is observed to be structurally similar to that of $\Sigma_{\psi, \text{Gaussian}}^{-1}$. The results here suggest that some form of row sparsity assumption on Σ_ψ^{-1} is reasonable even for Ising models if the maximum degree is expected to be small.

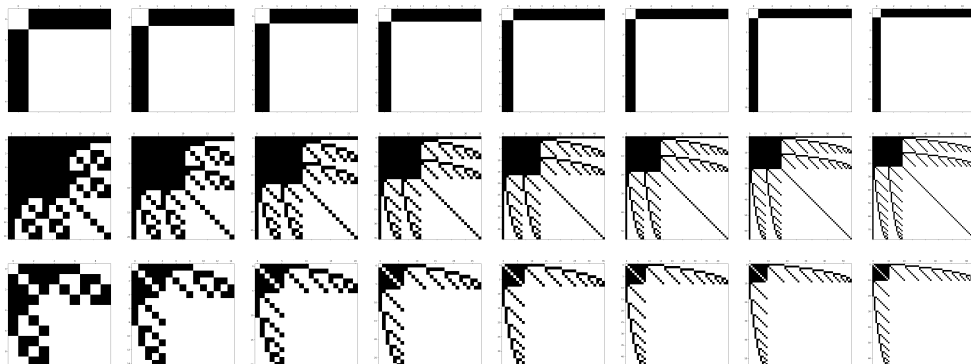
(a) chains



(b) cycles



(c) stars



D.3 When are the rows of Σ_ψ^{-1} sparse?

For our method, one sufficient condition for theoretical validity is consistent estimation of both θ^* and Σ_ψ^{-1} . It is well-understood that when parameters satisfy structural assumptions, they can be estimated consistently even in high-dimensional settings; this is what motivated us to use ℓ_1 -regularized procedures for sparse or approximately sparse θ^* and Σ_ψ^{-1} . However, we have $\Sigma_\psi^{-1} = \text{Cov}_x[\psi(\mathbf{x})]^{-1}$, and hence Σ_ψ^{-1} is determined by γ_x . Therefore, to see whether it is plausible to assume Σ_ψ^{-1} is a row-sparse matrix, it is helpful to understand how Σ_ψ^{-1} is related to γ_x .

Recall that f_x is an exponential family. Lemma 7 gives the map $\gamma_x \mapsto \Sigma_\psi^{-1}(\gamma_x)$ under the condition of regularity and minimality.

Lemma 7 (Essentially Lemma 1 in Loh and Wainwright (2013)). *Consider a regular, minimal exponential family*

$$f_x(\mathbf{x}) = \exp(\langle \gamma_x, \psi(\mathbf{x}) \rangle - A(\gamma_x)), \quad A(\gamma_x) = \log \left(\int \exp(\langle \gamma_x, \psi(\mathbf{x}) \rangle) d\mathbf{x} \right).$$

Then,

$$\left(\text{Cov}_x[\psi(\mathbf{x})] \right)^{-1} = \nabla^2 A^* \circ \nabla A(\gamma_x),$$

where A^* is the convex dual function to A

$$A^*(\boldsymbol{\mu}) = \sup_{\gamma \in \Omega} \{ \langle \boldsymbol{\mu}, \gamma \rangle - A(\gamma) \}.$$

Proof. The proof in Loh and Wainwright (2013) is a direct consequence of combining Proposition B.2 and Theorem 3.4 in Wainwright and Jordan (2008a); the former holds for *any* regular, minimal exponential family, and the latter, more generally. \square

Lemma 7 can be used to show that in the case of Gaussian graphical models, Σ_ψ^{-1} has sparse rows when the maximum degree of the underlying graph is small.

Example 3 (Gaussian graphical models). Suppose $\mathbf{x} \sim \mathcal{N}(\mathbf{0}, \Sigma)$ for some covariance matrix $\Sigma \in \mathbb{R}^{m \times m}$. Then, the probability density function is given by $f_x(\mathbf{x}) = \exp(\text{tr}[\mathbf{\Gamma}_x \Psi(\mathbf{x})] - A(\mathbf{\Gamma}_x))$, where $\mathbf{\Gamma}_x = 2^{-1} \Sigma^{-1}$, $\Psi(\mathbf{x}) = \mathbf{x} \mathbf{x}^\top$, and

$$A(\mathbf{\Gamma}_x) = \log Z(\mathbf{\Gamma}_x) = \frac{m}{2} \log(2\pi) - \frac{1}{2} \log \det(-2\mathbf{\Gamma}_x).$$

By direct computation,

$$\nabla A(\mathbf{\Gamma}_x) = \frac{1}{2} \mathbf{\Gamma}_x^{-1} = \Sigma,$$

and

$$\begin{aligned} A^*(\mathbf{M}) &= -\frac{m}{2} \log(2\pi e) - \frac{1}{2} \log \det(\mathbf{M}), \\ \nabla^2 A^*(\mathbf{M}) &= \frac{1}{2} \mathbf{D}_m^\top (\mathbf{M}^{-1} \otimes \mathbf{M}^{-1}) \mathbf{D}_m. \end{aligned}$$

where $\mathbf{D}_m : \mathbb{R}_{\binom{m+1}{2}} \rightarrow \mathbb{R}^{m^2}$ is the *duplication matrix*, which is defined by the property

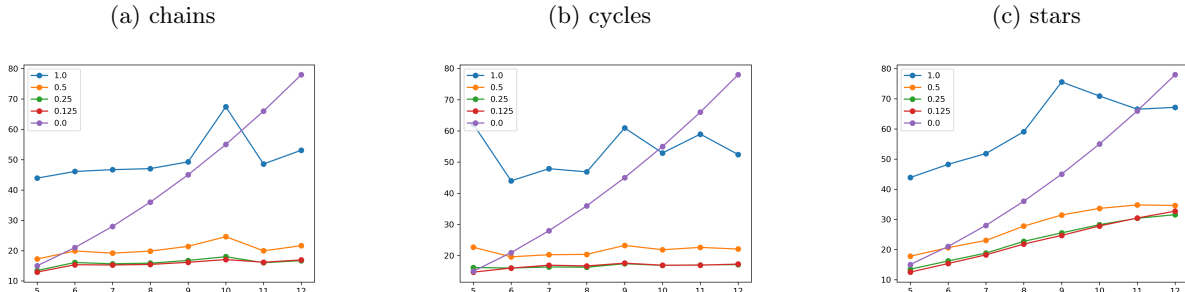
$$\mathbf{D}_m \text{vech}(\mathbf{M}) = \text{vec}(\mathbf{M}).$$

(Here, $\text{vech} : \mathbb{S}^m \rightarrow \mathbb{R}^{\binom{m+1}{2}}$ is the *half-vectorization* map that vectorizes only the lower-triangular part of a matrix.) Thus,

$$\Sigma_\psi^{-1} = \Sigma_\psi^{-1}(\mathbf{\Gamma}) = 2\mathbf{D}_m^\top (\mathbf{\Gamma} \otimes \mathbf{\Gamma}) \mathbf{D}_m,$$

so that Σ_ψ^{-1} is row sparse if Σ^{-1} is row sparse. In particular, the (ab, cd) -th component of Σ_ψ^{-1} is nonzero if and only if both $\gamma_{x,ab}$ and $\gamma_{x,cd}$ are nonzero.

Figure 3: **The growth of $\max_k \|\omega_k^*\|_{q_k}$ for some Ising models.** We plot $\max_k \|\omega_k^*\|_q$ as a function of the number of nodes m for $q = 1, 0.5, 0.25, 0.125, 0$. Except for $q = 0$, most sparse “norms” remain well-controlled even as m is increased. Thus, the assumption that $\max_k \|\omega_k^*\|_{q_k}$ is small appears to be reasonable for many Ising models.



For general Markov random fields, the usefulness of Lemma 7 is limited due to intractability of A . For the case of *discrete* Markov random fields, Loh and Wainwright (2013) study sufficient conditions under which the inverse of a *submatrix* of Σ_ψ reflects the structure of the underlying graph, but their proof techniques do not apply to the inverse of the full matrix.

Thus, we turn to numerical tools for verifying the plausibility of the row-sparsity assumption in the case of Ising models. For small values of the number of nodes $m = 5, 6, \dots, 12$, we first generate a graph by fixing a topology and drawing weights $\stackrel{iid}{\sim} \text{Unif}([-0.5, -0.2] \cup [0.2, 0.5])$. We then explicitly evaluate the population Σ_ψ^{-1} under an Ising model. We looked at three different topologies: a chain, a cycle, or a star.

The graph structures are displayed in the first rows of Figure 2 (a - c). The sparsity patterns of Σ_ψ^{-1} 's are in the second rows. Note that here, the sufficient statistics include the node potentials; the edge interaction parameters are associated with the last $\binom{m}{2}$ rows of Σ_ψ^{-1} . For ease of comparison, in the third rows, we also plot the symmetric differences of the support of $\Sigma_{\psi, \text{Gaussian}}^{-1}$, which is computed assuming a Gaussian model, and the support of the lower diagonal block of Σ_ψ^{-1} . (We ignored entries with magnitudes $< 10^{-10}$.) It is clear from the plots in the last rows that the edge interaction diagonal block of Σ_ψ^{-1} has a structure similar to that of $\Sigma_{\psi, \text{Gaussian}}^{-1}$. Σ_ψ^{-1} is typically denser compared to $\Sigma_{\psi, \text{Gaussian}}^{-1}$, but some form of row sparsity assumption still appears to be quite reasonable, at least for the examples we have considered.

As a further check, we tracked the evolution of $\max_k \|\omega_k^*\|_{q_k}$ over the edge interaction rows of Σ_ψ^{-1} as m was increased. (No thresholding was applied.) This resulted in Figure 3. We observe that although Σ_ψ^{-1} may violate exact sparsity — as evidenced by the curve corresponding to $q = 0$ — many sparse “norms” remain well-controlled even as m is increased. In fact, for chains and cycles, the plots are flat for $q = 0.5, 0.25, 0.125$.

Finally, following the ideas in Ma et al. (2017) and Yu et al. (2020), we remark that a modified procedure that uses sample splitting can be used to construct provably de-biased and asymptotically Gaussian estimators of the difference in situations when the rows of Σ_ψ^{-1} are only bounded in ℓ_1 -norm (without being sparse or approximately sparse). The modified procedure first splits the f_y -sample into two, and then uses only one part to obtain $\hat{\theta}$, and the other part to obtain $\hat{\Omega}$.

E Auxiliary results for the ℓ_1 -penalty case

E.1 Bounds on the gradients

The two lemmas in this section bound the gradients of the loss functions in (7) and (8).

Lemma 8. *Under Condition 1 with ℓ_1 -norm,*

$$\mathbb{P} \{ \|\nabla \ell_{KLIEP}(\theta^*)\|_\infty > t \} \leq 4p \exp(-ct^2n)$$

for some $c > 0$ depending on M_r, M_ψ only. In particular, if

$$\lambda_\theta \geq K \sqrt{\frac{\log p}{n}},$$

for some $K \geq \sqrt{2/c}$, then

$$\mathbb{P} \{2 \|\nabla \ell_{\text{KLIEP}}(\boldsymbol{\theta}^*)\|_\infty > \lambda_\theta\} \leq 4 \exp(-c' \lambda_\theta^2 n),$$

for some $c' > 0$.

Proof. Let $\boldsymbol{\mu}_\psi = (\mu_{\psi_k})_{k=1}^p = \mathbb{E}_x[\boldsymbol{\psi}(\mathbf{x})] = \mathbb{E}_y[\boldsymbol{\psi}(\mathbf{y})r_{\theta^*}(\mathbf{y})]$. Using $n_y^{-1} \sum_{j=1}^{n_y} \widehat{r}_{\theta^*}(\mathbf{y}^{(j)}) = 1$,

$$\begin{aligned} \nabla \ell_{\text{KLIEP}}(\boldsymbol{\theta}^*) &= -\frac{1}{n_x} \sum_{i=1}^{n_x} \boldsymbol{\psi}(\mathbf{x}^{(i)}) + \frac{1}{n_y} \sum_{j=1}^{n_y} \boldsymbol{\psi}(\mathbf{y}^{(j)}) \widehat{r}_{\theta^*}(\mathbf{y}^{(j)}) \\ &= -\frac{1}{n_x} \sum_{i=1}^{n_x} \boldsymbol{\psi}(\mathbf{x}^{(i)}) + \boldsymbol{\mu}_\psi + \frac{1}{n_y} \sum_{j=1}^{n_y} \{\boldsymbol{\psi}(\mathbf{y}^{(j)}) - \boldsymbol{\mu}_\psi\} \widehat{r}_{\theta^*}(\mathbf{y}^{(j)}) \\ &= -\frac{1}{n_x} \sum_{i=1}^{n_x} \boldsymbol{\psi}(\mathbf{x}^{(i)}) + \boldsymbol{\mu}_\psi + \frac{Z_y(\boldsymbol{\theta}^*)}{\widehat{Z}_y(\boldsymbol{\theta}^*)} \frac{1}{n_y} \sum_{j=1}^{n_y} \{\boldsymbol{\psi}(\mathbf{y}^{(j)}) - \boldsymbol{\mu}_\psi\} r_{\theta^*}(\mathbf{y}^{(j)}). \end{aligned}$$

Condition 1 implies that $Z_y(\boldsymbol{\theta}^*)/\widehat{Z}_y(\boldsymbol{\theta}^*) \in [M_r^{-1}, M_r]$. For any $t > 0$,

$$\begin{aligned} &\mathbb{P} \{ \|\nabla \ell_{\text{KLIEP}}(\boldsymbol{\theta}^*)\|_\infty > t \} \\ &\leq \mathbb{P} \left\{ \left\| \frac{1}{n_x} \sum_{i=1}^{n_x} \boldsymbol{\psi}(\mathbf{x}^{(i)}) - \boldsymbol{\mu}_\psi \right\|_\infty > \frac{t}{2} \right\} + \mathbb{P} \left\{ M_r \left\| \frac{1}{n_y} \sum_{j=1}^{n_y} \{\boldsymbol{\psi}(\mathbf{y}^{(j)}) - \boldsymbol{\mu}_\psi\} r_{\theta^*}(\mathbf{y}^{(j)}) \right\|_\infty > \frac{t}{2} \right\} \\ &\leq \sum_{k=1}^p \mathbb{P} \left\{ \left| \frac{1}{n_x} \sum_{i=1}^{n_x} \psi_k(\mathbf{x}_k^{(i)}) - \mu_{\psi_k} \right| > \frac{t}{2} \right\} \\ &\quad + \sum_{k=1}^p \mathbb{P} \left\{ M_r \left| \frac{1}{n_y} \sum_{j=1}^{n_y} \{\psi_k(\mathbf{y}_k^{(j)}) - \mu_{\psi_k}\} r_{\theta^*}(\mathbf{y}^{(j)}) \right| > \frac{t}{2} \right\}. \end{aligned}$$

Since $\{(\psi_k(\mathbf{x}_k^{(i)}) - \mu_{\psi_k})\}_{i=1}^{n_x}$ and $\{(\psi_k(\mathbf{y}_k^{(j)}) - \mu_{\psi_k}) r_{\theta^*}(\mathbf{y}^{(j)})\}_{j=1}^{n_y}$ are each i.i.d. bounded and mean zero random variables,

$$\mathbb{P} \left\{ \left| \frac{1}{n_x} \sum_{i=1}^{n_x} \psi_k(\mathbf{x}_k^{(i)}) - \mu_k^* \right| > \frac{t}{2} \right\} \leq 2 \exp(-c_1 t^2 n_x)$$

and

$$\mathbb{P} \left\{ M_r \left| \frac{1}{n_y} \sum_{j=1}^{n_y} \{\psi_k(\mathbf{y}_k^{(j)}) - \mu_{\psi_k}\} r_{\theta^*}(\mathbf{y}^{(j)}) \right| > \frac{t}{2} \right\} \leq 2 \exp(-c_2 t^2 n_y)$$

by Hoeffding's inequality, where $c_1, c_2 > 0$ are constants depending on M_r, M_ψ only. Thus,

$$\mathbb{P} \{ \|\nabla \ell_{\text{KLIEP}}(\boldsymbol{\theta}^*)\|_\infty > t \} \leq 2p \exp(-c_1 t^2 n_x) + 2p \exp(-c_2 t^2 n_y) \leq 4p \exp(-ct^2 n)$$

for some $c > 0$. □

Lemma 9. For $t \geq 2/n_y$,

$$\begin{aligned} &\mathbb{P} \left\{ \|\widehat{\mathbf{H}}(\boldsymbol{\theta}^*) \boldsymbol{\omega}_k^* - \mathbf{e}_k\|_\infty > t \right\} \\ &\leq 2 \exp \left(-\frac{ct^2 n_y}{(1 + \underline{\kappa}^{-1})^2 s_{k, q_k}^{2/(2-q_k)}} \right) + 2p \exp \left(-\frac{c' t^2 n_y}{(1 + \underline{\kappa}^{-1})^2 s_{k, q_k}^{2/(2-q_k)}} \right) \end{aligned}$$

for some $c, c' > 0$ depending on M_r, M_ψ only. In particular, if

$$\lambda_k \geq K(1 + \underline{\kappa}^{-1})s_{k,q_k}^{1/(2-q_k)} \sqrt{\frac{\log p}{n_y}},$$

for some $K \geq \sqrt{2/(c \wedge c')}$, then

$$\mathbb{P} \left\{ 2 \|\widehat{\mathbf{H}}(\boldsymbol{\theta}^*) \boldsymbol{\omega}_k^* - \mathbf{e}_k\|_\infty > \lambda_k \right\} \leq 4 \exp \left(- \frac{c'' \lambda_k^{*2} n_y}{(1 + \underline{\kappa}^{-1})^2 s_{k,q_k}^{2/(2-q_k)}} \right).$$

for some $c'' > 0$.

Proof. Let $\widehat{\mathbf{H}}(\boldsymbol{\theta}) = \nabla^2 \ell_{\text{KLIEP}}(\boldsymbol{\theta})$, and $\mathbf{H}(\boldsymbol{\theta}) = (\widehat{Z}_y^2(\boldsymbol{\theta})/Z_y^2(\boldsymbol{\theta}))\widehat{\mathbf{H}}(\boldsymbol{\theta})$. We have $\boldsymbol{\Sigma}_\psi \boldsymbol{\omega}_k^* = \mathbf{e}_k$ by definition, and $\mathbb{E}_y \mathbf{H}(\boldsymbol{\theta}^*) = (1 - n_y^{-1})\boldsymbol{\Sigma}_\psi$ by (27). Therefore,

$$\widehat{\mathbf{H}}(\boldsymbol{\theta}^*) \boldsymbol{\omega}_k^* - \mathbf{e}_k = \{\widehat{\mathbf{H}}(\boldsymbol{\theta}^*) - \mathbf{H}(\boldsymbol{\theta}^*)\} \boldsymbol{\omega}_k^* + \{\mathbf{H}(\boldsymbol{\theta}^*) - \mathbb{E}_y \mathbf{H}(\boldsymbol{\theta}^*)\} \boldsymbol{\omega}_k^* - n_y^{-1} \mathbf{e}_k.$$

For $t \geq 2/n_y$,

$$\begin{aligned} \mathbb{P} \left\{ \|\widehat{\mathbf{H}}(\boldsymbol{\theta}^*) \boldsymbol{\omega}_k^* - \mathbf{e}_k\|_\infty > t \right\} &\leq \mathbb{P} \left\{ \|\widehat{\mathbf{H}}(\boldsymbol{\theta}^*) \boldsymbol{\omega}_k^* - (1 - n_y^{-1}) \mathbf{e}_k\|_\infty > \frac{t}{2} \right\} \\ &\leq \mathbb{P} \left\{ \|\{\widehat{\mathbf{H}}(\boldsymbol{\theta}^*) - \mathbf{H}(\boldsymbol{\theta}^*)\} \boldsymbol{\omega}_k^*\|_\infty > \frac{t}{4} \right\} + \mathbb{P} \left\{ \|\{\mathbf{H}(\boldsymbol{\theta}^*) - \mathbb{E}_y \mathbf{H}(\boldsymbol{\theta}^*)\} \boldsymbol{\omega}_k^*\|_\infty > \frac{t}{4} \right\}. \end{aligned}$$

By Lemma 10,

$$\mathbb{P} \left\{ \|\{\widehat{\mathbf{H}}(\boldsymbol{\theta}^*) - \mathbf{H}(\boldsymbol{\theta}^*)\} \boldsymbol{\omega}_k^*\|_\infty > \frac{t}{4} \right\} \leq 2 \exp \left(- \frac{ct^2 n_y}{(1 + \underline{\kappa}^{-1})^2 s_{k,q_k}^{2/(2-q_k)}} \right),$$

where $c > 0$ is a constant depending only on M_r, M_ψ . By Lemma 11,

$$\mathbb{P} \left\{ \|\{\mathbf{H}(\boldsymbol{\theta}^*) - \mathbb{E}_y \mathbf{H}(\boldsymbol{\theta}^*)\} \boldsymbol{\omega}_k^*\|_\infty > \frac{t}{4} \right\} \leq 2p \exp \left(- \frac{c't^2 n_y}{(1 + \underline{\kappa}^{-1})^2 s_{k,q_k}^{2/(2-q_k)}} \right),$$

where $c' > 0$ is a constant depending only on M_r, M_ψ . Thus,

$$\begin{aligned} \mathbb{P} \left\{ \|\widehat{\mathbf{H}}(\boldsymbol{\theta}^*) \boldsymbol{\omega}_k^* - \mathbf{e}_k\|_\infty > t \right\} \\ \leq 2 \exp \left(- \frac{ct^2 n_y}{(1 + \underline{\kappa}^{-1})^2 s_{k,q_k}^{2/(2-q_k)}} \right) + 2p \exp \left(- \frac{c't^2 n_y}{(1 + \underline{\kappa}^{-1})^2 s_{k,q_k}^{2/(2-q_k)}} \right). \end{aligned}$$

□

E.2 Bounds on the Hessian

This section contains the technical lemmas that go into bounding the $\ell_1 \rightarrow \ell_\infty$ operator norm — a.k.a. the maximum magnitude component — of the Hessian. The ultimate goal is to control the ℓ_∞ -norm of the matrix-vector product $\nabla^2 \ell_{\text{KLIEP}}(\boldsymbol{\theta}^*) \boldsymbol{\omega}_k^*$. Since a bound on the ℓ_1 -norm of $\boldsymbol{\omega}_k^*$ is easily implied by our structural assumptions on $\boldsymbol{\omega}_k^*$, it is natural to consider the $\ell_1 \rightarrow \ell_\infty$ operator norm of the Hessian in bounding the matrix-vector product.

To compute the bound, we first observe that $\nabla^2 \ell_{\text{KLIEP}}(\boldsymbol{\theta}^*) \approx \boldsymbol{\Sigma}_\psi$, and decompose the Hessian into a sum of three terms:

$$\widehat{\mathbf{H}}(\boldsymbol{\theta}^*) = \underbrace{\{\widehat{\mathbf{H}}(\boldsymbol{\theta}^*) - \mathbf{H}(\boldsymbol{\theta}^*)\}}_{\text{Lemma 10}} + \underbrace{\{\mathbf{H}(\boldsymbol{\theta}^*) - \mathbb{E}_y \mathbf{H}(\boldsymbol{\theta}^*)\}}_{\text{Lemma 11}} + (1 - n_y^{-1})\boldsymbol{\Sigma}_\psi,$$

where $\widehat{\mathbf{H}}(\boldsymbol{\theta}) = \nabla^2 \ell_{\text{KLIEP}}(\boldsymbol{\theta})$, and $\mathbf{H}(\boldsymbol{\theta}) = (\widehat{Z}_y^2(\boldsymbol{\theta})/Z_y^2(\boldsymbol{\theta}))\widehat{\mathbf{H}}(\boldsymbol{\theta})$.

Lemma 10 reduces the difference $\widehat{\mathbf{H}}(\boldsymbol{\theta}^*) - \mathbf{H}(\boldsymbol{\theta}^*)$ to the deviation of the sample average of the ratios from their expectation. Lemma 11 is the usual concentration bound for U-statistics applied to our problem.

Lemma 10. *Suppose Condition 1 holds, and let $\boldsymbol{\theta} \in \bar{\mathcal{B}}_\rho(\boldsymbol{\theta}^*)$. For any $\mathbf{v} \in \mathbb{R}^p$,*

$$\mathbb{P}\{\|\{\widehat{\mathbf{H}}(\boldsymbol{\theta}) - \mathbf{H}(\boldsymbol{\theta})\}\mathbf{v}\|_\infty > t\} \leq 2 \exp\left(-\frac{t^2 n_y}{2M_\psi^4 M_r^8 (M_r + 1)^2 (M_r - M_r^{-1})^2 \|\mathbf{v}\|_1^2}\right).$$

In particular,

$$\mathbb{P}\{\|\widehat{\mathbf{H}}(\boldsymbol{\theta}) - \mathbf{H}(\boldsymbol{\theta})\|_\infty > t\} \leq 2 \exp\left(-\frac{t^2 n_y}{2M_\psi^4 M_r^8 (M_r + 1)^2 (M_r - M_r^{-1})^2}\right).$$

Proof. Condition 1 implies that $\widehat{Z}_y(\boldsymbol{\theta})/Z_y(\boldsymbol{\theta}) \in [M_r^{-1}, M_r]$, and that $\widehat{\mathbf{H}}(\boldsymbol{\theta})$ has uniformly bounded components. In particular, on $\bar{\mathcal{B}}_\rho(\boldsymbol{\theta}^*)$, for any $k, \ell \in [p]$,

$$\begin{aligned} |\widehat{H}_{k\ell}(\boldsymbol{\theta})| &= \left| \frac{1}{n_y^2} \sum_{1 \leq j < j' \leq n_y} (\psi_k(\mathbf{y}_k^{(j)}) - \psi_k(\mathbf{y}_k^{(j')})) (\psi_\ell(\mathbf{y}_\ell^{(j)}) - \psi_\ell(\mathbf{y}_\ell^{(j')})) \widehat{r}_\theta(\mathbf{y}^{(j)}) \widehat{r}_\theta(\mathbf{y}^{(j')}) \right| \\ &\leq \frac{1}{n_y^2} \sum_{1 \leq j < j' \leq n_y} \left| \psi_k(\mathbf{y}_k^{(j)}) - \psi_k(\mathbf{y}_k^{(j')}) \right| \left| \psi_\ell(\mathbf{y}_\ell^{(j)}) - \psi_\ell(\mathbf{y}_\ell^{(j')}) \right| \widehat{r}_\theta(\mathbf{y}^{(j)}) \widehat{r}_\theta(\mathbf{y}^{(j')}) \leq 2M_\psi^2 M_r^4. \end{aligned}$$

Now,

$$\widehat{\mathbf{H}}(\boldsymbol{\theta}) - \mathbf{H}(\boldsymbol{\theta}) = \left(1 - \frac{\widehat{Z}_y(\boldsymbol{\theta})}{Z_y(\boldsymbol{\theta})}\right) \widehat{\mathbf{H}}(\boldsymbol{\theta}) = \left(1 - \frac{\widehat{Z}_y(\boldsymbol{\theta})}{Z_y(\boldsymbol{\theta})}\right) \left(1 + \frac{\widehat{Z}_y(\boldsymbol{\theta})}{Z_y(\boldsymbol{\theta})}\right) \widehat{\mathbf{H}}(\boldsymbol{\theta}),$$

so that

$$\begin{aligned} \mathbb{P}\{\|\{\widehat{\mathbf{H}}(\boldsymbol{\theta}) - \mathbf{H}(\boldsymbol{\theta})\}\mathbf{v}\|_\infty > t\} &\leq \mathbb{P}\left\{\|\widehat{\mathbf{H}}(\boldsymbol{\theta})\|_\infty \|\mathbf{v}\|_1 \left|\frac{\widehat{Z}_y(\boldsymbol{\theta})}{Z_y(\boldsymbol{\theta})} + 1\right| \left|\frac{\widehat{Z}_y(\boldsymbol{\theta})}{Z_y(\boldsymbol{\theta})} - 1\right| > t\right\} \\ &\leq \mathbb{P}\left\{2M_\psi^2 M_r^4 (M_r + 1) \|\mathbf{v}\|_1 \left|\frac{\widehat{Z}_y(\boldsymbol{\theta})}{Z_y(\boldsymbol{\theta})} - 1\right| > t\right\}. \end{aligned}$$

It then follows by Lemma 6 that

$$\mathbb{P}\{\|\{\widehat{\mathbf{H}}(\boldsymbol{\theta}) - \mathbf{H}(\boldsymbol{\theta})\}\mathbf{v}\|_\infty > t\} \leq 2 \exp\left(-\frac{t^2 n_y}{2M_\psi^4 M_r^8 (M_r + 1)^2 (M_r - M_r^{-1})^2 \|\mathbf{v}\|_1^2}\right).$$

□

Lemma 11. *Suppose Condition 1 holds, and let $\boldsymbol{\theta} \in \bar{\mathcal{B}}_\rho(\boldsymbol{\theta}^*)$. For any $\mathbf{v} \in \mathbb{R}^p$ and any $k \in [p]$,*

$$\mathbb{P}\left\{\left|\mathbf{e}_k^\top \{\mathbf{H}(\boldsymbol{\theta}) - \mathbb{E}_y \mathbf{H}(\boldsymbol{\theta})\}\mathbf{v}\right| > t\right\} \leq 2 \exp\left(-\frac{t^2 n_y}{16M_\psi^4 M_r^4 \|\mathbf{v}\|_1^2}\right).$$

In particular,

$$\mathbb{P}\left\{\|\{\mathbf{H}(\boldsymbol{\theta}) - \mathbb{E}_y \mathbf{H}(\boldsymbol{\theta})\}\mathbf{v}\|_\infty > t\right\} \leq 2 \exp\left(-\frac{t^2 n_y}{16M_\psi^4 M_r^4 \|\mathbf{v}\|_1^2} + \log p\right).$$

and

$$\mathbb{P}\left\{\|\{\mathbf{H}(\boldsymbol{\theta}) - \mathbb{E}_y \mathbf{H}(\boldsymbol{\theta})\}\|_\infty > t\right\} \leq 2 \exp\left(-\frac{t^2 n_y}{16M_\psi^4 M_r^4} + \log p\right).$$

Proof. For any $k \in [p]$ and for any $a > 0$,

$$\begin{aligned} \mathbb{P}\left\{\mathbf{e}_k^\top \{\mathbf{H}(\boldsymbol{\theta}) - \mathbb{E}_y \mathbf{H}(\boldsymbol{\theta})\}\mathbf{v} > t\right\} &= \mathbb{P}\left\{\|\mathbf{v}\|_1 a \cdot \mathbf{e}_k^\top \{\mathbf{H}(\boldsymbol{\theta}) - \mathbb{E}_y \mathbf{H}(\boldsymbol{\theta})\}(\mathbf{v}/\|\mathbf{v}\|_1) > at\right\} \\ &\leq \mathbb{P}\left\{\exp(\|\mathbf{v}\|_1 a \cdot \mathbf{e}_k^\top \{\mathbf{H}(\boldsymbol{\theta}) - \mathbb{E}_y \mathbf{H}(\boldsymbol{\theta})\}(\mathbf{v}/\|\mathbf{v}\|_1)) > \exp(at)\right\} \\ &\leq \exp(-at) \mathbb{E}_y \left[\exp(\|\mathbf{v}\|_1 a \cdot \mathbf{e}_k^\top \{\mathbf{H}(\boldsymbol{\theta}) - \mathbb{E}_y \mathbf{H}(\boldsymbol{\theta})\}(\mathbf{v}/\|\mathbf{v}\|_1))\right] \\ &\leq \exp(-at + 4M_\psi^4 M_r^4 \|\mathbf{v}\|_1^2 a^2 / n_y), \end{aligned}$$

where in the last line, we have used Lemma 12. Optimizing the bound, we get

$$\mathbb{P} \left\{ \mathbf{e}_k^\top \{ \mathbf{H}(\boldsymbol{\theta}) - \mathbb{E}_y \mathbf{H}(\boldsymbol{\theta}) \} \mathbf{v} > t \right\} \leq \exp \left(- \frac{t^2 n_y}{16 M_\psi^4 M_r^4 \|\mathbf{v}\|_1^2} \right).$$

A similar argument applied to the other side gives us

$$\mathbb{P} \left\{ | \mathbf{e}_k^\top \{ \mathbf{H}(\boldsymbol{\theta}) - \mathbb{E}_y \mathbf{H}(\boldsymbol{\theta}) \} \mathbf{v} | > t \right\} \leq 2 \exp \left(- \frac{t^2 n_y}{16 M_\psi^4 M_r^4 \|\mathbf{v}\|_1^2} \right).$$

Taking the union bound over all $k \in [p]$,

$$\mathbb{P} \left\{ \| \{ \mathbf{H}(\boldsymbol{\theta}) - \mathbb{E}_y \mathbf{H}(\boldsymbol{\theta}) \} \mathbf{v} \|_\infty > t \right\} \leq 2 \exp \left(- \frac{t^2 n_y}{16 M_\psi^4 M_r^4 \|\mathbf{v}\|_1^2} + \log p \right).$$

□

Lemma 12. *Suppose Condition 1 holds, and let $\boldsymbol{\theta} \in \bar{\mathcal{B}}_\rho(\boldsymbol{\theta}^*)$. For any $\mathbf{u}, \mathbf{v} \in \mathbb{R}^p$ with $\|\mathbf{u}\|_1 = \|\mathbf{v}\|_1 = 1$ and any $t \in \mathbb{R}$,*

$$\mathbb{E}_y \left[\exp \left(t \cdot \mathbf{u}^\top \{ \mathbf{H}(\boldsymbol{\theta}) - \mathbb{E}_y \mathbf{H}(\boldsymbol{\theta}) \} \mathbf{v} \right) \right] \leq \exp(4 M_\psi^4 M_r^4 t^2 / n_y).$$

Proof. Define

$$U := \frac{2}{1 - 1/n_y} \mathbf{u}^\top \mathbf{H}(\boldsymbol{\theta}) \mathbf{v} = \frac{2}{n_y(n_y - 1)} \sum_{1 \leq j < j' \leq n_y} g(\mathbf{y}^{(j)}, \mathbf{y}^{(j')}),$$

where

$$g(\mathbf{y}, \mathbf{y}') = \langle \boldsymbol{\psi}(\mathbf{y}) - \boldsymbol{\psi}(\mathbf{y}'), \mathbf{u} \rangle \langle \boldsymbol{\psi}(\mathbf{y}) - \boldsymbol{\psi}(\mathbf{y}'), \mathbf{v} \rangle r_\theta(\mathbf{y}) r_\theta(\mathbf{y}').$$

Let

$$V(\mathbf{y}^{(1)}, \dots, \mathbf{y}^{(n_y)}) := \frac{1}{\lfloor n_y/2 \rfloor} \left(g(\mathbf{y}^{(1)}, \mathbf{y}^{(2)}) + g(\mathbf{y}^{(3)}, \mathbf{y}^{(4)}) + \dots + g(\mathbf{y}^{(2\lfloor n_y/2 \rfloor - 1)}, \mathbf{y}^{(2\lfloor n_y/2 \rfloor)}) \right)$$

and write

$$U = \frac{1}{n_y!} \sum_{\sigma \in \mathfrak{S}_{n_y}} V(\mathbf{y}^{(\sigma(1))}, \dots, \mathbf{y}^{(\sigma(n_y))}),$$

where \mathfrak{S}_{n_y} is the group of permutations on $[n_y]$. For any $t \in \mathbb{R}$,

$$\begin{aligned} & \mathbb{E}_y \left[\exp \left(t \cdot \mathbf{u}^\top \{ \mathbf{H}(\boldsymbol{\theta}) - \mathbb{E}_y \mathbf{H}(\boldsymbol{\theta}) \} \mathbf{v} \right) \right] \\ &= \mathbb{E}_y \left[\exp \left(\frac{1 - 1/n_y}{2} t \cdot (U - \mathbb{E}_y U) \right) \right] \\ &= \mathbb{E}_y \left[\exp \left(\frac{1 - 1/n_y}{2} t \right. \right. \\ &\quad \left. \left. \times \frac{1}{n_y!} \left(\sum_{\sigma \in \mathfrak{S}_{n_y}} \left(V(\mathbf{y}^{(\sigma(1))}, \dots, \mathbf{y}^{(\sigma(n_y))}) - \mathbb{E}_y \left[V(\mathbf{y}^{(\sigma(1))}, \dots, \mathbf{y}^{(\sigma(n_y))}) \right] \right) \right) \right) \right] \\ &\leq \frac{1}{n_y!} \sum_{\sigma \in \mathfrak{S}_{n_y}} \mathbb{E}_y \left[\exp \left(\frac{1 - 1/n_y}{2} t \right. \right. \\ &\quad \left. \left. \times \left(V(\mathbf{y}^{(\sigma(1))}, \dots, \mathbf{y}^{(\sigma(n_y))}) - \mathbb{E}_y \left[V(\mathbf{y}^{(\sigma(1))}, \dots, \mathbf{y}^{(\sigma(n_y))}) \right] \right) \right) \right] \\ &\leq \exp(4 M_\psi^4 M_r^4 t^2 / n_y), \end{aligned}$$

where the second-to-last inequality follows from the Jensen's inequality and the last inequality follows from Lemma 13. □

Lemma 13. Let $V(\mathbf{y}^{(1)}, \dots, \mathbf{y}^{(n_y)})$ be as in the proof of Lemma 12. For any $t \in \mathbb{R}$,

$$\mathbb{E}_y \left[\exp \left(t \cdot \left(V(\mathbf{y}^{(1)}, \dots, \mathbf{y}^{(n_y)}) - \mathbb{E}_y \left[V(\mathbf{y}^{(1)}, \dots, \mathbf{y}^{(n_y)}) \right] \right) \right) \right] \leq \exp(16M_\psi^4 M_r^4 t^2 / n_y).$$

Proof. Consider a random variable G with $|G| \leq D$ and $\mathbb{E}G = g$. Using the convexity of the exponential function,

$$e^{tG} \leq \frac{D-G}{2D} e^{-Dt} + \frac{G+D}{2D} e^{Dt},$$

so that

$$\begin{aligned} \mathbb{E}[e^{t(G-g)}] &\leq e^{-tg} \frac{(D-g)e^{-Dt} + (D+g)e^{Dt}}{2D} \\ &= e^{-tg} \frac{e^{-Dt}(D-g + (D+g)e^{2Dt})}{2D} \\ &= \exp \left(-(D+g)t + \log \left(1 - \frac{D+g}{2D} + \frac{D+g}{2D} e^{2Dt} \right) \right). \end{aligned}$$

Put $\tilde{t} = 2Dt$ and $p = (D+g)/2D$, and write

$$h(\tilde{t}) = -p\tilde{t} + \log(1 - p + pe^{\tilde{t}}).$$

Then,

$$h'(\tilde{t}) = -p + \frac{pe^{\tilde{t}}}{1 - p + pe^{\tilde{t}}}$$

and

$$h''(\tilde{t}) = \frac{(1-p)pe^{\tilde{t}}}{(1-p+pe^{\tilde{t}})^2} = \left(\frac{pe^{\tilde{t}}}{1-p+pe^{\tilde{t}}} \right) \left(1 - \frac{pe^{\tilde{t}}}{1-p+pe^{\tilde{t}}} \right) \leq \frac{1}{4},$$

since $p \exp(\tilde{t}) / (1 - p + p \exp(\tilde{t})) \in (0, 1)$. By Taylor's theorem,

$$h(\tilde{t}) \leq h(0) + h'(0)\tilde{t} + \frac{1}{8}\tilde{t}^2 = \frac{1}{8}\tilde{t}^2,$$

so that

$$\mathbb{E}[e^{t(G-g)}] \leq e^{D^2 t^2 / 2}. \quad (87)$$

Now, $g(\mathbf{y}^{(j)}, \mathbf{y}^{(j')})$'s occurring in $V(\mathbf{y}^{(1)}, \dots, \mathbf{y}^{(n_y)})$ are i.i.d. with

$$\begin{aligned} |g(\mathbf{y}^{(j)}, \mathbf{y}^{(j')})| &= \left| \left\langle \boldsymbol{\psi}(\mathbf{y}^{(j)}) - \boldsymbol{\psi}(\mathbf{y}^{(j')}), \mathbf{u} \right\rangle \left\langle \boldsymbol{\psi}(\mathbf{y}^{(j)}) - \boldsymbol{\psi}(\mathbf{y}^{(j')}), \mathbf{v} \right\rangle r_\theta(\mathbf{y}^{(j)}) r_\theta(\mathbf{y}^{(j')}) \right| \\ &\leq \left\| \boldsymbol{\psi}(\mathbf{y}^{(j)}) - \boldsymbol{\psi}(\mathbf{y}^{(j')}) \right\|_\infty^2 r_\theta(\mathbf{y}^{(j)}) r_\theta(\mathbf{y}^{(j')}) \leq 4M_\psi^2 M_r^2, \end{aligned} \quad (88)$$

since $\|\mathbf{u}\|_1 = \|\mathbf{v}\|_1 = 1$. Applying (87) to the random variable $g(\mathbf{y}^{(1)}, \mathbf{y}^{(2)})$,

$$\mathbb{E}_y \left[\exp \left(\frac{t}{\lfloor n_y/2 \rfloor} \cdot \left(g(\mathbf{y}^{(1)}, \mathbf{y}^{(2)}) - \mathbb{E}_y \left[g(\mathbf{y}^{(1)}, \mathbf{y}^{(2)}) \right] \right) \right) \right] \leq \exp(32M_\psi^4 M_r^4 t^2 / n_y^2).$$

By independence,

$$\begin{aligned} &\mathbb{E}_y \left[\exp \left(t \cdot \left(V(\mathbf{y}^{(1)}, \dots, \mathbf{y}^{(n_y)}) - \mathbb{E}_y \left[V(\mathbf{y}^{(1)}, \dots, \mathbf{y}^{(n_y)}) \right] \right) \right) \right] \\ &= \mathbb{E}_y \left[\exp \left(\frac{t}{\lfloor n_y/2 \rfloor} \cdot \left(g(\mathbf{y}^{(1)}, \mathbf{y}^{(2)}) - \mathbb{E}_y \left[g(\mathbf{y}^{(1)}, \mathbf{y}^{(2)}) \right] \right) \right) \right]^{\lfloor n_y/2 \rfloor} \leq \exp(16M_\psi^4 M_r^4 t^2 / n_y). \end{aligned}$$

□

E.3 Restricted strong convexity

In the following,

$$\mathcal{K}(S, \beta, \rho) = \{\mathbf{v} \in \mathbb{R}^p : \|\mathbf{v}_{S^c}\|_1 \leq \beta \|\mathbf{v}_S\|_1 + (1 + \beta)\rho, \|\mathbf{v}\| \leq 1\},$$

where $S \subseteq [p]$ is nonempty, $\beta \geq 0$, and $\rho \geq 0$.

Lemma 14. *Suppose $Z_y^2(\boldsymbol{\theta}^*)/\widehat{Z}_y^2(\boldsymbol{\theta}^*) \geq c$ for some $c > 0$, and*

$$\|\mathbf{H}(\boldsymbol{\theta}^*) - \mathbb{E}_y \mathbf{H}(\boldsymbol{\theta}^*)\|_s \leq \underline{\kappa}/(2(2 + \beta)^2)$$

for some $s \in [p]$ and $\beta \geq 0$. Then for all nonempty $S \subseteq [p]$ with $|S| \leq s$ and for all $\rho \geq 0$,

$$\mathbf{v}^\top \widehat{\mathbf{H}}(\boldsymbol{\theta}^*) \mathbf{v} \geq \frac{c\underline{\kappa}}{2} \left(\|\mathbf{v}\|^2 - \frac{\rho^2}{s} \right) \quad \text{for all } \mathbf{v} \in \mathcal{K}(S, \beta, \rho),$$

as well as

$$\mathbf{v}^\top \widehat{\mathbf{H}}(\boldsymbol{\theta}) \mathbf{v} \geq \exp(-2M_\psi(M_r^2 + 1)\|\boldsymbol{\theta} - \boldsymbol{\theta}^*\|_1) \cdot \frac{c\underline{\kappa}}{2} \left(\|\mathbf{v}\|^2 - \frac{\rho^2}{s} \right) \quad \text{for all } \mathbf{v} \in \mathcal{K}(S, \beta, \rho).$$

Proof. We have

$$\mathbf{v}^\top \widehat{\mathbf{H}}(\boldsymbol{\theta}^*) \mathbf{v} = \frac{Z_y^2(\boldsymbol{\theta}^*)}{\widehat{Z}_y^2(\boldsymbol{\theta}^*)} \mathbf{v}^\top \mathbf{H}(\boldsymbol{\theta}^*) \mathbf{v} = \left[\left(1 - \frac{1}{n_y}\right) \mathbf{v}^\top \boldsymbol{\Sigma}_\psi \mathbf{v} + \mathbf{v}^\top \{\mathbf{H}(\boldsymbol{\theta}^*) - \mathbb{E}_y \mathbf{H}(\boldsymbol{\theta}^*)\} \mathbf{v} \right].$$

For n_y large enough, under the conditions of the lemma and applying Lemma 16,

$$\begin{aligned} \mathbf{v}^\top \widehat{\mathbf{H}}(\boldsymbol{\theta}^*) \mathbf{v} &\geq c \left(\underline{\kappa} \|\mathbf{v}\|^2 - \frac{\underline{\kappa}}{2(2 + \beta)^2} \left(\|\mathbf{v}\| + \frac{\|\mathbf{v}\|_1}{\sqrt{s}} \right)^2 \right) \\ &\geq c \left(\underline{\kappa} \|\mathbf{v}\|^2 - \frac{\underline{\kappa}}{2} \left(\|\mathbf{v}\| + \frac{\rho}{\sqrt{s}} \right)^2 \right) \\ &\geq \frac{c\underline{\kappa}}{2} \left(\|\mathbf{v}\|^2 - \frac{\rho^2}{s} \right). \end{aligned} \tag{89}$$

For the second part of the statement, first note

$$\begin{aligned} \mathbf{v}^\top \widehat{\mathbf{H}}(\boldsymbol{\theta}) \mathbf{v} &\geq \min_{j, j'} \frac{\widehat{r}_\theta(\mathbf{y}^{(j)}) \widehat{r}_\theta(\mathbf{y}^{(j')})}{\widehat{r}_{\boldsymbol{\theta}^*}(\mathbf{y}^{(j)}) \widehat{r}_{\boldsymbol{\theta}^*}(\mathbf{y}^{(j')})} \mathbf{v}^\top \widehat{\mathbf{H}}(\boldsymbol{\theta}^*) \mathbf{v} \\ &= \min_{j, j'} \exp \left\{ \left(\psi(\mathbf{y}^{(j)}) + \psi(\mathbf{y}^{(j')}) \right)^\top (\boldsymbol{\theta} - \boldsymbol{\theta}^*) - 2 \log \frac{\widehat{Z}_y(\boldsymbol{\theta})}{\widehat{Z}_y(\boldsymbol{\theta}^*)} \right\} \mathbf{v}^\top \widehat{\mathbf{H}}(\boldsymbol{\theta}^*) \mathbf{v}. \end{aligned}$$

By convexity of LogSumExp,

$$\begin{aligned} -\log \widehat{Z}_y(\boldsymbol{\theta}) + \log \widehat{Z}_y(\boldsymbol{\theta}^*) &\geq -\nabla[\log \widehat{Z}_y(\boldsymbol{\theta})]^\top (\boldsymbol{\theta} - \boldsymbol{\theta}^*) \\ &= -\frac{1}{n_y} \sum_{j=1}^{n_y} \widehat{r}_\theta(\mathbf{y}^{(j)}) \psi(\mathbf{y}^{(j)})^\top (\boldsymbol{\theta} - \boldsymbol{\theta}^*) \geq -M_\psi M_r^2 \|\boldsymbol{\theta} - \boldsymbol{\theta}^*\|_1, \end{aligned}$$

so that

$$\exp \left\{ (\boldsymbol{\theta} - \boldsymbol{\theta}^*)^\top \left(\psi(\mathbf{y}^{(j)}) + \psi(\mathbf{y}^{(j')}) \right) - 2 \log \frac{\widehat{Z}_y(\boldsymbol{\theta})}{\widehat{Z}_y(\boldsymbol{\theta}^*)} \right\} \geq -2M_\psi(M_r^2 + 1)\|\boldsymbol{\theta} - \boldsymbol{\theta}^*\|_1,$$

and hence,

$$\mathbf{v}^\top \widehat{\mathbf{H}}(\boldsymbol{\theta}) \mathbf{v} \geq \exp(-2M_\psi(M_r^2 + 1)\|\boldsymbol{\theta} - \boldsymbol{\theta}^*\|_1) \mathbf{v}^\top \widehat{\mathbf{H}}(\boldsymbol{\theta}^*) \mathbf{v}.$$

Combining with (89) from the first part finishes the proof. \square

Lemma 15. For $c > 0$, $\beta \geq 0$, $\varepsilon \in (0, 1)$, whenever

$$n_y \geq C(\bar{\kappa}/\underline{\kappa}^2)M_\psi^2M_r^2s \log^2(s) \log(p \vee n_y) \log(n_y)c^2(2 + \beta)^4/\varepsilon^2,$$

where $C > 0$ denotes a known, absolute constant, we have

$$\|\mathbf{H}(\boldsymbol{\theta}^*) - \mathbb{E}_y \mathbf{H}(\boldsymbol{\theta}^*)\|_s = \sup_{\|\mathbf{v}\|_0 \leq s, \|\mathbf{v}\|=1} |\mathbf{v}^\top \{\mathbf{H}(\boldsymbol{\theta}^*) - \mathbb{E}_y \mathbf{H}(\boldsymbol{\theta}^*)\} \mathbf{v}| \leq \underline{\kappa}/(c(2 + \beta)^2)$$

with probability $1 - \varepsilon$.

Proof. Similar to the proof of Lemma 12, let

$$U_{\mathbf{v}} := \frac{2}{1 - 1/n_y} \mathbf{v}^\top \mathbf{H}(\boldsymbol{\theta}^*) \mathbf{v} = \frac{2}{n_y(n_y - 1)} \sum_{1 \leq j < j' \leq n_y} g_{\mathbf{v}}(\mathbf{y}^{(j)}, \mathbf{y}^{(j')}),$$

where

$$g_{\mathbf{v}}(\mathbf{y}, \mathbf{y}') = \langle \boldsymbol{\psi}(\mathbf{y}) - \boldsymbol{\psi}(\mathbf{y}'), \mathbf{v} \rangle \langle \boldsymbol{\psi}(\mathbf{y}) - \boldsymbol{\psi}(\mathbf{y}'), \mathbf{v} \rangle r_\theta(\mathbf{y}) r_\theta(\mathbf{y}').$$

Let

$$\begin{aligned} V_{\mathbf{v}}(\mathbf{y}^{(1)}, \dots, \mathbf{y}^{(n_y)}) \\ := \frac{1}{\lfloor n_y/2 \rfloor} \left(g_{\mathbf{v}}(\mathbf{y}^{(1)}, \mathbf{y}^{(2)}) + g_{\mathbf{v}}(\mathbf{y}^{(3)}, \mathbf{y}^{(4)}) + \dots + g_{\mathbf{v}}(\mathbf{y}^{(2\lfloor n_y/2 \rfloor - 1)}, \mathbf{y}^{(2\lfloor n_y/2 \rfloor)}) \right), \end{aligned}$$

and write

$$U_{\mathbf{v}} = \frac{1}{n_y!} \sum_{\sigma \in \mathfrak{S}_{n_y}} V_{\mathbf{v}}(\mathbf{y}^{(\sigma(1))}, \dots, \mathbf{y}^{(\sigma(n_y))}),$$

where \mathfrak{S}_{n_y} is the group of permutations on $[n_y]$. Then

$$\begin{aligned} \mathbb{E}_y \left[\sup_{\substack{\|\mathbf{v}\|_0 \leq s \\ \|\mathbf{v}\|=1}} |U_{\mathbf{v}} - \mathbb{E}_y U_{\mathbf{v}}| \right] \\ = \mathbb{E}_y \left[\sup_{\substack{\|\mathbf{v}\|_0 \leq s \\ \|\mathbf{v}\|=1}} \left| \frac{1}{n_y!} \sum_{\sigma \in \mathfrak{S}_{n_y}} V_{\mathbf{v}}(\mathbf{y}^{(\sigma(1))}, \dots, \mathbf{y}^{(\sigma(n_y))}) - \mathbb{E}_y V_{\mathbf{v}}(\mathbf{y}^{(\sigma(1))}, \dots, \mathbf{y}^{(\sigma(n_y))}) \right| \right] \\ \leq \mathbb{E}_y \left[\sup_{\substack{\|\mathbf{v}\|_0 \leq s \\ \|\mathbf{v}\|=1}} |V_{\mathbf{v}}(\mathbf{y}^{(1)}, \dots, \mathbf{y}^{(n_y)}) - \mathbb{E}_y V_{\mathbf{v}}(\mathbf{y}^{(1)}, \dots, \mathbf{y}^{(n_y)})| \right]. \end{aligned}$$

Denoting $\mathbf{z}^{(i)} = (\boldsymbol{\psi}(\mathbf{y}^{(2i-1)}) - \boldsymbol{\psi}(\mathbf{y}^{(2i)})) \sqrt{r_\theta(\mathbf{y}^{(2i-1)})r_\theta(\mathbf{y}^{(2i)})}$, we have

$$\begin{aligned} \mathbb{E}_y \left[\sup_{\substack{\|\mathbf{v}\|_0 \leq s \\ \|\mathbf{v}\|=1}} |\mathbf{v}^\top \{\mathbf{H}(\boldsymbol{\theta}^*) - \mathbb{E}_y \mathbf{H}(\boldsymbol{\theta}^*)\} \mathbf{v}| \right] \\ \leq \frac{1 - 1/n_y}{2} \mathbb{E}_y \left[\sup_{\substack{\|\mathbf{v}\|_0 \leq s \\ \|\mathbf{v}\|=1}} \left| \mathbf{v}^\top \left(\sum_{i \in [n_y/2]} \mathbf{z}^i \mathbf{z}^{i\top} - \mathbb{E}_y [\mathbf{z}^i \mathbf{z}^{i\top}] \right) \mathbf{v} \right| \right]. \end{aligned}$$

Note that $\|\mathbf{z}^i\|_\infty \leq 2M_\psi M_r$. Then an application of Lemma 11 of [Belloni and Chernozhukov \(2013\)](#) gives us

$$\mathbb{E}_y \left[\sup_{\substack{\|\mathbf{v}\|_0 \leq s \\ \|\mathbf{v}\|=1}} |\mathbf{v}^\top \{\mathbf{H}(\boldsymbol{\theta}^*) - \mathbb{E}_y \mathbf{H}(\boldsymbol{\theta}^*)\} \mathbf{v}| \right] \leq a_n^2 + a_n \sqrt{\bar{\kappa}},$$

where $a_n^2 = CM_\psi^2 M_r^2 s \log^2(s) \log(p \vee n_y) \log(n_y)/n_y$, $C > 0$ is a known, absolute constant inherited from the lemma. Using Markov's inequality, we get that

$$\sup_{\substack{\|\mathbf{v}\|_0 \leq s \\ \|\mathbf{v}\| = 1}} |\mathbf{v}^\top \{\mathbf{H}(\boldsymbol{\theta}^*) - \mathbb{E}_y \mathbf{H}(\boldsymbol{\theta}^*)\} \mathbf{v}| \leq \underline{\kappa}/(c(2 + \beta)^2)$$

with probability $1 - \varepsilon$. □

Lemma 16 (Lemma 4.9 of Barber and Kolar (2018)). *For any $\mathbf{M} \in \mathbb{R}^{p \times p}$ and $s \geq 1$,*

$$\mathbf{v}^\top \mathbf{M} \mathbf{v} \leq \|\mathbf{M}\|_s \left(\|\mathbf{v}\| + \frac{\|\mathbf{v}\|_1}{\sqrt{s}} \right)^2 \quad \text{for all } \mathbf{v} \in \mathbb{R}^p.$$

F Auxiliary results

F.1 Gaussian approximation lemmas

Lemma 17. *For $\boldsymbol{\omega} \in \mathbb{R}^p$, let*

$$A_n = A_n(\boldsymbol{\omega}) = \left\langle \boldsymbol{\omega}, \frac{1}{n_x} \sum_{i=1}^{n_x} (\boldsymbol{\psi}(\mathbf{x}^{(i)}) - \boldsymbol{\mu}_\psi) + \frac{1}{n_y} \sum_{j=1}^{n_y} (\boldsymbol{\mu}_\psi - \boldsymbol{\psi}(\mathbf{y}^{(j)})) r_{\theta^*}(\mathbf{y}^{(j)}) \right\rangle,$$

and

$$\sigma_n^2 = \sigma_n^2(\boldsymbol{\omega}) = \text{Var} [\sqrt{n} A_n(\boldsymbol{\omega})].$$

Then,

$$\sup_{t \in \mathbb{R}} |\mathbb{P} \{ \sqrt{n} A_n / \sigma_n \leq t \} - \Phi(t)| \leq \frac{2CM_r M_\psi \|\boldsymbol{\omega}\|}{\eta_{x,n} \eta_{y,n} \sigma_n \sqrt{n}},$$

where $C > 0$ denotes a known, absolute constant.

Proof. Write

$$\sqrt{n} A_n / \sigma_n = \frac{1}{\sqrt{n}} \left\{ \sum_{i=1}^{n_x} \frac{\langle \boldsymbol{\omega}, \boldsymbol{\psi}(\mathbf{x}^{(i)}) - \boldsymbol{\mu}_\psi \rangle}{\eta_{x,n} \sigma_n} + \sum_{j=1}^{n_y} \frac{\langle \boldsymbol{\omega}, \boldsymbol{\mu}_\psi - \boldsymbol{\psi}(\mathbf{y}^{(j)}) \rangle r_{\theta^*}(\mathbf{y}^{(j)})}{\eta_{y,n} \sigma_n} \right\}.$$

Now,

$$\frac{|\langle \boldsymbol{\omega}, \boldsymbol{\psi}(\mathbf{x}) - \boldsymbol{\mu}_\psi \rangle|}{\eta_{x,n} \sigma_n} \leq \frac{2M_\psi \|\boldsymbol{\omega}\|}{\eta_{x,n} \sigma_n} \quad \text{and} \quad \frac{|\langle \boldsymbol{\omega}, \boldsymbol{\mu}_\psi - \boldsymbol{\psi}(\mathbf{y}) \rangle r_{\theta^*}(\mathbf{y})|}{\eta_{y,n} \sigma_n} \leq \frac{2M_r M_\psi \|\boldsymbol{\omega}\|}{\eta_{y,n} \sigma_n}.$$

Noting that $M_r \geq 1$, the Berry-Esseen inequality (Theorem 3.4 of Chen et al. (2011)) yields

$$\sup_{t \in \mathbb{R}} |\mathbb{P} \{ \sqrt{n} A_n / \sigma_n \leq t \} - \Phi(t)| \leq \frac{2CM_r M_\psi \|\boldsymbol{\omega}\|}{\eta_{x,n} \eta_{y,n} \sigma_n \sqrt{n}},$$

where $C > 0$ is a known, absolute constant from the theorem. □

Lemma 18 (Lemma D.3 of Barber and Kolar (2018)). *If*

$$\sup_{z \in \mathbb{R}} |\mathbb{P}\{A \leq z\} - \Phi(z)| \leq \varepsilon_A \quad \text{and} \quad \mathbb{P}\{|B| \leq \delta_B, |C| \leq \delta_C\} \geq 1 - \varepsilon_{BC}$$

for some $\delta_B, \delta_C, \varepsilon_A, \varepsilon_{BC} \in [0, 1)$, then

$$\sup_{z \in \mathbb{R}} |\mathbb{P}\{(A + B)/(1 + C) \leq z\} - \Phi(z)| \leq \delta_B + \frac{\delta_C}{1 - \delta_C} + \varepsilon_A + \varepsilon_{BC}.$$

F.2 Consistency of the variance estimator

Lemma 19. *On the event that*

$$\|\boldsymbol{\theta} - \boldsymbol{\theta}^*\| \leq \delta_\theta, \quad \|\check{\boldsymbol{\omega}}_k - \boldsymbol{\omega}_k^*\| \leq \delta_k, \quad \text{and} \quad \|\widehat{\mathbf{S}}_\psi - \boldsymbol{\Sigma}_\psi\|_* \leq \delta_\sigma/4,$$

the variance estimate (11) satisfies

$$|\widehat{\sigma}_k^2 - \sigma_k^2| \leq (\eta_{x,n}\eta_{y,n})^{-1} \left\{ \|\boldsymbol{\omega}_k^*\|^2 (\delta_\sigma + 2L_3 \delta_\theta) + (\delta_\sigma + 2L_3 \delta_\theta + \|\boldsymbol{\Sigma}_\psi\|_* + \|\boldsymbol{\Sigma}_{\psi r}\|_*) \delta_k^2 \right\}.$$

Proof. Let

$$\boldsymbol{\Sigma}_{\text{pooled}} = \eta_{x,n}^{-1} \boldsymbol{\Sigma}_\psi + \eta_{y,n}^{-1} \boldsymbol{\Sigma}_{\psi r}.$$

We have

$$\begin{aligned} \widehat{\sigma}_k^2 - \sigma_k^2 &= \check{\boldsymbol{\omega}}_k^\top \widehat{\mathbf{S}}_{\text{pooled}} \check{\boldsymbol{\omega}}_k - \boldsymbol{\omega}_k^{*\top} \boldsymbol{\Sigma}_{\text{pooled}} \boldsymbol{\omega}_k^* \\ &= \check{\boldsymbol{\omega}}_k^\top \left\{ \eta_{x,n}^{-1} \widehat{\mathbf{S}}_\psi + \eta_{y,n}^{-1} \widehat{\mathbf{S}}_{\psi r}(\boldsymbol{\theta}) \right\} \check{\boldsymbol{\omega}}_k - \boldsymbol{\omega}_k^{*\top} \left\{ \eta_{x,n}^{-1} \boldsymbol{\Sigma}_\psi + \eta_{y,n}^{-1} \boldsymbol{\Sigma}_{\psi r} \right\} \boldsymbol{\omega}_k^* \\ &= \eta_{x,n}^{-1} \left(\check{\boldsymbol{\omega}}_k^\top \widehat{\mathbf{S}}_\psi \check{\boldsymbol{\omega}}_k - \boldsymbol{\omega}_k^{*\top} \boldsymbol{\Sigma}_\psi \boldsymbol{\omega}_k^* \right) + \eta_{y,n}^{-1} \left(\check{\boldsymbol{\omega}}_k^\top \widehat{\mathbf{S}}_{\psi r}(\boldsymbol{\theta}) \check{\boldsymbol{\omega}}_k - \boldsymbol{\omega}_k^{*\top} \boldsymbol{\Sigma}_{\psi r} \boldsymbol{\omega}_k^* \right). \end{aligned}$$

The first term is bounded as

$$\begin{aligned} \left| \check{\boldsymbol{\omega}}_k^\top \widehat{\mathbf{S}}_\psi \check{\boldsymbol{\omega}}_k - \boldsymbol{\omega}_k^{*\top} \boldsymbol{\Sigma}_\psi \boldsymbol{\omega}_k^* \right| &\leq \left| \check{\boldsymbol{\omega}}_k^\top \{ \widehat{\mathbf{S}}_\psi - \boldsymbol{\Sigma}_\psi \} \check{\boldsymbol{\omega}}_k \right| + |(\check{\boldsymbol{\omega}}_k - \boldsymbol{\omega}_k^*)^\top \boldsymbol{\Sigma}_\psi (\check{\boldsymbol{\omega}}_k - \boldsymbol{\omega}_k^*)| \\ &\leq \|\widehat{\mathbf{S}}_\psi - \boldsymbol{\Sigma}_\psi\|_* \|\check{\boldsymbol{\omega}}_k\|^2 + \|\boldsymbol{\Sigma}_\psi\|_* \|\check{\boldsymbol{\omega}}_k - \boldsymbol{\omega}_k^*\|^2 \\ &\leq \frac{1}{2} \delta_\sigma (\|\boldsymbol{\omega}_k^*\|^2 + \delta_k^2) + \|\boldsymbol{\Sigma}_\psi\|_* \delta_k^2. \end{aligned}$$

Similarly,

$$\begin{aligned} \left| \check{\boldsymbol{\omega}}_k^\top \widehat{\mathbf{S}}_{\psi r}(\boldsymbol{\theta}) \check{\boldsymbol{\omega}}_k - \boldsymbol{\omega}_k^{*\top} \boldsymbol{\Sigma}_{\psi r} \boldsymbol{\omega}_k^* \right| &\leq \left| \check{\boldsymbol{\omega}}_k^\top \{ \widehat{\mathbf{S}}_{\psi r}(\boldsymbol{\theta}) - \boldsymbol{\Sigma}_{\psi r} \} \check{\boldsymbol{\omega}}_k \right| + |(\check{\boldsymbol{\omega}}_k - \boldsymbol{\omega}_k^*)^\top \boldsymbol{\Sigma}_{\psi r} (\check{\boldsymbol{\omega}}_k - \boldsymbol{\omega}_k^*)| \\ &\leq \|\widehat{\mathbf{S}}_{\psi r}(\boldsymbol{\theta}) - \boldsymbol{\Sigma}_{\psi r}\|_* \|\check{\boldsymbol{\omega}}_k\|^2 + \|\boldsymbol{\Sigma}_{\psi r}\|_* \|\check{\boldsymbol{\omega}}_k - \boldsymbol{\omega}_k^*\|^2 \\ &\leq \left(\|\widehat{\mathbf{S}}_{\psi r}(\boldsymbol{\theta}) - \widehat{\mathbf{S}}_{\psi r}(\boldsymbol{\theta}^*)\|_* + \|\widehat{\mathbf{S}}_{\psi r}(\boldsymbol{\theta}^*) - \boldsymbol{\Sigma}_{\psi r}\|_* \right) \|\check{\boldsymbol{\omega}}_k\|^2 + \|\boldsymbol{\Sigma}_{\psi r}\|_* \|\check{\boldsymbol{\omega}}_k - \boldsymbol{\omega}_k^*\|^2 \\ &\leq \left(L_3 \|\boldsymbol{\theta} - \boldsymbol{\theta}^*\| + \|\widehat{\mathbf{S}}_{\psi r}(\boldsymbol{\theta}^*) - \boldsymbol{\Sigma}_{\psi r}\|_* \right) \|\check{\boldsymbol{\omega}}_k\|^2 + \|\boldsymbol{\Sigma}_{\psi r}\|_* \|\check{\boldsymbol{\omega}}_k - \boldsymbol{\omega}_k^*\|^2 \\ &\leq (2L_3 \delta_\theta + \frac{1}{2} \delta_\sigma) (\|\boldsymbol{\omega}_k^*\|^2 + \delta_k^2) + \|\boldsymbol{\Sigma}_{\psi r}\|_* \delta_k^2, \end{aligned}$$

where the penultimate line is by Lemma 20. Thus,

$$|\widehat{\sigma}_k^2 - \sigma_k^2| \leq (\eta_{x,n}\eta_{y,n})^{-1} \left\{ \|\boldsymbol{\omega}_k^*\|^2 (\delta_\sigma + 2L_3 \delta_\theta) + (\delta_\sigma + 2L_3 \delta_\theta + \|\boldsymbol{\Sigma}_\psi\|_* + \|\boldsymbol{\Sigma}_{\psi r}\|_*) \delta_k^2 \right\}.$$

□

Lemma 20. *There exists $L_3 > 0$ depending on M_r, M_ψ only such that*

$$\|\widehat{\mathbf{S}}_{\psi r}(\boldsymbol{\theta}) - \widehat{\mathbf{S}}_{\psi r}(\boldsymbol{\theta}^*)\|_* \leq L_3 \|\boldsymbol{\theta} - \boldsymbol{\theta}^*\| \quad \text{for all } \boldsymbol{\theta} \in \bar{\mathcal{B}}_\rho(\boldsymbol{\theta}^*).$$

Proof. By applying Lemma 5 after computing the form of each $\widehat{\mathbf{S}}_{\psi r_{k'k}}(\boldsymbol{\theta}) - \widehat{\mathbf{S}}_{\psi r_{k'k}}(\boldsymbol{\theta}^*)$. □

Lemma 21. *Under Condition 1 with ℓ_1 -norm, there exist constants $K, c, c' > 0$ depending on M_ψ only such that for any $t \in [K\sqrt{\log p/n_x}, 1]$,*

$$\mathbb{P} \left\{ \|\widehat{\mathbf{S}}_\psi - \boldsymbol{\Sigma}_\psi\|_\infty > t \right\} \leq c \exp(-c't^2 n_x).$$

Proof. Let $k, k' \in [p]$.

$$\begin{aligned} \widehat{S}_{\psi_{k'k}} - \Sigma_{\psi_{k'k}} &= \frac{1}{n_x} \sum_{i=1}^{n_x} \left(\psi_{k'}(\mathbf{x}_{k'}^{(i)}) - \mu_{\psi_{k'}} \right) \left(\psi_k(\mathbf{x}_k^{(i)}) - \mu_{\psi_k} \right) - \Sigma_{\psi_{k'k}} \\ &\quad - \left\{ \frac{1}{n_x} \sum_{i=1}^{n_x} \psi_{k'}(\mathbf{x}_{k'}^{(i)}) - \mu_{\psi_{k'}} \right\} \left\{ \frac{1}{n_x} \sum_{i=1}^{n_x} \psi_k(\mathbf{x}_k^{(i)}) - \mu_{\psi_k} \right\}. \end{aligned}$$

Suppose t satisfies the conditions of the lemma, and suppose

$$\begin{aligned} \left| \frac{1}{n_x} \sum_{i=1}^{n_x} \psi_k(\mathbf{x}_k^{(i)}) - \mu_{\psi_k} \right| &\leq t \quad \forall k, \\ \left| \frac{1}{n_x} \sum_{i=1}^{n_x} \left(\psi_{k'}(\mathbf{x}_{k'}^{(i)}) - \mu_{\psi_{k'}} \right) \left(\psi_k(\mathbf{x}_k^{(i)}) - \mu_{\psi_k} \right) - \Sigma_{\psi_{k'k}} \right| &\leq t \quad \forall k, k'. \end{aligned}$$

On this event,

$$\begin{aligned} &\|\widehat{\mathbf{S}}_\psi - \Sigma_\psi\|_\infty \\ &= \max_{k, k'} |\widehat{S}_{\psi_{k'k}} - \Sigma_{\psi_{k'k}}| \\ &\leq \max_{k, k'} \left| \frac{1}{n_x} \sum_{i=1}^{n_x} \left(\psi_{k'}(\mathbf{x}_{k'}^{(i)}) - \mu_{\psi_{k'}} \right) \left(\psi_k(\mathbf{x}_k^{(i)}) - \mu_{\psi_k} \right) - \Sigma_{\psi_{k'k}} \right| + \max_k \left| \frac{1}{n_x} \sum_{i=1}^{n_x} \psi_k(\mathbf{x}_k^{(i)}) - \mu_{\psi_k} \right|^2 \\ &\leq t + t^2 \leq 2t, \end{aligned}$$

using the upper bound on t .

Now, the boundedness of $\psi(\mathbf{x})$ implies

$$\begin{aligned} \mathbb{P} \left\{ \left| \frac{1}{n_x} \sum_{i=1}^{n_x} \psi_k(\mathbf{x}_k^{(i)}) - \mu_{\psi_k} \right| > t \right\} &\leq 2 \exp(-c_1 t^2 n_x), \\ \mathbb{P} \left\{ \left| \frac{1}{n_x} \sum_{i=1}^{n_x} \left(\psi_{k'}(\mathbf{x}_{k'}^{(i)}) - \mu_{\psi_{k'}} \right) \left(\psi_k(\mathbf{x}_k^{(i)}) - \mu_{\psi_k} \right) - \Sigma_{\psi_{k'k}} \right| > t \right\} &\leq 2 \exp(-c_2 t^2 n_x), \end{aligned}$$

where $c_1, c_2 > 0$ are constants depending on M_ψ only.

Thus,

$$\mathbb{P} \left\{ \|\widehat{\mathbf{S}}_\psi - \Sigma_\psi\|_\infty > t \right\} \leq 2p \exp(-c_1 t^2 n_x) + 2p^2 \exp(-c_2 t^2 n_x) \leq 4p^2 \exp(-c_3 t^2 n_x), \quad (90)$$

where $c_3 > 0$ is another constant depending on M_ψ only. (90) can be simplified by using the lower bound on t :

$$\mathbb{P} \left\{ \|\widehat{\mathbf{S}}_\psi - \Sigma_\psi\|_\infty > t \right\} \leq c \exp(-c' t^2 n_x),$$

where $c, c' > 0$ are constants depending on M_ψ only. \square

Lemma 22. *Under the bounded density ratio model (Condition 1), there exist constants $K, c, c' > 0$ depending on M_r, M_ψ only such that for any $t \in [K\sqrt{\log p/n_y}, 1]$,*

$$\mathbb{P} \left\{ \|\widehat{\mathbf{S}}_{\psi r}(\boldsymbol{\theta}^*) - \Sigma_{\psi r}\|_\infty > t \right\} \leq c \exp(-c' t^2 n_y).$$

Proof. Let $k, k' \in [p]$. We have

$$\widehat{S}_{\psi \widehat{r}_{k'k}}(\boldsymbol{\theta}^*) - \Sigma_{\psi r_{k'k}} = \left\{ \widehat{S}_{\psi \widehat{r}_{k'k}}(\boldsymbol{\theta}^*) - \frac{Z_y^2(\boldsymbol{\theta}^*)}{\widehat{Z}_y^2(\boldsymbol{\theta}^*)} \Sigma_{\psi r_{k'k}} \right\} + \left(\frac{Z_y^2(\boldsymbol{\theta}^*)}{\widehat{Z}_y^2(\boldsymbol{\theta}^*)} - 1 \right) \Sigma_{\psi r_{k'k}}$$

with

$$\begin{aligned} & \widehat{S}_{\psi\widehat{r}_{k'k}}(\boldsymbol{\theta}^*) - \frac{Z_y^2(\boldsymbol{\theta}^*)}{\widehat{Z}_y^2(\boldsymbol{\theta}^*)} \Sigma_{\psi r_{k'k}} \\ &= \frac{Z_y^2(\boldsymbol{\theta}^*)}{\widehat{Z}_y^2(\boldsymbol{\theta}^*)} \left[\frac{1}{n_y} \sum_{j=1}^{n_y} \left(\psi_{k'}(\mathbf{y}_{k'}^{(j)}) r_{\theta^*}(\mathbf{y}^{(j)}) - \mu_{\psi_{k'}} \right) \left(\psi_k(\mathbf{y}_k^{(j)}) r_{\theta^*}(\mathbf{y}^{(j)}) - \mu_{\psi_k} \right) - \Sigma_{\psi r_{k'k}} \right. \\ & \quad \left. - \left\{ \frac{1}{n_y} \sum_{j=1}^{n_y} \psi_{k'}(\mathbf{y}_{k'}^{(j)}) r_{\theta}(\mathbf{y}^{(j)}) - \mu_{\psi_{k'}} \right\} \left\{ \frac{1}{n_y} \sum_{j=1}^{n_y} \psi_k(\mathbf{y}_k^{(j)}) r_{\theta}(\mathbf{y}^{(j)}) - \mu_{\psi_k} \right\} \right] \end{aligned}$$

and

$$\frac{Z_y^2(\boldsymbol{\theta}^*)}{\widehat{Z}_y^2(\boldsymbol{\theta}^*)} - 1 = \frac{Z_y^2(\boldsymbol{\theta}^*)}{\widehat{Z}_y^2(\boldsymbol{\theta}^*)} \left(1 + \frac{\widehat{Z}_y(\boldsymbol{\theta}^*)}{Z_y(\boldsymbol{\theta}^*)} \right) \left(1 - \frac{\widehat{Z}_y(\boldsymbol{\theta}^*)}{Z_y(\boldsymbol{\theta}^*)} \right).$$

Condition 1 implies that $Z_y(\boldsymbol{\theta}^*)/\widehat{Z}_y(\boldsymbol{\theta}^*) \in [M_r^{-1}, M_r]$, as well as that $\|\Sigma_{\psi r}\|_\infty$ is bounded by some constant. So,

$$\begin{aligned} & \left| \widehat{S}_{\psi\widehat{r}_{k'k}}(\boldsymbol{\theta}^*) - \frac{Z_y^2(\boldsymbol{\theta}^*)}{\widehat{Z}_y^2(\boldsymbol{\theta}^*)} \Sigma_{\psi r_{k'k}} \right| \\ & \leq M_r^2 \left[\left| \frac{1}{n_y} \sum_{j=1}^{n_y} \left(\psi_{k'}(\mathbf{y}_{k'}^{(j)}) r_{\theta^*}(\mathbf{y}^{(j)}) - \mu_{\psi_{k'}} \right) \left(\psi_k(\mathbf{y}_k^{(j)}) r_{\theta^*}(\mathbf{y}^{(j)}) - \mu_{\psi_k} \right) - \Sigma_{\psi r_{k'k}} \right| \right. \\ & \quad \left. + \left| \frac{1}{n_y} \sum_{j=1}^{n_y} \psi_{k'}(\mathbf{y}_{k'}^{(j)}) r_{\theta}(\mathbf{y}^{(j)}) - \mu_{\psi_{k'}} \right| \left| \frac{1}{n_y} \sum_{j=1}^{n_y} \psi_k(\mathbf{y}_k^{(j)}) r_{\theta}(\mathbf{y}^{(j)}) - \mu_{\psi_k} \right| \right] \end{aligned}$$

and

$$\left| \left(\frac{Z_y^2(\boldsymbol{\theta}^*)}{\widehat{Z}_y^2(\boldsymbol{\theta}^*)} - 1 \right) \Sigma_{\psi r_{k'k}} \right| \leq M_r^2 (1 + M_r) \|\Sigma_{\psi r}\|_\infty \left| 1 - \frac{\widehat{Z}_y(\boldsymbol{\theta}^*)}{Z_y(\boldsymbol{\theta}^*)} \right|.$$

Suppose t satisfies the conditions of the lemma, and suppose

$$\left| \frac{\widehat{Z}_y(\boldsymbol{\theta})}{Z_y(\boldsymbol{\theta})} - 1 \right| \leq t,$$

$$\left| \frac{1}{n_y} \sum_{j=1}^{n_y} \psi_k(\mathbf{y}_k^{(j)}) r_{\theta}(\mathbf{y}^{(j)}) - \mu_{\psi_k} \right| \leq t \quad \forall k,$$

$$\left| \frac{1}{n_y} \sum_{j=1}^{n_y} \left(\psi_{k'}(\mathbf{y}_{k'}^{(j)}) r_{\theta^*}(\mathbf{y}^{(j)}) - \mu_{\psi_{k'}} \right) \left(\psi_k(\mathbf{y}_k^{(j)}) r_{\theta^*}(\mathbf{y}^{(j)}) - \mu_{\psi_k} \right) - \Sigma_{\psi r_{k'k}} \right| \leq t \quad \forall k, k'.$$

On this event,

$$\left| \widehat{S}_{\psi\widehat{r}_{k'k}}(\boldsymbol{\theta}^*) - \frac{Z_y^2(\boldsymbol{\theta}^*)}{\widehat{Z}_y^2(\boldsymbol{\theta}^*)} \Sigma_{\psi r_{k'k}} \right| \leq M_r^2 (t + t^2) \leq 2M_r^2 t$$

and

$$\left| \left(\frac{Z_y^2(\boldsymbol{\theta}^*)}{\widehat{Z}_y^2(\boldsymbol{\theta}^*)} - 1 \right) \Sigma_{\psi r_{k'k}} \right| \leq M_r^2 (1 + M_r) \|\Sigma_{\psi r}\|_\infty t,$$

and hence,

$$\|\widehat{\mathbf{S}}_{\psi\widehat{r}}(\boldsymbol{\theta}^*) - \Sigma_{\psi r}\|_\infty \leq K t$$

for some constant $K > 0$.

We finish the proof by bounding the probability of the complementary event. By Lemma 6,

$$\mathbb{P} \left\{ \left| \frac{\widehat{Z}_y(\boldsymbol{\theta})}{Z_y(\boldsymbol{\theta})} - 1 \right| > t \right\} \leq 2 \exp(-c_1 t^2 n_y),$$

for some constant $c_1 > 0$ depending on M_r only. On the other hand, the boundedness of $\psi(\mathbf{y})r_{\theta^*}(\mathbf{y})$ implies

$$\mathbb{P} \left\{ \left| \frac{1}{n_y} \sum_{j=1}^{n_y} \psi_k(\mathbf{y}_k^{(j)}) r_{\theta^*}(\mathbf{y}^{(j)}) - \mu_{\psi_k} \right| > t \right\} \leq 2 \exp(-c_2 t^2 n_y),$$

$$\mathbb{P} \left\{ \left| \frac{1}{n_y} \left(\psi_{k'}(\mathbf{y}_{k'}^{(j)}) r_{\theta^*}(\mathbf{y}^{(j)}) - \mu_{\psi_{k'}} \right) \left(\psi_k(\mathbf{y}_k^{(j)}) r_{\theta^*}(\mathbf{y}^{(j)}) - \mu_{\psi_k} \right) - \Sigma_{\psi_{r_{k'k}}} \right| > t \right\} \leq 2 \exp(-c_3 t^2 n_y),$$

where $c_2, c_3 > 0$ are constants depending on M_r, M_ψ only.

Thus,

$$\mathbb{P} \left\{ \|\widehat{\mathbf{S}}_{\psi_r}(\boldsymbol{\theta}^*) - \Sigma_{\psi_r}\|_\infty > t \right\} \leq 2 \exp(-c_1 t^2 n_y) + 2p \exp(-c_2 t^2 n_y) + 2p^2 \exp(-c_3 t^2 n_y) \leq 6p^2 \exp(-c_4 t^2 n_y), \quad (91)$$

where $c_4 > 0$ is another constant depending on M_r, M_ψ only. (91) can be simplified by using the lower bound on t :

$$\mathbb{P} \left\{ \|\widehat{\mathbf{S}}_{\psi_r}(\boldsymbol{\theta}^*) - \Sigma_{\psi_r}\|_\infty > t \right\} \leq c \exp(-c' t^2 n_y),$$

where $c, c' > 0$ are constants depending on M_r, M_ψ only. \square

G Implementation details

G.1 Autoscaling

G.1.1 Sparse KLIEP with self-normalizing penalty

The default option in KLIEPInference.jl (<https://github.com/mlakolar/KLIEPInference.jl>) replaces (7) in the initial KLIEP estimation step with the following modified version

$$\check{\boldsymbol{\theta}} \leftarrow \arg \min_{\boldsymbol{\theta}} \ell_{\text{KLIEP}}(\boldsymbol{\theta}; \mathbf{X}_{n_x}, \mathbf{Y}_{n_y}) + \lambda_{\theta 0} \sum_{k=1}^p \tau_k |\theta_k|, \quad (92)$$

where $\lambda_{\theta 0} = (1+a)\Phi^{-1}(1-b/p)$ for some small $a, b > 0$ is the universal penalty and $\tau_k > 0$ is the k th penalty loading. For $\lambda_{\theta 0}$, we used $a = 0.01$ and $b = 0.05$. The k th penalty loading is chosen to match the sample standard deviation of $\partial_k \ell_{\text{KLIEP}}(\boldsymbol{\theta}^*)$; this has the effect of penalizing components with larger variance more.

As $\boldsymbol{\theta}^*$ is unavailable to us, we take the following two-step approach:

Procedure 4. Two-step procedure for minimizing (92)

Initialize $\check{\boldsymbol{\theta}} \leftarrow \mathbf{0}$.

Compute the initial penalty loadings: for $k = 1, \dots, p$,

$$\tau_k \leftarrow \widehat{\mathbf{S}}_{\text{pooled},kk}(\check{\boldsymbol{\theta}}).$$

Compute $\check{\boldsymbol{\theta}}$:

$$\check{\boldsymbol{\theta}} \leftarrow \arg \min_{\boldsymbol{\theta}} \ell_{\text{KLIEP}}(\boldsymbol{\theta}; \mathbf{X}_{n_x}, \mathbf{Y}_{n_y}) + \lambda_{\theta 0} \sum_{k=1}^p \tau_k |\theta_k|.$$

Update the penalty loadings: for $k = 1, \dots, p$,

$$\tau_k \leftarrow \widehat{\mathbf{S}}_{\text{pooled},kk}(\check{\boldsymbol{\theta}}).$$

Estimate $\check{\boldsymbol{\theta}}$ with the updated penalty loadings.

The intuition behind $\lambda_{\theta_0} = (1 + a)\Phi^{-1}(1 - b/p)$ and $\tau_k \approx \sqrt{\widehat{\text{Var}}[\partial_k \ell_{\text{KLIEP}}(\boldsymbol{\theta}^*)]}$ is as follows. Estimation using (92) is consistent provided that

$$\mathbb{P} \left\{ \max_k |\partial_k \ell_{\text{KLIEP}}(\boldsymbol{\theta}^*) / \tau_k| > \lambda_{\theta_0} \right\} \text{ is small.} \quad (93)$$

For sufficiently large sample sizes, we would have $\partial_k \ell_{\text{KLIEP}}(\boldsymbol{\theta}^*) / \sqrt{\widehat{\text{Var}}[\partial_k \ell_{\text{KLIEP}}(\boldsymbol{\theta}^*)]} \approx \mathcal{N}(0, 1)$, and hence for $\lambda_{\theta_0} = (1 + a)\Phi^{-1}(1 - b/p)$, an upper bound for the probability in (93) is about $b > 0$. Thus, b can be interpreted as a tolerance parameter that controls the probability of the undesirable event. Similar approach was taken in Belloni et al. (2011, 2014, 2019) in the context of linear regression, nonparametric regression, and error-in-variables regression problems. For detailed discussions of the motivation and the relationship to the moderate deviations theory, we refer the reader to these works and the references therein. In particular, a rigorous proof in the context of our problem would involve establishing a moderate deviation bound (de la Peña et al., 2009, Jing et al., 2003) for the self-normalized gradient $[\partial_k \ell_{\text{KLIEP}}(\boldsymbol{\theta}^*) / \sqrt{\widehat{\text{Var}}[\partial_k \ell_{\text{KLIEP}}(\boldsymbol{\theta}^*)]}]_{k=1}^p$, which we leave up to future work.

G.1.2 Sparse Hessian inversion via the scaled lasso

The default option in KLIEPInference.jl (<https://github.com/mlakolar/KLIEPInference.jl>) replaces (8) in the Hessian inversion step with a scaled lasso formulation (Sun and Zhang, 2012). In particular, we use the approach described in Sun and Zhang (2013) that allows us to estimate a sparse inverse of the Hessian without hyperparameter tuning. This implementation is used for all of our experiments.

In the below, we describe the procedure in more detail. The equation (8) is modified so that $\check{\boldsymbol{\omega}}_k = -\check{\tau}_k \check{\mathbf{d}}_k$, where

$$\check{\mathbf{d}}_k, \check{\tau}_k \leftarrow \arg \min_{\mathbf{d}, \tau: d_k = -1} \frac{\mathbf{d}^\top \nabla^2 \ell_{\text{KLIEP}}(\check{\boldsymbol{\theta}}) \mathbf{d}}{2\tau} + \frac{\tau}{2} + \lambda_0 \sum_{k'=1}^p \partial_{k'k'}^2 \ell_{\text{KLIEP}}(\check{\boldsymbol{\theta}}) |d_{k'}| \quad (94)$$

and the universal penalty level $\lambda_0 = \sqrt{2 \log p / n_y}$ does not depend on the unknown problem specific parameters. Following Sun and Zhang (2013), the solution $(\check{\mathbf{d}}_k, \check{\tau}_k)$ is obtained from the following iterative procedure:

Procedure 5. Iterative procedure for solving (94)

Initialize $\check{\mathbf{d}}_k \leftarrow \mathbf{e}_k$.

repeat

$$\check{\tau}_k \leftarrow \check{\mathbf{d}}_k^\top \nabla^2 \ell_{\text{KLIEP}}(\check{\boldsymbol{\theta}}) \check{\mathbf{d}}_k,$$

$$\lambda \leftarrow \lambda_0 \check{\tau}_k,$$

$$\check{\mathbf{d}}_k \leftarrow \arg \min_{\mathbf{d}} \frac{1}{2} \mathbf{d}^\top \nabla^2 \ell_{\text{KLIEP}}(\check{\boldsymbol{\theta}}) \mathbf{d} - \mathbf{d}^\top \mathbf{e}_k + \lambda \|\mathbf{d}\|_1.$$

until converged

For a detailed discussion of the procedure and its theoretical properties, the reader is referred to Sun and Zhang (2013).

G.2 Regularization parameter tuning

In all our experiments, including the experiments published only in Appendix, we used Procedure 5 for Step 2 with the universal penalty level $\lambda_0 = \sqrt{2 \log p / n_y}$. For Experiments 1 – 3, we use Procedure 4 for Step 1 with the universal penalty level $\lambda_{\theta_0} = 1.01\Phi^{-1}(1 - 0.05/p)$. Experiments 4 – 5 use the original sparse KLIEP

formulation (Liu et al., 2017) *without* autoscaling. For Experiment 4, we used $\lambda_\theta = \sqrt{4 \log p / n_x}$, because for Ising models, the components of the gradient $\nabla \ell_{\text{KLIEP}}(\boldsymbol{\theta}^*)$ are bounded by 2 when $\boldsymbol{\theta}^* \approx \mathbf{0}$.

Parameter tuning is an issue for most, if not all, high-dimensional estimation procedures, and ours is no exception. As noted by one reviewer, it is at least unclear how the regularization parameter pair can be chosen to achieve the best performance. In the case of the bounded model, it is possible to make an educated guess for the first-stage regularization parameter λ_θ (Lemma 8), and this is what we do in our experiments. Choosing the second-stage regularization parameters λ_k is a more delicate matter.

One heuristic is to cross-validate the *three-stage procedure in its entirety* over a 2D grid of $(\lambda_\theta, \lambda_k)$ pairs using the empirical KLIEP loss. A clear drawback of this strategy is that it is computationally intensive. It also has very little theory.

A good alternative is to use autoscaling procedures for the initial estimation steps. In our simulations, the combination of Procedure 4 and Procedure 5 has been seen to yield excellent performance while removing the need for hyperparameter tuning. For theory, we need the initial estimates obtained using Procedure 4 and Procedure 5 to be consistent. While we leave this up for future work, theoretical results for similar problems (e.g., Belloni et al. (2011) in the case of Step 1 and Sun and Zhang (2013) in the case of Step 2) lend support to our claim.

Additionally, to study the sensitivity of the overall procedure to the choice of the regularization parameter when the original sparse KLIEP formulation (Liu et al., 2017) is used, we ran additional experiments where we varied λ_θ on a grid of five values under the same set-up as that of Experiment 1. For Step 2, we still use Procedure 5 with the universal penalty level $\lambda_0 = \sqrt{2 \log p / n_y}$. We record the coverage and the median width of the 95% confidence intervals as well as the bias of the final estimate over 1000 independent replications. The regularization parameter settings are detailed in Table 4. The results are shown in Tables 5 to 10. The coverage, the median width, and the bias are all stable for both SparKLIE+ procedures. The reversed and the symmetrized procedures do show some instability, but it is likely that this has more to do with the fact that both procedures have a larger sample complexity relative to KLIEP. See Remark 5 in Section 4.2.

G.3 Studentized bootstrap

Consider the studentized analogue of the statistic in (12)

$$W = W_{n_x, n_y} = \max_{k=1, \dots, p} \sqrt{n} |\hat{\theta}_k - \theta_k^*| / \hat{\sigma}_k, \quad (95)$$

where $\hat{\theta}_k$ is either SparKLIE+1 or SparKLIE+2 estimator and $\hat{\sigma}_k$ is the estimator of the standard error from (11). W can replace T as the reference distribution in carrying out statistical inference. Letting $c_{W,q}$ be the q -quantile of T , $\hat{\boldsymbol{\theta}} \pm (c_{W,1-\alpha} / \sqrt{n}) \hat{\boldsymbol{\sigma}}$, where $\hat{\boldsymbol{\sigma}} = (\hat{\sigma}_k)_{k=1}^p$, is a $100 \times (1 - \alpha)\%$ confidence region for $\boldsymbol{\theta}^*$. Similarly, the test that rejects if $\max_k |\hat{\theta}_k| / \hat{\sigma}_k > c_{W,1-\alpha} / \sqrt{n}$ controls the family-wise error rate at level α for the null hypothesis $H_0 : \theta_k^* = 0$ for all $k \in [p]$. This approach has the advantage of being adaptive to the heterogeneity in variance across multiple components.

The bootstrap procedures of Section 3.2 can be easily modified to yield estimates of the quantiles of W . In Procedure 2, this is accomplished by replacing (13) with

$$\widehat{W}^{(b)} = \max_k \frac{1}{\hat{\sigma}_k \sqrt{n}} \left| \left\langle \hat{\boldsymbol{\omega}}_k, \frac{n}{n_x} \sum_{i=1}^{n_x} (\boldsymbol{\psi}(\mathbf{x}^{(i)}) - \bar{\boldsymbol{\psi}}) \boldsymbol{\xi}_x^{(b,i)} - \frac{n}{n_y} \sum_{j=1}^{n_y} (\boldsymbol{\psi}(\mathbf{y}^{(j)}) \hat{r}_{\hat{\boldsymbol{\theta}}}(\mathbf{y}^{(j)}) - \hat{\boldsymbol{\mu}}(\hat{\boldsymbol{\theta}})) \boldsymbol{\xi}_y^{(b,j)} \right\rangle \right|. \quad (96)$$

In the case of Procedure 3, one replaces (14) with

$$\widehat{W}^{(b)} = \max_k \sqrt{n} |\hat{\theta}_k^{(b)} - \hat{\theta}_k| / \hat{\sigma}_k. \quad (97)$$

H Supplementary material for Section 5

H.1 Competing procedures

The *oracle* refers to the following procedure:

$$\hat{\boldsymbol{\theta}}^{\text{oracle}} \leftarrow \arg \min_{\boldsymbol{\theta}} \ell_{\text{KLIEP}}(\boldsymbol{\theta}; \mathbf{X}_{n_x}, \mathbf{Y}_{n_y}) \text{ subject to } \text{supp}(\boldsymbol{\theta}) \subseteq \{k\} \cup \text{supp}(\boldsymbol{\theta}^*).$$

This is clearly infeasible due to the occurrence of $\boldsymbol{\theta}^*$ in the constraint. It is meant to be a performance benchmark rather than an actual alternative.

The *naïve* re-estimation is the procedure obtained by replacing the unknown $\boldsymbol{\theta}^*$ in the constraint with a sample estimate $\check{\boldsymbol{\theta}}$:

$$\hat{\boldsymbol{\theta}}^{\text{naïve}} \leftarrow \arg \min_{\boldsymbol{\theta}} \ell_{\text{KLIEP}}(\boldsymbol{\theta}; \mathbf{X}_{n_x}, \mathbf{Y}_{n_y}) \text{ subject to } \text{supp}(\boldsymbol{\theta}) \subseteq \{k\} \cup \text{supp}(\check{\boldsymbol{\theta}}).$$

This can have a near oracle behavior if $\check{\boldsymbol{\theta}}$ recovers the true support with high probability. Unfortunately, the sufficient conditions are often not met for many interesting applications; they are also notoriously difficult to check from the data (Liu et al., 2017). As such, the procedure is expected to be brittle to errors in model selection.

Finally, *SparKLIE+2* is the procedure obtained by choosing double-selection rather than one-step approximation in Step 3 of SparKLIE+1 (Procedure 2):

Step 3. (Re-estimation on the combined support)

$$\hat{\boldsymbol{\theta}}^{2+} \leftarrow \arg \min_{\boldsymbol{\theta}} \ell_{\text{KLIEP}}(\boldsymbol{\theta}; \mathbf{X}_{n_x}, \mathbf{Y}_{n_y}) \text{ subject to } \text{supp}(\boldsymbol{\theta}) \subseteq \{k\} \cup \text{supp}(\check{\boldsymbol{\theta}}) \cup \text{supp}(\check{\boldsymbol{\omega}}_k).$$

This looks deceptively like the naïve re-estimation, but the inclusion of the coordinates with large correlations with k makes the procedure robust to model selection mistakes. SparKLIE+2 is first-order equivalent to SparKLIE+1 (Chernozhukov et al., 2015b).

H.2 Parameter generation for Experiment 1

Figure 4: **Chain 1 pair, realized edge weights.** The displayed weights are the actual values used in the experiments. Excluding the difference graph, all the weights, including the ones not shown here, were generated i.i.d. $\text{Unif}(-1, 1)$. The target of inference is marked in red.

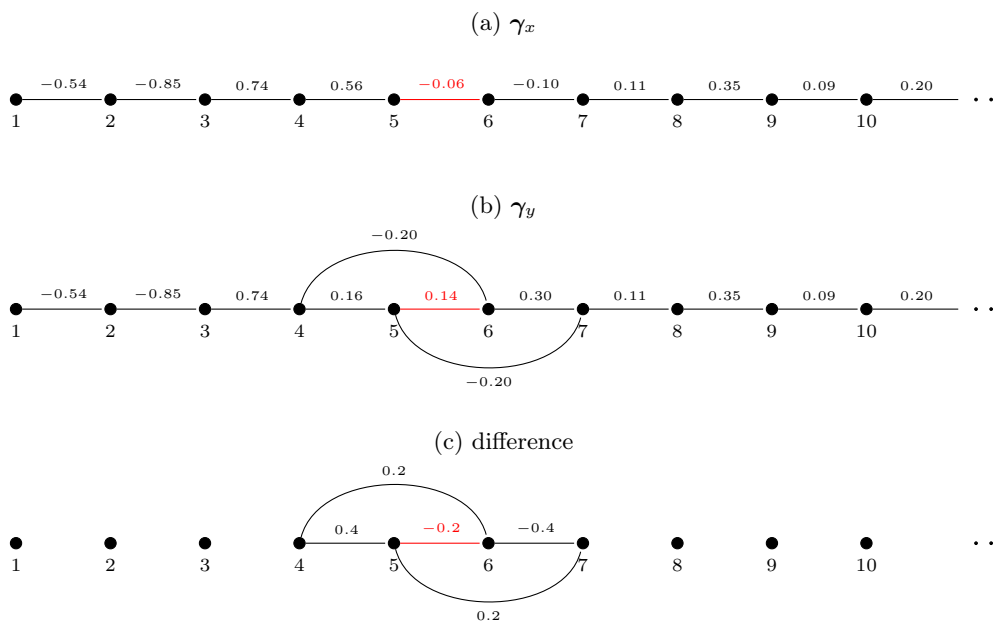


Figure 5: **Chain 2 pair, realized edge weights.** The displayed weights are the actual values used in the experiments. Excluding the difference graph, all the weights, including the ones not shown here, were generated i.i.d. $\text{Unif}(-1, 1)$. The target of inference is marked in red.

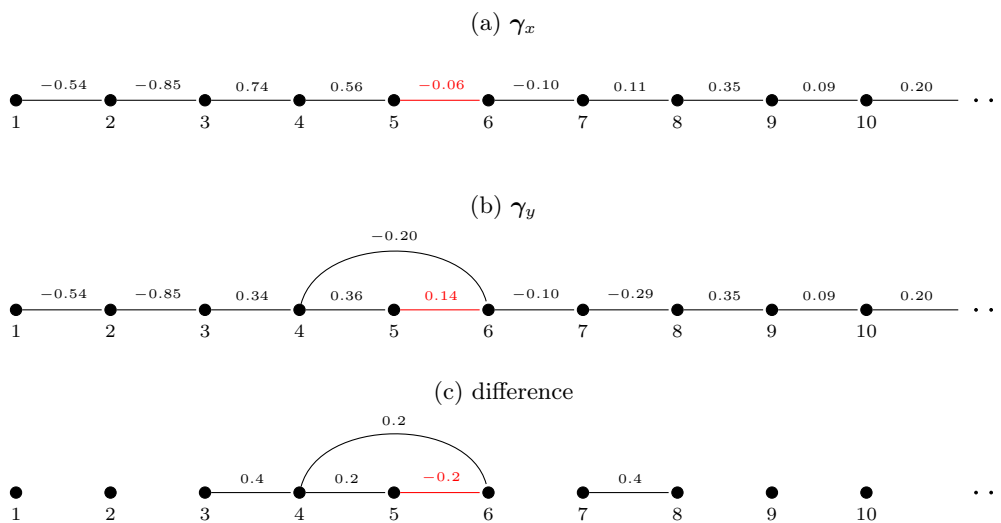


Figure 6: **Tree 1 pair, realized edge weights.** The displayed weights are the actual values used in the experiments. Excluding the difference graph, all the weights, including the ones not shown here, were generated i.i.d. $\text{Unif}(-1, 1)$. The target of inference is marked in red.

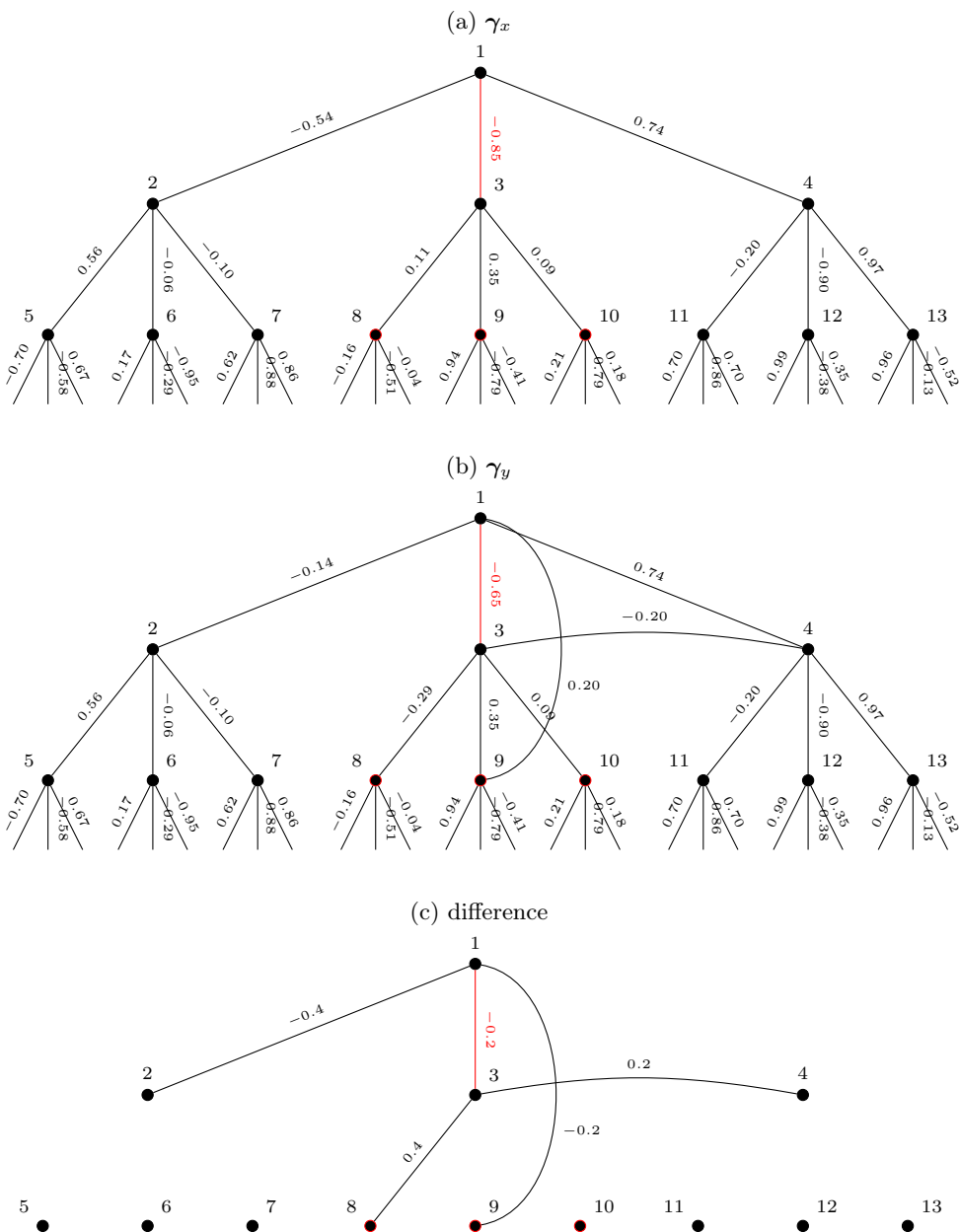
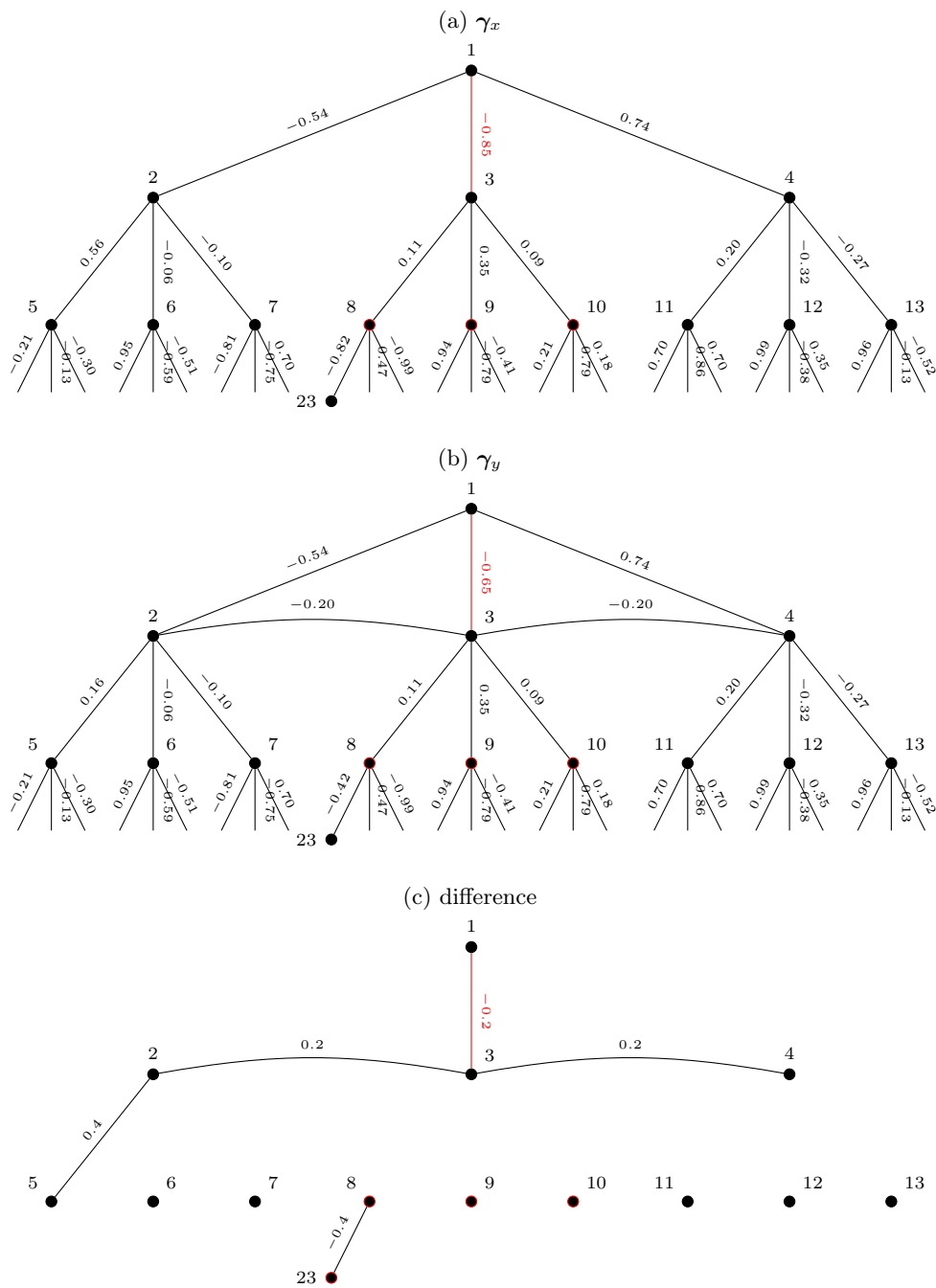


Figure 7: **Tree 2 pair, realized edge weights.** The displayed weights are the actual values used in the experiments. Excluding the difference graph, all the weights, including the ones not shown here, were generated i.i.d. $\text{Unif}(-1, 1)$. The target of inference is marked in red.



The advantage of our method is most clearly illustrated in settings in which initial sparse estimates are likely to miss parts of the support that are nonetheless important for inference. That is to say, both SparKLIE+ and the naïve procedure described in Appendix H.1 are expected to do well when the support is recovered with high probability. However, when this is no longer true, only SparKLIE+ will perform well.

We constructed eight graph pairs to highlight this difference. See Figures 4 to 7. We have four designs, and each design has a 25-node version and a 50-node version. The designs are labeled as Chain 1, Chain 2, Tree 1, and Tree 2, where the first part refers to the structure of γ_x and the second, the type of modification used to obtain γ_y from γ_x .

The edge weights were picked in the following manner. First, the weights for γ_x were generated i.i.d. $\text{Unif}(-1, 1)$. Next, γ_y was obtained from γ_x by modifying five edges. Thus, the difference graph always contained *five* nonzero edges.

Each design has a fixed inference target, a.k.a. the edge of interest. For Chain 1 and Chain 2, this was always the edge (5, 6). For Tree 1 and Tree 2, this was always the edge (1, 3). The magnitude was always fixed at 0.2. By contrast, two of the nuisance edges had magnitude 0.4, while the two others had magnitude 0.2. The signs were chosen so that the none of the edge weights had magnitudes exceeding 1.

For each design, we first generated a 25-node version, and then embedded the 25-node version into a 50-node one.

H.3 Data generation

In Experiments 1 – 5, the data were generated as i.i.d. draws from an Ising model with zero node potentials. A Gibbs sampler (Geman and Geman, 1984) was used. For Experiments 1, 2, and 5 burn-in was 3000 and thinning was 1000. For Experiments 3 and 4, burn-in was 3000 and thinning was 2000.

H.4 Additional figures and tables for Experiment 1

Table 3: **Empirical bias** $\times 10^2$. We estimate the bias $\mathbb{E}[\hat{\theta}_k - \theta_k^*] \times 10^2$, where $\hat{\theta}_k$ is either the oracle, the naïve re-fitted, the SparKLIE+1, or the SparKLIE+2 estimator. The results are averages over 1000 independent replications.

γ_x	γ_y	m	n_x	n_y	oracle	naïve	SparKLIE	
							+1	+2
chain	(1)	25	150	300	-0.505	8.033	-1.894	-0.621
		50	300	600	-0.360	7.692	-2.301	-1.673
	(2)	25	150	300	-0.819	6.920	0.526	-1.013
		50	300	600	-0.039	7.636	1.516	-0.369
ternary tree	(1)	25	150	300	-1.763	6.698	-2.323	-4.143
		50	300	600	0.256	8.975	0.875	-0.539
	(2)	25	150	300	-0.770	3.803	1.168	-0.587
		50	300	600	-0.611	5.306	-0.248	-0.826

Figure 8: **The quality of Gaussian approximation for Chain 1 pair.** We plot the distributions of the naïve re-fitted (left), the SparKLIE+1 (middle), and the SparKLIE+2 (right) estimators after studentization (i.e., standardizing by the standard error estimate (11)), first as a Normal Q-Q plot (top) and then as a histogram (bottom). In each Q-Q plot, the distribution of the oracle estimator after studentization (gray dots) is also provided for easy comparison. The orange curves in each histogram represents the density of $\mathcal{N}(0, 1)$ and is provided for reference.

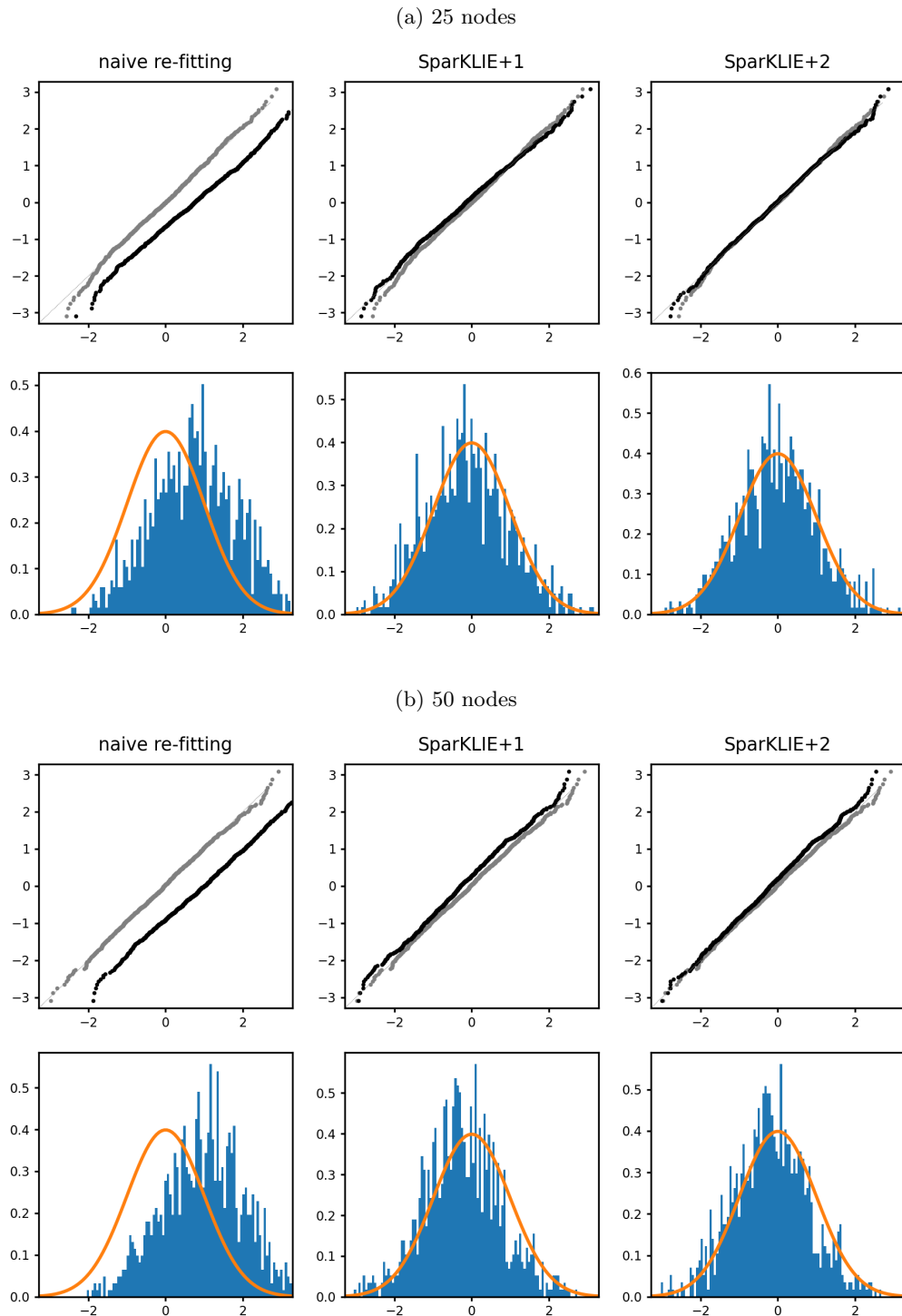


Figure 9: **The quality of Gaussian approximation for Chain 2 pair.** We plot the distributions of the naïve re-fitted (left), the SparKLIE+1 (middle), and the SparKLIE+2 (right) estimators after studentization (i.e., standardizing by the standard error estimate (11)), first as a Normal Q-Q plot (top) and then as a histogram (bottom). In each Q-Q plot, the distribution of the oracle estimator after studentization (gray dots) is also provided for easy comparison. The orange curves in each histogram represents the density of $\mathcal{N}(0, 1)$ and is provided for reference.

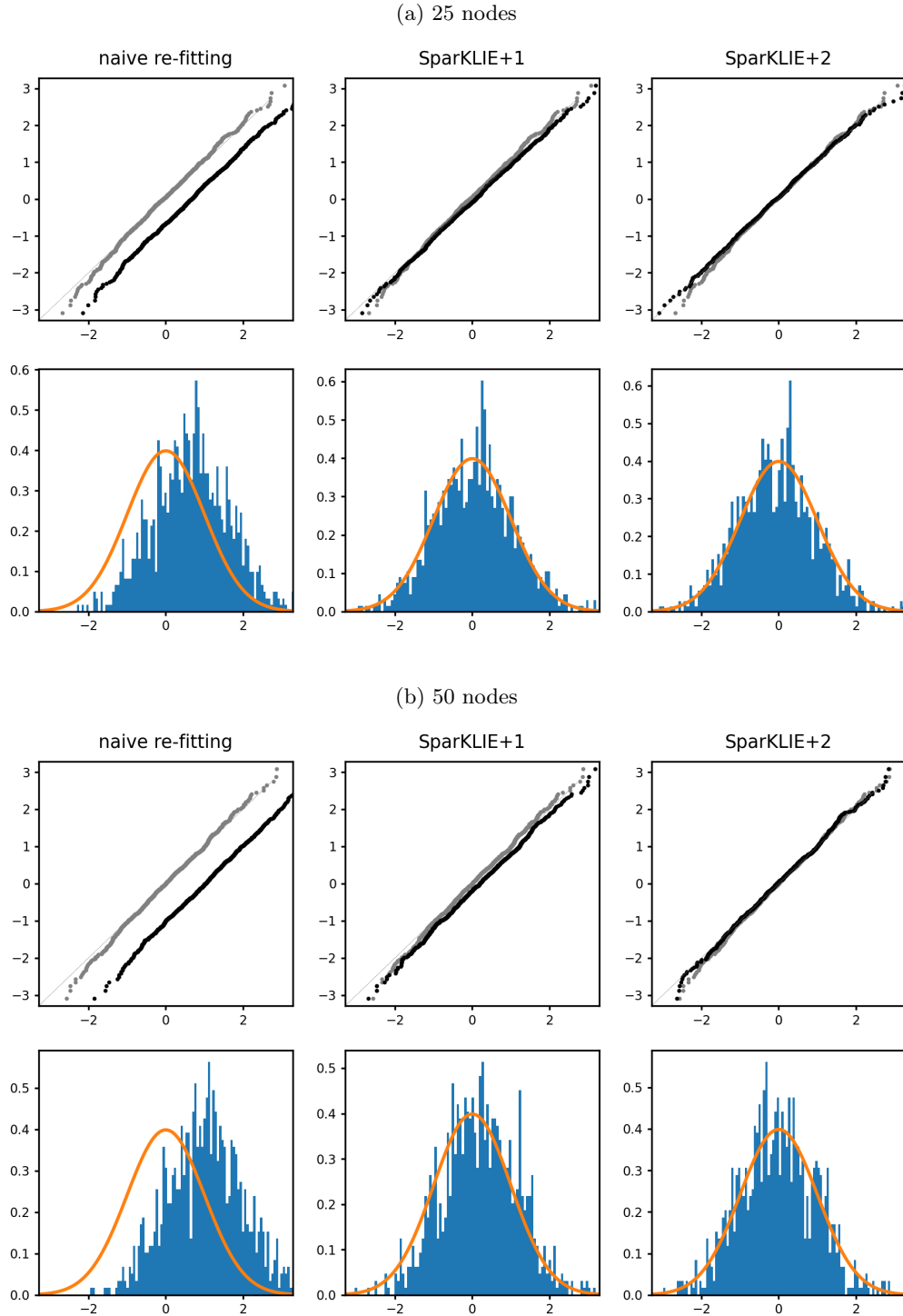


Figure 10: **The quality of Gaussian approximation for Tree 1 pair.** We plot the distributions of the naïve re-fitted (left), the SparKLIIE+1 (middle), and the SparKLIIE+2 (right) estimators after studentization (i.e., standardizing by the standard error estimate (11)), first as a Normal Q-Q plot (top) and then as a histogram (bottom). In each Q-Q plot, the distribution of the oracle estimator after studentization (gray dots) is also provided for easy comparison. The orange curves in each histogram represents the density of $\mathcal{N}(0, 1)$ and is provided for reference.

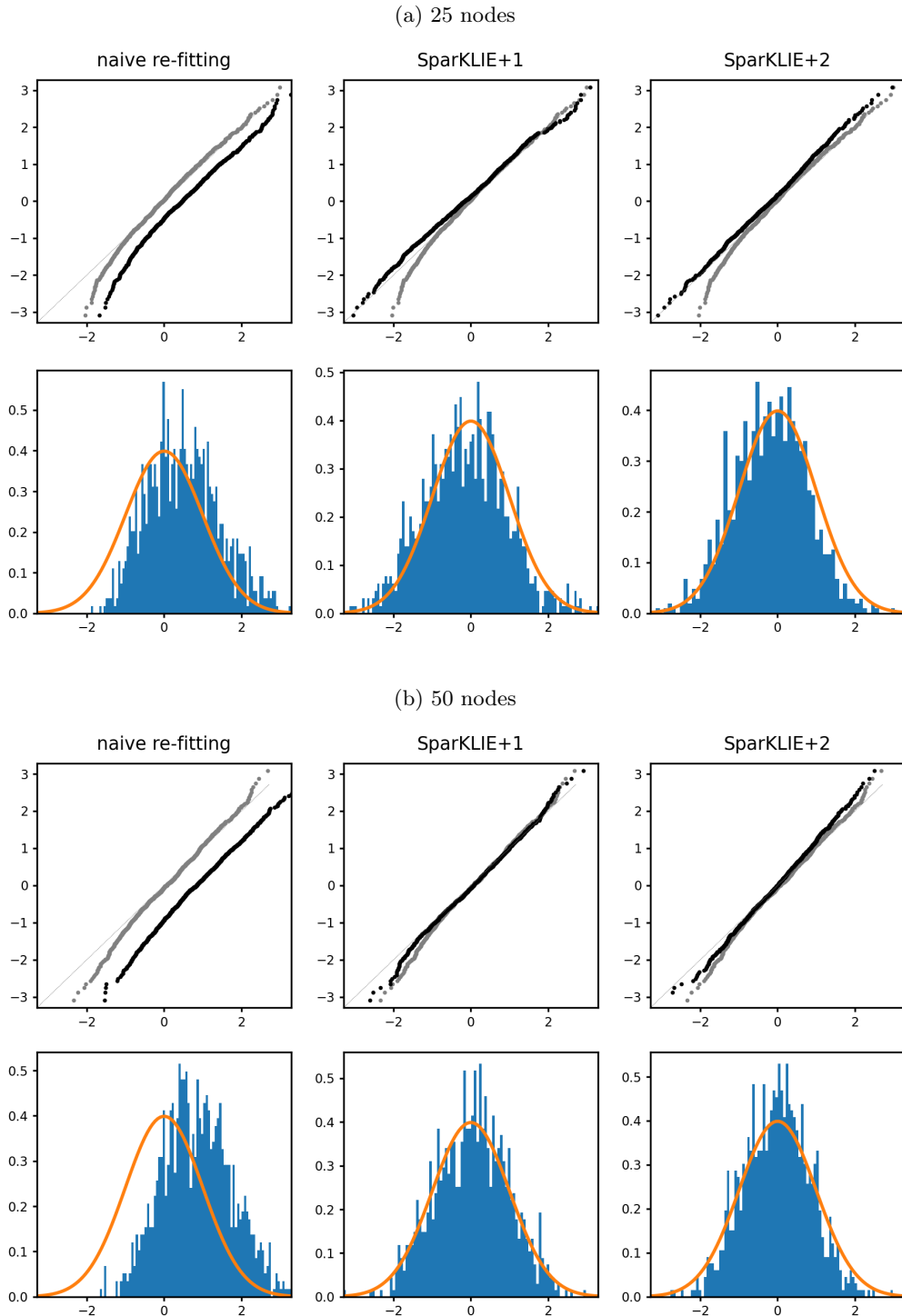
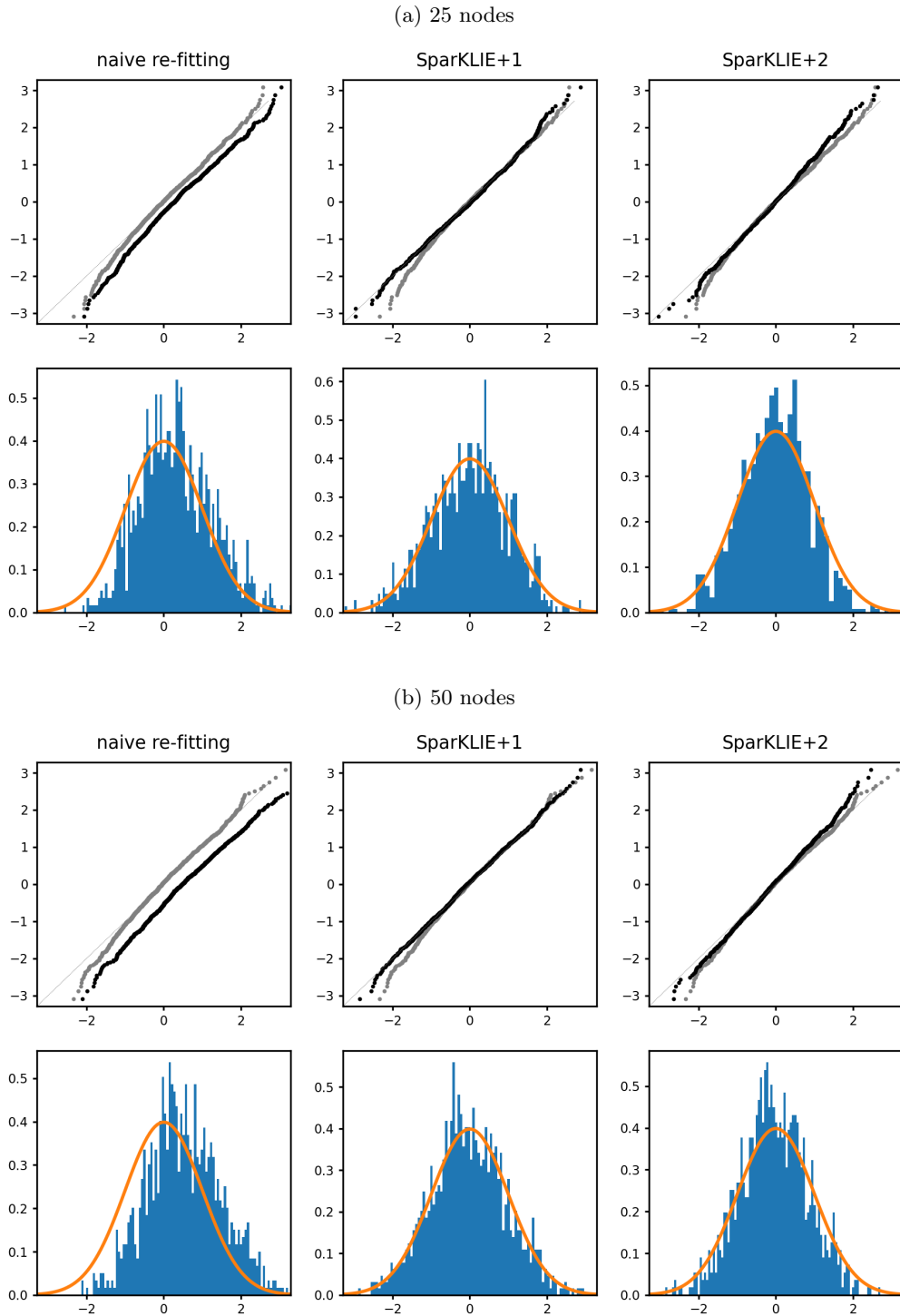


Figure 11: **The quality of Gaussian approximation for Tree 2 pair.** We plot the distributions of the naïve re-fitted (left), the SparKLIE+1 (middle), and the SparKLIE+2 (right) estimators after studentization (i.e., standardizing by the standard error estimate (11)), first as a Normal Q-Q plot (top) and then as a histogram (bottom). In each Q-Q plot, the distribution of the oracle estimator after studentization (gray dots) is also provided for easy comparison. The orange curves in each histogram represents the density of $\mathcal{N}(0, 1)$ and is provided for reference.



I Additional experiments

I.1 Experiment 2: Power of the normal-theory based test

We study the power of the normal-theory based test with SparKLIE+1 and +2 estimators. The parameters for this experiment were generated by first fixing γ_y at the γ_y of the 25-node Chain 1 pair from Experiment 1, and then obtaining 124 distinct graphs for γ_x by varying the value of the change of interest over a grid $\delta = -0.75, -0.60, \dots, 0.75$ in one of the four settings described below:

- Setting 1.* (NONE) the edge of interest is the only edge that changes from γ_y to γ_x ,
- Setting 2.* (STRONG) there are two additional strong changes of magnitude 0.4,
- Setting 3.* (WEAK) there are two additional weak changes of magnitude 0.2, or
- Setting 4.* (MIXED) there are both weak and strong changes.

See Figures 12 – 15 for illustration.

Figure 12: **NONE, realized edge weights.** γ_y is the same as the γ_y of Chain 1 pair. γ_x is obtained from γ_y by applying the change δ to the target edge marked in red.

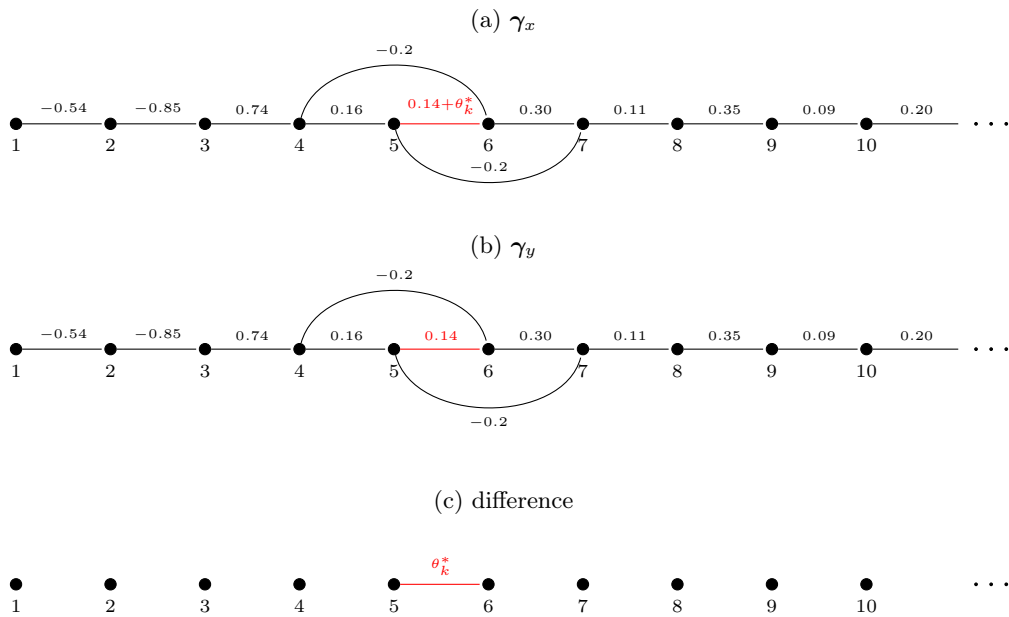


Figure 13: **STRONG, realized edge weights.** γ_y is the same as the γ_y of Chain 1 pair. γ_x is obtained from γ_y by applying the change δ to the target edge marked in red, as well as changes of magnitude 0.4 to two neighboring edges.

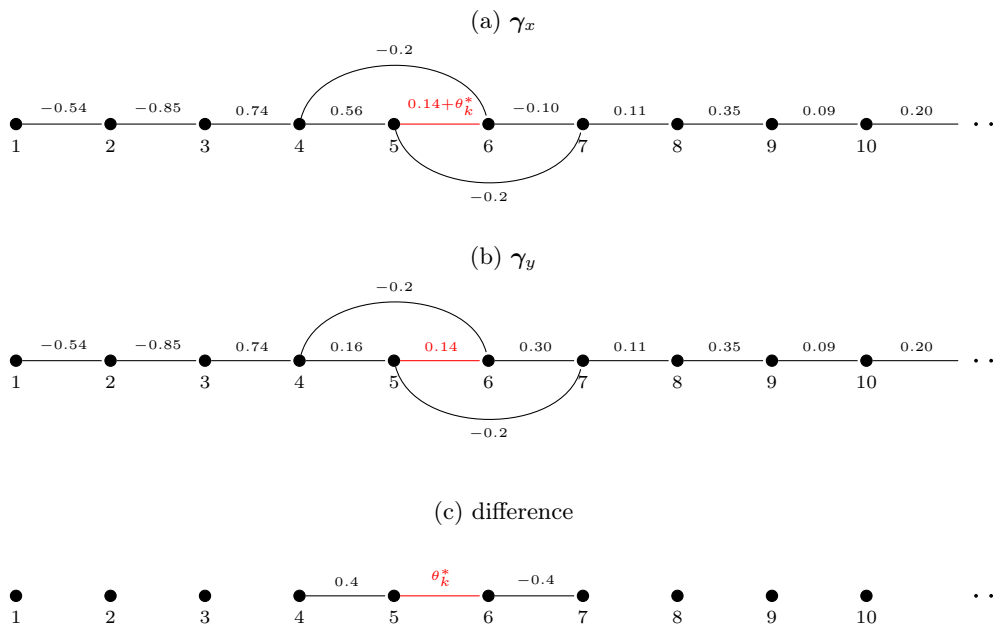


Figure 14: **WEAK, realized edge weights.** γ_y is the same as the γ_y of Chain 1 pair. γ_x is obtained from γ_y by applying the change δ to the target edge marked in red, as well as changes of magnitude 0.2 to two neighboring edges.

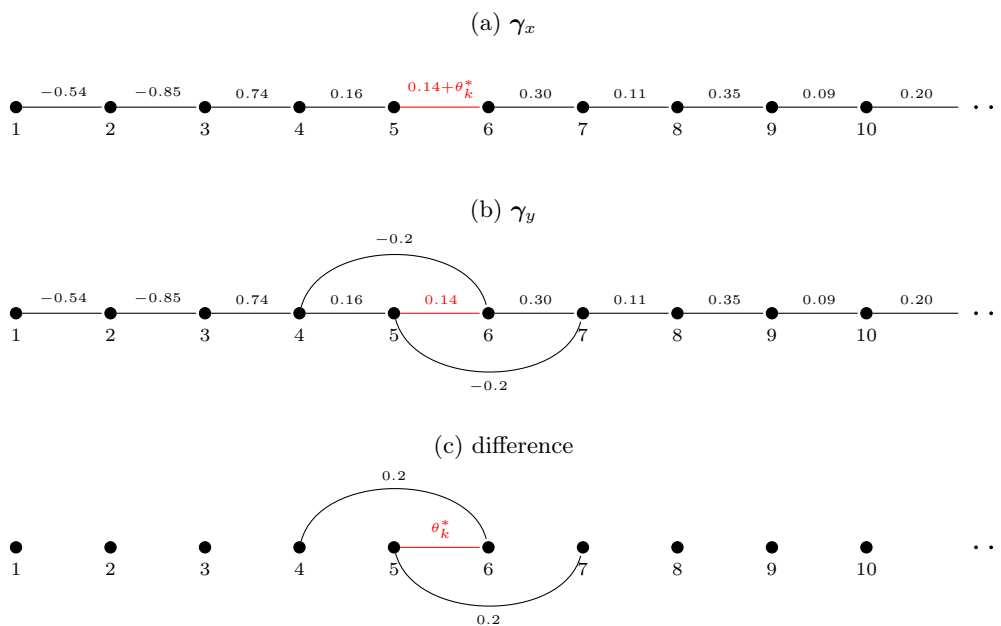
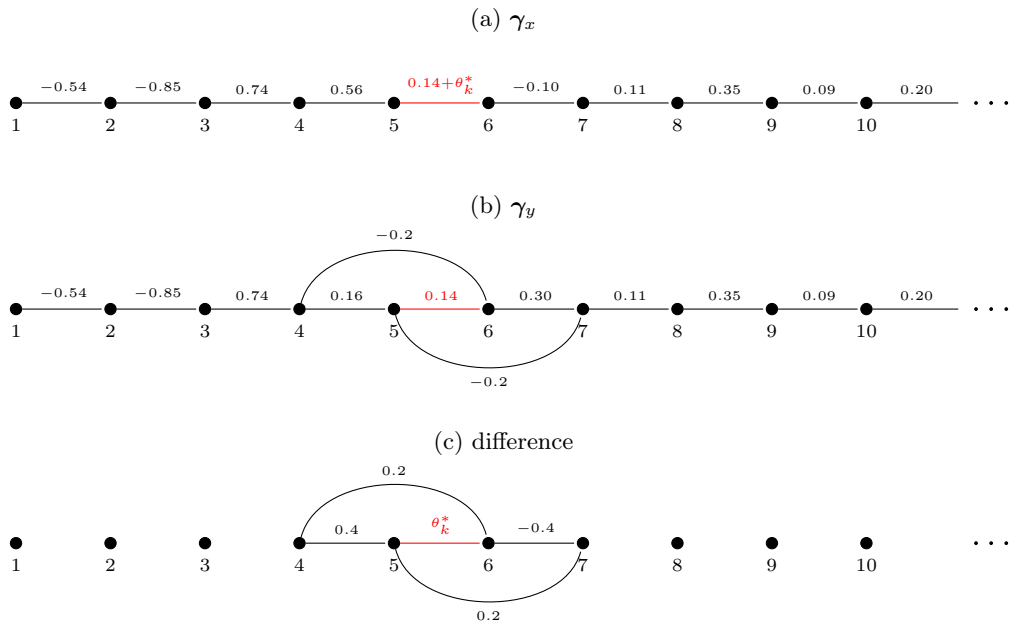


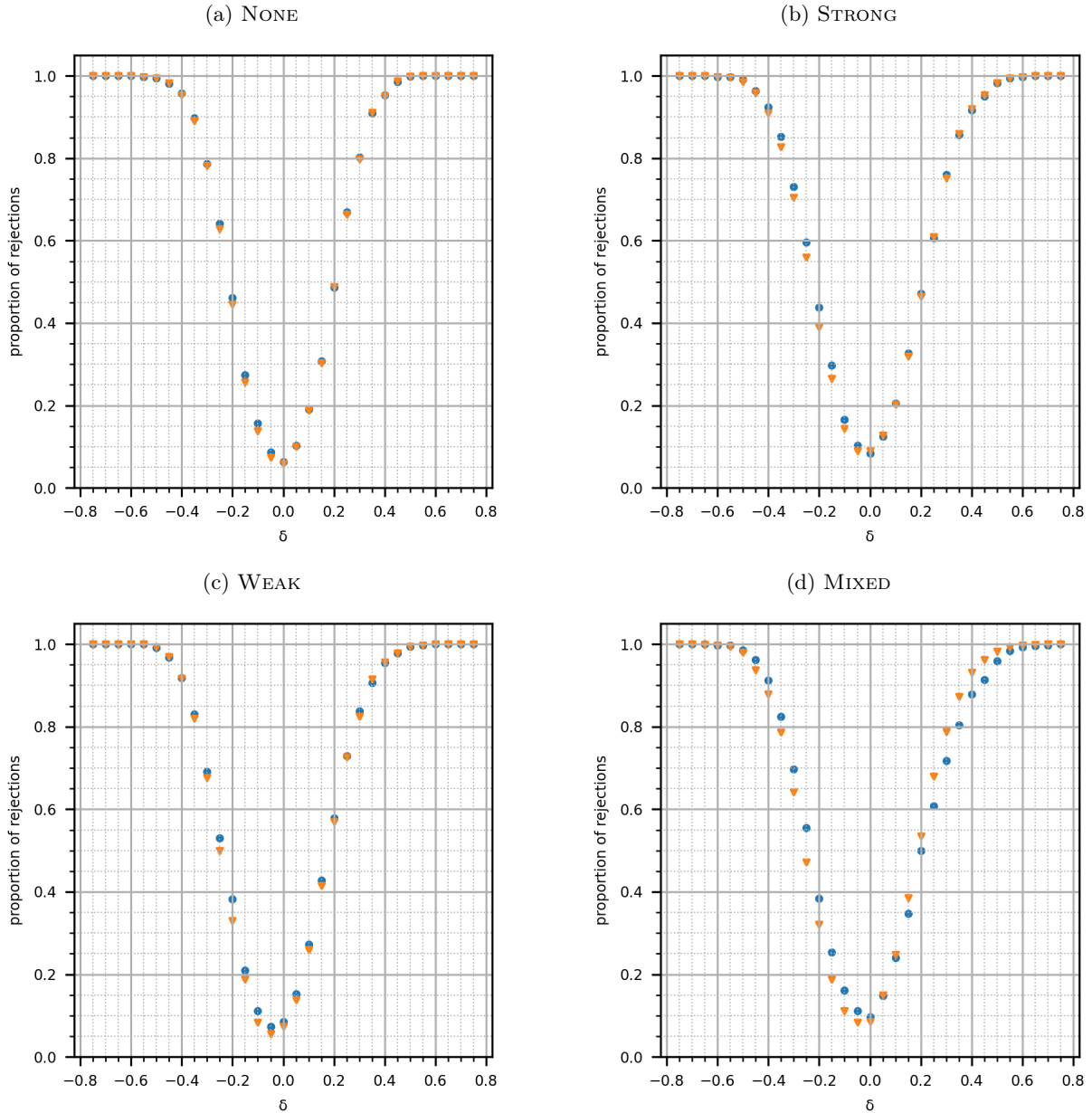
Figure 15: **MIXED, realized edge weights.** γ_y is the same as the γ_y of Chain 1 pair. γ_x is obtained from γ_y by applying the change δ to the target edge marked in red, as well as both types of nuisance changes in STRONG and WEAK.



We expect NONE and STRONG to be easy in the sense that all four estimators are projected to perform equally well. By contrast, WEAK and MIXED represent hard problems for the naïve re-estimation procedure.

Figure 16 gives a summary of the results. The power is estimated as the proportion of rejections out of 1000 independent replications at level 0.05. As in Experiment 1, both SparKLIE+ estimators behave similarly.

Figure 16: **Power of the test** $|\hat{\theta}_k|/\hat{\sigma}_k > z_{0.975}/\sqrt{n}$ **for the hypothesis** $\mathcal{H}_0 : \theta_k^* = 0$. Here, $\hat{\theta}_k$ is either the SparKLIE+1 or the SparKLIE+2 estimator, $\hat{\sigma}_k$ is the estimator of the standard error from (11), and $z_{0.975}$ is the 0.975-quantile of $\mathcal{N}(0, 1)$. The blue line with \bullet indicates SparKLIE+1. The orange line with \blacktriangledown indicates SparKLIE+2.



I.2 Experiment 4: Power of the empirical bootstrap test

We look at the power of the empirical bootstrap test as a function of the number of the changes and their magnitudes. For each $m \in \{25, 500, 100\}$, we fix γ_x at the γ_x from Experiment 3, and then modify γ_x to obtain γ_y . This was done by first picking $s_\theta \in \{1, 3, 5\}$ edges uniformly at random from the set of all possible edges, next drawing $\delta \sim \text{Unif}(l, l + 0.1)$ for $l \in \{0, .05, .10, \dots, .50\}$ for each edge in the difference graph independently of everything else, and finally subtracting the chosen δ 's from γ_x .

Here, we focused on bootstrapping SparKLIE+2 only. Also, we considered the studentized version $W = \max_k \sqrt{n} |\hat{\theta}_k - \theta_k^*| / \hat{\sigma}_k$, where $\hat{\sigma}_k$ is the estimate of the standard error (11). $\hat{c}_{W,\alpha}$ refers to the estimated $(1 - \alpha)$ -quantile of W (see Appendix G.3).

The results are summarized in Figure 17 at level 0.05. In the plots, the label "unnormalized" refers to the testing procedure using the unnormalized statistics T , and the label "normalized", to the studentized version W . There is a moderate gain in power when the latter is used.

I.3 Experiment 5: Reversed and symmetrized procedures and sensitivity to λ_θ

We study the performance of the reversed and the symmetrized procedures using the same synthetic data as in Experiment 1 for easier comparison with SparKLIE+. The reversed procedure is obtained by replacing ℓ_{KLIEP} with the reversed loss

$$\ell_{\text{RevKLIEP}}(\boldsymbol{\theta}; \mathbf{X}_{n_x}, \mathbf{Y}_{n_y}) = \frac{1}{n_y} \sum_{j=1}^{n_y} \boldsymbol{\theta}^\top \boldsymbol{\psi}(\mathbf{y}^{(j)}) + \log \left\{ \frac{1}{n_x} \sum_{i=1}^{n_x} \exp \left(-\boldsymbol{\theta}^\top \boldsymbol{\psi}(\mathbf{x}^{(i)}) \right) \right\}.$$

It is easy to see that this is just ℓ_{KLIEP} with the roles of \mathbf{x} and \mathbf{y} switched. ℓ_{RevKLIEP} also occurs as a result of minimizing the reverse KL divergence from f_x/r_θ to f_y . The symmetrized procedure minimizes the sum of ℓ_{KLIEP} and ℓ_{RevKLIEP}

$$\begin{aligned} \ell_{\text{SymKLIEP}}(\boldsymbol{\theta}; \mathbf{X}_{n_x}, \mathbf{Y}_{n_y}) &= \ell_{\text{KLIEP}}(\boldsymbol{\theta}; \mathbf{X}_{n_x}, \mathbf{Y}_{n_y}) + \ell_{\text{RevKLIEP}}(\boldsymbol{\theta}; \mathbf{X}_{n_x}, \mathbf{Y}_{n_y}) \\ &= -\frac{1}{n_x} \sum_{i=1}^{n_x} \boldsymbol{\theta}^\top \boldsymbol{\psi}(\mathbf{x}^{(i)}) + \frac{1}{n_y} \sum_{j=1}^{n_y} \boldsymbol{\theta}^\top \boldsymbol{\psi}(\mathbf{y}^{(j)}) \\ &\quad + \log \left\{ \frac{1}{n_x} \sum_{i=1}^{n_x} \exp \left(-\boldsymbol{\theta}^\top \boldsymbol{\psi}(\mathbf{x}^{(i)}) \right) \right\} + \log \left\{ \frac{1}{n_y} \sum_{j=1}^{n_y} \exp \left(\boldsymbol{\theta}^\top \boldsymbol{\psi}(\mathbf{y}^{(j)}) \right) \right\}. \end{aligned}$$

To measure performance, we looked at the coverage and the median width of 95% confidence intervals, as well as the bias of the estimator over the same 1000 replications as in Experiment 1. The results are in Tables 5 to 10. The reversed and the symmetrized procedures are expected to have worse sample complexity compared to SparKLIE+. This is indeed what we observe.

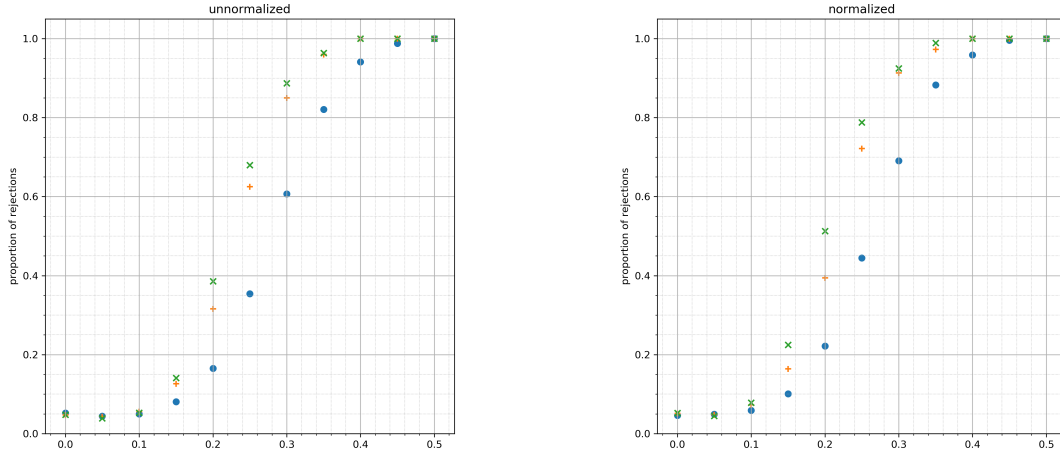
Also, to study the sensitivity to the regularization parameter choice, we tried five difference values of λ_θ as detailed in Table 4. The results in Tables 5 to 10 tell us that all performance measures are quite stable for both SparKLIE+ procedures. The reversed and the symmetrized procedures do show some instability, but it is likely that this has more to do with the fact that both procedures have larger sample complexity relative to KLIEP. See Remark 5 in Section 4.2.

Table 4: Regularization parameter settings for Experiment 5.

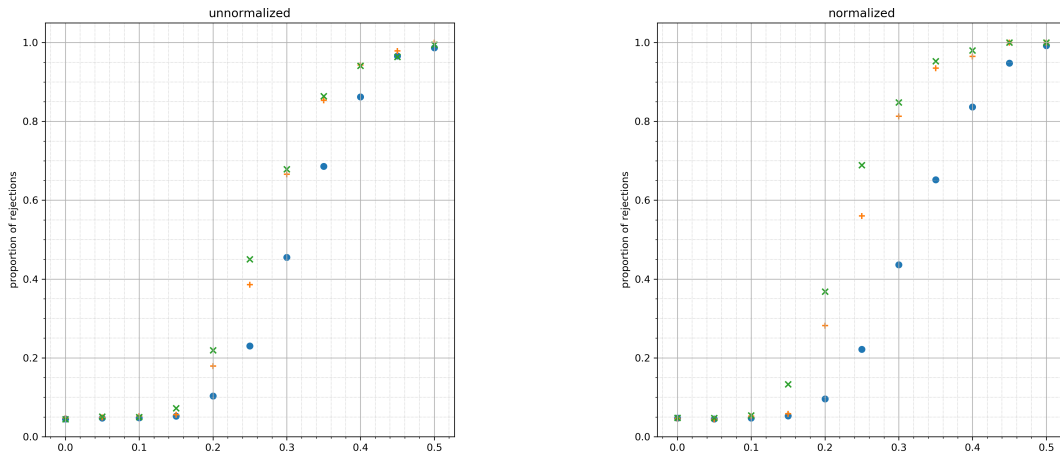
Divergence	λ_θ	λ_k
KL	$\sqrt{j \log p / \min\{n_x, n_y\}}$, $j = 4, 3.5, \dots, 2$	$\sqrt{2 \log p / n_y}$
Reverse	$\sqrt{j \log p / \min\{n_x, n_y\}}$, $j = 16, 12.5, \dots, 2$	$\sqrt{2 \log p / n_x}$
Symmetric	$\sqrt{j \log p / \min\{n_x, n_y\}}$, $j = 16, 12.5, \dots, 2$	$\frac{1}{2} \sqrt{2 \log p / n_x} + \frac{1}{2} \sqrt{2 \log p / n_y}$

Figure 17: **Power of the empirical bootstrap test for the global hypothesis $\mathcal{H}_0 : \theta^* = \mathbf{0}$.** We plot the power curves for $m = 25, 50, 100$ and the number of changes = 1, 3, 5 using two different test statistics. The three panels on the left correspond to the test $\max_k |\hat{\theta}_k| > \hat{c}_{T,1-\alpha}/\sqrt{n}$. The three panels on the right correspond to the *studentized* test $\max_k |\hat{\theta}_k|/\hat{\sigma}_k > \hat{c}_{W,1-\alpha}/\sqrt{n}$. The blue \bullet 's correspond to the case of the difference graph with 1 change; the orange $+$'s, 3 changes; and the green \times 's, 5 changes.

(a) 25 nodes



(b) 50 nodes



(c) 100 nodes

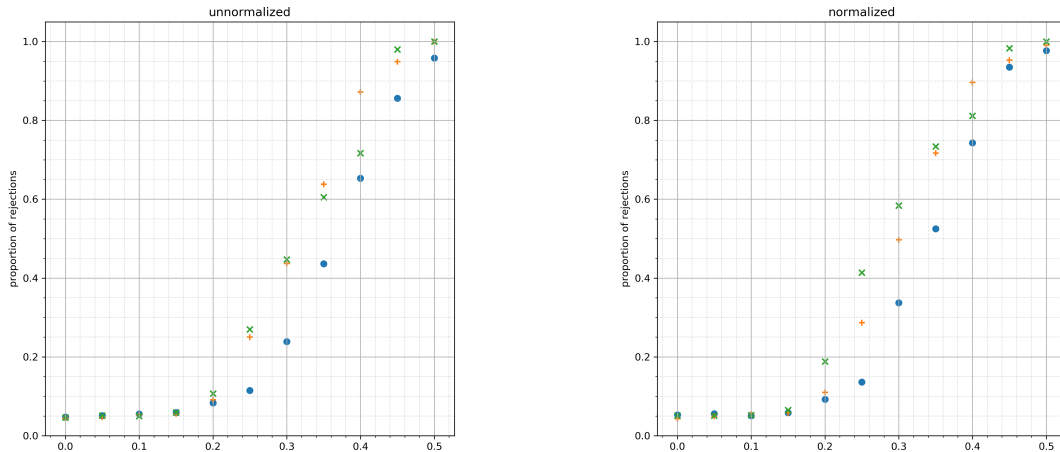


Table 5: **Empirical coverage of the 95% CI $\hat{\theta}_k \pm z_{0.975}\hat{\sigma}_k/\sqrt{n}$ for Chain 1 and Chain 2.**

γ_y	m	Divergence	De-biasing	Coverage as a function of λ_θ				
(1)	25	KL		0.934	0.941	0.942	0.943	0.953
		Reverse	+1	0.920	0.919	0.921	0.917	0.902
		Symmetric		0.911	0.895	0.893	0.876	0.875
		KL		0.963	0.965	0.964	0.965	0.964
		Reverse	+2	0.967	0.965	0.956	0.936	0.915
		Symmetric		0.940	0.930	0.897	0.781	0.567
	50	KL		0.951	0.955	0.953	0.955	0.957
		Reverse	+1	0.888	0.876	0.859	0.919	0.891
		Symmetric		0.909	0.914	0.887	0.868	0.708
		KL		0.970	0.972	0.974	0.970	0.964
		Reverse	+2	0.947	0.930	0.889	0.930	0.895
		Symmetric		0.940	0.933	0.871	0.525	0.978
(2)	25	KL		0.956	0.951	0.947	0.948	0.957
		Reverse	+1	0.900	0.900	0.891	0.898	0.877
		Symmetric		0.938	0.929	0.917	0.895	0.889
		KL		0.959	0.955	0.956	0.955	0.961
		Reverse	+2	0.953	0.953	0.951	0.948	0.910
		Symmetric		0.949	0.948	0.903	0.783	0.568
	50	KL		0.924	0.930	0.938	0.943	0.928
		Reverse	+1	0.877	0.877	0.873	0.878	0.857
		Symmetric		0.927	0.926	0.887	0.836	0.718
		KL		0.937	0.942	0.943	0.952	0.945
		Reverse	+2	0.926	0.925	0.927	0.920	0.883
		Symmetric		0.936	0.935	0.859	0.487	0.987

Table 6: Empirical coverage of the 95% CI $\hat{\theta}_k \pm z_{0.975} \hat{\sigma}_k / \sqrt{n}$ for Tree 1 and Tree 2.

γ_y	m	Divergence	De-biasing	Coverage as a function of λ_θ				
(1)	25	KL		0.940	0.945	0.947	0.955	0.952
		Reverse	+1	0.798	0.801	0.831	0.862	0.893
		Symmetric		0.880	0.892	0.925	0.946	0.895
		KL		0.977	0.976	0.974	0.972	0.977
		Reverse	+2	0.939	0.939	0.939	0.940	0.934
		Symmetric		0.909	0.903	0.905	0.865	0.728
	50	KL		0.954	0.957	0.961	0.961	0.959
		Reverse	+1	0.743	0.755	0.820	0.843	0.860
		Symmetric		0.871	0.883	0.903	0.964	0.435
		KL		0.985	0.985	0.985	0.981	0.982
		Reverse	+2	0.906	0.914	0.940	0.942	0.934
		Symmetric		0.905	0.908	0.878	0.734	0.987
(2)	25	KL		0.955	0.961	0.959	0.959	0.958
		Reverse	+1	0.860	0.861	0.856	0.862	0.889
		Symmetric		0.887	0.905	0.937	0.970	0.906
		KL		0.982	0.987	0.988	0.985	0.985
		Reverse	+2	0.941	0.941	0.939	0.927	0.929
		Symmetric		0.925	0.918	0.917	0.896	0.731
	50	KL		0.954	0.956	0.950	0.954	0.955
		Reverse	+1	0.859	0.859	0.855	0.860	0.873
		Symmetric		0.903	0.910	0.932	0.972	0.435
		KL		0.990	0.988	0.982	0.980	0.980
		Reverse	+2	0.954	0.951	0.939	0.936	0.932
		Symmetric		0.935	0.921	0.914	0.784	0.990

Table 7: Median width of the 95% CI $\hat{\theta}_k \pm z_{0.975}\hat{\sigma}_k/\sqrt{n}$ for Chain 1 and Chain 2.

γ_y	m	Divergence	De-biasing	Median width as a function of λ_θ				
(1)	25	KL		0.479	0.481	0.485	0.490	0.497
		Reverse	+1	0.500	0.500	0.494	0.478	0.503
		Symmetric		0.420	0.438	0.503	0.701	1.467
		KL		0.511	0.517	0.519	0.523	0.532
		Reverse	+2	0.540	0.540	0.531	0.502	0.528
		Symmetric		0.454	0.483	0.531	0.669	1.605
	50	KL		0.347	0.347	0.346	0.347	0.351
		Reverse	+1	0.353	0.351	0.331	0.316	0.344
		Symmetric		0.300	0.310	0.384	0.776	766.6
		KL		0.366	0.364	0.364	0.365	0.369
		Reverse	+2	0.382	0.381	0.346	0.324	0.359
		Symmetric		0.333	0.340	0.385	0.649	936.7
(2)	25	KL		0.436	0.446	0.454	0.466	0.483
		Reverse	+1	0.483	0.483	0.494	0.524	0.573
		Symmetric		0.443	0.463	0.528	0.727	1.503
		KL		0.444	0.454	0.465	0.481	0.504
		Reverse	+2	0.521	0.522	0.537	0.568	0.630
		Symmetric		0.458	0.480	0.535	0.680	1.569
	50	KL		0.318	0.323	0.329	0.336	0.349
		Reverse	+1	0.341	0.344	0.362	0.380	0.410
		Symmetric		0.319	0.328	0.390	0.787	756.2
		KL		0.322	0.327	0.336	0.348	0.363
		Reverse	+2	0.368	0.372	0.395	0.413	0.445
		Symmetric		0.331	0.342	0.388	0.654	953.3

Table 8: Median width of the 95% CI $\hat{\theta}_k \pm z_{0.975} \hat{\sigma}_k / \sqrt{n}$ for Tree 1 and Tree 2.

γ_y	m	Divergence	De-biasing	Median width as a function of λ_θ				
(1)	25	KL		0.754	0.765	0.776	0.792	0.815
		Reverse	+1	0.711	0.712	0.740	0.781	0.865
		Symmetric		0.707	0.772	0.969	1.467	2.925
		KL		0.845	0.865	0.881	0.903	0.940
		Reverse	+2	0.786	0.788	0.804	0.831	0.925
		Symmetric		0.783	0.853	1.014	1.508	4.574
	50	KL		0.581	0.578	0.575	0.575	0.584
		Reverse	+1	0.508	0.516	0.559	0.580	0.676
		Symmetric		0.527	0.558	0.717	1.709	2.008
		KL		0.659	0.654	0.651	0.652	0.669
		Reverse	+2	0.577	0.583	0.607	0.614	0.746
		Symmetric		0.592	0.619	0.758	1.733	411.9
(2)	25	KL		0.815	0.826	0.835	0.842	0.867
		Reverse	+1	0.686	0.686	0.696	0.770	0.889
		Symmetric		0.740	0.802	0.990	1.533	3.451
		KL		0.893	0.906	0.928	0.933	0.973
		Reverse	+2	0.726	0.726	0.738	0.814	0.948
		Symmetric		0.783	0.852	1.014	1.514	4.893
	50	KL		0.620	0.621	0.620	0.617	0.632
		Reverse	+1	0.485	0.486	0.524	0.599	0.735
		Symmetric		0.539	0.579	0.755	1.848	1.954
		KL		0.687	0.684	0.679	0.679	0.693
		Reverse	+2	0.515	0.517	0.558	0.629	0.797
		Symmetric		0.574	0.611	0.752	1.754	416.6

Table 9: **Empirical bias of $\hat{\theta}_k$ for Chain 1 and Chain 2.**

γ_y	m	Divergence	De-biasing	Bias as a function of λ_θ				
(1)	25	KL		-0.009	-0.014	-0.019	-0.021	-0.023
		Reverse	+1	-0.061	-0.062	-0.046	-0.002	0.003
		Symmetric		0.006	-0.006	-0.033	-1.591	-1.9×10^{15}
		KL		0.009	-0.001	-0.012	-0.017	-0.021
		Reverse	+2	-0.058	-0.059	-0.045	-0.005	-0.038
		Symmetric		0.005	-0.009	-0.041	-0.541	-12.007
	50	KL		-0.018	-0.017	-0.017	-0.017	-0.017
		Reverse	+1	-0.058	-0.054	-0.005	0.023	0.005
		Symmetric		0.008	-0.002	-0.043	-0.775	-96.784
		KL		-0.011	-0.013	-0.012	-0.012	-0.014
		Reverse	+2	-0.054	-0.052	-0.007	0.019	-0.002
		Symmetric		0.006	-0.004	-0.050	-2.337	-22.035
(2)	25	KL		0.012	0.007	0.004	-0.000	-0.004
		Reverse	+1	-0.070	-0.070	-0.076	-0.073	-0.078
		Symmetric		-0.023	-0.029	-0.047	-0.118	-10.152
		KL		-0.004	-0.006	-0.008	-0.012	-0.014
		Reverse	+2	-0.067	-0.067	-0.073	-0.140	-0.237
		Symmetric		-0.023	-0.031	-0.054	-0.282	-9.502
	50	KL		0.022	0.018	0.013	0.005	-0.003
		Reverse	+1	-0.066	-0.067	-0.073	-0.069	-0.074
		Symmetric		-0.019	-0.022	-0.054	-0.696	-83.982
		KL		-0.006	-0.007	-0.008	-0.010	-0.014
		Reverse	+2	-0.063	-0.064	-0.070	-0.070	-0.083
		Symmetric		-0.020	-0.023	-0.061	-2.634	-18.973

Table 10: **Empirical bias of $\hat{\theta}_k$ for Tree 1 and Tree 2.**

γ_y	m	Divergence	De-biasing	Bias as a function of λ_θ				
(1)	25	KL		-0.021	-0.017	-0.014	-0.012	-0.012
		Reverse	+1	-22.828	-21.619	-21.573	-21.307	-20.354
		Symmetric		-0.042	-0.085	-0.129	-0.300	-11.936
		KL		-0.030	-0.031	-0.031	-0.034	-0.039
		Reverse	+2	-4.351	-3.258	-4.820	-4.550	-3.982
		Symmetric		-3.215	-3.624	-3.284	-3.849	-11.791
	50	KL		0.001	-0.000	-0.003	-0.007	-0.011
		Reverse	+1	-0.381	0.008	-2.644	-1.543	-2.899
		Symmetric		-0.046	-0.063	-0.105	-0.341	-56.174
		KL		-0.012	-0.012	-0.014	-0.017	-0.021
		Reverse	+2	-0.331	0.038	-0.226	-0.343	-0.684
		Symmetric		-0.056	-0.080	-0.140	-2.748	-14.916
(2)	25	KL		0.020	0.021	0.017	0.016	0.012
		Reverse	+1	-20.257	-19.118	-19.523	-20.280	-19.418
		Symmetric		-0.062	-0.074	-0.106	-0.251	-9.982
		KL		0.005	0.005	0.005	0.005	-0.001
		Reverse	+2	-3.518	-3.371	-3.643	-3.835	-4.016
		Symmetric		-3.006	-3.024	-2.678	-3.294	-10.106
	50	KL		0.001	-0.001	-0.003	-0.004	-0.005
		Reverse	+1	-1.360	-0.999	-0.880	-2.011	-2.479
		Symmetric		-0.046	-0.052	-0.084	-0.756	-60.579
		KL		-0.007	-0.008	-0.007	-0.007	-0.008
		Reverse	+2	-0.200	-0.104	-0.284	-0.121	-0.918
		Symmetric		-0.048	-0.057	-0.101	-2.445	-13.089

J Supplementary material for Section 6

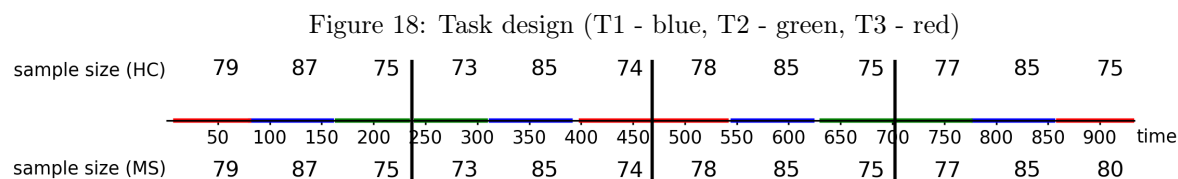
J.1 Preprocessing

The data were preprocessed in SPM12 (Wellcome Trust Centre for Neuroimaging, <http://www.fil.ion.ucl.ac.uk/spm>). The default SPM12 steps were used, except in normalization, the voxel size was set to $2 \times 2 \times 2$ and the bounding box was changed to match the automated anatomical labelling atlas (Tzourio-Mazoyer et al., 2002).

J.2 Experiment

The fMRI measurements were made while the participants were asked to go through four blocks of task sequences, each made up of three types of tasks arranged in some order. During the experiment, the participants were asked to look at a screen, through which they received instructions about the tasks. All three tasks involved squeezing and releasing a hand dynamometer while looking at the screen. For the sensorimotor task (T1), the participants were asked to squeeze and release the hand dynamometer freely at their own pace while paying heed to the images on the screen. By contrast, in the intrinsic alertness task (T2) or the extrinsic alertness task (T3), the participants were supposed to squeeze the hand dynamometer only after seeing a white square. In the case of T3, a black screen always preceded each occurrence of the white square. For T2, there was no forewarning.

Figure 18 gives the task sequence used in the pilot study.



K Additional real data example: Voting records of the 109th United States Senate

We apply Section 3.1 and Procedure 3 to compare the voting records in the 109th US Senate between the first half (January 3, 2005 – January 16, 2006) and the second half (January 16, 2006 – January 3, 2007). The data were taken from a larger dataset covering a longer period (1979 – 2012) originally extracted from the website www.voteview.com and then processed by the authors of Roy et al. (2017). We are grateful to the authors of Roy et al. (2017) for sharing their data with us.

We focus on the two halves of the 109th Senate. This is to ensure a sparse network difference as well as homogeneity of the data. Only one seat changed hands between the two periods from one Democrat to another. On January 16, 2006, Democrat Jon Corzine resigned in order to assume his new position as Governor of New Jersey, naming Democrat Bob Menendez to succeed. In spite of the change in membership, one would not expect there to be significant changes in the overall voting pattern, as the votes tend to split along the party lines, and nothing in our research suggests that the two Democrats were exceptional in this respect. This leads to the hypothesis

$$\mathcal{H}_{\text{NJ}} : \gamma_{\text{1st half, Corzine / Menendez},v} = \gamma_{\text{2nd half, Corzine / Menendez},v} \text{ for all } v \neq \text{Corzine / Menendez}.$$

There were 251 votes in the first half, and 177 votes in the second. Following Roy et al. (2017), we code “Yea” as +1 and “Nay” as -1, and model the votes as independent observations from one of two Ising models with zero node potentials, one for each period. Admittedly, our model is far too simple to capture all the nuances of the complex political process. What we are hoping to observe with this toy example is whether the pattern recovered by SparkLIE+ aligns well with our knowledge of past political events, which in this case corresponds to an empty graph for the neighborhood of the New Jersey seat of interest.

We test \mathcal{H}_{NJ} at level 0.05. We use Procedure 1 to estimate the differential network in the neighborhood of the New Jersey seat. We use the version of Procedure 1 employing autoscaling formulations for Steps 1 and 2 with the universal penalty levels, as explained in Remark 2 in Section 3.1. The rejection threshold for the test statistic

$$T_0 = \max_{v \neq \text{Corzine / Menendez}} |\hat{\theta}_{\text{Corzine / Menendez},v}|$$

was estimated using Procedure 3. Comparing T_0 with the estimated rejection threshold yielded no statistically significant edges in this neighborhood differential network. We conclude that Senator Menendez’s records did not differ significantly from those of his predecessor, as expected.